UNIVERSITY OF CAPE COAST

MERCURY AND OTHER ELEMENTS IN THE PRA RIVER BASIN, GHANA

BY

CHRISTIANA ODUMAH HOOD

Thesis submitted to the Department of Physics of the School of Physical Sciences, College of Agriculture and Natural Sciences, University of Cape Coast, in partial fulfilment of the requirements for the award of Doctor of Philosophy degree in Physics

November, 2017

UNIVERSITY OF CAPE COAST

MERCURY AND OTHER ELEMENTS IN THE PRA RIVER BASIN, GHANA

BY

CHRISTIANA ODUMAH HOOD

Thesis submitted to the Department of Physics of the School of Physical Sciences, College of Agriculture and Natural Sciences, University of Cape Coast, in partial fulfilment of the requirements for the award of Doctor of Philosophy degree in Physics

November, 2017

DECLARATION

Candidate's Declaration

I hereby declare that this thesis is the result of my own original research and that no part of it has been presented for another degree in this university or elsewhere.

Candidate's Signature:................................... Date: 8/04/2019
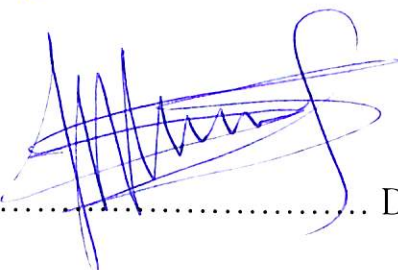
Name: Christiana Oduamh Hood

Supervisors' Declaration

We hereby declare that the preparation and presentation of the thesis were supervised in accordance with the guidelines on supervision of thesis laid down by the University of Cape Coast.

Principal Supervisor's Signature:..................... Date: 14.12.2018

Name: Prof. Dr. Milena Horvat

Co-Supervisor's Signature:........................... Date: 14/12/2018

Name: Prof. Samuel Yeboah Mensah

ABSTRACT

Total mercury (THg) concentrations in sediment cores (0-10 cm depth), soil profiles (0-6 cm), carnivorous/herbivorous fish tissues, and "Black" samples were determined using Cold Vapour Atomic Absorption Spectroscopy (CVAAS). The samples were obtained from twenty-one, twenty, seven, and four sites respectively in the Pra River Basin. k0-Instrumental Neutron Activation Analysis (k_0-INAA) method was used to validate HNO_3/HF/HCl digestion in the determination of THg in the geological samples, and thirty-four elements in soil (0-1 cm) samples. Precision and accuracy for all reference materials were good. Hydrofloric (HF) acid combination was best digestion procedure for THg determination in all geological samples from the basin. The least (2.20-3.23 mg/kg) and highest (103-770 mg/kg) THg in the soil from twenty sites were recorded at Twenedurase and Dunkwa-on-Offin sites respectively. Also, the least (0.01-0.02 mg/kg) and highest (0.23-20.8 mg/kg) THg in sediments from twenty-one sites were recorded at Kwahu Praso and Beposo sites respectively. The highest THg (1,673 mg/kg) in "Black" samples was recorded at Dunkwa-on-Offin 1. All carnivorous fish muscle from Nkontinso site had THg (0.376-0.983 µg/g) above 0.3 µg/g and THg (0.014-0.262 µg/g) in herbivorous fish muscles were below 0.3 µg/g. The elements, As, Hf, Se, Zr, U, Sb, W and Au in the soil were found to bind THg. Monazite-Ce was found in the 0-1 cm soil from Kibi site. HF acid digestion was the best procedure for THg determination in the geological samples in the river basin. All soils had THg above background levels of 0.07 mg/kg. Dunkwa-on-Offin site is THg "hotspot" in the basin and carnivorous fish from Nkontinso site are not safe for consumption.

KEY WORDS

Anthropogenic

Contamination

Mercury

Methylmercury

Sediment

Soil

ACKNOWLEDGEMENTS

DEDICATION

I dedicate this work to my daughters, Ewurakuwa Arko Anderson and Ewurabena Mbraye Anderson.

TABLE OF CONTENTS

CHAPTER FIVE: SUMMARY, CONCLUSIONS AND

RECOMMENDATIONS

LIST OF TABLES

LIST OF FIGURES

LIST OF SYMBOLS

α ray	Alpa ray
β ray	Beta ray
γ ray	Gamma ray
ρ_a	Concentration of analyte a (μg/g)
N_p	Net peak area
A_{sp}	(N_p/t_c)/SDCW, the specific count rate (s^{-1})
G_{th}	Correction factor for thermal neutron self-shielding
G_e	Correction factor for epithermal neutron self-shielding
f	Thermal to epithermal neutron fluence rate ratio(ϕ_{th}/ϕ_e)
Φ	Neutron flux density (neutron $cm^{-2}s^{-1}$)
n	Number of atoms of target present
θ	Isotopic abundance of the nuclide
M	Chemical atomic weight of the nuclide
m	Mass of nuclide
A	Absolute activity of samples (s^{-1})
$\varepsilon(E)$	Photo peak detection efficiency for gamma ray energy E
P_A	Detector photo peak area (m^2)
W	Weight of the sample (g)
t_i	Irradiation time (s^{-1})
t_d	Delay Time (s^{-1})
t_c	Counting time (s^{-1})
λ	Decay constant (s^{-1})
R	Reaction rate
S	Saturation factor $[1-\exp(-\lambda t_{irr})]$

D	Delay factor $[1 - \exp(-\lambda t_d)]$
C	Counting factor $[1 - \exp(-\lambda t_c)]/\lambda t_c$
I_0	Resonance integral
$\bar{E}r$	Effective resonance energy (eV)
LA	Probability for loss
SA	Probability for gain
E_{Cd}	Effective Cd cut-off energy
k0	Kay Zero

LIST OF ACRONYMS

AA	Atomic Absorption
AAS	Atomic Absorption Spectroscopy
AFS	Atomic Florescence Spectroscopy
AMAP	Arctic Monitoring Assessment
ASGM	Artisanal and Small-scale Gold Mining
BCR	Community Bureau of Reference
BMD	Benchmarch Dose
CAMEP	Carnegie Amazon Ecosystem Mercury Project
CF	Carousel Facility
CRM	Certified Reference Material
CV	Cold Vapour
CVAAS	Cold Vapour Atomic Absorption Spectroscopy
CVAFS	Cold Vapour Atomic Florescence Spectroscopy
DO	Dissolved Oxygen
DOM	Dissolve Organic Matter
DSNR	Department of Sustainable Natural Resources
EDL	Electrodeless Discahrge Lamp
GEM	Gasouse Elemental Mercury
GC	Gas Chromatography
GHG	Greenhouse Gas
GOM	Gaseous Organic Mercury
GSS	Ghana Statistical Service
HG	Hybride Generation
HNOAE	Highest No Observed Adverse Effect

HPLC	High Performance Liquid Chromatography
HREE	Heavy Rare Earth Element
ICC	Interclass Correlation Coefficient
INAA	Instrumental Neutron Activation ANalysi
LA	Lanthanide
LOAEC	Lowest Observable Adverse Effect Concentration
LREE	Light Rare Earth Element
LSGM	Large Scale Gold Mining
MAC	Maximum Allowable Concentration
MCA	Multi-Channel Analyzer
MMHg	Monomethylmencury
MoFA	Ministry of Food and Agriculture
MRI	Magnetic Resonance Imaging
NAA	Neutron Activation Analysis
NOx	Oxides of Nitrogen
RE	Relative Error
REE	Rare Earth Element
RSD	Relative Standard Deviation
RPD	Relative Percentage Difference
TAV	Trigger Allowable Value
THg	Total Mercury
UNEP	United Nation Environmental Programme
VOC	Volatile Organic Compounds
WRC	Water Resource Commission
WQA	Water Quality Assessment

WQI   Water Quality Index

CHAPTER ONE

INTRODUCTION

The study is based on anthropogenic released of mercury into different compartment of the environment by Artisanal and Small-Scale miners in the Pra River Basin. The mercury released is bonded to other elements in the basin and may need vigorous analytical procedures for true determination of mercury concentrations in geological samples. Thus, accumulation and magnification of mercury in the environment and food chain in the Basin which may affect the health of the populace was determined.

Background to the Study

All natural soils contain some amount of trace metals; however, the presence of metals in soil does not necessary mean the soil is contaminated. Thus, the concentration of metals in contaminated soil is primarily related to the local geology of the parent material from which the soil was formed (McLean & Bledsoe, 1992). In general, soils are the reservoir for toxic and trace metals (Cottenie & Verloo, 1984). The metal-soil interactions introduces metals at the soil surface but are not transported downward unless the metal retention capacity of the soil is exceeded. Numerous physical and chemical factors in soil, such as degradation of organic waste matrix, pH, redox potential, soil solution composition, chemical type of the element in the environment, over time may increase metal mobility, ionization and availability (Hooper & Anderson, 2008; McLean & Bledsoe, 1992). The degree of vertical contamination is closely related to the soil solution and surface chemistry of the soil matrix with reference to the metal involved

1

(McLean & Bledsoe, 1992). Mercury has a long retention time in soil. As a result, the majority of anthropogenic mercury accumulated in soil may be released to surface waters through surface runoff over long periods of time (Chemicals, 2002; Hissler & Probst, 2006). Surface runoff of mercury from rain or snow is a very important source of mercury contamination in aquatic systems in urban areas(CAMEP, 2013; Wan et al., 2004). Mercury deposition in soil takes place in three major forms that are, wet Hg (II), dry Hg (0) and particulate Hg.

Mercury (Hg) is a natural element that has existed on the planet since the earth was formed. It is mostly in the form of the ore cinnabar (mercury sulfide) and also found in its pure state. In its chemical form, mercury exists as elemental (metallic), organic (methylmercury and ethylmercury) and inorganic (Bose-O'Reilly, Mccarty, Steckling, & Lettmeier, 2010). Based on its unusual physiochemical properties, high specific gravity, fluidity at normal temperatures, electric conductivity, uniform volume expansion, toxicity-giving pesticidal activity, and ability to alloy with other metals like gold, silver, copper, etc, mercury has found widespread use in industries, hence its commercial importance. Even though mercury once released into the environment becomes exposed to several processes, including biological, chemical, and photochemical reactions (Kaiser & Olge, 1980), it circulates between major environmental compartments (air, soils and waters) until it is eventually removed from the system through deposition in deep ocean sediments and mineral soils. The total amount of mercury cycling through the land surface, oceans, and atmosphere have increased dramatically (Selin et al., 2008; Sunderland, Krabbenhoft, Moreau, Strode, & Landing, 2009).

2

Anthropogenic activities, such as mining, burning of coal, incinerators, and recycling of automobiles have elevated the levels of mercury and other elements in the environment (Clarkson & Magos, 2006). In gold mining areas, where gold is associated with sulphide minerals, in particular, arsenopyrite (FeAsS), mercury has over ten times the average crystal abundances of gold and arsenic (Kesse, 1985; Griffis, Barning, Agezo, & Akosah, 2002).

Early gold mining produced large quantities of mercury enriched tailings because of mercury amalgamation with gold (Bonzongo, Heim, Warwick, & Lyon, 1996). Tailings, along open mines passages, reckless disposal of mining waste at homes, river banks and other places allow rain to leach as it mobilizes mercury into the environment. Smaller scale mining activities, in particular, has produced a significant amount of waste matter that is enriched in mercury into the environment (Veiga, Baker, Fried, & Withers, 2006). Research conducted on the urban watershed of Anacostia in the United States of America during a normal flow shows less concentration of mercury (10 ng/L); however, this increases 3-5 times during storm flow due to high particulate loading (Mason & Sullivan, 1998). Mercury in aquatic environments raises a cause for concern as it is converted into methylmercury and become bioavailable in water, sediments and wetland soils (AMAP/UNEP, 2013). Mercury in its methyl form is a powerful neurotoxin to human, which arises due to consumption of contaminated fish tissues. Methylmercury accumulation in seafood and fish products poses severe health risks to the public and is an emergent global concern (Griesbauer, 2007). Regions where both marine and fresh water fish are important sources of protein, especially for subsistence and recreational fisheries, may be at risk, if

3

mercury becomes bioavailable and is being accumulated in the environment. Thus, Artisanal and Small Scale Gold Mining (ASGM) communities are of greater concern since bioavailability and bioaccumulation may affect the health of the indigenes (AMAP/UNEP, 2013). Average mercury levels increased in ten of eleven (90 %) fish species analysed between 2009 and 2012 including species with mercury concentrations below the international mercury reference limit indicates the aquatic ecosystems, are increasingly impacted by mercury (CAMEP, 2013). Considerable number of research shows that natural and anthropogenic activities can redistribute mercury through a complex combination of transport and transformations in the atmospheric, soil and water ecosystems. Globally, ASGM are the largest source of anthropogenic mercury emissions, followed closely by coal combustion, then non-ferrous metals production and cement production (AMAP/UNEP, 2013).

The primary mechanisms for transporting atmospheric Hg to the terrestrial and aquatic systems is through wet and dry depositions with the dry deposition being more than twofold greater than wet deposition (Schroeder & Munthe, 1998a; Pacyna et al., 2008). Elemental Hg circulates in the air for a long period of time (0.5-2 years) before depositing because of its high dispersion. The effect of Hg pollution may therefore not just be limited to the geographical location of the discharge point (local pollutant) but several kilometres radius from the point of original discharge (Harada et al., 2001; Johansson, Bergbäck & Tyler, 2001). Reactive Gaseous Mercury (RGM) and particulate mercury tend to fall out of the atmosphere more quickly than

4

elemental Hg and are more likely to deposit closer to the source from which they are emitted (Schroeder & Munthe, 1998).

Gold is a popular and well-known mineral for its value and special properties. In the quest for this precious mineral, mercury amalgamation has been the cheapest way for extraction. In any case, one hundred million people in over fifty-five (55) countries depend on ASGM, directly or indirectly, for their livelihood mainly in Africa, Asia and South America (Telmer & Veiga, 2008). This accounts for an estimated gold production between 500 to 800 tonnes per annum, representing 20 to 30 % gold production worldwide (Pacyna et al., 2008). As a result of these activities, there has been an increase in use of liquid metallic mercury in the extraction of gold (AMAP/UNEP, 2013; World Bank Group, 1998). Thus, ASGM have contibuted the largest anthropogenic intentional release of mercury worldwide (Pacyna et al., 2008). About 1,000 tons of mercury per year is released into the atmosphere by natural sources, at the same time, approximately 2,600 tones, is emitted from anthropogenic sources (Honda, Hylander, & Sakamoto, 2006). As ASGM relies on rudimentary methods and technologies with inefficient mining practices, mercury amalgamation results in the consumption and release of an estimated 650 to 1000 tonnes of mercury per annum into the environment (Pacyna et al., 2008).

Across Africa, in countries with rich mineral reserves and barren economies, thousands of the unemployed dig for fortunes functioning illegally and unregulated. These miners apply primitive extraction techniques, with dynamite, pickaxes, mercury and the strength of their arms (Harkinson, 2003). West Africa was formerly considered as having minimal ASGM in 2005 but is

now recognized as a region with considerable activity (AMAP/UNEP, 2013).

In Ghana alone, small-scale/artisanal sector employs about 300,000 people - most of whom are illiterates and employ primitive methods in mining (Amponsah-Tawiah & Dartey-Baah, 2011). Therefore, ASGM activities have become the principal anthropogenic source of environmental Hg (Hilson & Pardie, 2006). In 2003, a major newspaper, "Daily Graphic" in Ghana, reported illegal mining groups of more than 300 diverse groups, involving over 5,000 individuals on the Pra River operating from Assin Praso to Daboase. These miners operate with their self-styled floating dredging mining equipment, using mercury and other dangerous chemicals to extract the gold. These activities lead to the discharge of heavy metals into the water. In 2007, about 239,331 ounces, representing 9.6 % of total gold production, was recorded by the small-scale gold mining sector in Ghana (Bermudez-Lugo, 2008). The "rule of thumb", to obtain satisfactory recovery rates of gold indicates that for each ounce of gold in the ore, one ounce of Hg was used (Richards, 1940; Agbesinyale, 2003). At most stamp mills, 10-25 % of the mercury used in the process was lost to the environment through flouring (i.e. subdivision of the amalgam into fine particles), sickening of the mercury (formation of Hg-sulfides), and evaporative losses during retorting, and careless handling of mercury by mill personnel.

Ghana is endowed with many natural resources, especially gold, timber, industrial diamonds, bauxite, manganese, fish, rubber, hydropower, petroleum, silver, salt, limestone, rivers, etc. of which some are exploited and others not exploited. Some of the naturally occurring minerals that were discovered but not exploited are Rare Earth Elements (REEs). Monazite has

been found in some stream gravels in many parts of Ghana (Overstreet, 1967) but not yet exploited. Meanwhile, the historical value of mining in the economic development of Ghana is considerable and well documented, with the country's colonial name Gold Coast, reflecting the importance of the mining sector, particularly, the gold trade to the country (Agbesinyale, 2003; Akabzaa, 2001). Thus, an estimated 2,488 metric tons (80 million ounces) of gold was produced between the first documentation of gold mining in 1493 and 1997 (Coakley, 2003). Currently, Ghana is the second largest gold producer in Africa; the third-largest African producer of aluminium metal and manganese ore and a significant producer of bauxite and diamond (Coakley, 2003). At present, there are eleven large-scale mining companies operating eight gold mines, one bauxite, one diamond and one manganese mine, in various communities in the country (Amponsah-Tawiah & Dartey-Baah, 2011).

In Ghana, a research conducted in 2006 indicated that the average concentration of mercury in the Upper Pra (soil- 24.6 ng/g and sediment - 18.09 ng/g), lower Pra (soil- 75.6 ng/g and sediment- 25.89 ng/g) and Offin (soil- 263.8 ng/g and sediment- 23.0 ng/g) from the Pra River Basin (Donkor, Bonzongo, Nartey, & Adotey, 2006). Meanwhile, the concentrations have elevated as reported in another research with mercury in soil ranging from 0.042-0.145 µg/g; sediment ranging from 0.390-0.707 µg/g; and fish (<0.001-0.370 µg/g, $n = 6$) in the Pra River Basin (Oppong, Voegborlo, Agorku, & Adimado, 2010). In addition, Hg and Arsenic pollution was observed in soils, food crops and fish around Obuasi, a mining town and its environs. Another study on Hg contamination in water, sediment, soil and food crops in the

7

Apopre River Basin at Dumasi, a well-known artisanal gold mining town in Ghana has been carried out (Babut et al., 2003; Amonoo-Neizer, Nyamah, & Bakiamoh, 1996). The impact of mining operations in Ghana both from the large, small-scale and illegal miners are diverse and devastating, and have affected the land, water and air. Nearly all the large-scale mining companies in the country employ the open-pit method of mining in addition to cyanide heap leach operations (Amponsah-Tawiah & Dartey-Baah, 2011) and the illegal miners also known as 'galamsey' use mercury amalgamation in extracting gold. These methods used by both small-scale/artisanal miners and large-scale miners have far-reaching consequences on human health and environmental safety (Akabzaa, 2001). Thus, the small-scale/artisanal miners and the large-scale miners are the two main players in the industry.

Table 1 is a summary of studied samples reviewed for mercury (Hg) in soil, sediment, fish, and tailings in all studies across Ghana, and those at or near ASGM and Large Scale Gold Mining (LSGM) which are near mining areas or in non-mining areas (Rajaee et al., 2015). Mining activities may introduce potentially most hazardous trace metals (Ag, Au, Cd, Cr, Hg, Mn, Pb, Sb, Sn, Te, W, and Zn) to the biosphere. As, Be, Cd, Cr, Cu, Hg, Ni, Pb, Se, Tl, V, Zn, and some Lanthanides and Actinides do not correspond closely to the list of elements considered to be of great risk to environmental health (Kabata-Pendias, 2011). Approximately, every mercury compound is toxic and can be dangerous at very low levels in both aquatic and terrestrial ecosystems.

Table 1: Summaries of Studies and Samples Reviewed for Mercury (Hg) in Soil, Sediment, Fish, and Tailings in all Studies across Ghana, and those at or near ASGM and/or LSGM (mining) or in Non-Mining Areas

Type of sample	Number of studies	Number of samples	Min. - Max. (Mean)
Soil (mg/kg):			
Total	11	727	ND - 186
Mining	10	565	0.020 - 186
Non–mining	5	54	ND - 0.190
Sediment (mg/kg):			
Total	15	193*	ND - 40.85
Mining	13	140*	ND - 40.85
Non-mining	5	53	ND - 0.494
Fish (mg/kg)	15	1305	0.004 - 0.430
Tailings (mg/kg)	7	37*	0.011 - 19.3

Source: Rajaee et al., 2015

In the first decade of the 20th Century, massive alluvial mining operations were begun on several major river systems of the Gold Coast Colony, particularly the Offin, Pra, Tano, and Ankobra rivers. In recent years anthropogenic activities have introduced a significant amount of trace metals into the aquatic environment (Puig, Palanques, Sanchez-Cabeza, & Masqué, 1999). The Pra River in southwestern Ghana is a site of ongoing application of metallic mercury in prospecting gold, in the different environmental compartments in its watershed (Donkor, Bonzongo, Nartey, & Adotey, 2006). The communities along this watershed such as the Shama Ahanta East Metropolitan Assembly depend on the Pra River as a source of drinking water, either directly (unfiltered) or through waterworks situated in the area (GSS, 2001). A research performed on chemical water quality shows that heavy

metals such as lead (Pb), arsenic (As) and uranium (U) were localised to mining areas whilst elements such as aluminium (Al, 95 %) and chloride (Cl, 5.7 %) were found above the provisional guideline value across Ghana (Rossiter et al., 2010). In 2011, Water Quality Assessment (WQA) conducted in forty (40) rivers indicated that, Lake Bosomtwe (the only Lake in the Pra Basin), Twifo-Praso (a major ASGM ongoing activity in the Pra River basin) and Dunkwa-On-Offin (a major town of ASGM activity along a major tributary of Pra River, river Offin) scored below 50 (poor water quality) in the Water Quality Index (WQI) (WRC, 2011).
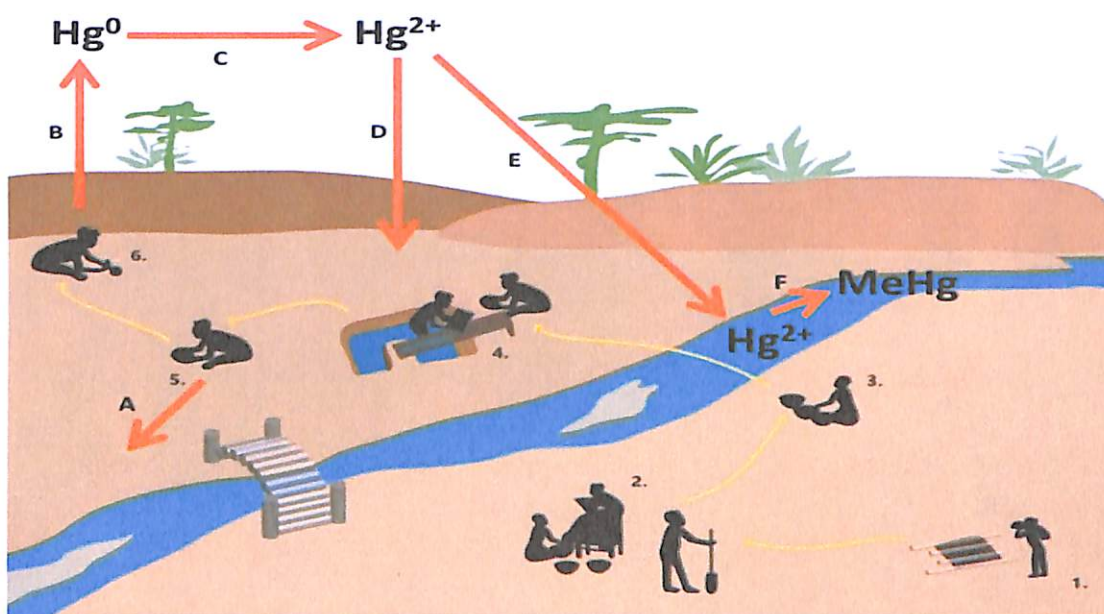
Figure 1: Mercury (Hg) cycle in a typical artisanal and small- scale gold mining (ASGM) process
Source: Rajaee et al., 2015

From Figure 1, the numbers represent key steps in the ASGM process: 1-excavation, 2-crushing and grinding, 3-shifting/shaking, 4-washing/sluicing, 5-mercury amalgamation, and 6-burning. Letters represent key steps in the mercury cycle: A-residual mercury from amalgamation may be discarded in local soil and water, B-volatilisation of elemental mercury into the

10

atmosphere, C-oxidation of elemental mercury, D-deposition onto local terrestrial systems, E-deposition onto local aquatic systems, F-methylation of inorganic mercury to methylmercury (Rajaee et al., 2015).

Fish absorbs minerals not only from their diets but also from the surrounding water via their gills and skin (AMAP/UNEP, 2013; Lall, 2002). They can accumulate substantial concentrations of trace metals like As, Be, Cd, Co, Cr, Hg, Mn, Ni, Pb, Sb, Se, in their tissues and thus can represent a major dietary source to humans through the food chain. Figure 2 illustrates the mercury cycle in the environment through anthropogenic sources through runoffs and precipitations, and then finally getting through the food chain to man.
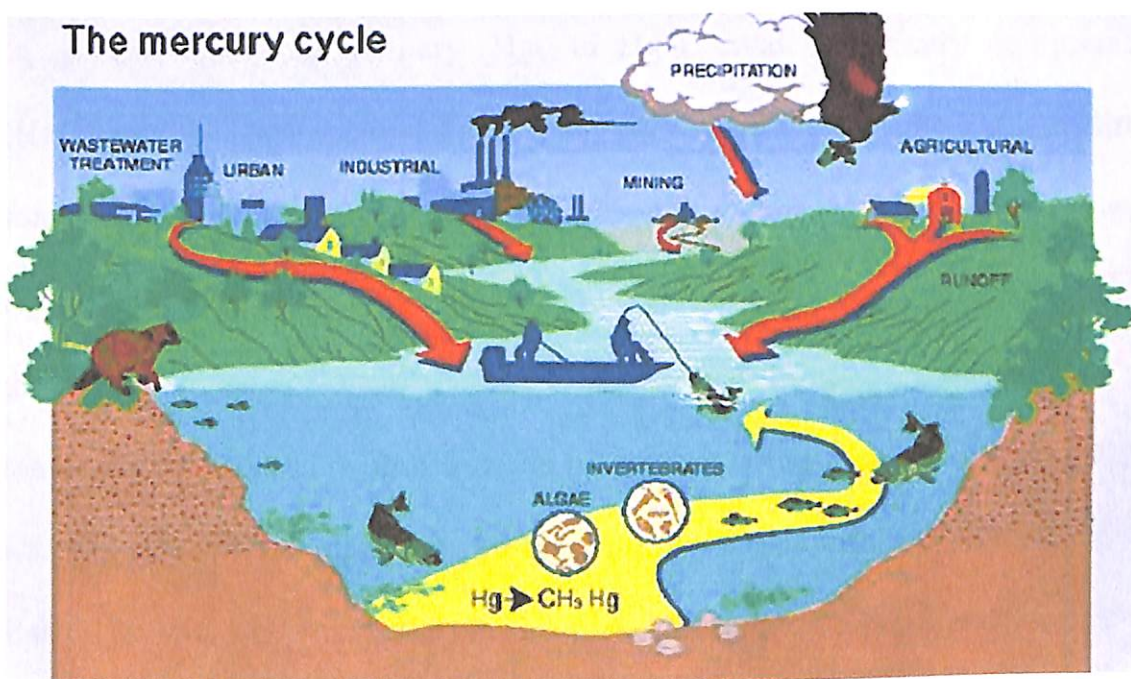
Figure 2: Mercury Cycle in the Environment and its Biomagnification as it moves through the Food Chain
Source: Connie, J. Dean, n. d

Statement of the Problem

Mercury is a naturally occurring element and may occur in soils due to the local geology of the parent material (McLean & Bledsoe, 1992). It is released into the environment through both natural or anthropogenic (intentionally or non-intentionally) sources. Mercury has unique properties which enable it to form amalgam with other elements; thus, it's used in gold amalgamation. Unfortunately, the residues of the amalgams end up been released intentionally into the environment. Among the anthropogenic sources of Hg releases, Artisanal and Small-scale Gold Mining (ASGM) activities releases the highest of 1,610 t/y of Hg (37 %) of which 727 t/y and 880 t/y are released to the air and hydrosphere respectively (UNEP/AMAP, 2013). Mercury exist in many forms, that is, organic (e.g. methylmercury), and inorganic ($HgCl_2$, HgS, HgO). Three main forms of emission of Hg exist that is, gaseous elemental mercury (Hg0 or Hg^0), divalent mercury compounds (Hg^{2+}), and particulate associated mercury (Hg-P). Together, these three forms comprise the total mercury (THg) emissions in the environment. Once Hg is released into the environment, it persistently and actively circulates in the environment for years before being buried in the ocean. Hg^0 is an atmospheric reservoir with a lifetime between 0.5 and 3 years (Bank, 2012), and can travel a distance of 2,500 km from its origin within 72 hours (Glass, Easterly, Jones, & Walsh, 1991). This makes Hg, once released, a point source pollutant which is distributed locally, regionally and globally.

Mercury once released into the environment can get into the air, soil and water bodies. It can be converted to methylmercury in soils, sediments, river water and in biota as its bioaccumulated and biomagnified through the

12

food chain to the highest trophic level in the water bodies. Fish is a good source of protein and helps in good health, however, exposure to mercury even in minute quantity may cause serious health problems and is a threat to the development of the foetus in the uterus. Mercury can cross the placenta and accumulate in the fetal tissue, thus developing foetuses are most at risk. In babies, mercury can be transferred from mother to child through breast milk. However, health effects of highly exposed populations and wildlife are also a concern (Gundacker & Hengstschläger, 2012; Driscoll, Mason, Chan, Jacob, & Pirrone, 2013). Mercury may have toxic effects on the nervous, digestive and immune systems, and on lungs, kidneys, skin and eyes (WHO, 2017). Aside health issues, impacts of Hg have been also assessed for three potential future anthropogenic Greenhouse Gas (GHG) emissions on climate change (Driscoll, Mason, Chan, Jacob, & Pirrone, 2013).

Mercury is being used extensively in gold amalgamation by ASGM activities in the Pra River Basin (Donkor et al., 2006). During ASGM activities, Hg are discriminately disposed off directly or indirectly into different compartment (air, soils, river) of the environment. A population census conducted in 2010 indicated that, the Pra River Basin has a population of about 5.8 million people, which include children and pregnant women (GSS, 2012). This populace in the Basin engage in subsistence farming coupled with commercial farming and uses the river water directly or indirectly as drinking water and other domestic activities. Also, fishing is also done in the basin for food. Meanwhile fish is the main source of protein in Ghana (Aggrey-Fynn, 2001). However, given the current crude mining process used by artisanal miners, the presence and possible accumulation of

13

mercury in the important water body, soil and air cannot be underestimated. People living in the Pra Basin are at risk of mercury pollution.

With the current boom in small scale mining along the basin, there is the need to conduct a cross-section survey to assess the rate of deposition of THg in the soils, sediments and the fish in the basin. However, this can be achieved by using validated analytical methods to ascertain the true concentration levels of Hg and its other forms in the basin. Establishing the levels of mercury and their concentration in the Pra River Basin will provide requisite information needed for management of the Basin.

Objectives of the Study

The main objective of this study is to use different analytical methods to investigate the distribution of total mercury (THg) concentrations in different compartments (soil profile, sediment core and biota along the food chain) from the Main Pra River and three of its tributaries (Anum, Birim, and Offin Rivers) and the Pra Estuary using Cold Vapour Atomic Absorption Spectroscopy (CVAAS). The specific objectives include:

➤ To identify the best acid digestion procedures which totally digest Hg from the matrix into solution, with maximum digestion yield.

➤ To validate these acid digestion procedures by using K_0 Instrumental Neutron Activation Analysis (k_0-INAA) as a validation tool.

➤ To identify potential enrichment trend of total mercury concentrations (mg/kg) in the vertical profile of soils (0-6 cm into 1 cm section) from twenty (20) sampling sites in the Pra River Basin, Ghana.

14

➤ To identify potential enrichment trend of total mercury concentrations (mg/kg) in the vertical sediments (0-10 cm into 1 cm sections) cores from twenty-one (21) sampling sites from the Pra River Basin, Ghana.

➤ To identify Hg species in some selected geological studied materials using temperature fractionation method.

➤ To obtain the bioavailability and bioaccumulation of THg and MeHg in carnivorous, and herbivorous fish muscles and skin in the trophic levels in the catchment areas using Cold Vapour Absorption Fluorescence Spectroscopy (CVAFS).

➤ To identify mineral bearing REEs deposits in the Pra River Basin using k_0-INAA method.

➤ To identify the concentration (mg/kg) levels of some selected elements that are in the topsoils (0-1 cm depth).

Significance of the Study

The findings of this study will go a long way to inform decision-makers and stakeholders including, the Ministry of Health, Ministry of Environment, Ministry of Local Government and Ministry of Energy, about:

➤ The estimated Hg released from ASGM activities into the Pra River Basin.

➤ Mining and environmental hotspots of mercury in the Pra River Basin which need immediate attention for remediation.

➤ Mercury available in the different environmental compartment in the study area to help in bioavailability control.

➤ Mercury species that has become available in the catchment area.

15

- The amount of total mercury and methylmercury in the herbivorous and carnivorous fish.

- Rare Earth Elements (REE) mineral deposits in the Pra River Basin, Ghana.

- The levels monazites $((Ce, La, Nd, Th)PO_4)$ mineral deposits in the Pra River Basin.

Scope of the Study

The main Pra River (Ghana) and its estuary (Shama and Anlo) together with its major three tributaries which include Anum, Birim, and Offin rivers, will be the main sampling sites in this research. The towns along the catchment areas are (1) Anum River Basin: Nnoboamu and Wobiri in the Ashante Region, (2) Birim River Basin: Dadientem (upstream), Kibi (upstream), Adonkrono, Kade, Akim Oda and Akim Oda (an old town downstream) all from the Eastern region of Ghana; (3) Offin River Basin: Nkontinso, Dunkwa-On-Offin (1) and Dunkwa-On-Offin (2) in the Central region of Ghana; and (4) main Pra River and Estuary: Twenedurase (upstream), Kwahu Praso (upstream), and Apreja all in the Eastern Region; Assin Praso, Twifo Praso (1) and, Twifo Praso (2) from the Central region; and Daboase, Beposo, Anlo and Shama in the Western Region of Ghana.

The Department of Fisheries and Aquatic Sciences laboratory at the University of Cape Coast, Ghana was used in preparing the fish samples for analysis of both THg and MeHg concentration. Total mercury was determined in twenty-one (21) sediment cores (0-10 cm), twenty (20) soil profile (0-6 cm) samples, carnivorous and herbivorous fish muscle and skin, "Black" and

16

special mining waste. Grid method of sampling was used for sampling the soil, whilst random sampling was employed in sampling sediment core at the bank of the rivers. Purposive sampling was used in obtiaining fish samples using fishermen in seven (7) sampling sites (Nkontinso, Dunkwa-On-Offin (1), Twifo Praso, Daboase, Anlo and Shama) along the Pra River Basin. Methylmercury was determined in both the carnivorous and herbivorous fish muscle

Sample analysis (sponsored by the ICTP/IAEA STEP programme) was done at the Environmental Science Department, Jožef Stefan Institute, Ljubljana, Slovenia. Cold Vapour Atomic Absorption Spectrometry (CVAAS), Cold Vapour Atomic Fluorescence Spectrometry (CVAFS), Lumex Atomic Spectroscopy, Temperature Fractionation using Zeeman Background correction and the Research reactor TRIGA MARK II with Hot Cell all these instruments from Environmental Science Department, Jožef Stefan Institute was used to determine trace metals in all the samples. Maestro software, k_0-software, special MS Excel, relative standardization method and mercury "GURU" was used in this research.

Limitations of the Study

Time constraint was one of the limitations encountered in this research work since the sampling sites were at four different regions (Ashanti, Central, Eastern and Western Regions) along the Pra River Basin which was far apart, therefore, enough time was needed to go through all the twenty-one (21) sampling sites in all the four (4) regions for the samples. Also, stipulated time for analysis (by sponsors) was limited since analysis for all samples was three

17

(3) months each year at the Environmental Science Department, Jožef Stefan Institute, Ljubljana, Slovenia. Finally, financial constraint was an important factor which limited the scope of this research.

Organisation of the Study

In this thesis, Chapter One deals with the introduction of the thesis. Chapter Two gives an overview of Analytical methods, the theory of Instrumental Neutron Activation Analysis and k_0-Instrumental Neutron Activation Analysis (k0-INAA), what reactors are the various types of methods for neutron activation analysis, and various types of elements under investigation. Chapter Three deals with the description of sampling sites, sampling procedure, analytical methods and the experimental work whilst Chapter Four deals with the results and discussions of the findings. Chapter Five deals with conclusion and recommendations based on the previous chapters.

Chapter Summary

Brief background information of the study has been given. The problem has been identified with the objectives to achieve the goals spelt out. Also, the scope, justification, and the importance of the research to look at the environmental issues in the Pra River Basin were also looked at. The chapter concludes with a summary of the organization of the thesis.

18

CHAPTER TWO

LITERATURE REVIEW

Introduction

The environment plays a critical role in the physical, mental and social well-being of human beings; thus, the quality of human life depends on the quality of the environment. Soil is a specific component of the biosphere which is not only a geochemical sink for contaminants, but also acts as a natural buffer controlling the transport of chemical elements and substances to the atmosphere, hydrosphere and biota. Heavy metals contamination in both soil and sediment has become a problem worldwide.

Soils can naturally have a high concentration of metals as a result of the weathering of parental material with high amounts of metal minerals or due to contamination associated with several human activities (Das, Sherameti, & Varma, 2012). Many authors have proved that increase in the level of certain metals in soils are due to anthropogenic activities such as mining, industry, traffic, agriculture and many others (Birke, Rauch, & Stummeyer, 2011; Bityukova & Birke, 2011; Flight & Scheib, 2011; Locutura & Bel-Lan, 2011; Sajn, 2003; Wei & Yang, 2010).

Mercury

Mercury with a symbol of Hg is unique among elements because it is liquid under ambient conditions and has an extraordinary low melting point as a metal (Kozin & Hansen, 2013). In its high-purity state, it is a dense, silvery-white element. This element has an atomic number of 80, relative atomic mass of 200.59, a boiling point of 356.6 °C, melting point of -38.80 °C, density of

19

13.456 g/cm^3, vapour pressure of 1.22 x 10^{-3} mm at 20 °C (2.8 x 10^{-3} mm at 30 °C) and solubility in water of 6 x 10^{-6} g per 100 ml (25 °C). Mercury is present in a large number of physical and chemical forms with an extensive range of properties. It has seven (7) stable isotopes in nature (^{195}Hg, ^{198}Hg, ^{199}Hg, ^{200}Hg, ^{201}Hg, ^{202}Hg, and ^{204}Hg) and exist in three oxidation states: elemental mercury (Hg^0), mercurous mercury (Hg$_2^{2+}$) and mercuric mercury (Hg^{2+}) (Adriano, 1986; Rice, Ambrose, Bullock, & Swartout, 1997). It also has seventeen (17) synthetic and radioactive isotopes with mass numbers ranging from185 to 206. The isotope with mass number 194 (^{194}Hg) has a half-life of 130 days, ^{203}Hg 47 days and ^{199}Hg 2.4 x 10^{-9} s. The thermal neutron capture cross-section for natural mercury is 380±20 barns (Kozin & Hansen, 2013).

Naturally, the earth crust contains approximately 0.05 mg/kg of mercury (Adriano, 1986) and diverge among deposit types (Rytuba, 2005), nevertheless, almost all production comes from the main ore mineral, cinnabar (HgS). Some of the natural sources include volcanic and geothermal emissions (Nriagu & Becker, 2003), mercury ore deposits (Rytuba, 2003), marine environments (Horvat et al., 2003), and emissions of mercury from terrestrial environments such as soil with background or elevated mercury concentrations (Gustin & Stamenkovic, 2005; Kocman & Horvat, 2010; Xin, Gustin, & Johnson, 2007). On the average mercury is present in natural soils and in uncontaminated soil at 0.1 mg/kg while areas with mercury deposit can range from 1 mg/kg to 100 mg/kg (Salminen et al., 2005) and in other places can be as higher as 1000 mg/kg or more (Health, Services, & others, 1991). The average background mercury concentration in Europe were determined for different types of soil as follows: topsoil (0.061 mg/kg), subsoil (0.035

mg/kg), humus (0.226 mg/kg) (Salminen et al., 2005). Agricultural soil and grazing soils were 0.03 mg/kg and 0.035 mg/kg respectively in Europe (Ottesen et al., 2013). In the environment, Hg is found in various chemical and physical forms, such as Hg^0, $HgCl_2$, HgO, HgS, CH_3HgCl, and $(CH_3)_2Hg$, and each species behaves differently in various ecosystems (Drasch, Böse-O'Reilly, Maydl, & Roider, 2004). To divide primary emissions between three main types of mercury/mercury compounds are Gaseous Elemental Mercury (GEM, also abbreviated as Hg0 or Hg^0), divalent mercury compounds (Hg^{2+}), and particulate associated mercury (Hg-P); together these comprise the total mercury (THg) emissions.

Metallic Mercury (Elemental mercury)

Metallic mercury also known as elemental mercury (Hg^0) is the purest form of mercury; it is referred as Hg vapour when present in the atmosphere or metallic Hg when in the liquid form. It is a shiny, silver white, odourless liquid, much heavier than water. Most natural waters are nearly saturated, or are supersaturated with respect to atmospheric Hg^0 (Hammerschmidt, Lamborg, & Fitzgerald, 2007). In natural environment it exists in gaseous or liquid state. The atmosphere is an important reservoir of Hg which mainly exists as GEM. The relatively low deposition velocity and anomalously high vapour pressure of Hg^0 at ambient conditions makes it has longer its lifetime which is between 0.5 and three (3) years in the atmosphere (Brown, Brown, Corns, & Stockwell, 2008; Bank, 2012). In the gaseous phase, the chemical processes are controlled by oxidation reactions that change Hg^0 into reactive gaseous mercury. These are representations of a mixture of gaseous divalent

21

mercuric compounds (Reactive Gaseous Mercury, RGM) and particulate mercury (mercury associated with atmospheric particulate matter, PHg) which represent mercury species bound to airborne particles (Swartzendruber & Jaffe, 2012). Important oxidants are ozone, hydroxyl radical, hydrogen peroxide, nitrate radicals and reactive halogen species which are made up of atomic, molecular and radical forms of chlorine, bromine and iodine.

The daytime oxidant, ozone, is the product of photochemical reactions which involves Volatile Organic Compounds (VOC), oxides of nitrogen (NOx), and molecular oxygen. Also, stratosphere ozone can enter the troposphere through vertical mixing (Robertson, 2006). Equation (1) is an oxidation of Hg^0 by O_3:

$$Hg^0 + O_3 \longrightarrow HgO_{(s)} + O_{2(g)} \tag{1}$$
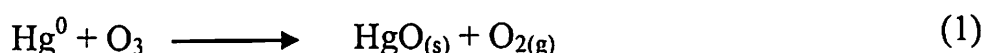
Hg might react with ozone to form an HgO_3 which is an intermediate (Pacyna et al., 2008). It is more likely that the HgO is an artefact from the decomposition of HgO_3 intermediate which is possibly an oxidation pathway via homogeneous, exothermic gas-phase reaction with HgO_3 as the primary product (Calvert & Lindberg, 2005). Limited data available suggests that the energy profile of reaction decrease with the number of the water molecule, therefore mercury oxidation processes with ozone increase with relative humidity (Vahedpour, Tozihi, & Nazari, 2011).

The hydroxyl radical can be produced from the reactions of water vapour and excited atomic oxygen, nitrous acid (HNO_2), nitric acid (HNO_3), hydrogen peroxide (H_2O_2) and peroxynitric acid (HO_2NO_2). A probable step of the reaction between the hydroxyl radical and Hg is suggested in Equation (2).

22

$$\mathrm{Hg^0_{(g)} + OH_{(g)} \longrightarrow HgOH_{(g)}} \tag{2}$$

In view of that the oxidation of $\mathrm{Hg^0}$ by $\mathrm{OH^-}$ leads to an HgOH intermediate which was found to be short-lived and susceptible to thermal decomposition. Also, the oxidation of $\mathrm{Hg^0}$ by $\mathrm{NO_3}$ is produced mostly from the reaction of $\mathrm{O_3}$ and $\mathrm{NO_2}$ which occur during the daytime by the production of this radical by photolysis of dinitrogen pentoxide ($\mathrm{N_2O_5}$) is also possible but in this instance, $\mathrm{NO_3}$ can be rapidly photolyzed. The oxidation process is presented in Equation (3)

$$\mathrm{Hg^0_{(g)} + NO_{3\,(g)} \longrightarrow HgO_{(g)} + NO_{2\,(g)}} \tag{3}$$
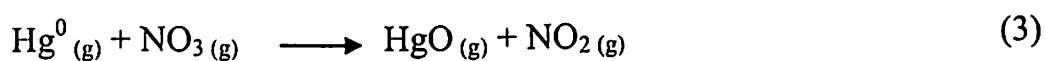
Also, Equation (4) represents the possible oxidation between $\mathrm{Hg^0}$ by $\mathrm{H_2O_2}$.

$$\mathrm{Hg^0_{(aq)} + H_2O_2 \longrightarrow Hg\,(OH)_{2\,(g,s)}} \tag{4}$$
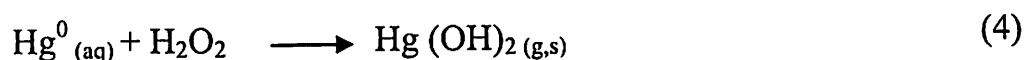
There is also an oxidation of $\mathrm{Hg^0}$ via gaseous reactive halogen species. Reactive halogen atoms, molecules and monoxides can also be formed autocatalytically from sea salt aerosols or come from the anthropogenic release of $\mathrm{NO_x}$ and halogenated compounds followed by atmospheric processing (Liu, O'Driscoll, Feng, & Jiang, 2011). Under certain conditions, their concentrations can be high enough to cause oxidation of $\mathrm{Hg^0}$. When it comes to studies about gas-phase reactions between elemental mercury and halogen species, one study has revealed that methyl iodide is nonreactive under atmospheric conditions ($k < 1.23 \times 10^{-21}$ $\mathrm{cm^3}$ $\mathrm{molecule^{-1}}$ $\mathrm{s^{-1}}$) and in a further studies, chlorine was proposed to have a relatively modest reaction rate, 4×10^{-16} $\mathrm{cm^3}$ $\mathrm{molecule^{-1}}$ $\mathrm{s^{-1}}$ and which is considered as an upper limit (Ariya, Khalizov, & Gidas, 2002).

Another oxidation is Hg^0 by means of Halogen atoms and molecules. The chemical reaction of Hg^0 with chloride ions is shown in Equation (5)

$$Hg^0_{(g)} + Cl_{(g)} \longrightarrow HgCl_{(g)} \tag{5}$$

Oxidation of Hg^0 by Br atom follows two-step processes and it is also represented by Equations (6) and (7).

$$Hg^0_{(g)} + Br_{(g)} \longrightarrow HgBr_{(g)} \tag{6}$$

$$HgBr_{(g)} + Br_{(g)} \longrightarrow HgBr_{2(g)} \tag{7}$$
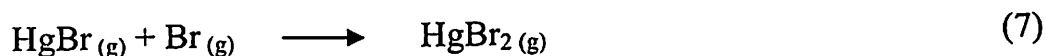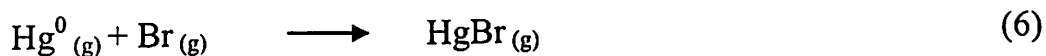
These reactions play an important role when atmospheric Hg^0 is rapidly depleted following the polar springtime sunrise. Mercury depletion match with an ozone hole at the ground driven by sunlight and bromine atoms derived from reactions of atmospheric reactive halogen gases with marine sea salt in surface snow and ice (Ariya et al., 2002). The effects and relative significance of Br and Cl atoms in mercury depletion events in the troposphere during the polar spring have been studied by Calvert and Lindberg (2005). Besides in earlier studies, only Br atoms could be a major reactant responsible for the observed Hg loss. The bromine-initiated reactions lead to formation of RGM and also reaction with Br atoms is a major and possibly the dominant global sink for Hg^0, with most of the oxidation taking place in the middle and upper troposphere (Hynes, Donohoue, Goodsite, & Hedgecock., 2008). Other studies are requisite to clarify this mechanism because it is likely that this is a key reaction both in polar mercury depletion measures and in the global Hg^0 oxidation cycle. Similarly, additional potential reactant which has been considered is the BrO radical, since in the O_3-rich troposphere the probable BrO concentration is higher than the concentration of Br. Gaseous depletion rates of Hg are strongly dependent on the initial concentrations of BrCl, as

well as rate coefficient for the BrO and Hg reaction. Mechanisms of these chemical reactions are represented by the following Equations (8) to (11)

$$Br_2 + h\nu \longrightarrow Br + Br \qquad (8)$$

$$Br + Hg \longrightarrow HgBr \qquad (9)$$

$$Br + O_3 \longrightarrow BrO + O_2 \qquad (10)$$

$$BrO + Hg \longrightarrow HgO + Br \qquad (11)$$

Also, halogen molecules (Cl_2, Br_2, and I_2) participate in the oxidation reactions which shown in Equations (12) to (14) below

$$Hg^0_{(g)} + Cl_{2(g)} \longrightarrow HgCl_{2(g)} \qquad (12)$$

$$Hg^0_{(g)} + Br_{2(g)} \longrightarrow HgBr_{2(g)} \qquad (13)$$

$$Hg^0_{(g)} + I_{2(g)} \longrightarrow Hg^{2+} + Products \qquad (14)$$
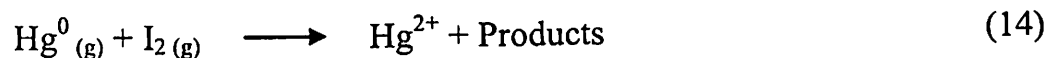
Other studies recommend that, based on the obtained kinetic data, the reactions of Hg^0 with molecular halogens are too slow to be vital in atmospheric mercury transformation. Then again, among these molecular halogen species, molecular bromine was found to react with mercury significantly faster than molecular chlorine. It was also pointed out the importance of researching into the $HgCl_2$ and $HgBr_2$ products, which formed in the halogen-initiated reactions of elemental mercury, as they are more soluble than elemental mercury hence, may be subject to bioaccumulation (Ariya et al., 2002).

Inorganic Mercury

Inorganic mercury compounds occur when mercury combines with elements such as chlorine, sulfur, or oxygen. These mercury compounds are also called mercury salts. The majority of inorganic mercury compounds are

white powders or crystals, excluding mercuric sulfide (cinnabar) which is red but turns black after exposure to light. Many salts of divalent mercury, Hg (II), are readily soluble in water, such as mercury sublimate ($HgCl_2$, 62 g L^{-1} at 20 °C), thus highly toxic. In order words, the water solubility of cinnabar (HgS) is extremely low (~10 ng L^{-1}) which is less toxic than $HgCl_2$ (Simon & Wuhl-Couturier, 2002). Free mercury ion, Hg^{2+} has a predominantly high affinity for sulfhydryl groups of amino acids such as cysteine and methionine in enzymes and this explains its high toxicity level. Thus its affinity for SeH-groups is even greater, which explains the protective role of selenium from Hg intoxication (Yoneda & Suzuki, 1997). Monovalent Hg, Hg (I), is found only in dimeric salts such as Hg_2Cl_2 (Cornelis, Caruso, Crews & Heumann, 2005). Some inorganic mercury compounds are used as fungicides. Inorganic salts of mercury, including ammoniated mercuric chloride and mercuric iodide, have been used in skin-lightening creams. Mercuric chloride is a topical antiseptic or disinfectant agent.

Organic Mercury

When mercury combines with carbon, the compounds which consist of diverse structures in which divalent Hg forms one covalent bond (R-Hg-X) or two covalent bonds (R-Hg-R) formed are called "organic" mercury compounds or organo-mercurials. There are potentially huge numbers of organic mercury compounds but the majority general organic mercury compound in the environment is methylmercury (also known as monomethylmercury). Organo-Hg cations ($R-Hg^+$) form salts with inorganic and organic acids (e.g. Chlorides and acetates) and react readily with

biologically key ligands, especially sulfhydryl groups. It also passes without any complexity across biological membranes, because the halides (e.g. CH_3HgCl) and dialkylmercury are lipid-soluble. The most key difference among these organo-Hg compounds is the stability of carbon-mercury bonds *in vivo* which varies considerably. Thus alkylmercury compounds have great resistance to biodegradation than both arylmercury and alkoxymercury compounds. The complete identity of organo-mercury compounds are not known except monomethlymercury (MMHg) cations, CH_3Hg^+, which is associated either with a simple anion, like chloride, or a large charged molecule (e.g. protein) (Horvat, 2005). Monomethylmercury compounds are exceedingly toxic and usually formed by microorganisms in sediments through bioaccumulation and biomagnification in aquatic food chains, as a result, the populace that eat fish are exposed to levels exceeding the safe level (Bank, 2012). Similar to the inorganic mercury compounds, both methylmercury and phenylmercury exist as "salts" (for example, methylmercuric chloride or phenylmercuric acetate). When pure, most forms of methylmercury and phenylmercury are white crystalline solids.

Mercury in Soil and Sediments

The soil is a very specific component of the biosphere because it not merely a geochemical sink for contaminants, but also acts as a natural buffer controlling the transfer of chemical elements and substances to the atmosphere, hydrosphere and biota. Conversely, the utmost vital role soil plays are its productivity for the survival of humans thus mankind's accountability to preserve the ecological and agricultural functions of soil.

Pollution arises when an element or a substance is present in greater than natural (background) concentrations as a result of human activity and has a net detrimental effect on the environment and its components (Kabata-Pendias, 2010). Various authors stated that soils are not considered polluted unless a threshold concentration exists that begins to affect biological processes.

Trace elements originating from a collection of sources may finally reach the surface soil, and their fate depends on soil chemical and physical properties as well as speciation. The persistence of contaminations in soil is much longer than in other compartments of the biosphere. Metals accumulated in soils are depleted bit by bit by leaching, plant uptake, erosion, or deflation (Kabata-Pendias & Pendias, 2001). In tropical rainforests, the rate of leaching of some elements in soils is greatly shorter and is calculated at about 40 years and related evaluation have clearly indicated that the complete removal of metallic contaminants from soils is nearly impossible (Kabata-Pendias, 2011). There are a number of indications that the composition of surface soil may be influenced by both local contamination and long-range transport of pollutants.

Soils have a large capacity to store Hg, and small changes in Hg dynamics can have great effects on ecosystem function biologic exposure. In the same Hg retention in soils varies depending on the sort of soil in a particular geographical area. Soil mineralogy can have an influence on the fate of Hg (Kitazume & Terash, 2013). Soils consisting of aluminosilicate minerals, such as those common in northern climates, perform differently from soils dominated by Al and Fe hydroxides, found in tropical regions.

Soil conditions such as pH, temperature and soil humic content are typically favorable for the development of inorganic Hg(II) compounds such

28

as $HgCl_2$, $Hg(OH)_2$ and complexes with soil particles of sulfur content (Rice et al., 1997). Mercury in soil and sediments arises in a number of mineral forms, in connection with oxygen, sulfur and chloride. Thus, the core Hg-related minerals in soil and sediments are cinnabar (α-HgS) and metacinnabar (β-HgS), but minerals such as montroydite (HgO), mercuric chloride ($HgCl_2$), terlinguite (Hg_2OCl), eglestonite ($Hg_3Cl_3O_2H$), corderoite ($Hg_3S_2Cl_2$), and schuetteite ($Hg_3O_2SO_4$) are also relatively abundant (Liu, O'Driscoll, Feng, & Jiang, 2012). The liquid form of mercury is also present in soils contaminated by industry from which mercury has been released into the environment.

Considering mercury (II) sulfides, metacinnabar (β-HgS) seems to be the major form in anoxic soils and sediments (Liu, Cai, O'Driscoll, Feng, & Jiang, 2012). As a consequence of the strong affinity for reduced sulfur groups, Hg^{2+} and $MeHg^{+}$ ions will be adsorbed to functional groups associated with Natural Organic Matter (NOM) and to metal sulfides (Liu, Cai, O'Driscoll, Feng, & Jiang, 2012). Hg^{2+} in soil can be simply changed into other mercury species. The reduction of Hg^{2+} to Hg^0 can be caused by bacteria and organic substances (USEPA, 1997). This reduction is mediated by humic substances and by light which is mediated by sulfate-reducing bacteria (Bouffard & Amyot, 2009). Roughly 1-3 % of total mercury in soil surfaces are methylmercury, and the other 97-99 % can be considered largely Hg(II) complexes, although a small fraction of mercury in typical soil will be Hg^0 (USEPA, 1997).

River bottom sediment is a mixture of minerals in accumulation to organic material that is deposited on the bottoms of the river channels (Taylor, 2007). In case of normal water flow, bottom sediment is repeatedly eroded or

resuspended within a channel by flowing water, so the composition of sediment is steadily changing. The chief natural sources of sediment to river are atmospheric dust deposition and wind erosion, mass movement events (landslides, debris flows, etc.) and erosion of soils by water. Within the river corridor, erosion of channel banks, floodplain deposits and resuspension of channel bed sediments add to sediments loads. Anthropogenic sources of sediment deposits consist of mines, construction sites, urban road network and mineral and organic material from point sources and industrial sites (Taylor, 2007).

Organomercury species are present in marine sediments. It is believed that monomethylmercury is the major and ubiquitous organomercury species in coastal deposits (Hammerschmidt et. al., 2007). Modern studies have shown that distribution coefficients of Hg (II) and dimethylmercury are positively correlated with the concentration of organic matter in sediments (Hammerschmidt et al., 2007).

Hg photoreduced near the surface could be bound to organic matter. On the other hand it can be produced in sediments by bacteria in a reaction linked to the mer-operon. Also, considering that sediment in a reducing environment, organic matter can reduce Hg. Studies has shown that Hg^0 concentration varies as sediment depth changes. In the first centimetre of sediment Hg^0 concentrations observed were 2.5 times higher than in the 10th centimetre. Surface sediments have newly deposited material with more organic matter while in deeper sediments the organic matter is degraded by bacteria. Also a possible explanation could be the oxygen concentration in

surface sediments which could affect sediment affinity for Hg^0 (Bouffard &

Amyot, 2009).

Effects of pH on Mercury Species in Soil

Adsorption of metals, including Hg species, onto organic and inorganic

surfaces commonly decreases with a decreasing pH because of competition of

H^+ with the metal. At a high pH, Hg may reduce the extent of adsorption onto

negatively charges surfaces, thereby resulting in a pH range of optimal

adsorption. The exact behavior of the pH-dependent adsorption of Hg,

depends on the adsorption that is adsorbate ratio (Amirbahman, Reid, Haines,

Kahl, & Arnold, 2002; Dzombak & Morel, 1990). There is an increase in the

binding of inorganic Hg and MeHg respectively, to aquatic humic substances

with pH within a range of 4 to 7, with the behavior at higher pH values

depending on the Hg that is DOM ratio (Amirbahman, Reid, Haines, Kahl, &

Arnold, 2002; Haitzer, Aiken, & Ryan, 2003). The distribution of mercury

species in soils, elemental mercury (Hg^0), mercurous ions (Hg_2^{2+}) and

mercuric ions (Hg^{2+}), is dependent on soil pH and redox potential. Both the

mercurous and mercuric Hg cations are adsorbed by clay minerals, oxides, and

organic matter. Adsorption is pH dependent, increasing with increasing pH.

Mercurous and mercuric mercury are also immobilized by forming various

precipitates. Mercurous mercury precipitates with chloride, phosphates,

carbonate, and hydroxide. At concentrations of Hg commonly found in soil,

only the phosphate precipitate is stable. In alkaline soils, mercuric mercury

will precipitate with carbonate and hydroxide to form a stable solid phase. At

lower pH and high chloride concentration, $HgCl_2$ is formed. Divalent mercury

31

also will form complexes with soluble organic matter, chlorides, and hydroxides that may contribute to its mobility (Millán et al., 2006; Sánchez-Rodas, Corns, Chen, & Stockwell, 2005).

Mercury in Biota

Mercury (Hg) is a wide spread danger to human and ecosystem health primarily due to the contamination of freshwater and marine food webs with methymercury (MeHg). In North America, MeHg in freshwater and marine fish have led the government to subject human consumption advisories on fish from thousands of individual water bodies, state or province-wide advisories, and blanket advisories for some marine fish species (Pesch & Wells, 2004). Since human and predatory fish face similar toxic risks from MeHg, the exposure and effects of MeHg are of significant concern (Wiener, Krabbenhoft, Heinz, & Scheuhammer, 2003).

The majority of Hg in soils, sediment, surface water, and atmosphere deposition is inorganic Hg (Wiener, Krabbenhoft, Heinz, & Scheuhammer, 2003). Nevertheless, only when this inorganic Hg is methylated in the environment does it become a vital toxicological risk to fish, wildlife and human. The most common organic form of Hg, methylmercury (MeHg), is of an actual concern because it is a potent neurotoxin and biomagnifies in aquatic food webs. From a toxicological point of view, the main procedure that aids in mercury entrance into coastal food webs is mercury methylation. Mercury reaches coastal habitats through river discharge into estuaries and a number of abiotic processes impact mercury cycling in tropical coastal waters (Costa et al., 2012; Muresan, Cossa, Coquery, & Richard, 2008; Paraquetti, Lacerda,

Almeida, Marins, & Mounier, 2007). Mercury methylation and its uptake by biota is of concern since the average mercury levels in biota once increased (Evers et al., 2008) and becomes concentrated in the tissues of higher trophic level (Wolfe, Schwarzbach, & Sulaiman, 1998) bioaccumulates and magnified.

Methylmercury in Freshwater Food Webs

Methylmercury in surface water and sediment simply crosses biological membranes into microscopic phytoplankton and bacteria at the bottom of aquatic food webs (Watras et al., 1998). This first step in MeHg biomagnification is where concentration increases mostly in aquatic food webs. Methylmercury also binds to organic matter in the water column and sediments. Zooplankton and benthic invertebrates consume plankton and organic matter as food, and bioaccumulate the MeHg contained in that food. Then zooplankton and the benthic invertebrates in turn, are consumed by smaller fish, which in turn are eaten by larger fishes. Thus ninety percent (90 %) of the MeHg in the fish come from dietary uptake (Hall et al., 1997; Rodgers, 1994) and any species of wildlife that consume these fishes will also contain the MeHg that the fishes has eaten and therefore bioaccumulate it. At each step going up the food web, MeHg concentrations increase in the organisms through biomagnification, often two (2) to five (5) folds in magnitude (Meili, 1997). Thus, MeHg concentration in fish can be 10^6 to 10^7 times those in the surrounding lake water (Becker & Bigham, 1995; Watras & Bloom, 1992). Not only do MeHg concentrations increase along aquatic food webs, but also the percentage of MeHg verse Total mercury (THg) also

33

increases. In two freshwater studies, the mean percentages of MeHg were 5-10 % in lake water, 15-22 % in phytoplankton, 30-40 % in zooplankton and macro invertebrates, and 95-96 % in fish (Becker & Bigham, 1995; Watras & Bloom, 1992) were observed. A small fresh water fish of approximately 10-15 cm of length naturally contain greater than 94 % MeHg (Drysdale, Burgess, d'Entremont, Carter, & Brun, 2005; Scheuhammer, Atchison, Wong, & Evers, 1998). Larger predatory fish, muscle tissue contains 40>90 % MeHg, while liver tissue contgains 40-80 % MeHg (Lasorsa & Allen-Gil, 1995). The top level of food chain in both ecosystems is fish and this is shown in Figure 3. The food of fish-eating wildlife contain a high amount of MeHg (Parsons & Percival, 2005) hence some tissues of fish eating predators contain MeHg.
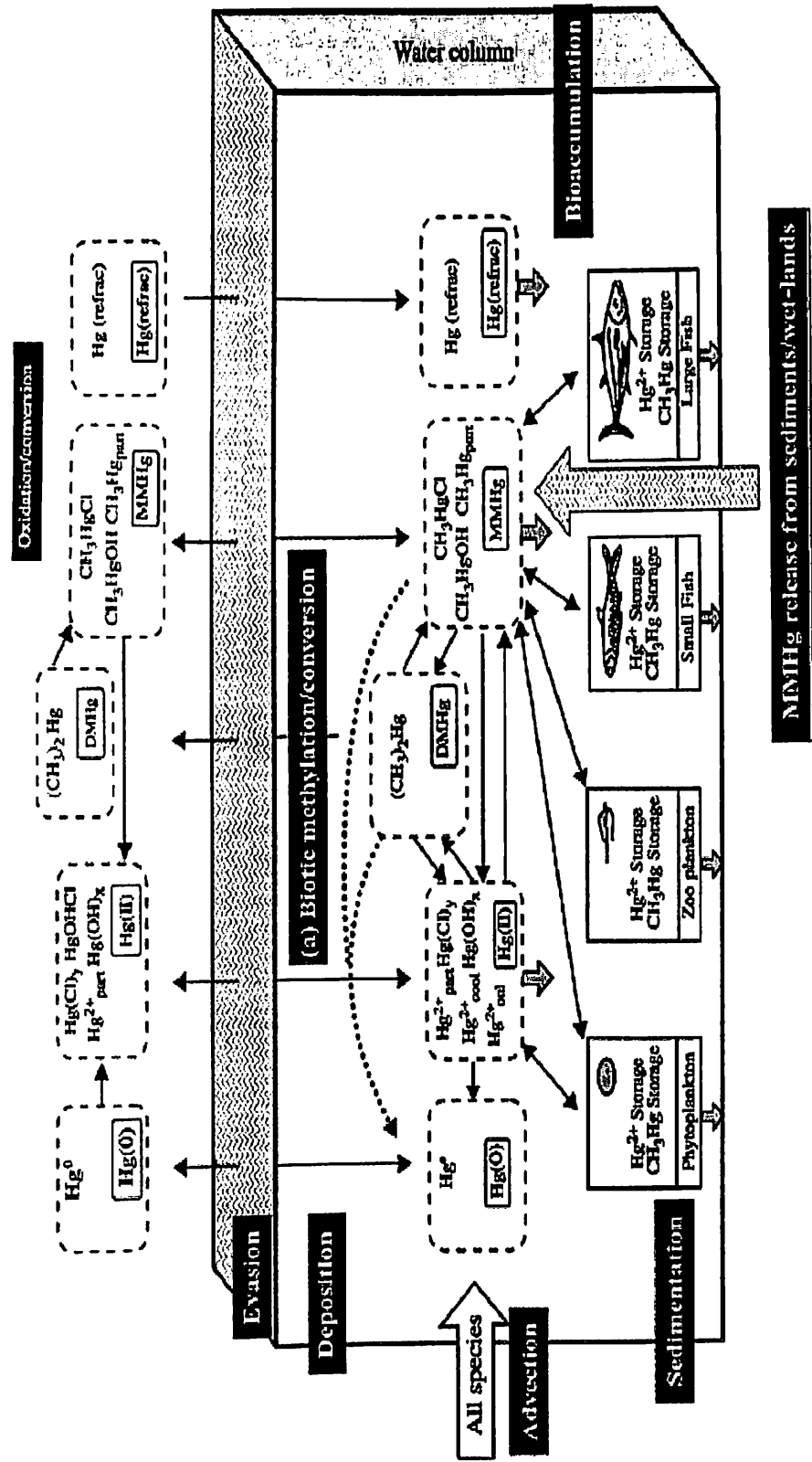
Figure 3: Generalized view of mercury biochemistry in the aquatic environment
Source: Fitzgerald & Lamborg, 2005

35
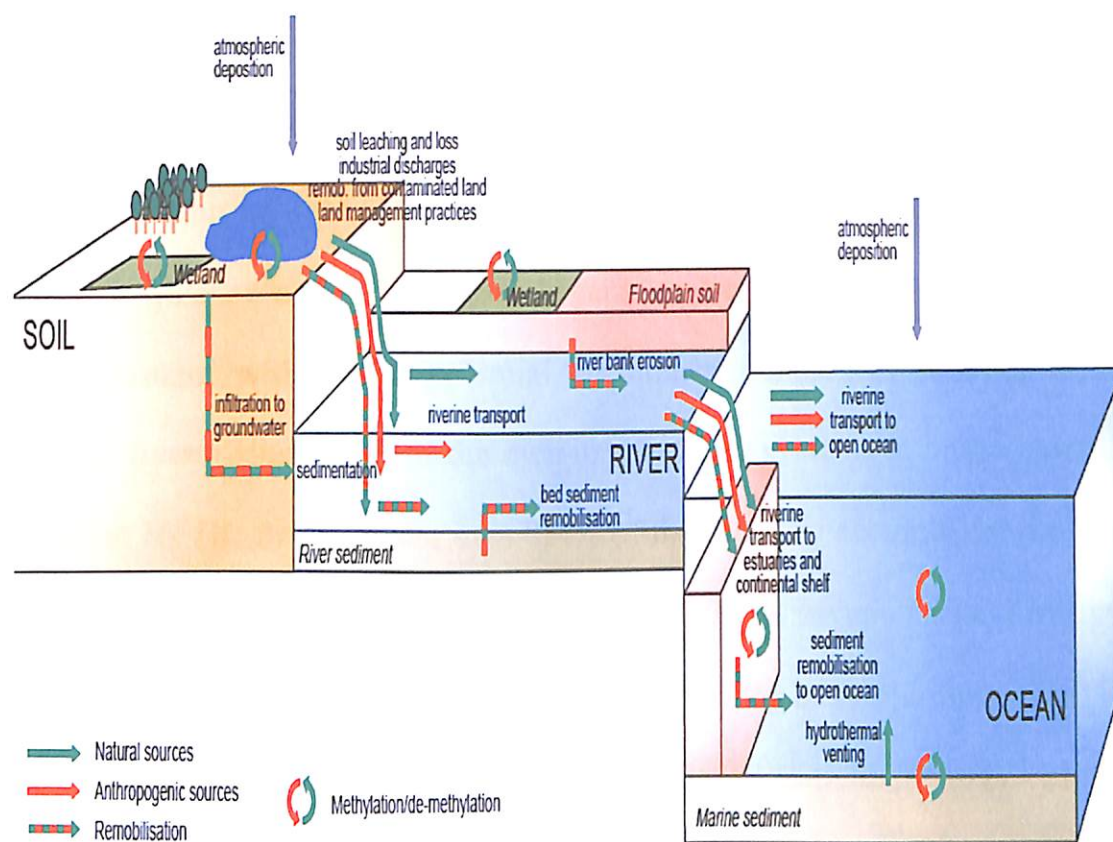
Figure 4: Transport pathways of mercury between soil and water systems and general sites of methylation/demethylation
Source: AMAP/UNEP, 2013

Mercury cycling in biota is most important process where methylation of inorganic mercury affecting the fate of mercury in aquatic systems occurs. Most of the methylmercury in biota is as a result of MeHg production in deep-sea sediments and/or hydrothermal systems (Ogrinc et al., 2007). MeHg can be formed either in biotic or abiotic processes and the possibility for biomethylation is greatest in anoxic conditions (Žižek, Horvat, Gibičar, Fajon, & Toman, 2007) with biotic production dominant. In natural environment, methylation is the result of the activity of sulfate-reducing bacteria (Rimondi, Gray, Costagliola, Vaselli, & Lattanzi, 2012) and iron-reducing bacteria (Bravo et al., 2014). In situ methylation of Hg by sulfate-reducing bacteria has been documented to result in the accumulation of MeHg in water food webs and fish (Fitzgerald & Lamborg, 2005). Migratory pelagic fish such as tuna is

36

important component of MeHg exposure and therefore any reduction in anthropogenic releases of Hg and associated deposition will result in decrease in human exposure and risk also (Soerensen et al., 2012). Mercury can enter organisms through many pathways. It can be directly absorbed from water through gills or other respiratory organs or from the food (prey) such as phytoplankton with highest potential for bioaccumulation of both Hg (II) and MeHg. Even though most of the mercury in water systems is in the inorganic divalent Hg (II) form, greater than 95 % of the mercury accumulated in fish is in the form of MeHg (USEPA, 1997). A report on seventeen (17) analysed fish muscle samples indicated more than 90 % of Hg has been methylated into MeHg (Rimondi, Gray, Costagliola, Vaselli, & Lattanzi, 2012). Migrant pelagic fish for example tuna is an important source of MeHg exposure and therefore any reduction in anthropogenic releases of Hg and associated deposition will result in decrease in human exposure and risk to MeHg (Mason, Fitzgerald, & Morel, 1994).

Health effects of Mercury

Elemental and MeHg are toxic to the central and peripheral nervous systems (WHO, 2017). The inhalation of mercury vapour can cause harmful effects on the nervous, digestive and immune systems, lungs and kidneys. Of all the organic mercury compounds, methylmercury occupies a superior position such that, large populations are exposed to it. MeHg toxicity is more than other organic mercury compounds. The inorganic salts of mercury are corrosive to the skin, eyes and gastrointestinal tract, and may stimulate kidney toxicity if ingested. Neurological and behavioral disorders may be observed

after inhalation, ingestion or dermal exposure of different mercury compounds. Symptoms include tremors, insomnia, memory loss, neuromuscular effects, headaches and cognitive and motor dysfunction. Mild, subclinical signs of central nervous system toxicity can be seen in workers exposed to an elemental mercury level in the air of 20 $\mu g/m^3$ or more for several years (Mercury, 1991).

An estimated Benchmark Dose (BMD) of MeHg of 58 $\mu g/l$, total mercury in cord blood (or 10 $\mu g/g$ THg in maternal hair) using data from the Faroe Islands study of human mercury exposures has been established (Grandjean et al., 1997). This BMD level is the lower 95 % confidence limit for the exposure level that causes a doubling of a 5 % prevalence of abnormal neurological performance that is, developmental delays in attention, verbal memory and language (Murata, Budtz-Jørgensen, & Gradjean, 2002) in children exposed in-utero in the Faroe Islands study. An average daily intake of about 1 μg MeHg per kg body weight is the tissue levels estimated intake per day (Grandjean, Cordier, Kjellström, Weihe, & Jørgensen, 2005).

Mercury Released by Artisanal and Small-scale Mining

Mercury-based artisanal and small-scale gold mining (ASGM) causes more Hg pollution than any other anthropogenic activities (UNEP, 2013). Currently, ASGM practices use large amounts of Hg, such that they constitute the most significant source of anthropogenic Hg emissions in the world (Mercury UNEP, 2013). They release estimation of Hg between 410 and 1400 tonnes of emission each year, accounting for 37 % of global Hg emissions (Kessler, 2013). In the extraction of gold from the ore by ASGM, metal Hg is

used in gold amalgamation and the amalgam is heated to evaporate the Hg to isolate the gold. In this process, huge amounts of Hg handled directly by the miners are released into the environment (Gibb, & O'Leary, 2014). In ASGM, the amalgamation process, tailings processing, and gold recovery from the amalgam result in substantial Hg which exceed 1 million kg each year released into the environment (UNEP, 2013). The primary sources of these emissions are from tailings discharge to land and water and mercury gas emissions during amalgam roasting through evaporation. In milling gold ore and Hg in trommels can result in the formation of tiny Hg droplets that become finely dispersed in the tailings which can be easily washed away and transported far from the mining site (Diringer et al., 2015; Appel & Na-Oy, 2014; Vieira & Cleaner Prod, 2006). Mercury-rich tailings can travel in rivers hundreds of kilometers from the mine (Diringer et al., 2015). The floured mercury is also difficult to recover because it does not coalesce efficiently (Appel & Na-Oy, 2014; Vieira & Cleaner Prod, 2006). These tailings may contain between 50 and 5000 mg mercury per kg ore, resulting in a substantial loss of mercury into the environment (Cordy et al., 2011; Veiga et al., 2009). In roasting, the gold amalgams are processed near the home or in gold shops in villages or cities, so the Hg vapour generated in the process affects both miners and non-miners living in these areas. Also if huge amount of Hg are exposed to a particular area, the area tends to be a point source which later distribute Hg to other areas.

Other Metals

Metals are natural constituents of the earth's crust. The haphazard human activities have drastically rehabilitated their geochemical cycles and biochemical balance. It can also be said to be referred to as any metallic element that has a relatively high density and is toxic or poisonous even at low concentration (Lenntech, 2010; Obodai et al., 2011; Yahaya, Adegbe, & wmurotu, 2012). Metals consist of the transition metals (Sc, Ti, Cr, Fe, Co, Zn, Cu, Zr, Mo, Ag, Cd, Hf, Ta, W, Au), metalloids (Ge, As, Sb), other metals (Ga, Sn), lanthanides (e.g. Ce, Ne, Sm, Eu, Te, Dy, Yb), and actinides (e.g. U, Th) (Singh, Gautam, Mishra, Gupta, & others, 2011). Amid the metals, are also noble metals (Ag, Au etc.), Alkali metals (e.g. Ga, Sn), Alkaline earth metals (e.g. Ca, Ba, Sr) and trace metals (e.g. Co, Cu, Fe, Zn, Se etc). Table 2 shows the mean background content of some metals and trace elements (Kabata-Pendias, 2011).

Even though some metals are very toxic even at a very low concentration, some are very important. Iron (Fe) plays an important roles in the behaviour of several trace element (Kabata-Pendias, 2011). It is an element that is in the transitional position between macro and micronutrients in plants, animals, and humans thus its importance (Kabata-Pendias, 2011). Aside the important role Fe plays in biological processes, goethite one of the most common occurring Fe-mineral in soils is involved in sorption processes such as: (1) absorption of metals on external surface, (2) solid state diffusion of metals, and (3) metal binding and fixation at position inside the mineral particles. This strong ability of goethite to bind selected metals might suggest

that goethite and other Fe hydroxides could be used to advance metal-polluted soils.

Table 2: Mean Background Contents of Trace Elements (mg/kg) in Surface Soils Worldwide

Element	Mean background content mg/kg (n)	Element	Mean Background content mg/kg (n)
Ag	0.003(4)	Rd	68.0 (6)
As	6.83 (4)	Sb	0.67 (5)
Au	0.13 (3)	Sc	11.7 (5)
Ba	460 (5)	Se	0.44 (4)
Br	10.0 (2)	Sm	4.60 (5)
Cd	0.41 (6)	Sn	2.50 (4)
Ce	56.7 (6)	Sr	175 (5)
Co	11.3 (6)	Ta	1.39 (5)
Cr	59.5 (6)	Tb	0.63 (5)
Cs	5.06 (5)	Th	9.20 (6)
Eu	1.40 (5)	U	3.00 (6)
Ga	15.2 (6)	W	1.70 (6)
Hf	6.40 (5)	Yb	2.60 (6)
Hg	0.07 (5)	Zn	7.00 (6)
La	27.0 (6)	Zr	267 (6)
Mo	1.1 (6)		
Nd	26.0 (6)		

Source: Kabata-Pendias, 2011

Rare Earth Elements in Soils

Rare Earth Elements (REEs) are related to the Lanthanide (LA) Series which include Yttrium and Scandium as proposed by the IUPAC (Kabata-Pendias, 2011). Lanthanides (LAs) covers the group of fifteen elements (Lanthanum-La, Cerium-Ce, Praseodymium-Pr, Neodymium-Nd, Samarium-Sm, Europium-Eu, Gadolinium-Gd, Terbium-Tb, Dysprosium-Dy, Holmium-Ho, Erbium-Er, Thulium-Tm, Ytterbium-Yb and Lutetium-Lu), of which only one, Promethium (Pm) does not occur naturally in the Earth's crust with an

exception of very small amounts in U and Th ores, while the other fourteen are relatively abundant in rocks and soils (Connelly, 2005). The terrestrial allocation of the LAs shows a universal uniqueness; their contents decrease with an increase in atomic weights, and according to the Oddon–Harkins rule, the element with the even atomic number is more frequent than the next element with an odd atomic number (Kabata-Pendias, 2011).

There are two subgroups of LAs notable Light Rare Earth Elements (LREEs), from La to Gd, and Heavy Rare Earth Elements (HREEs), from Tb to Lu. LAs are components of abundant different minerals and also are probably to be concentrated in phosphorites being incorporated in relatively common minerals such as monazite (Ce, La, Nd, Th)PO_4; bastnaside, (CeF)CO_3; cheralite, (Ce, La, Y, Th)PO_4; and xenotime, YPO_4 (Williams, Jercinovic, & Hetherington, 2007). The most abundant REEs are found primarily in the bastnaesite and monazite. Monazite occur in three different minerals (Monazite-Ce: (Ce, La, Nd, Th, Y)PO_4; Monazite-La (La, Ce, Nd,)PO_4; and Monazite-Nd (Nd, La, Ce,)PO_4). Bastnaesite typically contains LREEs and a small amount of the HREEs, while monazite also contains mostly the LREEs, but the fraction of the HREEs is two to three times larger. According to the U.S. Geological Survey, bastnaesite deposits in China and the U.S. make up the major percentage of economic rare earth resources of which China controls roughly 97 percent in the world (Hurst, 2010).

The use of LAs is relatively broad in several industries from glass production (mainly as colorants) to sophisticated electronic devices, as well as to catalytic converters, metallic alloys, rechargeable batteries, radars, fiber optics in communications, Magnetic Resonance Imaging (MRI) etc. Binding

activity of HS and particularly of DOM toward the LAs is affected by pH values with acid soils containing typically less the LAs than alkaline soils (Kabata-Pendias, 2010). Even so, the LAs contents of diverse soils are fairly analogous and indicate a strong positive relation between several LAs (mainly La, Ce, Pr, Nd, Sm) and fine soil granulometric fractions (Chojnicki, 2000). Elevated concentrations of some lanthanides (La, Ce, Sm, Eu, and Tb) originate in the air of industrial and urban areas indicate that these elements are likely to be released into the environment mainly from coal burning and nuclear energy materials processing (Kabata-Pendias, 2011). Also refining and petrochemical industries are known to be a source of LAs enrichment in ambient fine particles (Kulkarni, Chellam, & Fraser, 2006). It must be noted that REEs have a radiological impact on the environmrnt since it naturally contain an amount of U and Th (Ault, Krahn, & Croff, 2015).

Analytical Method for Total Mercury

Methods for measuring total mercury (THg) include absorption spectrometry (dithizone colorimetry), Instrumental Neutron Activation Analysis (INAA), Cold Vapour Atomic Absorption Spectrometry (CVAAS), direct analysis by thermal decomposition, and Cold Vapour Atomic Fluorescence Spectroscopy (CVAFS).

In measuring mercury using absorption spectrometry, dithizone forms a complex with the metal ions and produces a coloured (colour intensity varies with mercury concentration) organic solution. This method has been used previously because of the simplicity of the procedures, its use declined seriously with the introduction of highly sensitive atomic absorption

spectrometry in the 1960s (Akagi, Nishimura, Suzuki, Imura, & Clarkson, 1991a). In Instrumental Neutron Activation Analysis (INAA), neutrons in a nuclear reactor are irradiated and gamma radiation from generated ^{197}Hg is measured for relative quantification with the standard sample. It is the most suitable nuclear analytical technique for acquiring substantial information on the elemental composition of various environmental and biological samples. The abilities of INAA, that is, simultaneously and sequentially determinate many elements in a single sample; non-destructive assays, broad dynamic range and good sensitivity are other outstanding characteristic (Diaz, Herrera, Alvarez, & Manso, 2002) that makes INAA one of the powerful tool for validation in environmental and biological research (Janesseus et al., 1999; Gelinas, Venkatesh Iyungar, & Barnes, 1998). The detection limit is about 0.005 ng (Pfeil, 2011). CVAFS instruments are available in two configurations; one employing simple atomic fluorescence and one that employs gold amalgamation to preconcentrate mercury prior to measurement by atomic fluorescence. The detection limit via the simple fluorescence approach is about 0.2 ppt whereas using the preconcentration with fluorescence detection can be as low as 0.02 ppt (Pfeil, 2011). On the other hand, the CVAAS technique is a usually used technique for mercury trace analysis because of its simplicity, robustness, and relative freedom from interferences. In CVAAS, Hg is converted into elemental Hg vapour, which is introduced into an absorption cell and the absorption measured at 253.7 nm for determination of the quantity of mercury. A high-frequency driven electrodeless Hg low pressure discharge lamp (EDL) is used as a UV light source. This lamp generates emission lines of an extremely narrow bandwidth

44

which are congruent with the absorption lines of the Hg atoms. CVAAS is much more sensitive method as compared with CFAAS. Other advantages include its ability to measure Hg in the samples with a UV spectrophotometer or a simple Hg lamp. It is classified into the reduction/aeration procedure and the sample combustion procedure according to the generation mode for Hg in the elemental form. The former entail wet digestion with a mixture of strong acids followed by the addition of a reducing agent to generate elemental mercury vapour (Hg^0). In the latter, elemental mercury vapour (Hg^0) is generated through direct combustion of the sample to be analysed. Currently, the most common method is based on the former technique. Among these highly sensitive analytical methods, a method relating to wet digestion, reduction and CVAAS (the circulation-open air flow system) offers substantial enhancements over the conventional method.

Apart from INAA mention above all the other method of measurement needs acid digestion of the analyte into solution before measurements. To optimize the yield of the analyte, reagents play an important role in acid digestion (Mohammed, Mohammed, Mohammed, 2017) and this depends on the sample matrix and the metals being analyzed. The most effective acids used in digestions of inorganic and organic samples are HCl, H_2SO_4, HF and HNO_3 because of their strong oxidizing ability (Xiao, 2004). HF very effective for the decomposition of silicate matrices and can digest minerals, ores, stone, soil and plant (Wiltsche, & Knapp, 2014). Its strong complexation capabilities prevent the formation of sparingly soluble products of various metals and increase their solubility and stability. In order to improve

digestions, HF is usually combined with other acids like HNO_3 (Garcia, & de Castro, 2002).

Overview of Atomic Absorption Spectrometry

Atomic Absorption Spectrometry (AAS) is an analytical technique commonly used for the quantitative and qualitative determination of elements in samples such as aqueous solutions, waters, sea-waters, metals and alloys, glass, drugs, food, environmental samples, industrial wastes, biological samples among others. This technique is based on measuring the amount of electromagnetic energy of a particular wavelength (ultraviolet or visible region), which is absorbed as it passes through a cloud of atoms of a particular chemical element (the analyte) coming from samples and standards. An appropriate mathematical treatment allows relating the amount of absorbed energy to the number of absorbed atoms by providing a measurement of the element concentration in the sample. This technique is established, relatively quickly, economically affordable and allows to determine more than 60 chemical elements from a huge type of samples. AAS techniques are used by most of research laboratories and industry quality control around the world in determing analyt in a wide range of samples.

Basic Principles of Atomic Absorption Spectroscopy

(1) Wave-particle duality of Light

Electromagnetic radiation is a form of energy described by classical physics as a wave made up of mutually perpendicular, fluctuating electric and magnetic field that propagates at a constant

46

speed. It is characterized by wavelength (λ), and frequency (v). The speed of light propagated in a vacuum is C = 299.792.458 m s^{-1}. This model explains the energy propagation, but cannot explain its interaction with the matter. That interaction can be explained if we treat energy as a particle, called photon. A photon is characterized by frequency and wavelength and can transfer an amount of energy which is represented in equation (16)

$$E = hv = hc/\lambda \qquad (16)$$

where h is planck constant ($4.135667516 \times 10^{-15}$ eV s or 6.63x10-34 J.s), c is the speed of light, v is the frequency and λ is the wavelength.

Electromagnetic spectrum is appropriately divided in wavelength rates with specific names (from gamma rays to radio waves). The visible region of light between 400 and 700 nanometers (nm) is directly detected by the human eye and perceived as visible light (1 nm = 10-9 m).

(2) The atom, energy of a quantum state and electronic transitions.

An atom consisting of a nucleus containing protons and neutrons surrounded by a cloud of electrons which are inhabit in a specific regions in space known as an orbital. The further an orbital gets from the nucleus, the more they gain potential energy associated to a determined orbital. In Quantum Mechanics, orbitals have quantized energy levels and to move an electron to another level, it has to receive or emit the exact amount of energy corresponding to the difference between the two electronic levels in equation (17)

47

$$\Delta E = E_1 - E_0 \qquad (17)$$

The amount of energy required to move an electron from energy level E_0 to energy level E_1 can be provided by heat due to a collision with other particles or absorb the energy of a photon. In this case, the energy of a Photon should be equal to the difference between the orbitals (ΔE), this is, and only a Photon of a particular wavelength is absorbed and can promote that transition. This phenomenon is known as atomic absorption. A more stable electron configuration of an atom is the one with less energy, also known as ground state configuration. The difference of energy between the last full orbital and the next empty orbital of the atom in a ground state is of the same order of magnitude of photons with wavelengths between 200 and 800 nm, this means, photons in ultraviolet regions and visible light of electromagnetic spectrum.

Theoretical concepts of Atom and Atomic Spectroscopy

Atomic spectroscopy has generated three techniques for analytical use: atomic emission, atomic absorption, and atomic fluorescence. The atom is made up of a nucleus surrounded by electrons with each element having a specific number of electrons which are associated with the atomic nucleus in an orbital structure which is unique to each element (Beaty & Kerber, 1993). The electrons occupy orbital positions in an orderly and predictable way. In most stable electronic configuration of an atom, the lowest energy level is known as the "ground state", is the normal orbital configuration for an atom. The right magnitude of energy is applied to an atom in the ground state and an outer electron will be promoted to a less stable configuration or "excited state" and this state is unstable. The unstable atom will immediately and

spontaneously return to its ground state configuration, and a radiant energy equivalent to the amount of energy initially absorbed in the excitation process will be emitted. This process is shown in Figure 5.

EXCITATION   **DECAY**

(1) Energy + Ground State Atom → Excited State Atom   (2) Excited State Atom → Ground State Atom + λ Light Energy
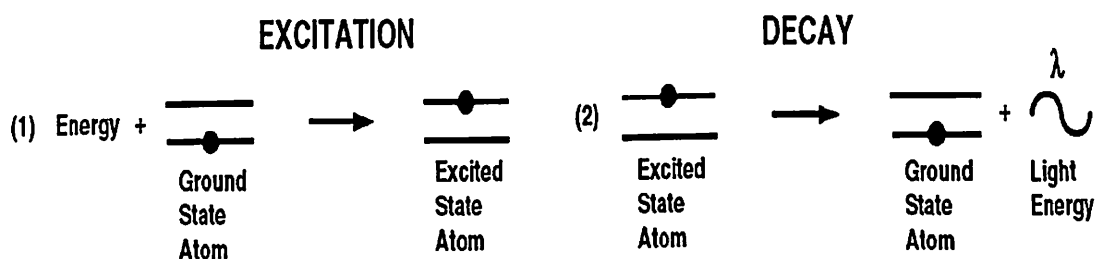
Figure 5: Excitation and Decay Process of an Atom
Source: Beaty & Kerber, 1993

The wavelength of the emitted radiant energy is directly associated to the electronic transition which has occurred. Meanwhile every element has a unique electronic structure with unique wavelength of light emitted which is a unique property of each individual element (Beaty & Kerber, 1993). As the orbital configuration of a large atom may be complex, there are many electronic transitions which can occur, each transition resulting in the emission of a characteristic wavelength of light, is shown in figure 6.

EXCITATION   **EMISSION**

Excited States / Ground State

Excited States / Ground State $\lambda 3$ $\lambda 2$ $\lambda 1$ Light Energy
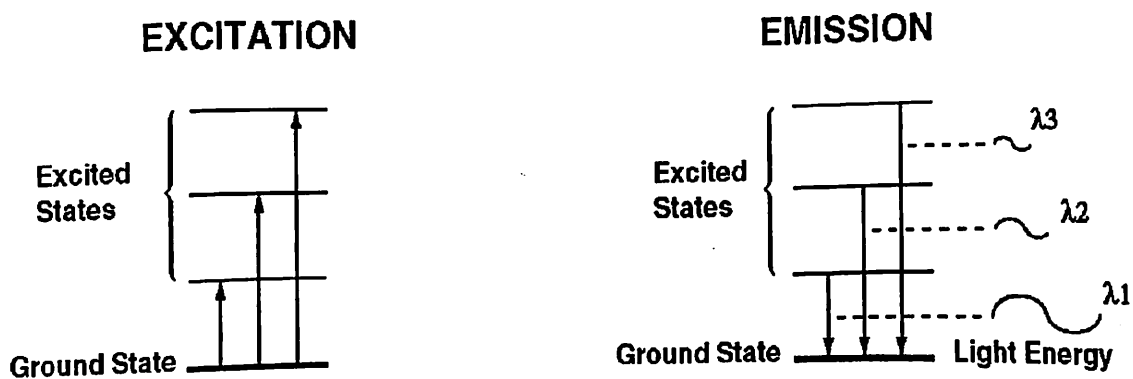
Figure 6: Energy transitions of an atom from the excited state to the emission state
Source: Beaty & Kerber, 1993

49

The method of excitation and decay to the ground state is involved in all the three fields of atomic spectroscopy. Either the energy absorbed in the excitation process or the energy emitted in the decay process is measured for analytical purposes. In atomic emission, a sample is subjected to a high energy, thermal environment in order to produce excited state atoms, capable of emitting light. The energy source can be an electrical arc, a flame, or more recently, plasma. The emission spectrum of an element exposed to such an energy source consists of a collection of the allowable emission wavelengths, commonly called emission lines, because of the discrete nature of the emitted wavelengths. This emission spectrum can be used as a unique characteristic for qualitative identification of the element. Atomic emission using electrical arcs has been widely used in qualitative analysis. Emission techniques can also be used to determine how much of an element is present in a sample. For a ''quantitative'' analysis, the intensity of light emitted at the wavelength of the element to be determined is measured. The emission intensity at this wavelength will be greater as the number of atoms of the analyte element increases. In many radiation/matter interactions, it is useful to emphasize the particle nature of light as a stream of photons or quanta (Skoog, West, Holler, Crouch, 2013). We relate the energy (Equation 16) of a single photon to its wavelength, frequency, and wave number.

Cold Vapor Atomic Absorption

Since atoms for most Atomic Absorption (AA) elements cannot exist in the free ground state at room temperature, heat must be applied to the sample to break the bonds binding the atoms into molecules (Beaty & Kerber,

1993). The only notable exception is Hg, the only metallic element with vapour pressure as high as 0.0016 mbar at 20 °C, which corresponds to a concentration of approximately 14 mg/m^3 of atomic Hg in the vapour phase (Welz & Sperling, 1999). Free Hg atoms exist at room temperature and can be measured by atomic absorption without heating cell (Csuros & Csuros, 2016). Therefore Hg can be directly be determine by Atomic Absorption Spectrometry (AAS) without an atomizer. In the cold vapour mercury technique, Hg is chemically reduced to the free atomic state by reacting the sample with a strong reducing agent like stannous chloride or sodium borohydride in the closed reaction system (Csuros & Csuros, 2016). The procedure is based on the absorption of radiation at 253.7 nm by the mercury vapour (Csuros & Csuros, 2016). The sensitivity of the cold vapour technique is far greater than can be achieved by conventional flame AA. This improved sensitivity is achieved, first of all, through a 100 % sampling efficiency (Zhang, 2007). Hallmarks of this method consist of detection limits in the single-digit parts-per-trillion (ppt) range, a dynamic range of 2-3 orders of magnitude, and an abundance of analytical methods that allow for the measurement of mercury in almost any sample matrix (Pfeil, 2011). The detection limit for mercury by this cold vapour technique is approximately 0.02 mg/L.

Mercury Speciation

Speciation is the identification and quantitation of the individual physicochemical forms of an element in a sample that together constitute its total concentration. It is well known that the various chemical forms (organic

and inorganic) of mercury in the natural environment behave differently, thereby affecting its biogeochemistry and toxicity to organisms. Mercury speciation is an analytical procedure that separates and measures the different forms (species) of mercury that are present in a sample. The development of analytical techniques able to differentiate the difference between inorganic and organomercury species has been a most important research area for scientists dealing with mercury in the environment. Principally, chromatography (Gas Chromatography (GC) and High-Performance Liquid Chromatography (HPLC))-based AFS, and purge and trap-based AFS are the two mainly widely used techniques for measuring inorganic and different forms of organomercury compounds, especially MeHg. Also, various Hg compounds are present in solid samples which and in present times are determined with various methods such as the leaching test (Issaro, Abi-Ghanem,& Bermond, 2009; Biester, & Schlz, 1999) and thermal fractionation (Coufalík, Zvěřina, & Komárek, 2014: Rumayor, Diaz-Somoano, Lopez-Anton, & Martinez-Tarazona, 2013; Coufalík, Krásenský, Dosbaba, & Komárek, 2012; Wu, Uddin, Nagano, Ozaki, & Sasaoka, 2011; Rallo, Lopez-Anton, Perry, & Maroto-Valer, 2010; Murakami, Uddin, Ochiai, Sasaoka, & Wu, 2010; Navarro, Cañadas, Martinez, Rodriguez, & Mendoza, 2009; Issaro, Abi-Ghanem, & Bermond, 2009; Do Valle, Santana, & Windmöller, 2006; Raposo, Windmöller, & Durao Jr., 2003; Milobowski, Amrhein, Kudlac, & Yurchison, 2001; Biester, & Scholz, 1996; Windmöller, Wilken, & Jardim, 1996). Hg compounds have different properties, including different vapour pressures at different temperatures and these properties of Hg can be used to know the

thermal stability of various Hg species in solid samples (Milobowski, Amrhein, Kudlac, & Yurchison, 2001).

Atomic Fluorescence Spectrometry Instrumentation

Atomic fluorescence Spectrometry (AFS) is a process which is centered on the absorption of radiation at a precise wavelength. In this technique, an atomic vapour with successive detection of radiationally deactivated states via emission in a direction in a typical orthogonal to the excitation state. Together, the absorption and the successive atomic emission processes occur at a wavelength which is characteristic of the atomic species present. AFS is a very sensitive and selective method for the determination of a number of environmentally and biomedically important elements such as mercury, arsenic, selenium, bismuth, antimony, tellurium, lead and cadmium. It is a well known technique in the determination of merthylmercury (CH_3Hg) in a varieties of samples (Cai, 2000). The key types of atomic fluorescence are resonance fluorescence, direct line fluorescence and stepwise line fluorescence. Resonance fluorescence happens when atoms absorb and re-emit radiation of the similar wavelength (Cai, 2000). Direct line fluorescence is quenched when an atom is excited from the ground state to a higher excited electronic state and then undergoes a direct radiational transition to a metastable level above the ground state. However, line fluorescence occurs when the upper energy levels of the exciting and the fluorescence line are different. The excited atoms may undergo deactivation, usually by collisions to a lower excited state rather than return directly to the ground state (Sanchez-Rodas, Corns, Chen, & Stockwell, 2010). The intensity of

fluorescence radiation depends on the intensity of the excitation source, concentrations of the atoms (atomiser), quantitative efficiency of the process, and the extent of any self-absorption in the atomiser. The fluorescence radiation is linearly dependent on the source radiation and the fluorescence quantum efficiency of the transition as long as saturation is avoided. The atomic concentration is low if, the fluorescence signal differs linearly against the total atomic concentration (Sanchez-Rodas, Corns, Chen, & Stockwell, 2010). Additionally, AFS intensity is proportional to the concentration of analyte in the sample and the optical efficiency of the instrument industry. The solid angles used for excitation and collection of radiation. The stated disadvantages of atomic fluorescence are quenching and interferences. In the quenching, excited atoms collide with other molecules in the atomisation sources. An additional disadvantage of "generic" AFS is source scatter and atomizer emission causing spectral interferences. These are then minimal when Hybride Generation (HG) and CV are used (Wang & Mulligan, 2006).

The rudimentary layout of an AFS instrument is related to AAS except for the light source and detectors are placed at right angles. Instruments for AFS can be classify into dispersive and non-dispersive, depending on wavelength selection. Dispersive instruments require a low resolution monochromator if a line radiation source is employed but in nondispersive instruments monochromators are not employed. In nondispersive instruments, interferences are bound to occur, due to stray light and background emission from the atomizer (Lajunen & Perämäki, 2004). This can be minimized by using a filter that allows a defined bandwidth to reach the detector. In most AFS systems wavelength selection is achieved using a filter located between

the source and the detector. Figure 7 shows a schematic diagram of the continuous flow vapour/hydride generator and optical configuration of an AFS system for mercury analysis.
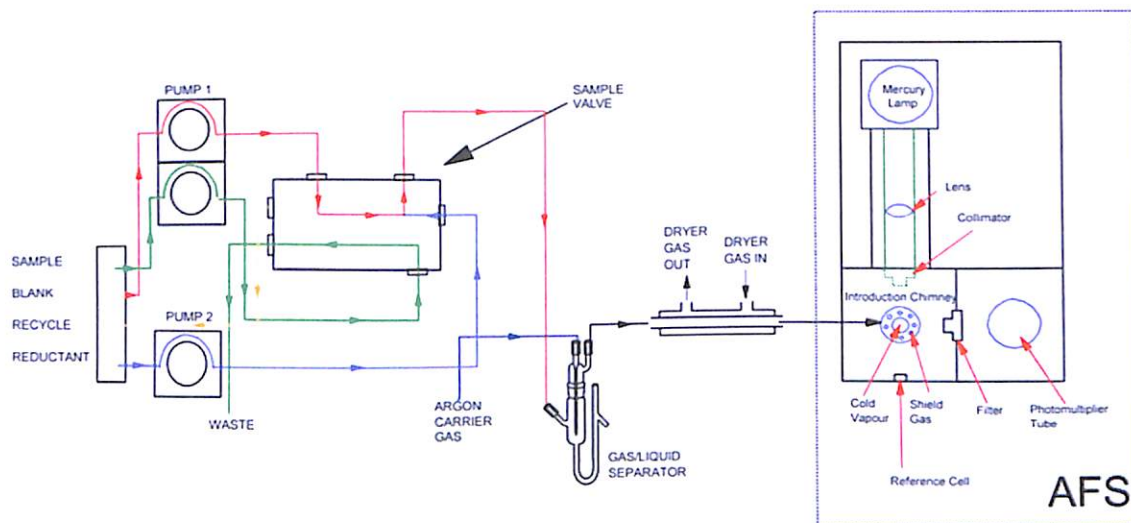
Figure 7: Schematic diagram of the Continuous Flow Vapour/Hydride Generator and Optical configuration of an AFS System for Mercury Analysis
Source: Sanchez-Rodas, Corns, Chen, & Stockwell, 2010

Mercury Arc Lamps

The mercury arc lamp is a type of vapor-discharge lamp that forms simple, robust sources of line spectra (Skoog et al., 1998). The low-pressure mercury-vapor lamp equipped with a fused-silica window has been the most common source for filter fluorometers. This source produces intense lines at 254, 366, 405, 546, 577, 691, and 773 nm. Individual lines can be isolated with suitable absorption or interference filters. The mercury lamp has been used in commercially available instruments with a 254-nm filter for mercury analysis (PSA, 1997).

Photomultiplier

The photomultiplier is an extremely sensitive light detector providing a current output proportional to light intensity it received. Photomultipliers are used to measure any process which directly or indirectly emits light. Some of the advantages of photomultiplier are large area light detection, high gain and the ability to detect single photons. Figure 8 is a diagram showing how photomultiplier works.
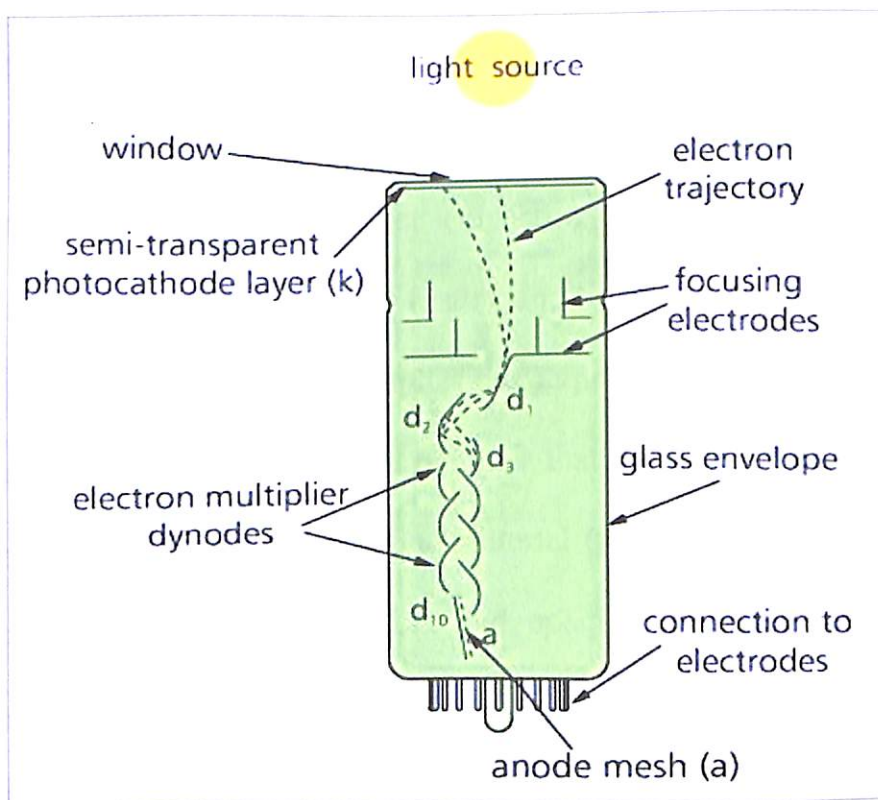
Figure 8: How the Photomultiplier Works

The photomultiplier detects light at the photocathode (k) which emits electrons by the principles of photoelectric effect. These photoelectrons are electrostatically accelerated and focused onto the first dynode (d_1) of an electron multiplier. On impact each electron liberates a number of secondary electrons which are in turn, electrostatically accelerated and focused onto the next dynode (d_2). The process is repeated at each subsequent dynode and the secondary electrons from the last dynode are collected at the anode (a). The

56

ratio of secondary to primary electrons emitted at each dynode depends on the energy of the incident electrons and is controlled by the inter-electrode potentials. By using a variable high voltage supply and a voltage divider network, to provide the inter-electrode voltages, the amplitude of photomultiplier output can be varied over a wide dynamic range.

A photomultiplier converts light into an electrical signal using the process of photoelectric effect, then amplifies that signal to a useful level by emission of secondary electrons. Figure 9 shows the essential elements of a photomultiplier: a photocathode which converts light flux into electron flux; an electron-optical input system which focuses and accelerates the electron flux; an electron multiplier consisting of a series of secondary-emission electrodes (dynodes); and, finally an anode which collects the electron flux from the multiplier and supplies the output signal. The photoemission is due to a fraction of the incident photons that impart all their energy to bonded electrons of the photocathode material (photoemissive semiconductor of two main kinds—semi transparent and opaque cathodes), giving some of them sufficient energy to escape. If the number of these photoelectrons that strike the first dynode is n_k, and the gain of the dynode is g_1, the number of resulting secondary electrons is $n_k g_1$. Then, if the second dynode has a gain g_2, it in turn emits $n_k g_1 g_2$ electrons. The process repeats from dynode to dynode up to the anode where the electrons are finally collected. If N is the number of dynodes, the number of electrons collected is shown in Equation (18)

$$n_a = n_k \prod_{i=1}^{N} g_i \tag{18}$$

The current amplification M is represent in Equation (19)

$$M = \frac{n_a}{n_k} = \prod_{i=1}^{N} g_i \tag{19}$$

The electrons are accelerated and focused by electric fields between the dynodes. The required potential gradients usually being obtained from a voltage divider across the terminals of a high-voltage supply.
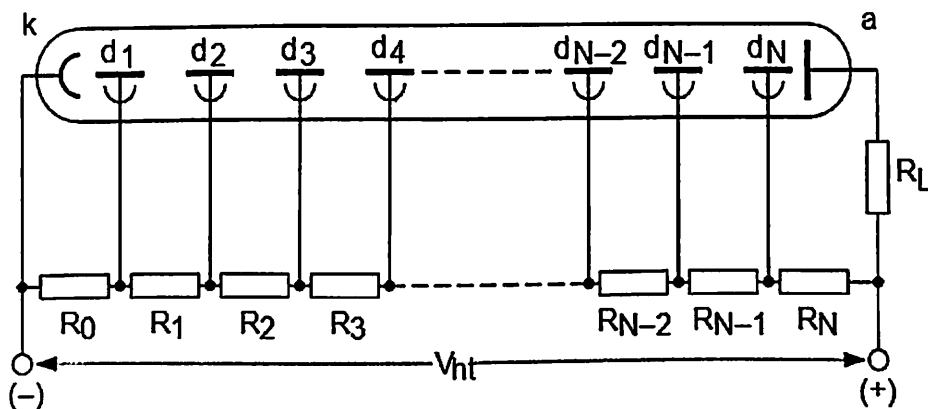
Figure 9: Voltage divider high tension supply
Source: Flyckt & Marmonier, 2002

The Zeeman Effect

Electrons in atoms can be characterized by a unique set of discrete energy states. When excited through heating or electron bombardment in a discharge tube, the atom is excited to a level above the ground state. When returning to a lower energy state, it emits the extra energy as a photon whose energy corresponds to the difference in energy between the two states. The emitted light forms a discrete spectrum, reflecting the quantized nature of the energy levels. In the presence of a magnetic field, these energy levels can shift. This effect is known as the Zeeman effect.

Qualitatively, in an atomic energy state, an electron orbits around the nucleus of the atom and has a magnetic dipole moment associated with its angular momentum. In a magnetic field, it acquires an additional energy and consequently the original energy level is shifted. The energy shift may be positive, zero, or even negative, depending on the angle between the electron magnetic dipole moment and the field. Due to the Zeeman effect, some

degenerate atomic energy levels will split into several levels with different energies. This allows for new transitions which can be observed as new spectral lines in the atomic spectrum. In quantum mechanics, a shift in the frequency and wavelength of a spectral line implies a shift in energy level of one or both of the states involves in the transition. The Zeeman effect that occurs for spectral lines resulting from a transition between singlet states is called the normal effect, while that which occurs when the total spin of either the initial or final states, or both is nonzero is called the analogous effect (Steane A., 2002).

Normal Zeeman Effect

The spin of a singlet state is zero, whilst the total angular momentum **J** is equal to the orbital angular momentum **L**. In an external field, the energy of the atom changes because of the energy of its magnetic moment in the field, which is given by equation (20)

$$\Delta E = -\mu . B = \mu_z B \qquad (20)$$

where the z direction is defined by the direction of B and $\mu_z = -m_\ell \mu_\ell = -m_\ell (e\hbar/2m_\ell)$, then ΔE becomes $\Delta E = + m_\ell \ (e\hbar/2m_\ell) B = m_\ell \mu_B B$

Since there are $2\ell + 1$ values of m_ℓ, each level splits into $2\ell + 1$ levels. Figure 10 shows the slpitting of the levels for the case of a transition between a stete with $\ell = 2$ and one with $\ell = 1$. The selection rule $\Delta m_\ell = \pm 1$ restricts the number of possible lines to the nine shown in the Figure 10.

Energy   No magnetic field   Magnetic field present
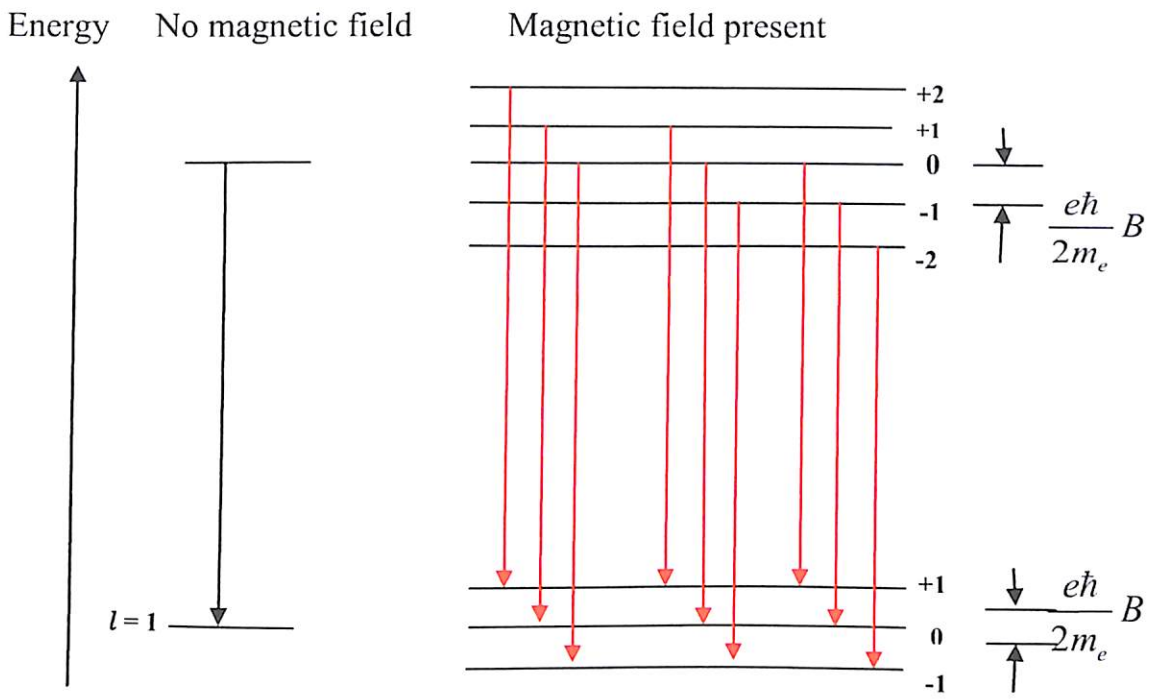
Figure 10: Zeeman Effect Splitting of Levels due to an External Magnetic Field

Thus, because of the uniforminity in th splitting in the levels, there are only three different transition energies, that is $E_0 + e\hbar/2m_e$, E_0, and $E_0 - e\hbar B/2m_e$, which correspond to the transitions with $\Delta m_\ell = +1$, $\Delta m_\ell = 0$ and $\Delta m_\ell = -1$. There will be these energies for the initial and final values of ℓ and changes in the frequency of the emitted spectral lines is the energy change divided by h. The frequency changes are therefore $\pm eB/2m_e$ or 0.

The Anomalous Zeeman Effect

The normal three-line Zeeman Effect is not commonly observed in practice. When a spectrometer with high resolution is used, it is often found that, the magnetic field splits the spectral lines into more that three components and the splitting increases more rapidly with applied field (Bohr

& Mottelson, 1969). In addition to the orbital angular momentum, electrons possess spin angular momentum S with quantum number $s = 1/2$. The total angular momentum of the electron is represented by equation (21)

$$J = L + S \tag{21}$$

Equation (21) corresponds to the total angular momentum quantum number which is given by the standard rules of addition of angular momenta thus $j = l + s, l + s - 1, ..., | l - s$. L is the the orbital angular momemtum and S is the spin of an atom. The total angular momemtum is presented in equation (22)

$$\mu = -g_l \mu_B \frac{L}{\hbar} - g_s \mu_B \frac{S}{\hbar} \tag{22}$$

where $g_l = 1$ and $g_s = 2$, we have equation (23)

$$\mu = -\frac{\mu_B}{\hbar} \left(L + 2S \right) \tag{23}$$

Each energy level split into $2j + 1$ levels corresponding to the possible values of m_j. In the case of thte singlet levels in the normal effect, the Zeeman splitting of these levels depends on j, ℓ, and s, and in general there are more than three different transition energies due to the fact that the upper and lower states are split by different amounts. The level splitting, that is, the energy shift relative to the position of the no-field energy level, can be written as equation (24) where g is called the Landé g factor (Fawcett, 1990).

$$g = 1 + \frac{j(j+1) + s(s+1) - \ell(\ell+1)}{2j(j+1)} \tag{24}$$

When s = 0, j = 1, and g = 1, equation (24) gives the splitting in the normal Zeeman effect. If the external magnetic field is sufficiently large, the Zeeman

slitting is greater than the fine structure splitting. If B is large enough, the Zeeman splitting is given by equation (25)

$$\Delta E = \left(m_\ell + 2m_s \right) \left(\frac{e\hbar B}{2m_\ell} \right) = \left(m_\ell + 2m_s \right) \mu_B B \qquad (25)$$

Neutron Activation Analysis

Activation analysis refers to the identification and quantitative determination of radionuclides produced from a target element. This is a nuclear technique that is used in determining the concentrations of elements in a wide variety of materials. Due to its high sensitivity and accuracy, simultaneous multielement analytical capability it used in wide fields of research (Menezes, Sabino, Amaral, & Maia, 2000; Lin & Henkelmann, 2003; Rahn & Sturdivan, 2004; Zaichick, 2006). Depending on the type of elements to be examined, one can use neutrons, charged particles or photons in bombarding the element in the samples. When neutrons are employed the technique is known as Neutron Activation Analysis (NAA).

In NAA naturally occurring stable isotopes of most elements in the samples are excited by neutron capture to intermediate state which de-excite by emitting prompt γ-ray in 10^{-14} sec after its formation. The radioactive product (that is, to become radioactive isotopes) then decays via α, β, γ or delayed gamma ray emission processes. This γ ray, which is emitted later, is known as delayed γ ray. The emitted α, β, γ rays are monitored to obtained both qualitative and quantitative analytical information.

In trace analytical work if no chemical separation is done to treat the samples before or after irradiation the process is called Instrumental Neutron

Activation Analysis, (INAA). In this technique, samples are simply packaged, irradiated for the specified length of time, allowed to decay, then counted, and the element results verified and reported. This type of NAA is as a result of increasing the probability of the required reaction between the neutron and target nucleus of analyte and to limit the formation of undesired activities of matrix (Kučera & Zeisler, 2004). Different types of reactors and different positions within a reactor (inner or outer core) can differ considerably with regard to their neutron energy distributions and fluxes due to the materials used to moderate or reduce the energies of the primary fission neutrons. Nevertheless, most neutron energy distributions are quite broad and consist of three principal components that is thermal at 20 °C 0.026 eV 2200 m/s, epithermal < 1 MeV > 0.026 eV, and fast > 1 MeV (Ehmann & Vance, 1991). When a neutron interacts with the target nucleus via a non-elastic collision, a compound nucleus forms in an excited state. The excitation energy of the compound nucleus is due to the binding energy of the neutron with the nucleus. The compound nucleus will almost instantaneously de-excite into a more stable configuration through emission of one or more characteristic prompt gamma rays. In several cases, this new configuration yields a radioactive nucleus rays, but at a much slower rate according to the unique half-life of the radioactive nucleus. Depending upon the particular radioactive species, half-lives can range from fractions of a second to several years. Figure 11 shows the process of neutron capture which follows the emission of gamma rays.
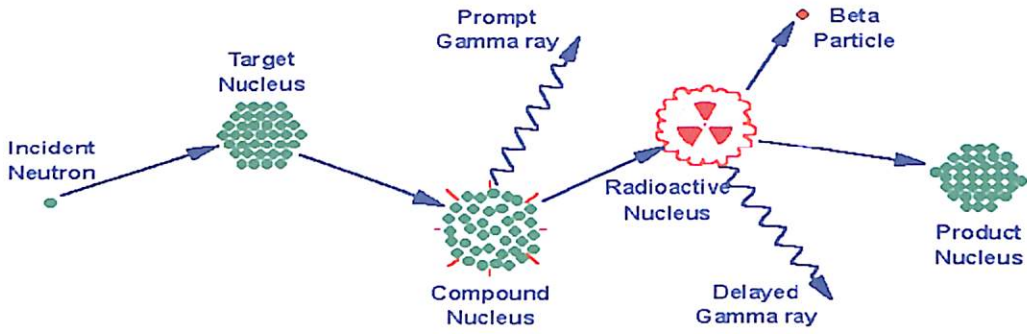
Figure 11: A process of neutron capture followed by emission of gammarays
Source: Glascock, 2011

Activation Equation

A nuclear fission reactor produces large number of neutrons. The neutron flux density (Φ) is the number of neutrons incident on a unit area of the target per unit time (neutron $cm^{-2}s^{-1}$). If a sample is placed in a nuclear research reactor, radiation capture reactions will occur.

$$A\ (n,\ \gamma)\ B \xrightarrow{\lambda_B} C \qquad (26)$$

The target atoms (A) capture neutrons to form the radioactive species B, which then decays to the product C and is displayed in equation (26). The rate of formation (R) of B is given by equation (27)

$$R = n_\phi \sigma \qquad (27)$$

Where n is the number of atoms of target present, which is assumed to be constant. The flux density is also assumed to remain constant throughout the target. The atoms of ith term are also decaying, at a rate equal to $-\lambda i N_i$, so the net rate of formation of active particles can be given by equation (28)

$$\frac{dN_i}{dt} = \text{rate of production} - \text{rate of radioactive decay} \qquad (28)$$

Where $n\phi\sigma$ is the rate of production and $\lambda_i N_i$ is the rate of radioactive

decay in equation (28) and the integral form in equation (30)

$$\frac{dN_i}{dt} = n\phi\sigma - \lambda_i N_i \tag{29}$$

$$\int_{N_i=0}^{N_i=N_i} \frac{dN_i}{n\phi\sigma - \lambda_i N_i} = \int_{t=0}^{t=t} dt \tag{30}$$

Integrating by standard form is represented in equation (31)

$$\int \frac{dx}{a+bx} = \frac{1}{b}\ln(a+bx) \tag{31}$$

Substitution yields the equation (32)

$$\frac{1}{\lambda_i}\ln(n_i\phi\sigma_i - \lambda_i N_i) - \frac{1}{-\lambda_i}\ln(n_i\phi\sigma_i) = t \tag{32}$$

Rearranging terms in equation (32), it becomes

$$n_i\phi\sigma_i - n_i\phi\sigma_i e^{-\lambda_i t} = \lambda_i N_i = A_i \tag{33}$$

This gives

$$A_i = n_i\phi\sigma_i(1 - e^{-\lambda_i t_i}) \tag{34}$$

A_i is the absolute activity of the sample at the end of irradiation and it is the

basic equation of activation analysis.

The n_i in equation (34) can be expressed as:

$$n_i = \frac{m_i\theta_i N_A}{M_i} \tag{35}$$

where m_i is mass of the ith nuclide, θ_i is isotopic abundance of the nuclide,

M_i is Chemical atomic weight of the nuclide, and N_A is Avogadro's number

(6.02×10^{23} atoms/mole)

At the end of the irradiation, the activity in equation (34) becomes

$$A_i(t_i) = \frac{\varphi\sigma_i\theta_i m_i N_A(1 - e^{-\lambda_i t_r})}{M_i} \tag{36}$$

After delaying for time t_d before counting, the activity of the end of the delay becomes

$$A_i(t_d) = A_i(t_i)e^{-\lambda_i t_d} \qquad (37)$$

If after the end of the delay, the sample is counted for a time t_c, then the number of disintegration that occurred during the counting period is obtained from equation (37) as:

$$N_i = \int_0^{t_c} A_i(t_d)e^{-\lambda_i t_d} dt = \frac{A_i(t_d)\left(1-e^{-\lambda_i t_c}\right)}{\lambda_i} \qquad (38)$$

putting equation (35), and (36) into equation (37) becomes:

$$N_i = \frac{\phi_i \sigma_i \theta_i m_i N_A \left(1-e^{-\lambda_i t_r}\right)\left(1-e^{-\lambda_i t_c}\right)e^{-\lambda_i t_d}}{\lambda_i m_i} \qquad (39)$$

Suppose $\varepsilon(E)$ is the photopeak detection efficiency for the gamma-ray energy E and total counts recorded by the detector (the photopeak area) are P_A then N_i can be expressed as;

$$N_i = \frac{P_A}{\varepsilon_i(E)\gamma_i} \qquad (40)$$

where γ_i is the gamma-ray emission probability.

Equating equation (39) and (40) and rearranging, we obtain

$$m_i = \frac{P_A \lambda_i M_i}{\varphi \sigma_i \theta_i N_A \varepsilon_i(E)\gamma_i (1-e^{-\lambda_i t_r})(1-e^{-\lambda_i t_c})e^{-\lambda_i t_d})} \qquad (41)$$

If W is the weight of the sample used, then the concentration or the amount ρ of a nuclide i in the sample is given by:

$$\rho = \frac{m}{W_i} = \frac{P_A \lambda_i M_i}{\phi \sigma_i \theta_i N_A \varepsilon_i(E)\gamma_i (1-e^{-\lambda_i t_r})(1-e^{-\lambda_i t_c})e^{-\lambda_i t_d})W_i} \qquad (42)$$

Equation (42) can be rewritten as:

66

$$\rho = \frac{m_i}{W} = \frac{[P_A/t_c]M_i}{\phi\sigma_i\theta_i\gamma_i\varepsilon(E_f)N_ASCDW} \tag{43}$$

S – Saturation factor = 1 - exp($-\lambda t_{irr}$) where t_{irr} is the irradiation time and λ =

(ln2/$T_{1/2}$ with $T_{1/2}$ –half-life;

D – Decay factor; = 1 - exp($-\lambda t_d$), with t_d is the decay time (from end of

radiation to start of counting);

C – Counting factor; = [1 q- exp($-\lambda t_c$)]/λt_c, is the correcting for decay during

counting;

W – Sample mass in grams

Methods of Standardization

The two features of neutron induced reaction - high penetrability for

neutrons and gamma radiation ensure that its standardization is potentially

easy and accurate. As the signal to concentration ratio is nearly matrix

independent, the sample preparation is rather easy; therefore, the risk of

systematic or random errors is reduced.

Absolute method

This method of quantification is based on equation (41). By measuring

P_A for known timing parameters, via t_i, t_d, and t_c, the amount of the element

present, p can be calculated. A consistent determination of ρ requires prior

knowledge of accurate ,σ, ε, ϕ, θ, and λ. Since these parameters are not usually

known with a high degree of accuracy, the absolute measurement does not

always provide reliable results; hence it is not used in many laboratories.

Where σ is the thermal neutron activation cross-section (m^2), ε is the

photopeak efficiency, ϕ is the neutron flux ($m^{-2}s^{-1}$), θ is the isotopic abundance, and λ is the decay constant (s^{-1}).

Relative Standardization

In the relative standardization method, a chemical standard (index std) of known mass, w, of the element is co-irradiated with the sample of known mass W. When the samples to be irradiated is short-lived radionuclide both the standard and sample are irradiated separately under the same conditions, usually with a monitor of the same neutron fluence rate and both are counted in the same geometrical arrangements with respect to the gamma-ray energy. It is assumed that the neutron flux, cross section, irradiation times and all other variables associated with counting are constant for the standard and the sample at a particular sample-to-detector geometry. The neutron activation equation then reduces to:

$$\rho_{sam} = \frac{[P_A/t_c]_{sam}(\rho WCD)_{std}}{[P_A/t_c]_{std}(WCD)_{sam}} \tag{44}$$

where $(P_A/t_c)_{std}$ and $(P_A/t_c)_{sam}$ are the counting rates for standard and sample respectively, ρ_{std} and ρ_{sam} are the counting concentrations of the standard and the element of interest respectively, C_{std} and C_{sam} are the counting factors for standard and sample, D_{std} and D_{sam} are decay factors for the standard and sample respectively. Equation (43) can be reduced to:

$$\rho_{sam} = \frac{[(P_A/t_c)CD]_{sam}W_{std}}{CD_{std}W_{sam}SA} \tag{45}$$

where SA is defined as $[P_A/t_c]_{std}/\rho_{std}$ and is the sensitivity of the element. Using the number of counts under the photopeak area from standardized

68

irradiation and counting conditions, the concentration of the element of concern can be determined.

Single Comparator (k_0-method) Standardization

The k_0-standardisation also known as the single comparator method of NAA is based on the fundamental equation for the calculation of the reaction rate R defined as:

$$R = \int_0^\infty \sigma(v)\phi(v)dv \tag{46}$$

-Integrating the equation (27) yields

$$R = \phi(v)\sigma(v) = \phi\sigma = nv_0\sigma_{ef}$$

This method involves the concurrent co-irradiation of the sample and the single nuclide such as ^{197}Au. The activation equation from equation (34) using the k_0 method with Au as comparator standards can be written in the form:

$$\rho = \frac{\left(\dfrac{P_A/t_c}{SCDW}\right)_i}{\left(\dfrac{P_A/t_c}{SCDW}\right)_{Au}} \frac{M_i \phi_{Au} \gamma_{Au} \sigma_{effAu} \varepsilon_p(E_{Au})}{M_{Au} \phi_{ii} \gamma_i \sigma_{effi} \varepsilon_p(E_i)} \tag{47}$$

Accurate knowledge of the nuclear data, the detector efficiencies and the specific activities of the nuclides in the sample and the monitor are needed for the determination of the concentration level in the sample. The application of the k_0-method avoids the problem associated with the preparation of individual standards for each element to be determined.

69

Fundamental equation of the k0-NAA Standardization

The k_0-standardisation also known as the single comparator method of NAA is based on the fundamental equation which determines the concentration of elements in a sample is obtained by:

$$\rho(\mu g / g) = \frac{\left(\frac{N_p/t_c}{SDCW}\right)a}{A_{sp,m}} \cdot \frac{1}{k_{o,m}(a)} \cdot \frac{G_{th,m} \cdot f + G_{e,m} \cdot Q_{o,m}(\alpha)}{G_{th,a} \cdot f + G_{e,a} \cdot Q_{o,a}(\alpha)} \cdot \frac{\varepsilon_{p,m}}{\varepsilon_{p,a}} \cdot 10^6 \qquad (48)$$

Below are the symbols figuring in equation (48) are explained as follows: ρ_a is the concentration of analyte a (in µg/g), m is the coirradiated neutron fluence rate monitor, N_p is the measured net peak area, corrected for pulse losses (dead time, random coincidence (pulse pile- up), true coincidence (cascade summing), and t_c is the counting time. A_{sp} = (N_p/t_c)/SDCW is the specific count rate, with W as the mass of the monitor and m as mas of element in grams.Meanwhile, G_{th} is the correction factor for thermal neutron self-shielding, and Ge is the correction factor for epithermal neutron self-shielding. $f - \phi_{th}/\phi_e$, the thermal (subcadnium) to epithermal neutron fluence rate ratio. $Q_0(\alpha) = \{(Q0 - 0.429)\bar{E}_r^{-\alpha} + 0.429/[(0.55)^\alpha(2\alpha + 1)]\}$ $(1eV)^\alpha$, where $Q0 = I0/\sigma0$,

where I_0 is the resonance integral is defined as:

$$I_0 = \int_{0.55eV}^{\infty} \sigma(E) dE/E \qquad (49)$$

where $\bar{E}_r$ — effective resonance energy in eV, σ is the measure for the deviation of the epithermal neutron fluence rate distribution from the 1/E shape, approximately by 1/E $^{1+\alpha}$ dependence, ε_p is the full- energy peak detection efficiency, ϕ_{th} is the conventional thermal neutron flux, and ϕ_c is the conventional epithermal neutron flux. Also $k_{0,m}(a)$ is the experimentally determined k_0 factor of analyte a versus monitor m, defined as

70

$$k_{o,m}(a) = \frac{\left(M_m \theta_a \sigma_{o,a} \gamma_a\right)}{\left(M_a \theta_m \sigma_{o,m} \gamma_m\right)}$$ (50)

Where M is the molar mass, θ is the isotopic abundance of the target nuclide, σo is the thermal neutron (n, γ) cross section at $v_0 = 2200$ m.s^{-1}, and γ – absolute gamma intensity. To obtain a good accuracy, the k_0-factor experimental determination is performed using high pure materials(Frans De Corte, 1987).

Monitor and Gold Comparator

The coirradiated monitor in equation (37) is not definitely the ultimate gold comparator [^{197}Au(n, γ) ^{198}Au; Eγ = 411.8 KeV], versus which k_0 factor ($k_{0,Au}$) are expressed in the formulations published by De Corte and Simonites (De Corte et al., 1993; De Corte & Simonits, 1989; Høgdahl, 1962). Nevertheless, by definition

$$k_0, m^{(a)} = \frac{k_{0,Au}(a)}{k_{0,Au}(m)}$$ (51)

And $k_{0,m}(a)$ in equation (51) can thus be replaced accordingly. Thus one can define a so called comparator factor as:

$$F_{c,Au} = \frac{A_{sp,m.}10^{-6}}{k_{o,Au}(m)\left[G_{th,m}.f + G_{e.m}.Q_{o,m}(\alpha).\varepsilon_{p.m}\right]}$$ (52)

Eqs (48) then become finally:

$$\rho_a(\mu g/g) = \frac{\left(\dfrac{N_p/t_c}{SDCW}\right)_a}{F_{c,Au}} \cdot \frac{1}{k_{o,Au}(a)} \cdot \frac{1}{G_{th.a}.f + G_{e.a}.Q_{o,a}(\alpha)} \cdot \frac{1}{\varepsilon_{p.a}}$$ (53)

Considering the definitions of the comparator factor Fc, Au in equations (48), it can also be stated as:

$$F_{c,Au} = \frac{N_A \theta_{Au} . \sigma_{o,Au} . \gamma_{Au}}{M_{Au}} \Phi_e . 10^{-6} \qquad (54)$$

$$F_{c,Au} = \frac{\Phi_{th}}{f} / 3.47 . 10^6 \qquad (55)$$

From equation (52), it is vivid that $F_{c,}$ Au experimentally obtained according to equation (52) is not only a useful intermediate factor in the calculation of elemental concentrations according to the k_0-Method, but is also a rough indicator of the accuracy of the neutron spectrum and the detector calibration. Obviously, this accuracy check is only possible on condition that comparison, through equation (55), of Fc, Au with the a priori estimated thermal neutron fluence rate ϕ_{th} and the thermal to epithermal fluence rate (f) is possible.

Detection Limits by Panoramic or Survey Analysis

If the gamma-ray spectra recorded show no considerable photopeak of a radionuclide of interest for a particular matrix, a concentration detection limit for the corresponding element can be calculated by replacing the term $N_{p,a}$ in the expression for the concentration calculation with the detection limit in the counts, according to Currie (1968):

$$DL\ (counts) = 2.706 + 4.653\ \sqrt{B} \qquad (56)$$

The background B in Equation (56) may be obtained as done in the software package KAYZERO version 3.01.

Peak Area for Correction for True Coincidence Effects

In equations (48), N_p is the measured net full-energy peak area, corrected for pulse losses caused by dead time, as well as for random and true coincidence effects. This can be attained by the use of an appropriate

computer code for the peak area determination and the application of proper correction methods for dead time and random coincidence. The correction for true coincidence effects is specifically bound to k_0 (or any absolute) standardization. True-coincidence effects originate from simultaneous detection of pulses generated on the detector by cascading photons.
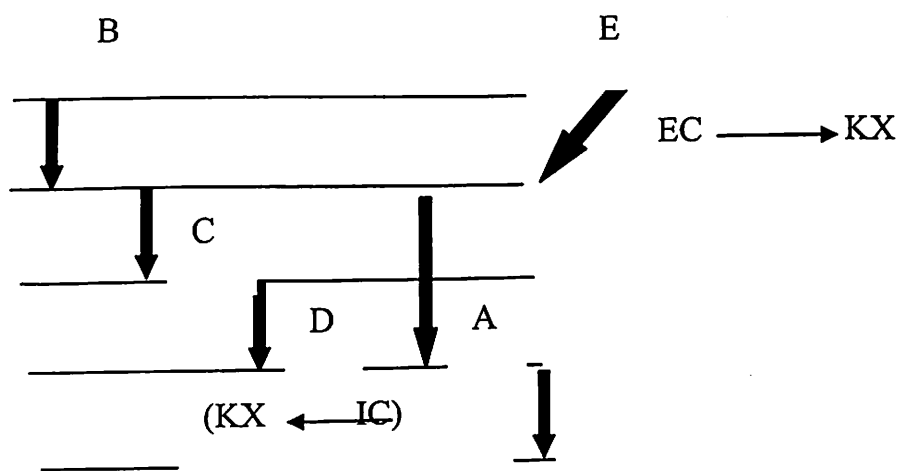
Figure 12: Simplified Decay Scheme, illustration of True-Coincidence Effects

In Figure 12, A is the measured gamma-ray under consideration, a count in its associated photopeak may be lost due to the simultaneous detection of another gamma-ray which are not certainly fully deposited in the detector but which can also be the earlier gamma-ray B and or the resulting gamma-ray E. Also an extra count in its peak may be gained by the simultaneous detection of fully deposited cascading gamma-ray C and D. If the probabilities for loss ("summing out") and gain ("summing-in") are denoted by L(A) and S(A), correspondingly, the so called true- coincidence correction factor is derived from:

$$COI\ (A) = [1 - L(\underline{A})][1 + S\ (\underline{A})] \tag{57}$$

Therefore

$$N_{p,\underline{A}}(\text{corrected}) = N_{p,\underline{A}}(\text{measured})/\ COI(\underline{A}) \qquad (58)$$

The sketch of calculated COI-factors takes into account up to three cascades for summing-in and up to five cascades for summing-out, is presented by De Corte (1987). It also considers summing-out with cascading KX-rays formed using internal conversion and/or electron capture (e.g. in Figure 12, the IC of transition E following A; EC preceding A). A Ge-detectors with a detection efficiency significantly decreasing below~100KeV photon energy, these γ-KX summing-out effects are only included for radionuclides from ^{175}Hf onwards, it KX > 50-60 KeV (a possibility to avoid coincidences with lower-energetic photons when measuring on a n-type Ge-detector, is to cover the end cap with a thin metallic shield such as for instance 0.5 mm Cu or Zn.

Also in the calculation process by De Corte (1987), the effect of delayed γ-γ emission was taken into account, as it would occur for example if the halftimes of the nuclear in Figure 12 are not negligible but of the same order of magnitude compared with the resolving time of the measuring system, thus, both the probability for gain S (A = B + C) and for loss L (A - E) would be reduced.

The probabilities for gain for the full-energy peak detection efficiencies ε_p of the involved gamma-rays are the detector characteristics of relevance, this is not so in the case of the probabilities for loss where the total detection efficiencies ε_t should be known. In the methodology k_0-standardization, ε_t is obtained from ε_p as:

$$\varepsilon_t = \frac{\varepsilon_p}{P/T} \qquad (59)$$

Thus shifting the problem to the determination of the peak to total ratio P/T finally, the methodology for true-coincidence correction is processed in a computer program COIN written in FORTRAN IV+ for a VAX (De Wispelaere, 1987).

Correction for Burn-up Effects

There may be a major loss of the target nuclei in some reactions (n, γ), which needs a change of the term Np/SDC or Asp which is presented in equation (48). When there is large cross- sections, high neutron fluence rates and long irradiation times are involved the burn up effect should be consider cautiously Formulas correcting for burn-up of the measured daughter or granddaughter are given by Simonits et al., (1980) and (De Corte, 1987). The feasible burnup is given in a user- oriented tabulation (De Corte & Simonits, 1989), where, whenever relevant σ_0, I_0 and $\bar{E}_r$ values for burn-up of the formed radionuclide are listed. A very essential case of the burnup concerns Au, the ultimate comparator in k_0-standardization. In the reaction scheme,

$$^{197}\text{Au} \xrightarrow{\text{n},\gamma} {}^{198}\text{Au} \xrightarrow{\text{n},\gamma}$$

$\sigma_0 = 98.65$ barn	$\sigma_0 = 25800$ barn
$I_0 = 1550$ barn	$I_0 = 31231$ barn
$\bar{E}_r = 5.65$ eV	$\bar{E}_r = 10$ eV (assumed)
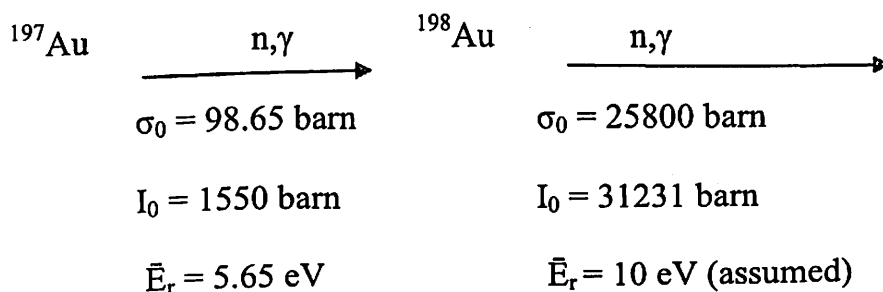
In this case both the target (^{197}Au) and the measure nuclide (^{198}Au) can undergo burn-up. The overall effect and thus the correction factor by which N_p/SDC is divided for example:

1) Negligible (0.999) for 7 hours irradiation at $\phi_{th} = 1.6 \times 10^{12}$ cm^{-2} S^{-1}, ϕ_e = 6.8×10^{10} cm^{-2}/S and α=0.015 (Channel 3)

2) Small but significant (0.983) for 10 hours irradiation at $\phi_{th} = 3.6 \times 10^{13}$ cm^{-2} S^{-1}, $\phi_e = 1.8 \times 10^{12}$ cm^{-2}/S and $\alpha = 0$ (Channel 17/2 of the former WWR-M reactor, Budapest).

3) Very large (0.509) for 14 days irradiation at $\phi_{th} = 10^{14}$ cm^{-2} S^{-1}, $\phi_e = 10^{13}$ cm^{-2}/S and $\alpha=0$ (Channel H323 of the BR-2 reactor, MOI).

In analysis conditions related to the latter case, a further monitor for coirradiation with the sample is needed. An example is a diluted Co-Al alloy [^{59}Co (n, γ)^{60}Co]. This also resolves the problem associated with the weighing of minute amounts of Au-Al alloy and/ or the large 198Au activities when performing long irradiations at high neutron fluence rates.

Variability of Neutron Fluence Rate during Irradiation

Throughout irradiation supposing the f and α remain constant, the variations occurring in the neutron fluence rate, the saturation factors for analyte and the monitor in equation (42), given by $S = 1 - \exp(-\lambda t_{irr})$, should be replaced by

$$S' = \int_0^{t_{irr}} F(t) e^{\lambda(t - t_{irr})} dt \tag{60}$$

Where F(t) is the time-dependent neutron fluence rate function, which may be normalized to unity at any arbitrarily chosen time. In the case of non-correction, the error vanishes when the analyte and the comparator radionuclides have similar half-lives. A more serious error is made if one of the half-lives (either the analyte or monitor radionuclide) is small.

Thermal and Epithermal Neutron Self-shielding Correction Factors

In equation (48), G_{th} and G_e are correction factors for thermal and epithermal neutron shielding correspondently. The $\sigma(v) \propto 1/v$ requirement in the thermal neutron energy region of all nuclides of homogeneous mixture undergo the same thermal shielding effect, and the same G_{th}-value applies to all (n,γ) reactions (Erdtmann & Petri, 1986; De Corte, 1987). Suitable expressions are given for G_{th} determination in case of simple shapes (spheres, foils, wires cylinders) irradiated in a homogeneous neutron spectrum. The elemental absorption cross section σ_{abs}, were taken from Walker et al., (1989) and are given in the k_0-compilations (De Corte & Simonits, 1989). The Gt_h and G_e values for the usual monitors applied in k_0-INAA. As to Au-Al~0.1 % Au content, thermal and epithermal effects are negligible, i. e. G_{th} and $G_e = 1$, for both 1mm diam wire and µm thick foil. For Au-Al wires with ~0.5 % Au content, $G_{th} = 1$, but $G_e = 0.985$ (Howe, 1962).

The Høgdahl Convention

The k_0-method is based on the Høgdahl convention (Høgdahl, 1962) in which the (n,γ) reaction rate per nucleus is described as in Equation (61)

$$R = G_{th}\phi_{th}\sigma_0 + G_e\phi_e I_0(\alpha) \tag{61}$$

In this case, the reaction rate is treated as a summation of a subcadmium part, through

$$\phi_{th} = v_0 \int_0^{E_{Cd}} \acute{n}\,(E)dE \tag{62}$$

With $\acute{n}\,(E)$, the neutron density per unit of energy interval, and an epithermal part, through Equation (63)

$$I_0(\alpha) = \int_{E_{Cd}}^\infty \frac{\sigma\,(E)dE}{E^{1+\alpha}} (1eV)^\alpha \tag{63}$$

77

Only equation (61) is valid on condition that as the cross section varies as the inverse of the neutron velocity that is σ is proportional to 1/v, up to approximately 1.5 eV. It is not adequate that the 1/v law is followed up to E_{Cd} = 0.55 eV, as to be expected from the Equation (61). This is because E_{Cd} is the "effective" Cd cut-off energy, whereas in reality the transmission of neutrons through a Cd-cover only comes up to unity at about 1.5 eV. Høgdahl convention was chosen for the use in the k_0-method based on the following: It is the most simple and most user friendly of the existing formalisms, it is as accurate as the more sophisticated formalisms if the condition σ(v) proportional to 1/v up to approximately 1.5 eV is met and, only a few (n, γ) reactions out of the 150 analytically interesting ones show a significant deviation from the 1/v behaviour and are thus excluded from being with.

Although such "forbidden" non 1/v reactions as $^{151}E(n,\gamma)^{152}Eu$, $^{151}Eu(n,\gamma)^{152m}Eu$, $^{168}Yb(n,\gamma)^{169}Yb$ and $^{176}Lu(n,\gamma)^{177}Lu$ are analytically important, the elements involved, however can in principle be determined via other isotopes formed by (n,γ) activation [^{154}Eu, ^{175}Yb, ^{177}Yb, ^{176m}Lu]. However, there are still some (n,γ) reactions showing slight deviations from the 1/v. Thus, small errors of maximum 1-2 % in the concentrations obtained via k_0-based NAA can be expected to formed radionuclides: $^{104(m)}Rh$, ^{116m}In, ^{154}Eu, $^{165(m)}Re$, ^{192}Ir and ^{194}Ir. Very small errors of maximum 0.1-0.2 % will be made for ^{110m}Ag, ^{134}Cs, ^{139}Ba, ^{182}W, ^{186}Re, ^{233}Th and ^{239}U. Also ^{198}Au comparator should be added to this last series.

Chapter Summary

In summary, a review of the literature on mercury and its forms (metalic, organic and inorganic mercury), and mercury in different compartments (soils, sediments, biota, fresh water foodwebs) were done. Also the effect of pH on mercury speciation in soil and health effect of mercury were reviewed. Other metals and rare earth elements (REEs) were also reviewed. The final reviews were on the analytical methods for the determination of THg (CVAAS), Hg species (CVAFS and Temperature Fractionation with Zeeman background correction) and the validation method (k0-INAA) which was also used for multielemental analysis.

CHAPTER THREE

MATERIALS AND METHODS

Introduction

This chapter provides information on the study areas, protocol used, materials and methodology used in sampling, preparations and analysis of data. Also, the quality controls of the analysis were also looked at.

Description of Sampling Sites

Originating from the eastern and north-western fringe and flowing southwards, the Pra River and its major tributaries (River Anum, Birim, Offin, and Oda) are located in south-central of Ghana. Its basin is between Latitude $5°$ N and $7° 30'$ N, and Longitudes $2° 30'$ W and $0° 30'$ W. Together with its major tributaries, the Pra River Basin forms the largest river basin of the three principal south-western basins (i.e Ankobra, Tano, and Pra) system of Ghana. The total basin area is approximately 23, 200 km^2 and it extends through almost 55 % of the Ashanti, 23 % of Eastern, 15 % of Central and 7 % of Western Regions. Table 3 presents the basic characteristics of the Pra River Basin, Ghana.

The Pra River takes its source from the highlands of Kwahu Plateau (Twenedurase) in the Eastern Region and flows for some 240 km before entering the Gulf of Guinea in Anlo and Shama (in the Western Region) where it forms an estuary of approximately 100 m wide at the point of entry into the sea. The Pra estuary banks are fringed by mangroves up to about 10 km inland (Obodai, Yankson, & Blay, 1991). The drainage area is bounded to the east by the Birim River, to the west by the Offin River and to the south by the Gulf of

Guinea. Also in addition to the river network is Lake Bosomtwe, the only significant natural freshwater lake in Ghana. It is a big crater lake with the highest depth of nearly 80 m and a rim diameter of about 8 km (WRC, 2012).

Table 3: Basic Characteristics of the Pra River Basin, Ghana. Integrated Water Resources Management Plan

Pra Basin Area	23,188 km^2
Inhabitants	5, 839,834 (2010) (GSS, 2012)
Length of main Pra river	240 km
Key Tributaries	Anum, Birim, Oda and Offin rivers
Natural Lake in the Pra Basin	Lake Bosomtwe-the only significant natural freshwater lake in Ghana.
Important water uses and services	Water abstraction (mining and irrigation), water supply (domestic and Industrial)

Source: WRC, 2012

The climate is sub-equatorial wet, with two rainy seasons, with the first season starting from May to July and second season starting from September to November. The mean annual rainfall in the basin is relatively high, about 1,500 mm with a range between 1300 mm and 1900 mm contributing 12 % to the flow of the main Pra (WRC, 2010c). Table 4 shows the seasonal variation of rainfall in the various meteological stations along the Pra River Basin from 2008 to 2011.

Table 4: Seasonal Variation of Rainfall in the Various Metrological Stations along the Pra River Basin from 2008 to 2011

Month	Mean monthly rainfall (mm)				
	Kumasi	Konongo	Kade	Twifo Praso	Dunkwa
January	20.1	10.4	22.2	30.2	12.3
February	93.6	95.3	101	103	75.6
March	123	86.2	113	129	120
April	118	132	170	141	125
May	153	231	163	231	232
June	283	290	177	214	281
July	167	159	168	123	141
August	96.0	190	86.9	99.8	93.8
September	148	166	95.2	120	184
October	147	163	266	130	188
November	45.8	28.6	120	107	73.3
December	36.0	24.9	84.7	72.8	48.5
Total	1426	1575	1567.9	1500	1470

Source: Ghana Metrological Service

The basin is moist during the year with drier seasons in August and temperature fluctuating between 26 °C and 30 °C. The meteorological statics demonstrate a mean annual number of rainy day between 90-100 days in the basin (WRC, 2012). The available surface water resources originate from an average annual rainfall of about 1,500 mm and the Pra river carries an average annual runoff of about 4,174 mm^3 (WRC, 2010a). The hydrogeology of the basin is dominated by aquifers of the crystalline basement of rocks and the Birimian Province (WRC, 2010b). Groundwater in the Pra basin mainly occurs in the Birimian geological formations which consist of lower Birimian, that is metasediment rocks and the upper Birimian with metavolcanic rocks. The key consumptive uses of water in the basin are for domestic, industrial, mining and agricultural.

The geography of the Pra Basin River is characterized by relatively flat land in the southern half, with a small number of peaks in the middle to

northern sections of the basin. Vegetation is of moist semi-deciduous forest which is made up of alfisols, (lixisols and luvisols), ultisols, plinthaqualfs and plinthaquuls (plinthosols), inceptisols (cambisols, and aquents and aquepts (Asiamah, 1987; Obeng, 2000). Presently, the main land cover types are estimated as follows: Agricultural (60 %), forest (30 %), grassland and human settlement cover 10 % (WRC, 2012) with isolated forest reserves (e.g. Atiwa Forest Reserve) and large established commercial tree plantations.

The population along the Pra River Basin was about 5.8 million people (including children) with an estimated average population growth rate at 2.5 % (GSS, 2012). Most towns are well-known for their mining activities in the basin with the largest mining company in Africa, AngloGold Ashanti at Obuasi from the Offin valley (Levich, 2010). Also, gold is mined at Konongo from the channel of Offin River at Dunkwa-On-Offin. Over 63 % of the population engaged in Agriculture and forestry, tourism and mining have taken other related sectors of the economy. Figure 8 shows a map of Pra River Basin from the upstream in the Kwahu plateau at Twenedurase (SS7) and three of its main tributaries (Anum, Birim, and Offin Rivers) through to the downstream at Shama (Estuary) where the Pra River enters the ocean. Whilst Figures 13 (the various sampling sites in the Pra River Basin), 14 (Main Pra River at Nkontinso), 15 (Offin River at Beposo sampling site), 16 (Main Pra River estuary with mangrove at the left towards Shama sampling site), 17 (Main Pra River estuary with mangrove at the left towards Anlo sampling site), and 18 (Pra River at the estuary showing wetlands, sandbar at the two (2) sampling sites at the Pra estuary).
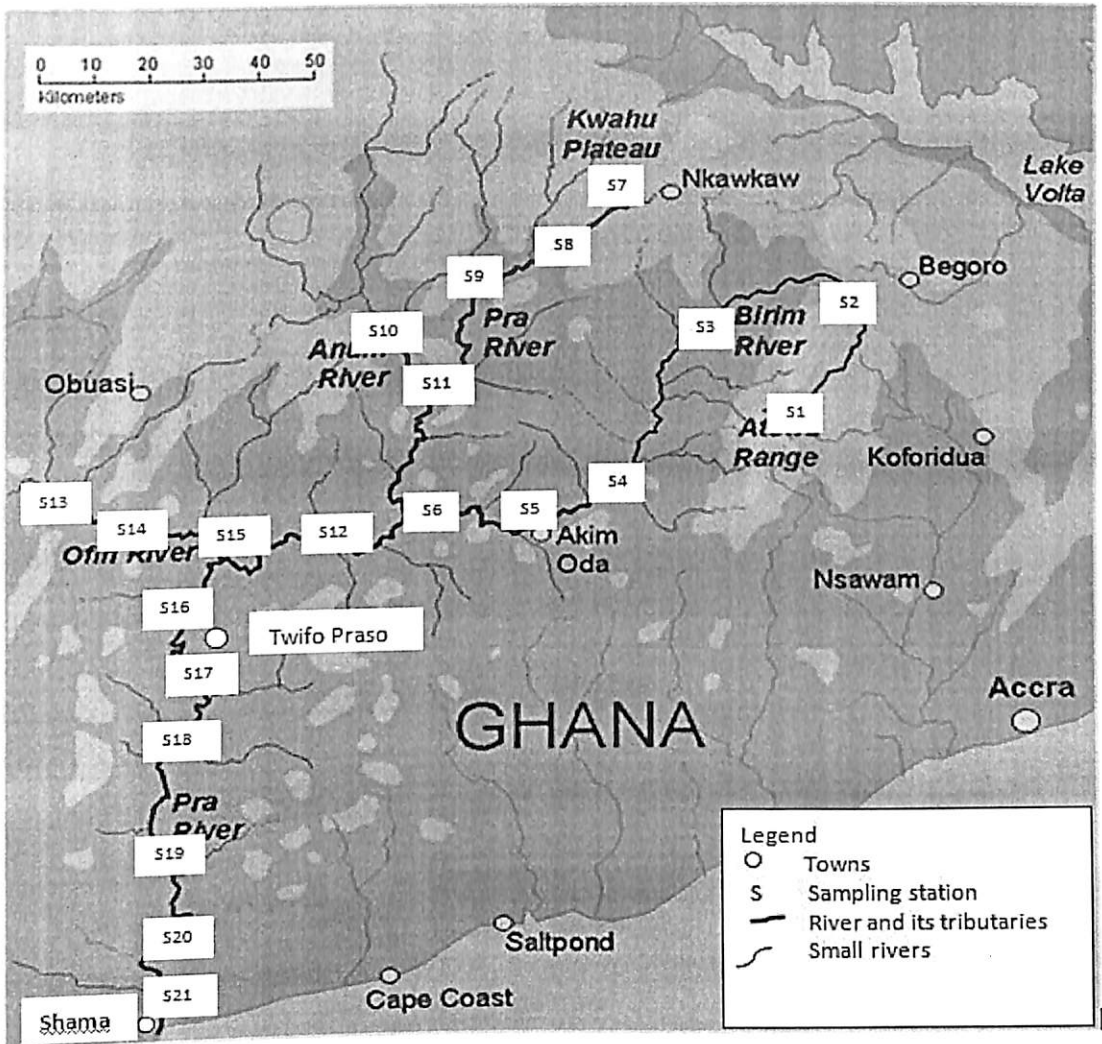
Figure 13: A map of Pra Basin from Kwahu plateau at Twenedurase (upstream) with three of its main tributaries (Anum, Birim, and Offin Rivers) the upstream to Shama (Estuary) where the Pra enters the ocean

Source: https://en.wikipedia.org/wiki/Pra_River_(Ghana)

Figure 14: Offin River at Nkontinso, one of the sampling sites in this study
Source: Author Data, 2013

Figure 15: Pra River at Beposo sampling site, a major tributary of the Pra
River Basin, Ghana
Source: Author Data, 2013

Figure 16: Mangroves at the middle of the Pra estuary; moving river inward during dry season

Source: Author Data, 2013

Figure 17: Mangroves grown at the middle of the Pra estuary with the river moving to Shama whilst the right shows Anlo Beach town, with the ocean moving inward during dry season.

Source: Author Data, 2013
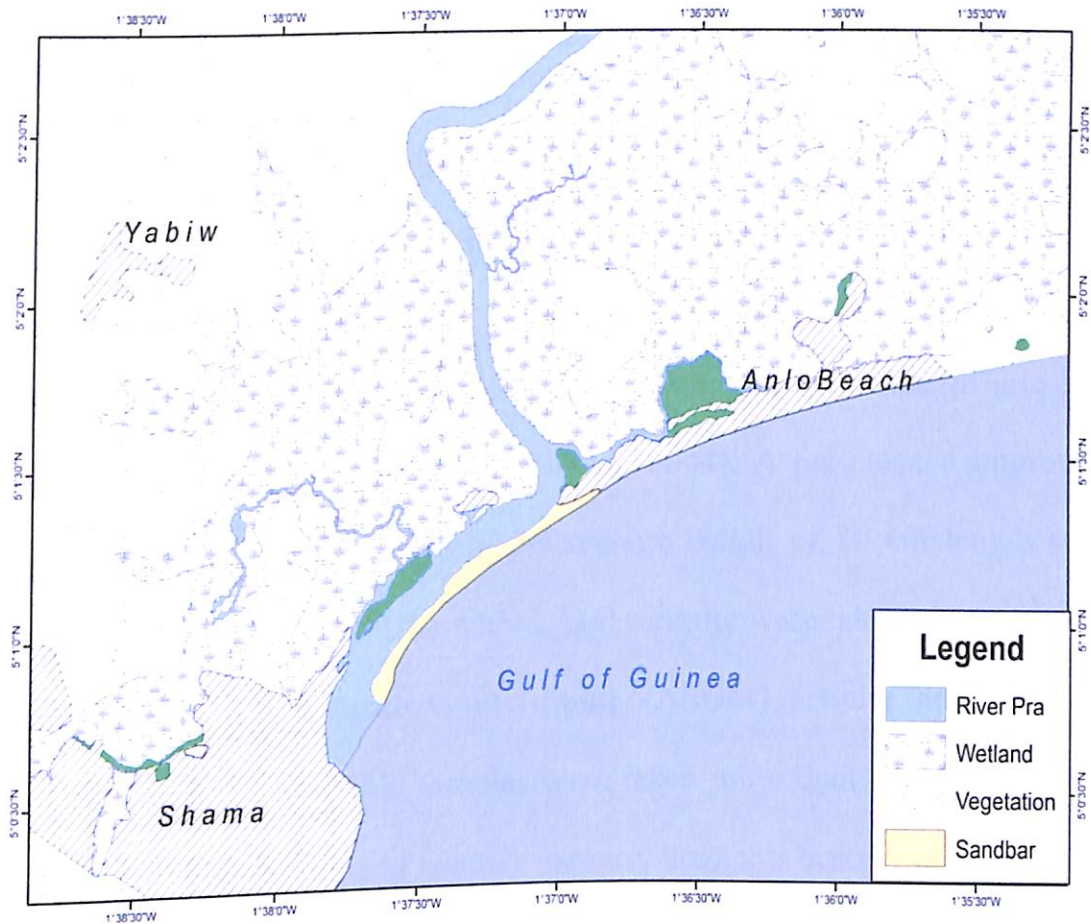
Figure 18: A map of Pra River at the estuary showing wetlands, sandbar at the two (2) sampling sites at the Pra estuary

Source: Department of Geography and Regional Planing, University of Cape Coast, Ghana

Sampling and Sample Preparation

Various protocols and sampling techniques will be used to sample soil (0-6 cm), sediment (0-10 cm), mining waste, "Black", carnivorous and herbivorous fish samples from the Pra River Basin. All containers, Teflon tubes, and volumetric flasks will be pre-cleaned before used. Also, all Samples will be prepared in duplicates, and appropriate reference materials and standards will be used for quality control purposes.

Soil Sampling

Mercury may be dispersed over extensive areas (km²) or concentrated in "hotspots" (100 m²). In identifying mining and environmental hotspot, the grid sampling technique was employed in sampling superficial soil profile samples of 10 cm depth at 100 m² (10 m x 10 m) at each sampling site of which each corner (east, west, north, and south) and the centre of grid were sampled (Veiga, Baker, Fried, & Withers, 2004). A pre-cleaned improvised polyethylene core (Figure 19) of an average length of 20 cm length and a diameter of 2 cm (Table 7) were used. Soil samples were taken either closed to Artisanal and Small Scale Gold Mining (ASGM) activity and where no ASGM activity is available samples were taken more than 100 m away from each river. This was done to identify mercury hot spots according to Veiga and Baker (2004). The coordinates of the various sampling locations were obtained using GARMIN hand-held Global Position System (GPS). The soil samples coded, names and coordinates of sampling sites, dates and time of sampling are shown in Table 5.

Table 5: Names of Sampling Sites, Location, Dates and Time of Sampling Soil Samples in the main Pra River Basin and Three of its Tributaries (Rivers Anum, Birim, and Offin), Ghana

Sampling Site	Name of Town	Name of River	Coordinates	Date	Time
SS1	Dadientem	Birim	6°09'43.20"N, 0°34'52.10"W	03/8/2013	11:29
SS2	Kibi	Birim	6°09'27.70"N, 0°32'53.20"W	03/8/2013	11:07
SS3	Adonkrono	Birim	6°05'17.70"N, 0°49'57.90"W	15/6/2013	12:17
SS4	Kade	Birim	6°05'02.20"N, 0°49'58.50"W	15/6/2013	12:21
SS5	Akim Oda (old)	Birim	5°57'01.96"N, 0°58'47.12"W	15/6/2013	09:38
SS6	Akim Oda	Birim	5°55'51.80"N, 0°59'58.60"W	15/6/2013	08:14

Table 5 Cont'd

Sampling Site	Name of Town	Name of River	Coordinates	Date	Time
SS7	Twenedurase	Pra	6°43'28.09"N, 0°56'04.06"W	10/8/2013	10:41
SS8	Kwahu Praso	Pra	6°37'11.65"N, 0°54'42.10"W	10/8/2013	12:27
SS9	Apreja	Pra	6°25'53.39"N, 1°01'13.57"W	03/8/2013	05:20
SS10	Nnoboamu	Anum	6°36'53.80"N, 1°16'36.70"W	13/7/2013	02:22
SS11	Wobiri	Anum	6°00'39.02"N, 1°54'40.16"W	13/7/2013	03:32
SS12	Nkontinso	Offin	6°00'38.80"N, 1°55'15.60"W	15/4/2013	03:25
SS13	Dunkwa-On-Offin (1)	Offin	5°58'22.10"N, 1°58'33.30"W	15/4/2013	10:19
SS14	Dunkwa-On-Offin (2)	Offin	5°55'24.31"N, 1°46'08.49"W	22/4/2013	11:05
SS15	Assin Praso	Pra	5°55'56.80"N, 1°22'00.40"W	12/7/2013	05:57
SS16	Twifo Praso	Pra	5°36'41.10"N, 1°33'36.30"W	30/5/2013	12:25
SS18	Daboase	Pra	5°08'41.70"N, 1°39'13.90"W	19/6/2013	12:31
SS19	Beposo	Pra	5°07'41.90"N, 1°37'12.74"W	19/6/2013	10:55
SS20	Anlo (Esturay)	Pra	5°01'30.47"N, 1°37'07.07"W	19/6/2013	3:55
SS21	Shama (Estuary)	Pra	5°00'54.12"N, 1°37'56.65"W	19/6/2013	1:56

Source: Author Data, 2013

The soil profile is a description of the vertical cross-sections of the soil that naturally occur in layers or horizons (Petersen, Sack, & Gabler, 2010). A composite of the 0 to 6 cm of the soil profile will be used in the determination of mercury. Also, soils are a complex and usually heterogeneous matrix which changes with depth along the soil profile and this happens typically in the first centimetre (Leo, 2005). In this study the immediate topsoil (0-1 cm) as previously sampled was used to determine other elements (Ag, As, Au, Ba, Br,

Ca, Cd, Ce, Co, Cr, Cs, Eu, Fe, Ga, Hf, Hg, K, La, Mo, Na, Nd, Rb, Sb, Sc, Se, Sm, Sn, Sr, Ta, Tb, Th, U, W, Yb, Zn, and Zr) using k_0-INAA.

Soil samples were prepared by measuring and cutting into 1cm section from the 0-1 cm, 1-2 cm, ..., 5-6 cm into plastic bowls which were labeled as follows: A (0-1 cm), B (1-2 cm), C (2-3 cm), D (3-4 cm), E (4-5 cm) and F (5-6 cm). Bigger stones, plant residues were removed before the samples were mixed using a plastic spoon to form composite samples and a section of the soil sample was taken. Each section was air dried at room temperature for three (3) days. The samples were packed into pre-cleaned plastic containers coded with date and time of sampling, using an indelible pen. The samples were kept in a clean, dried place which was later transported to the laboratory of the Department of Environmental Science, Jozef Stefan Institute, Ljubljana, Slovenia for further sample preparation and measurement. The samples were sieved a 2 mm nylon sieve mesh and then homogenized using FRITSCH (Planetary micro Mill Pulverisette 7, grinder for ten (10) minutes at a speed of 6.0 rpm) via Teflon balls. The Mill Pulverisette and the Teflon balls were washed with milli-Q water and dried in between each grinding process to avoid cross-contamination. During sample preparation, precautions were taken to avoid cross-contamination between the samples. Table 6 will summaries the types of samples obtained at various sampling sites and also the activities that the people in the catchment areas engage in along the Pra River Basin.

Table 6: Various Activities at Various Sampling sites with Samples taken During Sampling

Sampling Site	Activities at each sampling site	Sample type
SS1	Artisanal Small-scale and Gold Mining (ASGM) pits dug along the bank of the river with about 100 m away from residential houses.	Soil* & sediment*
SS2	ASGM pits dug along the bank of the Birim river.	Soil* & sediment*
SS3	Subsistence farming, residential houses along the bank of the river with previous AGSM activities.	Soil & sediment
SS4	Subsistence farms along the banks of the river with previous ASGM activities.	Soil & sediment
SS5	Diamond mining (in the river), palm and cocoa farm plantation along the bank of the river, petroleum station, timber company (100 m away), and old bridge and residential houses 200 m away.	Soil* & sediment*
SS6	Subsistence farming, oil palm plantation, residential with previous ASGM activities along river bank	Soil & sediment
SS7	The upstream of main Pra river with forest lands and few subsistence farming along the river. This site is located in the forest zone area where there are neither houses nor mining activities.	Soil & sediment
SS8	Upstream of main Pra river with residential houses, constructed road with bridge across the river.	Soil & sediment
SS9	AGSM activities along the bank of Pra river and around this sampling site. Benefication with "chanfan" machines along the Pra River throughout nearby villages.	Soil*, sediment* & "black"
SS10	Artisanal mining in the river with a bridge across the river. There are also wet lands around with subsistence farming along the river.	Soil* & sediment*
SS11	Artisanal mining in the river, with sand winning for building in the river. Palm and cocoa plantation few meters away with other cash crops.	Soil & sediment
SS12	Illegal mining with Bulldozers, trucks, hydraulic jet and mercury amalgamation are used. Roasting of gold in an open air scattered all over the township with gold buyers. The river is also used to transport heavy machinery into the forest. Panning by women and children are also a major activity around this sampling site. This sampling site has a lot of residential with congested housing.	Fish, soil, sediment, & "black"

Table 6 Cont'd

Sampling Site	Activities at each sampling site	Sample type
SS13	Alot of ASGM scattered all over this area. Beneficiation with "Chanfan" machine and washing of gold with blanket is a major activity in this sampling site. Amalgamation with mercury and burning of gold in an open air shops and buyers scattered all over Dunkwa-On-Offin. Fishing is also done in this sampling site.	Fish, soil*, sediment*, mining residue, & "black"
SS14	Anglo Gold Mining Company, ASGM with roasting of gold by gold buyers, and subsistence fishing in this catchment area. This sampling site is a suburb of SS12.	Soil*, sediment*, & "black"
SS15	ASGM activities used to take place in the main Pra River but since 2010, the construction of 60 km road with a bridge across the main Pra River and the outcry of the general public attracted the presence of security men guarding 24 hours stopped mining along the river.	Soil & sediment
SS16	Mining in the river with "chanfan" machine, palm nut oil production, timber production and car maintenance shops along the bank of the river.	Sediment & fish
SS18	Mining in the river, Water Reservoir for drinking water, subsistence farming and fishing.	Soil, fish& sediment
SS19	Mining for alluvial gold in the river by ASGM, Subsistence farming and fishing.	Soil*, fish & sediment*.
SS20	Wet lands, Fishing community, subsistence farming, and residential houses.	Soil, fish, & sediment,
SS21	Wet lands, lagoons, Fishing landing site, fish mocker along the estuary with residential houses.	Soil, fish, & sediment,
NOTE:	Soil and sediment samples that were sampled closed to ASGM activity are marked with an asterisk (*). "Chanfan" machines are basically sold and used by Chinese in Ghana. These machines are used for beneficiation by ASGM. "Black" as popularly known by ASGM in Ghana is tailing that is kept after amalgamation in big containers, cemented dug holes or kept in rooms especially made for them for safe keeping.	

Source: Author Data, 2013

Improvised Instruments in Sampling Soil and Sediments in this Studies

Polyethylene pipes were used in sampling soils and sediments in all the sampling sites along the Pra River Basin. Table 7 represents the diameters and length of the improvised corer that were used in sampling both soil and sediments in this research. To avoid contamination from metal corers polyethylene corers are preferred for sampling for mercury and other metals analysis. Figures 19 and 20 (A & B) represent the improvised corer designed for sampling soil and sediments respectively from the Pra River Basin in this research.
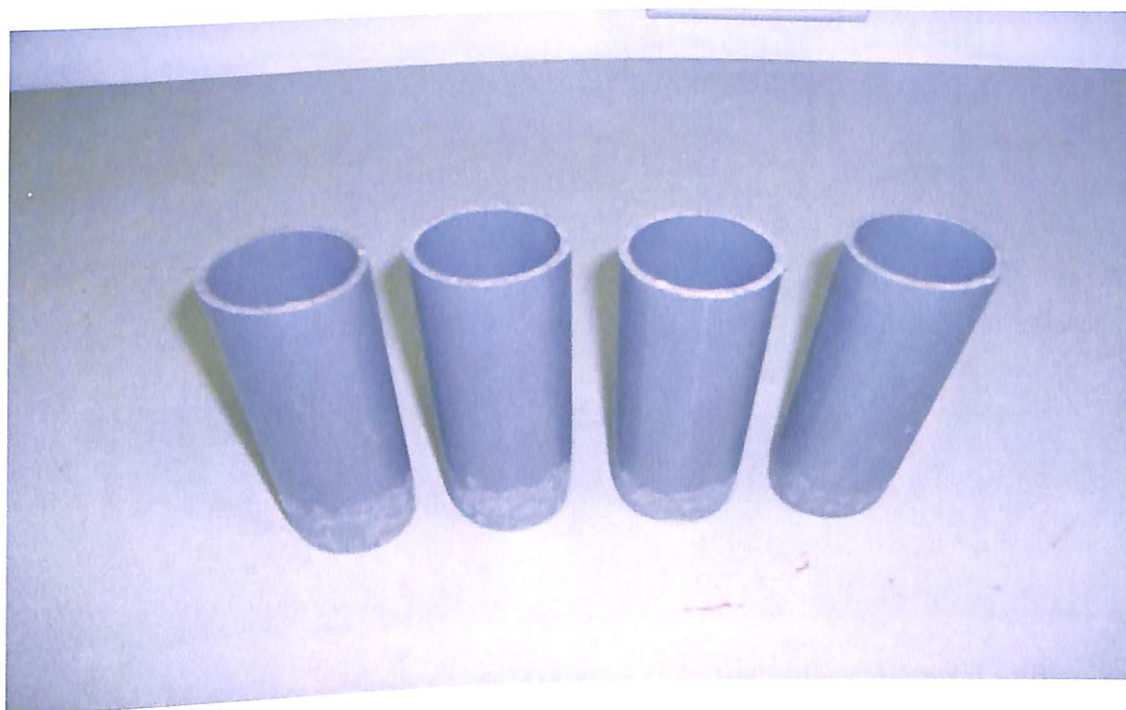
Figure 19: Improvised corer made from polyethylene material used in sampling soil in this study

Source: Author Data, 2013

(A)
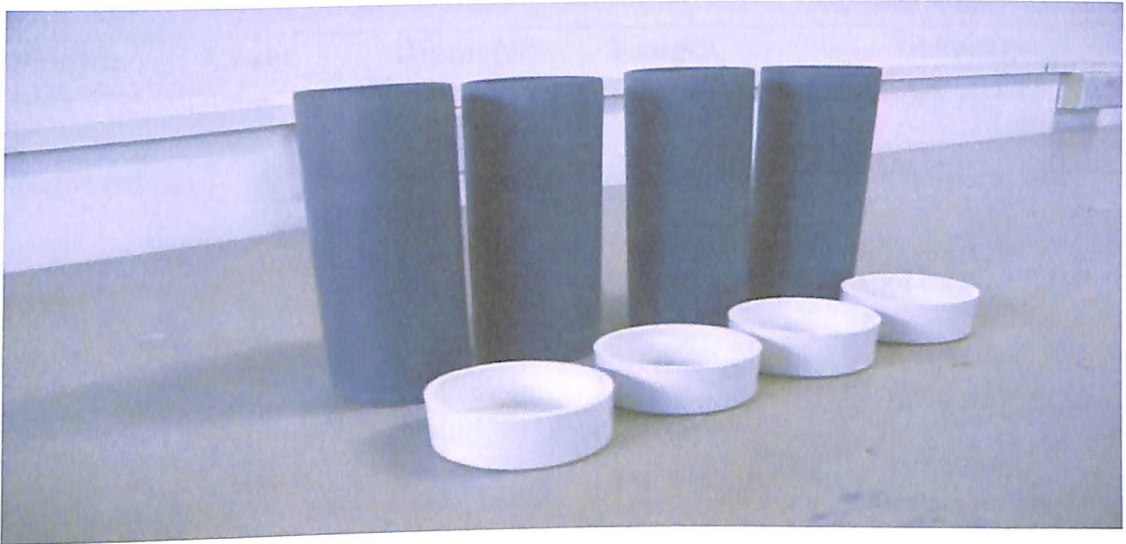
(B)

Figure 20: Improvised Corer (A & B) made of Polyethylene material with caps used in Sampling Sediment samples from the Pra River Basin in this Study

Source: Author Data, 2013

Table 7: Diameter and Length of Polyethylene Corer (Improvised) for Sediment, and Soils Samples

Sample type	Corer	Diameter (cm)	Length (cm)	Average Diameter (cm)	Length (cm)
Sediment	1	6.07	30.1	6.06	30.0
	2	6.04	30.0		
	3	6.06	29.8		
Soil	1	4.84	20.1	4.84	20.0
	2	4.87	20.0		
	3	4.80	20.0		
Cap	1	6.74	3.3	6.78	3.30
	2	6.81	3.3		
	3	6.79	3.4		

Source: Author Data, 2013

Sediment Sampling

The improvised polyethylene cores (Figure 20) with an average length of 30 cm, diameter; 6.06 cm was used to sample sediments (near the river banks) at a speed of 0.3 m/s in all the twenty-one (21) sampling sites. Random sampling technique was used on both sides of the river bank in all the twenty-one (21) sampling sites in triplicates. The corers were each capped at both ends and labelled after each sampling and kept in vertical position until all water has risen to the top (UNEP, 1997). Some physiochemical properties; pH, total dissolved solids, temperature, conductivity, salinity, and dissolved oxygen, of the water at each sampling sites were also measured using water quality checker OAKTON PCD650. The samples in the corer were bagged in a ziplock plastic bags and labeled with an indelible ink. They were placed in an ice chest with a temperature of about 4°C and transported to the lab for immediate samples pre-preparation.

Fish Sampling

Fish samples were purposively sampled with the help of local fishermen at seven (7) sampling sites namely Nkontinso (SS12), Dunkwa-On-Offin (SS13), Twifo Praso 1 (SS16), Twifo Praso 2 (SS17), Daboase (SS18), Anlo (SS20), and Shama (SS21). The fish samples were grouped according to their feeding habits (herbivorous, carnivorous and omnivorous) and standard length to determine mercury bioavailability (Veiga, Baker, Fred, & Withers, 2004). Appendices X and Y show some fish samples from the Pra River Basin which was used in this research. Each sample was ziplock in a polyethylene bags and labelled. The samples were immediately placed in an ice chest containing ice pack with a temperature of about -4°C which were immediately transported to the Fisheries and Aquatic laboratory, University of Cape Coast for further sample preparations.

"Black" Samples

"Black" is a milled gold stone, gravel or sand that is believed to contain gold. After extraction with mercury, the liquid tailings are thrown anywhere (whether in the bush, around the house etc.) but the residues are kept in big containers, or dug holes, or gathered in secured rooms. Mercury is used in extracting gold in these "blacks" after a week, two (2) weeks, a month or even up to one year till all gold are believed to have finished in the "black". Samples of "black" were purposively sampled from thirteen (13) miners from sampling sites Apreja (SS9), Nkontinso (SS12), Dunkwa-On-Offin 1 (SS13), and Dunkwa-On-Offin 2 (SS14). The "Black" samples were limited due to the fact that miners were reluctant to give out "black" as they believe it contains

some amount of gold which needs to be extracted after some time. In all, thirteen "blacks" were sampled from different artisanal and small-scale gold *miners from these sampling sites.*

Ice packs were placed on the "black" samples in an ice chest which was transported to the laboratory to be stored in a fridge for further sample preparation. The samples were later transported to the Department of Environmental Science, Jozef Stefan Institute, Ljubljana, for further samples preparation and measurement.

Mining Waste

After many extractions, "blacks" are also sold to another group of artisanal gold miners who are non-Ghanaians and mostly Francophone. In this type of extraction, pits are dug in the forest where accesses to their activities are very difficult. These group of illegal miners without using any protective gloves, mask, use other chemicals which are unknown, to extract almost all the gold in the "black". These chemicals when added to "black" produce fumes which when inhaled by the miners coughs yellowish substances. This is the final stage of gold extraction where mining wastes were purposively sampled. In all, six (6) residues were purposively sampled from abandoned pits in sampling site SS13 (Dunkwa-On-Offin) and were cut into 1 cm sections of six (6) for analysis.

Fish Sample Pre-Preparation

The weight of each fish sample was measured using analytical balance whilst a wooden board with a plastic measuring rule was used to measure both

total lengths and standard lengths of each fish in centimetres. In all five hundred and sixteen (516) fish samples were sampled in all the seven (7) sampling sites and are made up of various species with different standard length (cm). The fish samples were cleaned by removing scales (if any) and washed with de-ionized water. A pre-cleaned dissecting kit was used to dissect each fish samples into muscles, skin, and gills, in Fisheries laboratory, University of Cape Coast, Ghana. Care was taken in avoiding digestion track contents of each fish samples during dissecting to avoid cross-contamination. The samples were bagged in a ziplock polyethylene bag coded and stored in a freezer below -25 °C. Samples were transferred to the Department of Environmental Science, Jozef Stefan Institute, Ljubljana, Slovenia for further sample preparation and measurement.

In the lab at the Environmental Science Department, Ljubljana, each fish muscle sample was homogenized using a pre-cleaned glass Philips stainless blender and then packed in a pre-cleaned Teflon container with their codes (example, SS12FH-M or SS12FH-S, SS12FC-M or SS12FC-S which means Sampling Site 12 Fish Herbivorous-Muscle or Sampling Site 12 Fish Herbivorous Skin, Sampling Site 12 Fish Carnivorous-Muscle or Sampling Site 12 Fish Carnivorous-Skin) written with indelible pen. Since fish skin samples were in small quantities, a special technique was used in homogenizing the fish skin manually. The fish skin at -25 °C of each fish sample was homogenized using a pre-cleaned plastic chopping board and stainless-steel knife with the aid of liquid nitrogen. During this homogenization, the liquid nitrogen was used at least four (4) times to harden the fish skin sample and at each step, the fish skin sample was sliced into

about 0.2 mm until a desirable homogeneous was reached. To avoid cross-contamination, samples with least mercury were first homogenized followed by more contaminated fish. All equipment were cleaned with mercury-free detergent, rinsed with Milli-Q water and dried after each homogenization. The homogenized fish skin samples were packed in a pre-cleaned Teflon container with codes and then kept under −25 °C for further sample preparation and chemical analysis. Table 8 gives the number of fish samples obtained from each sampling site according to their standard length (cm) and eating behavior.

Table 8: Number of Fish Based on their Standard Length (cm) from each Sampling Sites

Standard length (cm)/ *Eating behaviuor*	Nkontinso	Dunkwa-On-Offin	Twifo Praso (1)	Twifo Praso (2)	Daboase	Anlo (Estuary)	Shama (Estuary)
0.00-5.10							
Carnivorous	-	-	-	-	-	5	–
5.10-10.0							
Herbivorous	6	-	8	7	6	40	5
Carnivorous	14	20	7	-	-	5	28
10.1-15.0							
Herbivorous	7	-20	13	19	10	-	15
Carnivorous	21	-	6	7	6	37	29
15.1-20.0							
Herbivorous	7	-	7	5	8	-	9
Carnivorous	11	7	9	-	4	23	13
20.1-25.0							
Herbivorous	6	-	8	3	-	-	–
Carnivorous	-	-	7	-	-	-	–
25.1-30.0							
Carnivorous	15	12	-	10	4	-	–

Table 8 Cont'd.

Standard length (cm)/ *Eating behaviuor*	Nkontinso	Dunkwa-On-Offin	Twifo Praso (1)	Twifo Praso (2)	Daboase	Anlo (Estuary)	Shama (Estuary)
25.1-30.0							
Carnivorous	15	12	-	10	4	-	–
35.1-40.0							
Carnivorous	-	-	-	-	3	-	–
55.1-60.0							
Carnivorous	-	-	-	-	4	-	–

Source: Author Data, 2013

101

Table 8 Cont'd.

Standard length (cm)/ *Eating behaviuor*	Nkontinso	Dunkwa-On-Offin	Twifo Praso (1)	Twifo Praso (2)	Daboase	Anlo (Estuary)	Shama (Estuary)
25.1-30.0							
Carnivorous	15	12	-	10	4	-	—
35.1-40.0							
Carnivorous	-	-	-	-	3	-	—
55.1-60.0							
Carnivorous	-	-	-	-	4	-	—

Source: Author Data, 2013

Sample preparation using HNO₃/HClO₃/H₂SO₄ Wet Acid Digestion (M1)

All volumetric flasks (100 ml) and stoppers were washed with 0.5 % of the $KMnO_4$ solution, rinsed with Milli-Q water until all the colour of the $KMnO_4$ was invisible, and then dried in a Termo Medicinski Aparati at 60 °C. About 0.2 g (air dry weight) of each sample (sediments, soil, mining residue, 'Black', fish muscle, and skin) were weighed using analytical balance in parallel with Reference material (BCR 277R, BCR 580, and DORM-4), Standard and sample blanks. All analytical samples, reference materials, standards, and sample blanks were prepared in duplicates for measurements. The samples were wet digested by adding 1 ml of Milli-Q water. This was followed by the addition of 2 ml of 1:1 $HNO_3/HClO_3$ and 5 ml of H_2SO_4. Mercury standard of 4 ng/ml and 10 ng/ml were also prepared with test samples by measuring 80 μl and 200 μl mercury respectively. Samples, references material, standards, and blanks were heated on a hot plate at 240 °C for 20 minutes. The samples were allowed to cool followed by topping it to a fixed volume of 100 ml with Milli-Q water.

Sample preparation using HNO₃/HF/HCl Acid Digestion (M2)

All Teflon (57.3 ml) with caps were pre-cleaned in detergent, soaked in 50 % Nitric acid for three (3) days on a heating block at 60 °C and then rinsed with Milli-Q water three times then soaked in 10 % HCl for one (1) day. The Teflon and caps were dried at 60 °C. Approximately 0.2 g (air dry weight) of each sample was weighed in duplicate using analytical balance, with reference material (BCR 580), standards and sample blank in duplicates. The samples were digested by adding 5 ml of HNO_3/HF (2:1) to each sample,

and then 1 ml of HCl was added to each sample. The samples were left at room temperature for 1 hour and later heated overnight at 100 °C on the heating plate. Each sample was diluted by bringing samples to a fixed volume by using 5 % H_3BO_3. Boric acid was used to neutralize excess HF and tetra fluoroboric acid in solution.

$$H_3BO_3 + 3HF \longrightarrow HBF_3(OH) + 2H_2O$$

$$HBF_3(OH) + HF \longrightarrow HBF_4 + H_2O$$
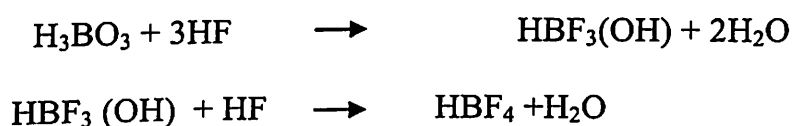
Sample Preparation Procedure for MeHg in Fish

Fish muscles samples of weight between 0.19-0.25 grams were weighed in duplicates into pre-cleaned and dried Teflon bottles and labeled. Duplicates of standard, reference material (DORM-4) and solution blanks were also prepared and labelled. A volume of 2.5 ml of 18 % KBr was added to each of the samples; followed by 2.5 ml of 5 % of H_2SO_4 and 1ml of $CuSO_4$. The samples were homogenized using a KS-15 shaker for 15 minutes between 250-300 Mut 1/minute. A dispenser was used to add 5 ml of Dichloromethane to each sample. The samples were shaken again at 15 minutes, 250-300 Mut 1/minutes using KS-15. Using the Centric 322A machine at a speed of 3200 rev/min, each sample was centrifuged for 2 minutes.

The organic phase of each sample was separated with the aid of a pre-cleaned (using dichloromethane) separating funnel into a pre-cleaned (using Dicholromathane) Teflon tubes. Thereafter, 5 ml of Dichloromethane was added to the residue of each fish sample and the inorganic phase was then centrifuged for 2 minutes at a speed of 3200 rpm for 2 minutes using the

Centric 322A machine. The organic phase of each sample was again separated using the separating funnel. The resultant solutions were heated at 80 °C using a heating block till all the dichloromethane evaporated. Each sample was purged using argon for 5 minutes. The samples were allowed to cool, weighed to ascertain the weight of MeHg extracted measured and later stored in a refrigerator for further analysis. Vial loading was done by adding prepared samples to 40 ml vials with Teflon® lined septa caps. Samples were buffered to pH 4.9, ethylated with the addition of NaBEt$_4$, topped off with Milli-Q water, capped, shaken and loaded into the autosampler. Sample information was entered into Mercury Guru™ software, and then sample analysis began. With the aid of MERX, MeHg was measured in each extracted fish sample solution.

Sample Preparation Procedure by k$_0$-INAA (K1)

Aliquots of about 0.18 to 0.20 g of air-dried soil samples were weighed and sealed into a pure polyethylene ampoule in triplicates. A sample and a standard, Al-0.1 % Au (IRMM-530R) disc of 6 mm diamond and 0.2 mm high were piled together and fixed in the polyethylene ampoule in a sandwich form. Reference material (BCR-320R) was irradiated with the samples for quality assurance and quality control in the determinations of the elements (Ag, As, Au, Ba, Br, Ca, Cd, Ce, Co, Cr, Cs, Eu, Fe, Ga, Hf, Hg, K, La, Mo, Na, Nd, Rb, Sb, Sc, Se, Sm, Sn, Sr, Ta, Tb, Th, U, W, Yb, Zn, and Zr). The samples were irradiated for 12 hours in the Carousel Facility (CF) of the TRIGA reactor with thermal neutron flux of 1.1 x 10^{12} cm^{-2}s^{-1} (Jaćimović, 2003; Snoj et al., 2011). Subsequent to irradiation, the aliquot was measured after 3, 7-14

and 35 days cooling time on absolutely calibrated High Purity Germanium (HPGe) detectors with 40 and 45 % relative efficiency. HyperLab 2002 program was used for peak area evaluation (HyperLab 2002 System, 2002). Thermal to epithermal flux ratio (f = 27.98) and epithermal flux deviation from the ideal 1/E distribution (α = −0.0076) were used to calculate element concentrations. The elemental concentrations and effective solid angle were calculated by using the software package Kayzero for Windows (KayZero for Windows, 2005). The target radioisotopes with their half-lives during irradiation using the TRIGA MARK II are presented in Table 9.

Table 9: Targeted Radioisotopes with their Half Lives during Irradiation with the TRIGA MARK II using k0-INAA Method

Element	Target Isotope	Formed Isotope	Half life	Element	Target Isotope	Formed Isotope	Half life
Ag	^{106}Ag	^{106m}Ag	8.28d	Mo	^{98}Mo	^{99}Mo	2.75d
As	^{73}As	^{74}As	17.8d	Na	^{23}Na	^{24}Na	15.0h
Au	^{197}Au	^{198}Au	2.70d	Nd	^{139}Nd	^{140}Nd	3.37d
Ba	^{130}Ba	^{131}Ba	11.5d	Rb	^{85}Rb	^{86}Rb	18.6d
Br	^{76}Br	^{77}Br	57.0h	Sb	^{125}Sb	^{126}Sb	12.4d
Ca	^{46}Ca	^{47}Ca	4.54d	Sc	^{46}Sc	^{47}Sc	3.35d
Cd	^{114}Cd	^{115}Cd	53.5h	Se	^{71}Se	^{72}Se	8.40d
Ce	^{133m}Ce	^{134}Ce	3.16d	Sm	^{155}Sm	^{156}Sm	9.40h
Co	^{54}Co	^{55}Co	17.5h	Sn	^{124}Sn	^{125}Sn	9.64d
Cr	^{47}Cr	^{48}Cr	21.6h	Sr	^{81}Sr	^{82}Sr	25.4d
Cs	^{135}Cs	^{136}Cs	13.2d	Ta	^{182}Ta	^{183}Ta	5.10d
Eu	^{151}Eu	^{152m}Eu	9.31h	Tb	^{152}Tb	^{153}Tb	2.34d
Fe	^{51}Fe	^{52}Fe	8.27h	Th	^{233}Th	^{234}Th	24.1d
Ga	^{66}Ga	^{67}Ga	3.26d	U	^{236}U	^{237}U	6.75d
Hf	^{178}Hf	^{179,2m}Hf	25.1d	W	^{177}W	^{178}W	21.6d
Hg	^{203}Hg	^{194m}Hg	41.6h	Yb	^{174}Yb	^{175}Yb	4.19d
K	^{42}K	^{43}K	22.3h	Zn	^{71}Zn	^{72}Zn	46.5h
La	^{139}La	^{140}La	1.68h	Zr	^{88}Zr	^{89}Zr	78.4h

Source: Audi, Wapstra, & Thibault, 2003

Soil Moisture Content Determination Procedure

Grounded soil samples, "Black" and mining wastes put in aluminum foils were weighed and dried to determine moisture content in each sample. The temperature of 105 °C was maintained until a constant mass of sample was achieved. The moisture content of each soil sample was calculated (Equation 64) as the moisture content of the soil as a percentage of the dry soil weight (DSNR, 1990).

$$MC \% = (W_2 - W_3 / W_3 - W_1) \times 100, \tag{64}$$

where W_1 – weight of the Al foil (g)

W_2 – weight of moist soil + foil tin (g)

W_3 – weight of dried soil + foil tin (g)

Sample Preparation in determining pH of Soil

A mass of 1.00 to 1.12 g homogenized soil samples were weighed into vials. A 1:5 soil: 0.01M $CaCl_2$ suspension was prepared to determine pH of the soil samples. The suspension was mechanically shaken for 1 hour at 15 rpm (Rayment et al., 1992). The suspensions were allowed to settle overnight. The pH meter (ID: 000070 MO69: METTLER TOLEDO SEVEN CO PRO pH/ION at 22.4 °C) was calibrated according to the manufacturer instructions by using a buffer at pH 6.86 (Rayment et al., 1992). The pH meter was used to read the pH of each solution and the results were tabulated. The electrode was washed with Milli-Q water in between measurements.

Preparation of Geological samples by Temperature Fractionation

A homemade device (Figure 21) which is made up of a gas cylinder, a flow meter (1 L/min), and a quartz tube was used in this research (Sedlar et al., 2015). About 0.20 g of each sample was weighed into the quartz boat and carefully positioned in the first quartz tube in the middle of the electric tube furnace which was linearly heated from room temperature to 800 °C at a heating rate of approximately 2.2 °C min^{-1}. The second quartz tube was filled with quartz wool kept heated at 800 °C by a small electric furnace to ensure the transformation of all volatile Hg compounds to elemental mercury and to retain any particles that might be released from the sample. A Lumex pyrolysis unit (Pyro 915$^+$) provided an additional decomposition of any remaining volatile mercury compounds that could interfere with the atomic absorption measurements (Sholupov et al., 2004). The elemental mercury was detected by a Lumex Ra-915$^+$ atomic absorption detector, based on Zeeman correction, which was connected directly to a computer for data collection. A trap containing H_2SO_4–$KMnO_4$ solution was connected to the exhaust from the Lumex Ra-915$^+$ to retain Hg(0) in solution by oxidation and to quantitatively trap recover mercury released from the sample this was used to assess the mass balance. Two parameters were controlled: the temperature of the sample at which the maximum mercury release peak was obtained, and the peak height/area. Figure 21 is a schmematic line for Temperature Fractionation by CVAAS method.
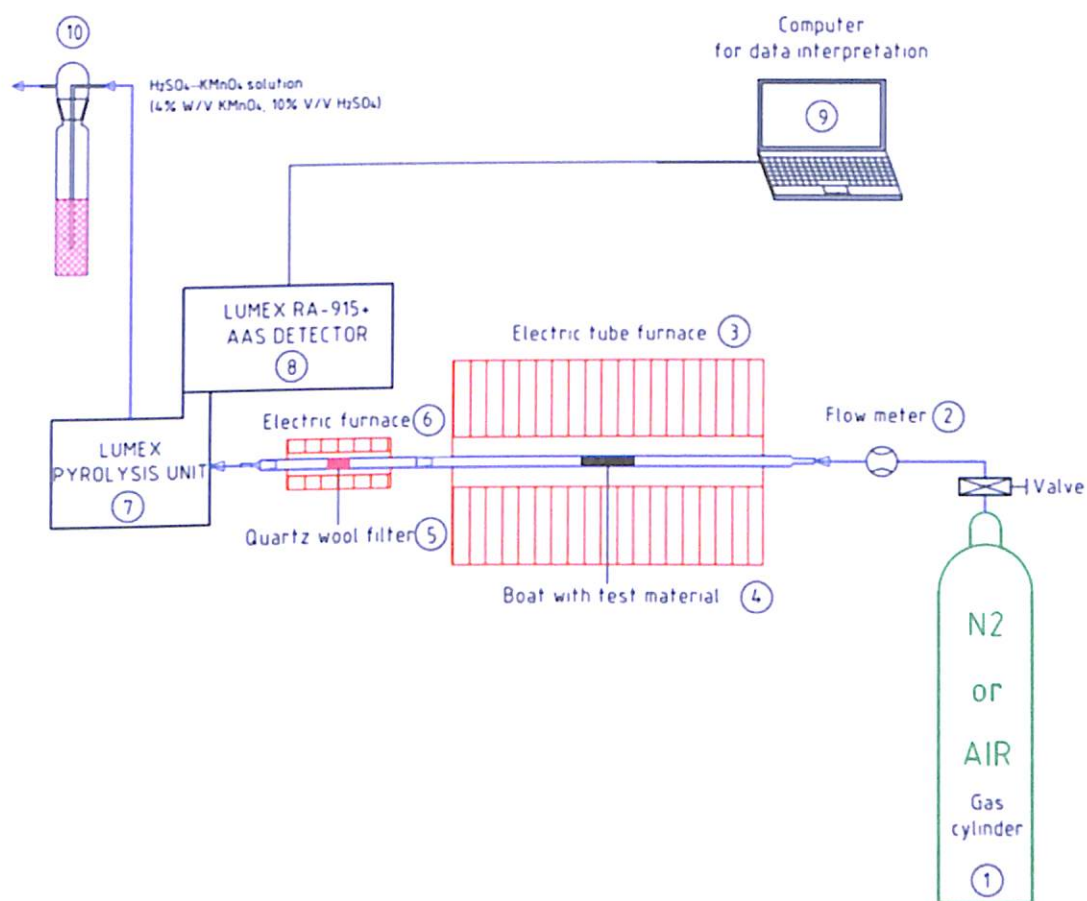
Figure 21: Scheme for measuring line
Source: Sholupov et al., 2004

The RA-915^{+} Mercury Analyser with PYRO-915^{+} pyrolyser was developed for direct mercury determination without pre-treatment procedures. Using the RA-915^{+} spectrometer with background correction and the PYRO-915^{+} pyrolser, two-chamber catalyst atomizer allowed direct mercury analysis of complex-matrix samples (Sholupov et al., 2004).

Test procedure for CVAAS using Automated Mercury Analyzer

A fixed volume V ml (maximum of 10 ml) of blank test solution, standard test solution, reference material test solution, and test solution was gently transferred into the reaction vessel of the mercury analyzer using a pipette (Eppendorf). With the aid of the accessory dispenser, 1 ml of 10 %

stannous chloride ($SnCl_2$) solution was added and the start bottom was pushed. The diaphragm pump ran and the generation of elemental mercury vapour circulated through the 4-way cock between the reaction vessel and the acidic gas which was trapped for 30 seconds to homogenize the concentration in the gas phase. The acidic gas generated from the sample test solution was collected in the alkaline solution. After 30 seconds, the 4-way cock turned automatically by 90 °C, which introduced the mercury vapour into the photoabsorption cell through an ice bath for measurement of the absorbance at 253.7 nm for the determination of total mercury quantity. The readings of the recorder increased sharply and decreased with a sharp peak. As the recorder readings began to decrease, the cock was opened on the lower part of the reaction vessel to discard the solution and was closed again which allowed aerating until it returned to the baseline. The procedure was repeated for the other measurements (Akagi et al., 1991). Figure 19 shows a schematic diagram of Reduction/Cold Vapor Atomic Absorption Spectrometry (CVAAS) Circulation-Open Air Flow System that was used in the determination of total mercury (Tsuguyoshi, 2004).
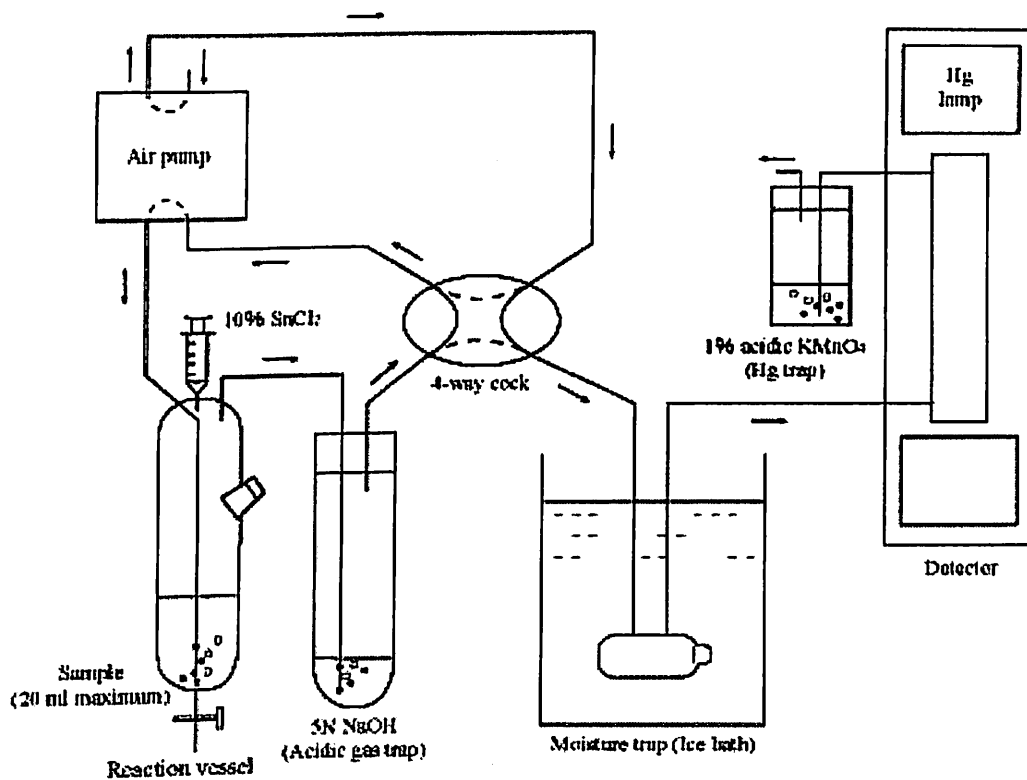
Figure 22: Schematic Diagram of Reduction/Cold Vapor Atomic Absorption Spectrometry (CVAAS) (Circulation-Open Air Flow System) for Total mercury determination

Source: Tsuguyoshi, 2004

The calculation of the THg concentration (μg/g of dry weight) in the sample is by using the peak heights (mm) obtained after measurement of the fixed volumes V ml (usually 5 ml, maximum 10 ml) of the each blank, the standard and the samples test solutions or the diluted solutions. The total mercury concentration (μg/g of dry weight) in the samples is calculated by the following formula:

Total mercury concentration in the sample (μg/g) = 0.10 μg ×

(Ps – Pbl)/(Pstd – Pbl) × dilution factor × 1/sample weight (g) ×

WW/DW,

where:

WW/DW: ratio of wet weight/dry weight

Pbl - Blank

111

Pstd - Standard

Ps - Sample test solution

Statistical tools used in this Study

The mean with the standard deviation (*std*) or Percentage Relative Standard Deviation (% RSD) was used to determine the central tendency of each result in this study. The minimum, maximum, and the range were also used to know how widely spread the data was. In determining the correlations between the THg and depth of both soil and sediment. The SPSS version 21 was used to determine the Partial and normal correlations (Pearson correlation) between total mercury (THg) and other elements concentrations in the Pra River Basin. The pH and percentage Moisture Content (% MC) were used as controlled variables in determining the partial correlations between THg concentration and other elements (As, Br, Cs, Hf, Se, Zr, Ba, Th, U, Sr, Sb, Rb, Sc, Ce, Eu, La, Nd, Sm, Tb, Yb, Fe, Na, K, Ca, Zn, Mo, Ag, Co, Cr, Ga, Ta, W, and Au) in the soil (0-1 cm) from the Pra River Basin. In all the correlations determined, *p-values* generated were used to determine how significant the results are. Anderson Darling test was also used to determine the normality of the distribution of the data and in case where the distribution is highly skewed, the data were log transformed to reduce the skewness of the data. Bland and Altman's plot were used to show the lower limit, upper limit and the mean difference between M1 and K1. Microsoft Excel software (2007) was used in graphically presenting the data (pie charts, bar charts, and line graphs).

The qualitative analysis involves the determination of the various elements in the fish samples by the identification of the spectra peaks and assigning corresponding radionuclides and hence the elements present. The quantitative analysis involves the calculation of the areas under the peaks of the identified elements and converting them into concentrations using an appropriate software or equation(s). The qualitative analysis was achieved by means of ORTEC EMCAPLUS Multi-Channel Analyzer (MCA) Emulation software. The quantitative measurements were done using the concentration equation (equation 53) in Microsoft Excel programme for calculating the elemental concentrations.

Quality of Analysis for M1, M2, and K1

The concentrations of THg of soil, sediments, carnivorous and herbivorous fish muscle and skin, mining waste and "black" samples were analysed in the Environmental Science Department labs, Institute of Jožef Stefan, Slovenia with Automatic mercury analyzer 201 after digestion of about 0.20 g with M1 ($HNO_3/HClO_3/H_2SO_4$ wet acid digestion), and M2 ($HNO_3/HF/HCl$). Validation of digestion with M1 and M2 were determined using k_0 methods using selected soil samples ($n = 20$).

Analytical sets of samples include soil samples ($n = 120$), sediment samples ($n = 210$), carnivorous fish muscles ($n = 20$) and skin ($n = 20$), herbivorous fish muscle ($n = 16$) and skin ($n = 16$), mining waste samples ($n = 34$), "black" samples ($n = 12$) and three (3) certified reference materials BCR 580R ($n = 53$), BCR 277R ($n = 45$), BCR 320R channel Sediment ($n = 3$), DORM 4-Hg ($n = 26$), and DORM 4-MeHg ($n = 4$) for quality analysis (QA).

To test for Quality Assurance (QA), accuracy, and precision were calculated. Accuracy of the analysis was estimated by calculating the absolute value of the Relative Error (RE) of the reference materials which was expressed as a percentage using the average value of the analyzed BCR measurements ($\bar{X}$) and referenced values (X_R) in equation (65)

$$|RE| = \frac{X_R - \bar{X}}{X_R} * 100 [\%] \qquad (65)$$

The precision of the analysis was predicted by calculating the relative standard deviation (RSD) expressed as a percentage using the standard deviation (stdev) and the average value of the analyzed BCR measurements ($\bar{X}$) in equation (66)

$$RSD = \frac{stdev}{\bar{X}} * 100 [\%] \qquad (66)$$

The accuracy and precision were estimated as good from 0-10 %, acceptable from 10 to 20 % and insufficient from >20 %. Also, recovery of CRMs were calculated using equation (67)

$$\% Recovery \frac{\bar{X}}{X_R} * 100 \qquad (67)$$

Recovery between 80 and 120 are acceptable. Also, the precision of the analysis was additionally tested by means of a double analysis, for which the random soil replicate samples ($n = 20$), sediment samples ($n = 21$).

Chapter Summary

Chapter three (3) gave information about the study geographical areas with various activities. Also, detailed information about materials, and methodology used to achieve the objectives were given. The descriptions of obtaining primary data and the various procedures and methods that were

undertaken for further analysis were also described. Finally, the statistical methods used in general and to check for quality assurance were also dealt with in this chapter.

CHAPTER FOUR

RESULTS AND DISCUSSION

Introduction

The results of THg concentrations in reference materials, soil profiles, sediment cores, mining wastes, "Black", and carnivorous and herbivorous fish muscles and skin are presented in this chapter. Also, methylmercury concentrations in both carnivorous and herbivorous fish muscle, mercury speciation results in soil (0-1 cm) are also presented in this chapter. Some results of other elements are also presented and discussed.

Quality Assurance and Quality Control

The accuracy and precision of measurements and instruments were estimated by the calculations (Table 10) of different certified reference materials; BCR 277R (THg), BCR 580 (THg), DORM 4 (THg and MeHg), BCR 320R (Hg, Co, Cr, Fe, Sc, Th, U, Zn and As). Both precision and accuracy were good or acceptable for all the elements. Therefore, the reliability of the chemical analysis was considered satisfactory and the results were used for further statistical and special analysis. Also, the accuracy of the analysis was tested using recovery and in all cases was satisfied as BCR 277R was between 100-101 %, BCR 580 was between 99.2-111 %, BCR 320R was 98.1-106 %, DORM 4 for THg was between 86.7-90.3 %, and DORM 4 for MeHg was 97.4 %.

In soil, the average RPD % values (n = 20) using M1 procedure (HNO$_3$/HClO$_3$/H$_2$SO$_4$) for THg were good and satisfactory in seventeen sampling sites except in SS5 (Akim Oda) was 29.6 %, SS8 (Kwahu Praso)

116

was 965 % and SS18 (Daboase) was 39.1 % whilst all the same soil samples

(n = 20) had good and satisfied precision using M2 (HNO_3/HF/HCl). RPD %

for sediment for both M1 (63.2 %) and M2 (41.8) in SSD19 (Beposo sampling

site) were not satisfactory and this indicates inhomogeneity of the sediment.

Also, RPD % for SSD9 (Apreja sampling site) was 44.9 %, SSD11 (Wobiri

sampling site) was 20.4 % for M1 and SSD1 (Dadientem sampling site) was

31.1 %, SSD20 (Anlo sampling site) was 36.2 % for M2. All RPD % for both

carnivorous and herbivorous fish muscle and herbivorous fish skin were good

and satisfactory except carnivorous fish skin for SS20FC_S (Anlo sampling

site) which was 27.0 % and SS21FC_S (Shama sampling site) was 25.6 %.

Table 10 represents the names of Certified Reference Materials (CRM) used in

this Research with their actual values, measured values (mean concentrations

(mg/kg), Std, uncertainties (Uc), percentage (%) recovery, number of Analysis

(n), Relative Error (RE), Relative Standard Deviation (RSD). Also Table 11

gives the Relative Percentage Difference (RPD %), Values of THg

Concentrations in the primary and duplicate soil (M2), sediments (M2),

carnivorous, and herbivorous fish muscle and skin samples.

Table 10: Certified Reference Materials used in this Research with their Actual Values, Measured Values (mean concentrations (mg/kg), Std, Uncertainties (Uc), Percentage (%) Recovery, Number of Analysis (n), Relative Error (RE), Relative Standard Deviation (RSD)

Certified Reference Material (CRM)	Actual (mg/kg)		Measured						RE %	RSD %	Sample
	Mean	Std	Mean	std	Uc.	% Recovery	n	Method			
BCR 277R (THg)	0.128	0.017	0.129	0.004	0.002	101	80	M1	-0.78	3.10	Soil
			0.128	0.012	0.002	100	84	M1	0.00	9.38	Sediment
			0.128	0.012	0.005	100	16	M1	0.00	9.38	"Black"
BCR 580R (THg)	132	3.00	131	10.0	2.55	99.2	80	M2	0.76	7.63	Soil
			131	10.0	2.55	99.2	84	M2	0.76	7.63	Sediment
			141	6.30	0.88	107	16	M2	-6.82	4.47	Black
			146	16.0	7.44	111	23	M1	-10.6	11.0	Mining Waste
			149	9.93	4.42	113	23	M2	-12.9	6.66	Mining waste
DORM 4(THg)	0.412	0.036	0.357	0.012	0.003	86.7	28	M1	13.3	3.36	Herbivorous fish muscle
			0.362	0.015	0.003	87.9	24	M1	12.1	4.14	Canivorous fish muscle
			0.371	0.016	0.005	90.1	28	M1	9.95	4.31	Herbivorous fish skin

Table 10 Cont'd

Certified Reference Material (CRM)	Actual (mg/kg) Mean	Std	Measured Mean	std	Uc.	% Recovery	n	Method	RE %	RSD %	Sample
			0.376	0.010	0.005	90.3	24	M1	8.74	2.66	Canivorous fish skin
DORM 4(MeHg)	0.355	0.028	0.345	0.036	0.028	97.2	8	CVAFS	2.82	10.4	Canivorous and Herbivorous fish muscle
BCR 320R (Hg)	0.850	0.09	0.854	0.056	0.09	105	3	k_0-INAA	-0.50	6.56	Soil (0-1 cm)
Co	9.70	0.60	10.0	0.14	0.01	103	3	k_0-INAA	-3.09	1.40	Soil (0-1 cm)
Cr	59.0	4.00	61.5	0.85	0.18	104	3	k_0-INAA	-4.24	1.38	Soil (0-1 cm)
Fe	25700	1300	25941	518	66978	101	3	k_0-INAA	-0.94	2.00	Soil (0-1 cm)
Sc	5.20	0.40	5.34	0.10	0.002	103	3	k_0-INAA	-2.69	1.89	Soil (0-1 cm)
Th	5.30	0.40	5.39	0.01	1.25E-05	102	3	k_0-INAA	-1.70	0.19	Soil (0-1 cm)
U	1.56	0.20	1.53	0.02	0.0001	98.1	3	k_0-INAA	11.9	1.31	Soil (0-1 cm)
Zn	319	20.0	330	4.95	6.13	103	3	k_0-INAA	-3.45	1.50	Soil (0-1 cm)
As	21.7	2.00	23.0	0.07	0.003	106	3	k_0-INAA	-5.99	0.30	Soil (0-1 cm)

NOTE: a denotes total mercury (THg) concentration in DORM 4, and b denotes methylmercury (MeHg) in DORM 4.
Source: Author Analysis, 2015

Table 11: Relative Percentage Difference (RPD %) Values of THg Concentrations in Primary and Duplicate Soil (M2), Sediments (M2), Carnivorous and Herbivorous Fish Muscle and Skin Samples

Soil Sample (0-6 cm)	Duplicate Sample	THg M1	THg M2	Sediment Sample (0-10 cm)	Duplicate sample	THg M1	THg M2	Fish samples	Duplicate Sample	THg
SS1	SS1D	12.1	12.9	SSD1	SSD1D	11.6	31.1	SS12FC_M	SS12FC_MD	1.59
SS2	SS2D	11.5	3.40	SSD2	SSD2D	6.78	1.71	SS13FC_M	SS13FC_MD	2.32
SS3	SS3D	12.8	2.90	SSD3	SSD3D	9.01	6.44	SS16FC_M	SS16FC_MD	7.31
SS4	SS4D	15.3	16.4	SSD4	SSD4D	9.39	9.70	SS17FC_M	SS17FC_MD	2.37
SS5	SS5D	29.6	5.30	SSD5	SSD5D	5.07	0.89	SS18FC_M	SS18FC_MD	2.70
SS6	SS6D	14.4	0.31	SSD6	SSD6D	7.71	2.70	SS20FC_M	SS20FC_MD	6.87
SS7	SS7D	10.3	5.71	SSD7	SSD7D	14.6	7.66	SS21FC_M	SS21FC_MD	7.97
SS8	SS8D	965	0.57	SSD8	SSD8D	34.5	3.48	SS12FC_S	SS12FC_SD	5.25
SS9	SS9D	3.31	0.82	SSD9	SSD9D	44.9	2.66	SS13FC_S	SS13FC_SD	2.32
SS10	SS10D	16.3	3.14	SSD10	SSD10D	19.4	10.8	SS16FC_S	SS16FC_SD	19.8
SS11	SS11D	11.5	11.3	SSD11	SSD11D	20.4	10.1	SS17FC_S	SS17FC_SD	15.0
SS12	SS12D	14.6	1.71	SSD12	SSD12D	13.4	1.94	SS18FC_S	SS18FC_SD	14.6
SS13	SS13D	18.7	0.59	SSD13	SSD13D	1.28	1.60	SS20FC_S	SS20FC_SD	27.0
SS14	SS14D	19.5	0.50	SSD14	SSD14D	16.8	15.5	SS21FC_S	SS21FC_SD	25.6
SS15	SS15D	7.00	0.53	SSD15	SSD15D	10.2	9.12	SS12FH_M	SS12FH_MD	3.73
SS16	SS16D	8.02	0.53	SSD16	SSD16D	16.9	3.42	SS16FH_M	SS16FH_MD	5.46

Table 11 Cont'd

Soil Sample (0-6 cm)	Duplicate Sample	THg M1	THg M2	Sediment Sample (0-10 cm)	Duplicate sample	THg M1	THg M2	Fish samples	Duplicate Sample	THg
SS17	SS17D	-	-	SSD17	SSD17D	8.92	3.53	SS17FH_M	SS17FH_MD	4.78
SS18	SS18D	39.1	1.44	SSD18	SSD18D	6.96	5.15	SS18FH_M	SS18FH_MD	1.75
SS19	SS19D	9.29	4.39	SSD19	SSD19D	63.2	41.8	SS20FH_M	SS20FH_MD	0.21
SS20	SS20D	7.23	8.68	SSD20	SSD20D	17.0	36.2	SS21FH_M	SS21FH_MD	15.4
SS21	SS21D	13.2	6.05	SSD21	SSD21D	19.2	16.6	SS12FH_S	SS12FH_SD	11.8
								SS16FH_S	SS16FH_SD	6.80
								SS17FH_S	SS17FH_SD	17.9
								SS18FH_S	SS18FH_SD	7.97
								SS20FH_S	SS20FH_SD	19.7
								SS21FS_S	SS21FC_SD	2.23

NB: The detection limits using k_0INAA for the multielemental analysis of the thirty six (36) elements are as follow: Ag, 1.97 mg/kg; Au, 0.0004; Ba, 286; Br, 29.0; Ca, 14213; Cd, 1.29; Eu, 0.30; Fe, 3112; Ga, 17.0; Mo, 0.80; Se, 0.37; Sn, 17.3; Sr, 28.3; U, 0.3; and W, 0.70. The following; Ce, Co, Cr, Eu, Hg, K, Na, Nd, Rb, Sb, Sc, Sm, ta, Tb, Th, Yb, Zn, and Zr had their concentrations below detection limit with this method.
Source: (Author Analysis, 2014)

This result, which is made up of M1, M2, and K1, are presented in APPENDIX H. To test the validity of the two digestion procedures (M1 and M2), three statistical tests were used to improve accuracy. The tests are paired *t-test*, Limit of agreement (Bland & Altman plot) and Reliability test using Interclass Correlation Coefficient (ICC).

Soil pH along the Pra River Basin, Ghana

Adsorption of metals, including Hg species into organic and inorganic surfaces normally decreases with a decreasing pH because of the competition of H^+ with the Hg (Sherene, 2010). The pH of the soil and mining waste samples from the Pra River basin were determined and presented in Appendices A, B, and C, and will be discussed in this chapter.

Along the Birim River, Kibi sampling site (upstream) gave a pH ranging between 4.03 and 4.16 ($n = 6$) which was acidic. Also, a strong negative correlation of 0.89 ($n = 6$, *p-value* = 0.02) between the depths (0-1 cm, 1-2 cm, 2-3 cm, 3-4 cm, 4-5 cm, and 5-6 cm) and the pH of the various soil profiles was significant. The pH in this sampling site, showed an extremely strong acidic soil according to the Soil Survey Manual (2011) and a significantly strong negative correlation indicating downward vertical distribution of extremely strong acidic soil along the soil profile. At the downstream of the Birim River, Akim Oda gave a range of pH from 8.18 to 8.34 ($n = 6$) that falls within moderately alkaline soil on the Soil Survey Manuel (2011) pH range. The correlation at this site was moderate 0.60 ($n = 6$, *p-value* = 0.21) for the depths (0-1 cm, 1-2 cm, 2-3 cm, 3-4 cm, 4-5 cm, and 5-6 cm) and the pH of the soil profile, which is not significant.

In the main Pra River Basin, Twifo Praso sampling site gave more acidic soils with a pH ranging from 4.08 to 5.25 ($n = 6$) along the soil profiles with significantly (*p-value* = 0.00) perfect negative correlation of 0.99 ($n = 6$) between the depth and pH of the soil profile ($n = 6$). Also, Shama sampling site gave an alkaline pH which ranges between 8.74 and 9.03 ($n = 6$). Shama is a town coastal town and the direction of the wind from the sea to the land may have influenced the pH of the soil profile along this sampling site. A moderate correlation of 0.38 ($n = 6$, *p-value* = 0.46) was established between the depth and pH of the soil profile which was not significant.

Nnoboamu and Wobiri sampling sites are located along the Anum River, one of the tributaries of the Pra River Basin and the two sampling sites gave a range of pH of 5.03 to 6.23 ($n = 6$) and 5.19 to 5.73 ($n = 6$) at Nnoboamu and Wobiri respectively. The pH at Nnoboamu ranges from strongly through to slightly acid. Also, the soil at Wobiri sampling site presented pH range between strong to moderate acidic soil pH. Both soils from Nnoboamu and Wobiri sampling sites gave significantly very strong negative correlation of 0.94 ($n = 6$, *p-value* = 0.01) between depth (0-1 cm, 1 - 2 cm, 2-3 cm, 3-4 cm, 4-5 cm, and 5-6 cm) and pH of the vertical soil profile showing a downward increase in acidity along both profiles which were both significant. This showed that, the topsoil (0-1 cm) was less acidic as the depth was increasing from 1-2 cm, 2-3 cm, 3-4 cm, 4-5 cm, and 5-6 cm.

Among the three (3) sampling sites from the Offin River Basin used in this research, Nkontinso gave a pH range which ranges from 3.89 to 4.49 ($n = 6$) showing extremely to very strongly acidic soil along the profile from the 0 to 6 cm depth. The correlation between the pH and the depth of the soil profile

was a strong negative correlation of 0.94 ($n = 6$, *p-value* = 0.01) which was significant showing increase in acidity along the vertical soil profile. Dunkwa-On-Offin (1) sampling site gave pH that was neutral to slightly neutral along the soil profile which ranges between 7.43 and 7.85 ($n = 6$). The correlation was negative and moderate 0.60 ($n = 6$, *p-value* = 0.208) between the depth and pH of the soil profile but insignificant. Even though the soil pH showed an alkaline property, the pH did not increase or decrease along the vertical profile but the pH were distributed in various degrees along the profile.

All the pH of the six (6) mining wastes which were sampled from six (6) pits from Dunkwa-On-Offin (1) sampling site exhibited alkaline properties. with the most alkaline 8.60 to 8.90 (SS13S–B sample; $n = 6$, $r = 0.94$, *p-value* = 0.005) and the least range of alkaline as 7.46 to 7.54 (SS13S-E; $n = 6$, $r = 0.68$, Among the twelve (12), "Black" four samples from Dunkwa-On-Offin (1) sampling site showed pH range from slightly acid (6.47 from sampling site C), neutral (7.13 from sampling site A), and slightly alkaline (7.51 and 7.56 from sampling site B and D respectively).

Many heavy metals become more water-soluble under acid conditions and can permeate through the soil profile and in some cases get into aquifers, surface streams, or lakes (Mulligan, Yong, & Gibbs, 2001). The soil pH along the Basin was basically acidic and the acidity increased downwards as the soil profile depth from 0-6 cm. Out of the twenty (20) soil profile (0-6 cm) tested for pH ranges, fourteen (14) sampling sites (Dadientem, Kibi, Adonkrono, Kade, Akim Oda (Old), Twenedurase, Kwahu Praso, Anlo, Apreja, Twifo Praso, Beposo, Nnoboamu, Wobiri, and Nkontinso) had

stronger correlations (p < 0.05) and in all soil pH acidity increased with depth along the soil profiles (0-6 cm).

Percentage Moisture Content of Soil (Air Dried) from Pra River Basin

Percentage Moisture Content (% MC) of all the soil samples from the Pra River Basin were determined and presented in Appendix E. The soil profiles (0-6 cm) from the Birim River Basin gave the highest % MC of 3.35 ($n = 36$, 4-5 cm) which was recorded at Dadientem sampling site, the upstream of the Birim River whilst the least % MC of 0.06 ($n = 36$, 0-1 cm) was recorded at Akim Oda (Old) sampling site at the downstream of the Birim River. The main Pra River had 3.53 ($n = 54$, 1-2 cm) as the highest % MC in soil which was recorded at Twenedurase sampling site (Upstream of the Pra River) and the 0.44 ($n = 54$, 1-2 cm) was recorded at Twifo Praso sampling site. The soil profile from the Offin River Basin gave the highest % MC to be 1.33 ($n = 18$, 1-2 cm) recorded at Nkontinso sampling site and Dunkwa-On-Offin (1) sampling site gave the least % MC to be 0.10 ($n = 18$, 5-6 cm). Also, the highest % MC (0.97, $n = 12$, 2-3 cm) of the soil profile from the Anum River was recorded at Nnoboamu sampling site with Wobirin sampling site recording the least % MC (0.39, $n = 12$, 0-1 cm).

Physiochemical properties of Water along Pra River Basin

The physiochemical properties of the water at each point of sampling sediments corer (0-10 cm) along the Pra River Basin in this study are represented in Table 11. In water, methylmercury (MeHg) is influenced by many factors which include temperature, pH, redox potential, the presence of

inorganic and organic complexing agents, total microbial activity and the concentration of bioavailability of Hg (Bravo et al., 2014). In this study, the pH of the water sample from the Pra River Basin ranges from 5.37 to 7.22 (n = 20, std = 0.38, $mean$ = 6.76) which is acidic to neutral. The least pH (5.37) was recorded at the Twenedurase sampling site, the upstream of the main Pra River. Five (5) sampling sites; Anlo, Shama, Dunkwa-On-Offin (1), Nkontinso, and Nnoboamu sampling sites gave neutral pH with the remaining fourteen (14) giving acidic pH. The dissolved oxygen (DO) of the Pra River ranges between 3.91 to 6.47 mg/L (n = 18, std = 1.11, $mean$ = 4.64) with the highest DO registered at the Twenedurase (upstream of the Pra River Basin) sampling sites whilst the least DO was recorded at Kwahu Praso sampling site. The conductivity of the water from the main Pra River Basin at the points of sampling river sediment ranges between 52.4and 153 µs/cm (n = 18, std = 35.2, $mean$ = 137). The highest conductivity of the river water at the Pra River Basin was recorded at Kwahu Praso (upstream of the Pra River Basin) sampling site, whilst the least conductivity was registered at Twenedurase (upstream of Pra River Basin) sampling site. Another physiochemical property that was determined was Total Dissolved Solid (TDS). The range of TDS of the river water in the Pra River Basin was between 27.9 and 78.3 ppm (n = 18, std = 17.9, $mean$ = 71.1). The maximum TDS of the river water was recorded at Nnoboanu sampling site, whilst the minimum TDS of the river water was registered at Twenedurase sampling site. Also the salinity of the river water at each sampling sites was determined. Salinity ranges between 32.3 and 78.3 ppm (n = 18, std = 17.2, $mean$ = 71.1). Nnoboamu sampling site gave the highest salinity; meanwhile Twenedurase sampling site gave the least salinity

in the Pra River Basin. Temperature at each sampling sites was noted and the range of temperature was from 22.5 to 27.6 °C ($n = 20$, $std = 2.39$, $mean = 26.7$). The least temperature of the River water at the point of sampling the river sediment core was registered at Twenedurase sampling site. However, the highest temperature of the river water in the Pra River Basin was registered at Kade sampling site from the Offin River Basin. The water depth at each sampling points at the banks of the rivers ranges from 2.50 to 8.20 m ($n = 20$, $std = 1.58$, $mean = 5.32$) respectively. The methylation of fish living in these catchment areas may be affected by physiochemical properties of the water. The physiochemeical properties of the water at each sampling sites including their names are presented in Table 12.

Table 12: Physiochemical Properties, Names of Sampling Sites for Water Samples from the Pra River Basin, Ghana

Sampling Sites	pH	DO (mg/L)	Conductivity (µs/cm)	TDS (ppm)	Salinity (ppm)	T (°C)	Water Depth (m)
Dadientem	6.71	4.06	150	77.6	77.7	23.1	3.80
Kibi	6.70	4.06	138	72.2	73.4	23.7	4.60
Adonkrono	6.69	4.32	100	52.4	54.6	27.4	7.00
Kade	6.73	4.91	105	55.4	57.6	27.6	6.20
Akim Oda (old)	6.79	4.99	107	56.9	58.0	26.2	5.10
Akim Oda	6.84	5.01	110	57.6	58.9	26.1	5.00
Twenedurase	5.37	6.47	52.4	27.9	32.3	22.5	3.40
Kwahu Praso	6.66	3.91	153	72.0	72.0	23.7	5.60
Apreja	6.95	4.14	134	70.2	70.4	24.2	5.40
Nnoboamu	7.16	4.51	150	78.3	78.3	27.3	6.80
Wobiri	6.58	4.09	142	76.4	73.9	27.2	2.50
Nkontinso	7.09	6.48	176	92.1	91.6	31.0	8.20
Dunkwa-On-Offin (1)	7.22	6.05	195	101	100	29.7	5.80
Dunkwa-On-Offin (2)	6.81	5.98	198	100	99.8	29.7	7.60
Assin Praso	6.96	3.81	122	57.0	59.0	26.1	5.00
Twifo Praso (1)	6.86	3.73	125	65.5	54.6	28.9	7.00

Table 12 Cont'd

Sampling Sites	pH	DO (mg/L)	Conductivity (μs/cm)	TDS (ppm)	Salinity (ppm)	T (oC)	Water Depth (m)
Twifo Praso (2)	6.80	5.90	128	67.6	68.2	28.6	4.20
Daboase	6.72	2.59	158	82.4	83.2	26.6	2.80
Beposo	6.77	3.22	169	87.5	88.1	27.4	5.00
Anlo	7.20	-	-	-	-	29.1	4.00
Shama	7.60	6.81	-	-	-	26	2.10
Mean	6.82	4.64	137.49	71.05	71.14	26.8	5.32
Std	0.41	1.11	35.22	17.92	17.21	2.34	1.67

Source: (Author Data, 2013)

129

Meeting assumptions of tests

The paired t–test assumes that the differences between pairs are normally distributed and the test is not very sensitive to deviations from normality, so unless the deviation from normality is really obvious, it could still be used. The paired difference between M1 and K1 from APPENDIX H yielded a normal distribution with a mean of -3.334 μg/g and standard deviation of 3.099 μg/g with a *p-value* 0.425 using the Anderson-Darling test of normality (Thode Jr., 2002). Again from APPENDIX H, a similar test done between M2 and K1 yielded non normal distribution. A log transformation was conducted for the M2 and K1 and the difference yielded a slightly skewed distribution (skewness -0.31) and a *p-value* of 0.04 (at 95 % confidence) which is significant. The Limit of agreement test has similar assumption as the paired *T-test* and hence the above test also applies.

For the reliability test, the variable must be normally distributed. Anderson-Darling test of normality for M1, M2 and K1 indicate a non -normal distribution with all *p value*<0.05. Inverse cube root transformation was performed on M1, M2 and K1 which yielded a normal distribution (using Anderson-Darling test of normality) with *p-values* 0.548, 0.074 and 0.326 respectively.

Statistical Analysis of Total Mercury using M1 and K1

M1 produced results between 1.884 to 4.785 mg/kg less than the validating method K1, at an average difference of -3.334 (3.334 less than the validating method). The limit of agreement fell between -9.41 to 2.73 mg/kg. The 95 % confidence interval for the lower bound ranges from -3.6380 to -

15.19 mg/kg and the upper bound ranges from -3.04 to 8.51 mg/kg. Figure 23

shows a Bland and Altman plot for M1 and K1 showing lower limit, an upper

limit and the mean difference for M1 and K1. Figure 20 shows the Bland &

Altman plot between M1 and K1 showing the lower, upperlimits and the mean

difference between M1 and K1.

Bland & Altman Plot for M1 and K1
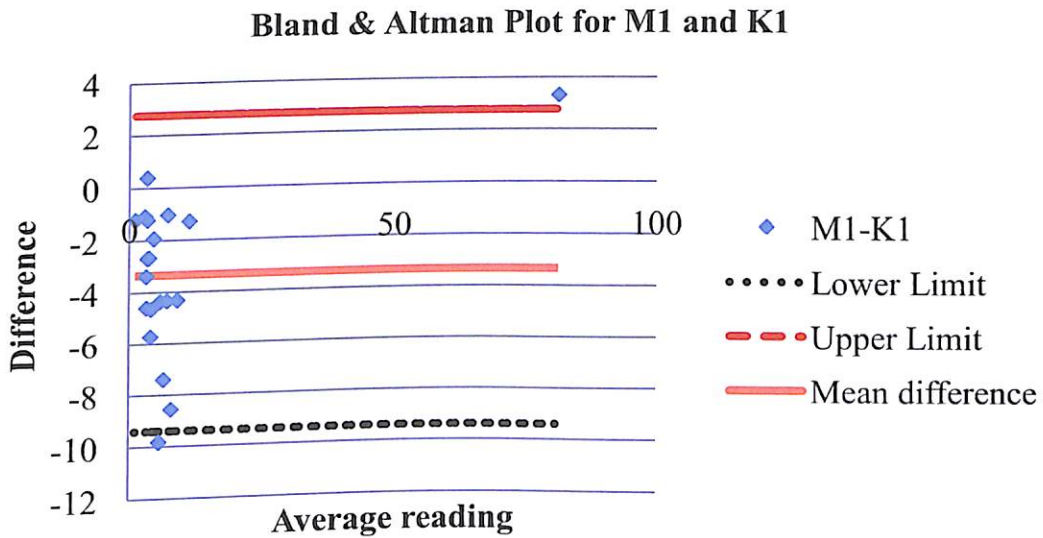
Figure 23: A graph showing the Lower, Upper Limits and the Mean difference
between M1 and K1

Reliability test performed yielded a moderate interclass correlation

coefficient (ICC), 52.2 % but at a wider confidence interval, -21.8 to 82.0.

The possibility of a zero ICC in the 95 % confidence interval suggests the

possibility of no agreement between the two measurements.

A paired *T-test* analysis with the hypothesis below was performed

Ho: M1 = K1

Ha: M1 ≠ K1

The *T- value* of -4.81 and a corresponding *p-value* of 0.00 (at 95 %

confidence) were obtained. This implies that we reject the null hypothesis and

concluded that there was no statistical agreement between the two

measurements (M1 and K1).

131

Statistical analysis of Total Mercury using M2 and K1

M2 produced results between 0.992 to 1.16 mg/kg more than the validating method K1, at an average difference of 1.07 mg/kg. The limit of agreement was 1.069 to 1.075. Since on the logarithms scale there are no units, the result indicates that M2 may be greater than K1 by 6.9 % to 7.5 %. A reliability test performed yielded a high interclass correlation coefficient, 98.4% with a narrower confidence interval, 95.9 to 99.4. This indicates that statistically, there is an excellent agreement between the two methods (M2 & K1).

A paired T- test analysis with the hypothesis below was performed

Ho: M2 = K1

Ha: M2 ≠ K1

The T-value obtained was 1.88 and a *p-value* of 0.075 (at 95 % confidence). This implies that we fail to reject the null hypothesis and concluded that there was a statistical agreement between the two measurements. M2 is a combination of 5ml (2:1) HNO_3/HF + 1 ml HCl digestion and HNO_3/HF dissolves silica matrices due to the presence of HF, therefore, THg was totally digested into solution for further analysis by CVAAS (Gaudino et al., 2007). This may be due to the fact that, there are binding elements and organic compounds which may be present in the geological samples from the Pra River Basin which made the matrix a difficult one for normal acid digestion (1 ml Milli-Q H_2O + 2 ml (1:1) $HNO_3/HClO_4$ + 5 ml H_2SO_4) for total digestion of THg in the samples for CVAAS analysis. The soil in the Pra River Basin is tropical soil, for which Fe and Al hydroxide minerals play a very vital role in binding Hg (Lacerda, de Souza, & Riberio,

2004; Roulet et al., 1998; Semu, Singh, Selmer-Olsen, 1987). Also, weathered

oxisols (laterites) contain high concentrations of Fe and Al hydroxides. In this

studies Fe content in the topsoil (0-1 cm) was high and Spear Rho correlation

drawn between Fe and THg in the soil gave a strong positive correlation of

0.67 with p<0.05 ($n = 20$, *p-value* = 0.001) which was very significant which

presupposed that, Fe increase with Hg levels in the Pra River Basin.

Table 13: Mean Concentration of Total Mercury (mg/kg) in 1cm Sections of Vertical Soil (Air dried mass) profile between a Depth of 0-6 cm, Using M2 (n = 4) for CVAAS and k0-INAA Methods (n = 3) from Twenty (20) Sampling Sites along the Pra River Basin, Ghana

| Name of Sampling site | M2 for CVAAS | | | | | | | | | | K1 |
| | Mean THg (mg/kg) in Soil Profile depth (cm) (n = 4) | | | | | | Min. (n = 6) | Max. (n = 6) | Range | %RSD | Mean THg mg/kg (n = 3) |
	0-1	1-2	2-3	3-4	4-5	5-6					0-1 cm
Dadientem[B]	11.1	3.32	4.42	3.86	4.20	5.44	3.32	11.1	3.32-11.1	8.73	11.9±0.50
Kibi[B]	9.25	8.42	7.83	7.67	6.54	7.83	6.54	9.25	6.54-9.25	0.71	8.00±0.30
Adonkrono[B]	6.27	6.17	8.91	6.05	7.35	7.83	6.05	8.91	6.05-8.91	2.26	5.54±0.20
Kade[B]	11.9	6.53	10.2	8.85	9.04	7.32	6.53	11.9	6.53-11.9	1.94	10.2±0.40
Akim Oda[B]	1.77	3.55	3.48	1.83	3.53	2.29	1.77	3.55	1.77-3.55	3.14	1.73±0.07
Akim Oda (Old)[B]	5.20	6.32	6.70	6.21	5.75	5.92	5.20	6.70	5.20-6.70	2.04	4.78±0.17
Twenedurase[P]	3.09	3.19	2.28	2.84	2.20	3.23	2.20	3.23	2.20-3.23	7.04	3.48±0.60
Kwahu Praso[P]	3.06	3.32	2.29	2.19	2.26	6.22	2.19	6.22	2.19-6.22	3.25	3.10±0.12
Apreja[P]	5.91	6.31	7.97	10.9	10.0	8.60	5.91	10.9	5.91-10.9	2.64	5.01±0.18
Nnoboamu[A]	5.74	7.01	7.95	12.5	20.1	14.8	5.74	20.1	5.74-20.1	2.64	5.52±0.21
Wobiri[A]	7.38	10.9	12.3	13.3	10.8	11.7	7.38	13.3	7.38-13.3	3.63	6.44±0.23

Table 13 Cont'd

Station									Range		Mean±SD
Nkontinso[O]	10.9	8.83	7.32	5.68	10.3	18.5	5.68	18.5	5.68-18.5	2.86	10.6±0.40
Dunkwa-On-Offin 1[O]	103	109	119	138	747	770	103	770	103-770	2.79	76.6±0.28
Dunkwa-On-Offin 2[O]	11.7	13.0	12.5	8.24	17.7	7.14	7.14	17.7	7.14-17.7	2.05	11.2±0.40
Assin Praso[P]	5.90	8.70	10.5	11.5	13.3	14.8	5.60	14.8	5.60-14.8	1.52	4.88±0.18
Twifo Praso[P]	12.8	11.2	11.4	10.2	13.0	9.57	9.57	13.0	9.57-13.0	1.76	12.2±0.50
Daboase[P]	3.18	2.58	8.65	8.00	6.87	9.99	2.58	9.99	2.58-9.99	2.59	3.95±0.15
Beposo[P]	7.87	8.75	11.7	11.0	10.0	14.0	7.87	14.0	7.87-14.0	2.59	6.87±0.24
Anlo[P]	9.34	4.63	1.57	1.54	1.62	1.30	1.30	9.34	1.30-9.34	1.26	9.29±0.35
Shama[P]	5.29	2.82	2.63	3.45	3.84	2.91	2.63	5.29	2.63-5.29	3.18	7.73±0.29

NOTE: M2- 5ml (2:1) HNO_3/HF + 1ml HCl digestion procedure; K1- k0.INAA method. (B)- Birim River; (A) - Anum River; (O)- Offin River; and (P)- Main Pra River.
Source: Author Data, 2014

Table 14: Mean Concentration (n = 4) of THg (mg/kg) of Sediment Core (0-10 cm divided into 10 sections), Using M2 (HF) by CVAAS from Twenty-one (21) Sampling Sites form the Pra River Basin, Ghana

Name of Sampling site	M2 for CVAAS Mean THg (mg/kg) in Sediment core (0-10 cm) (n = 4)/depth (cm)										Range	% RSD (n =10)
	0-1	1-2	2-3	3-4	4-5	5-6	6-7	7-8	8-9	9-10		
Dadientem	0.02	0.02	0.02	0.02	0.03	0.02	0.30	0.02	0.04	0.04	0.02-0.04	2.86
Kibi	0.02	0.02	0.02	0.02	0.02	0.02	0.03	0.02	0.03	0.02	0.02-0.03	6.33
Adonkrono	0.07	0.06	0.06	0.05	0.06	0.05	0.04	0.04	0.06	0.05	0.04-0.07	6.33
Kade	0.05	0.05	0.06	0.06	0.06	0.08	0.11	0.11	0.14	0.29	0.05-0.29	12.5
Akim Oda	0.04	0.04	0.03	0.03	0.03	0.03	0.03	0.03	0.03	0.03	0.05-0.29	4.03
Akim Oda (Old)	0.09	0.09	0.09	0.09	0.08	0.09	0.11	0.11	0.12	0.05	0.03-0.04	3.28
Twenedurase	0.01	0.01	0.01	0.01	0.01	0.01	0.02	0.01	0.02	0.01	0.05-0.12	9.34
Kwahu Praso	0.01	0.02	0.02	0.01	0.02	0.01	0.02	0.01	0.02	0.01	0.01-0.02	4.14
Apreja	0.07	0.32	0.07	0.14	0.24	0.07	0.06	0.05	0.05	0.16	0.01-0.02	4.19
Nnboamu	0.00	0.00	0.01	0.01	0.01	0.01	0.00	0.02	0.05	0.01	0.05-0.32	5
Wobiri	0.01	0.01	0.01	0.00	0.01	0.01	0.01	0.02	0.02	0.01	0.00-0.02	8.12
Nkontinso	0.01	0.01	0.01	0.00	0.01	0.01	0.01	0.01	0.01	0.02	0.01-0.02	6.26
Dunkwa-On-Offin[a]	0.08	0.05	0.06	0.08	0.06	0.05	0.05	0.05	0.08	0.06	0.05-0.08	2.52
	0.49	0.75	0.68	0.92	1.57	2.26	1.62	0.43	0.31	0.16	0.31-2.26	3.39

136

Table 14 Cont'd

Dunkwa-On-Offin[b]											
Assin Praso	0.09	0.07	0.07	0.08	0.06	0.07	0.07	0.06	0.10	0.06	0.06-0.10	2.26
Twifo Praso 1	0.05	0.04	0.04	0.04	0.03	0.07	0.03	0.04	0.04	0.11	0.03-0.11	2.75
Twifo Praso 2	0.14	0.12	0.11	0.10	0.11	0.12	0.14	0.17	0.07	0.08	0.07-0.14	3.24
Daboase	0.10	0.23	0.20	0.09	0.23	0.41	0.25	0.14	0.15	0.12	0.10-0.41	3.27
Beposo	0.16	0.17	0.14	0.14	0.13	0.12	0.09	0.09	0.11	0.13	0.09-0.17	3.26
Anlo	0.23	0.31	4.06	0.40	0.57	0.27	20.81	0.23	2.18	0.72	0.23-20.8	6.16
Shama	0.01	0.02	0.02	0.03	0.17	0.05	0.04	0.02	0.01	0.00	0.01-0.06	14.8
	0.01	0.01	0.01	0.01	0.02	0.02	0.02	0.02	0.02	0.02	0.01-0.02	4.04

Source: Author Data, 2014

The trend of Total Mercury along the Vertical Soil Profile (0-6 cm) and Sediment Core (0-10 cm) along the Pra River Basin.

In determining THg concentration in soil profile and sediment cores, a combination of HNO_3/HF/HCl was used to release THg from the silicate of the both soils and sediment. Tables 13 and 14 represents the results of THg in both soil profile (0-6 cm) and sediment cores (0-10 cm) from the Pra River Basin Ghana. Cold Vapor Atomic Absorption Spectrometry (CVAAS) method was used to measure the THg after digestion.

Along the Birim River, the highest range of THg concentration (3.32-11.1 mg/kg, $n = 6$) in the vertical soil profile (0-6 cm) was noted at Dadientem (upstream) sampling site, whilst the least range of mean THg concentration (5.20-6.70 mg/kg, $n = 6$) was recorded at Akim Oda (Old) (downstream) sampling site along the Birim River. Among the six (6) sampling sites, Kade (midstream) sampling site gave the highest mean THg concentration (11.9 mg/kg, 0-1 cm; $n = 36$) whilst Akim Oda (downstream) gave the least mean THg concentration (1.77 mg/kg, 0-1 cm, $n = 36$) along the Birim River. Even though the correlations between the depth of the soil profiles and THg concentration in all the six (6) sampling sites from the Birim River were positive (THg concentration increases as depth increases), only Kibi (upstream) sampling site showed a high correlation of 0.75 which was insignificant (p-$value = 0.08$). These show that THg concentrations in the soil profile (0-6 cm) along the Birim River are retained and bonded in each layer of the soil profile on which it was introduced. Also there were elevation of THg in the topsoil (0-1 cm) at Dadientem (11.1 mg/kg, $n = 6$), Kibi (9.25

mg/kg, n = 6) and Kade (11.9 mg/kg, n = 6) sampling sites along the Birim River. The correlations determined between THg concentration and soil profile depth (0-6 cm) for the six (6) sampling sites along the Birim River were all insignificant as *p-value*>0.05. In Table 14, the results of the THg concentration (mg/kg) in sediments core (0-10 cm) for the six (6) sampling sites (Dadientem, Kibi, Adonkrono, Kade, Akim Oda and Akim Oda (Old)) sampling sites along the Brim River are also presented. From the results, the mean THg concentration in the sediments core (0-10 cm) was elevated at Kade sampling site (midstream), as it recorded the highest range of THg (0.05 to 0.29 mg/kg, n = 36) and the highest mean THg concentration (0.29 mg/kg, 9-10 cm, n = 36) amidst all the six (6) sampling sites in the Birim River. Both the least range of THg concentration (16.2-29.7 ng/g, n = 10) and the least mean THg concentration (0.02 mg/kg, 1-2 cm, n = 36) determined in the sediment core (0-10 cm) were recorded at Kibi (upstream) sampling site in the Birim River. Both Dadientem and Kade sampling sites had a positive significant (P-value ≤ 0.01) correlation (0.81) which shows an increase in THg concentration with the depth of the sediment core (0-10 cm). This shows a previous sink of THg concentration in the sediment core in both Dadientem and Kade sampling sites. Figures 24, 25, and 26 show the trend of THg concentrations in both soil profile (0-6 cm) and sediment core (0-10 cm) for Dadientem, Kade and Akim Oda (Old) sampling site which is located at the upstream, midstream and downstream respectively at the Birim River Ghana. There were no significant correlations (r = 0.12-0.73, *p-value* =0.10-0.83, n = 6) between the THg concentrations in the soil profile and the sediment core in the six (6) sampling sites from the Birim River.
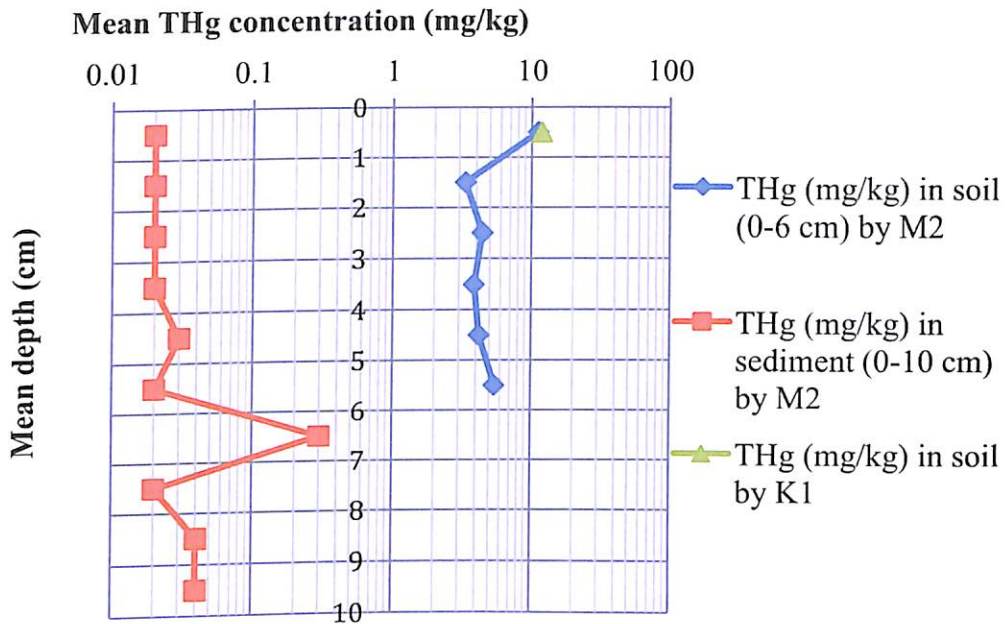
Figure 24: A Graph of Mean THg Concentrations (mg/kg) determined in the Vertical Soil Profile (0-6 cm) and Sediment Core (0-10 cm), from Dadientem Sampling site from Birim River, a Major Tributary in the Pra River Basin, Ghana
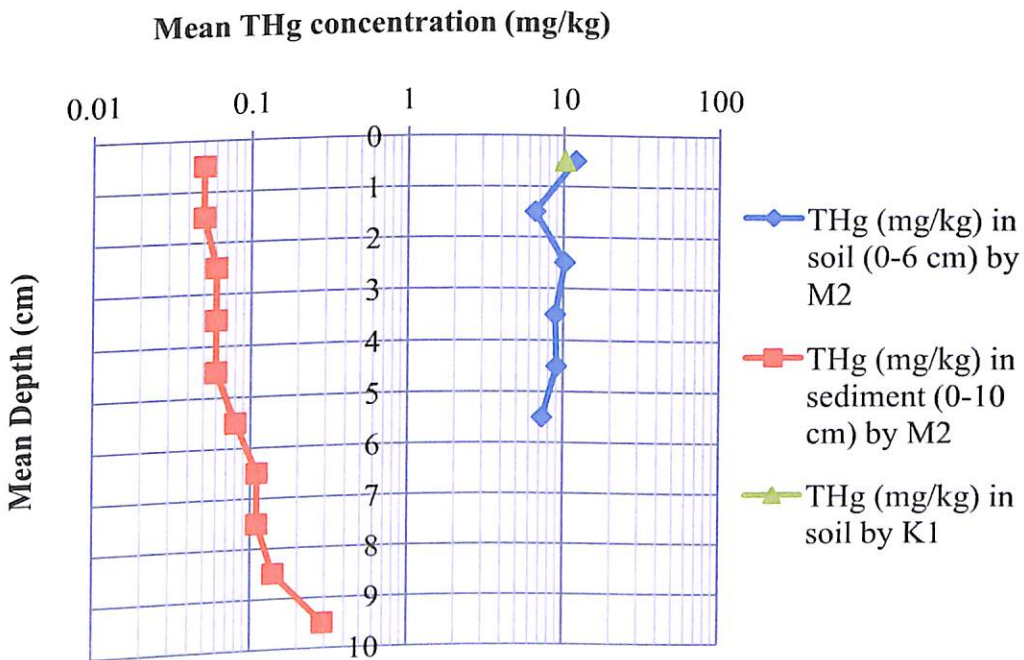
Figure 25: A Graph of mean THg Concentrations (mg/kg) determined in Vertical Soil Profile (0-6 cm) and Sediment Core (0-10 cm) from Kade Sampling site from Birim River, a Major Tributary in the Pra River Basin, Ghana
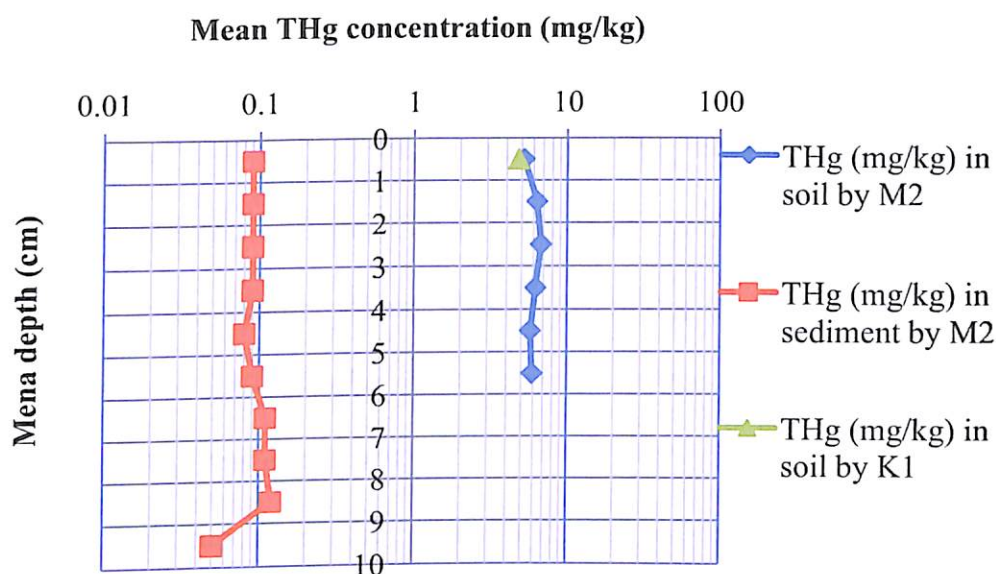
Figure 26: A Graph of Mean THg Concentrations (mg/kg) determined in Vertical Soil Profile (0-6 cm) and Sediment core (0-10 cm), from Akim Oda (Old) Sampling site along the Birim River, a Major Tributary in the Pra River Basin, Ghana

Anum River is another tributary of the Pra River Basin which was considered in this study for THg concentration determination in the vertical soil profile and sediment core from two (2) sampling sites Nnoboamu and Wobiri sampling sites. The results of the mean THg concentrations in both soil profile and sediments are also presented in Tables 13 and 14 respectively whilst Figure 27 and 28, presents graphically the result of THg concentration in soil (by M2 and K1) and sediment core for Nnoboamu and Nkontinso sampling site respectively. The maximum range of THg concentration (5.74 and 20.1 mg/kg, $n = 6$) in the soil profile was reported at Nnoboamu sampling site whilst the least range of THg concentration (7.38 and 13.3 mg/kg, $n = 6$) in the soil profile was registered at Wobiri sampling site. Both the least (5.74 mg/kg, $n = 12$, 0-1 cm) and highest (20.1 mg/kg, $n = 12$, 5-6 cm) mean of THg concentrations in the soil profiles from the Anum River Basin were recorded at Nnoboamu sampling site. There was a very strong positive correlation of

141

0.94 (*p-value* = 0.01, *n* = 6) between the vertical soil profile (0-6 cm) and THg concentrations in Nnoboamu sampling site. This shows that as the depth of the soil profile (0-6 cm) moved downward, THg concentration also increases showing previously deposition of THg than currently. The second sampling site from the Anum River, Wobiri sampling site gave a poor positive correlation of 0.37 (*p-value* = 0.47, *n* = 6) between the vertical soil profile (0-6 cm) and THg concentrations.

Even though all the results (Table 13) of mean THg concentrations (*n* = 18) in the soil profiles from the Offin River Basin were high, Dunkwa-On-Offin (1), a sampling site with a lot of ASGM (Table 6) gave extremely high THg concentration of 770 mg/kg (*n* = 18, 5-6 cm) and Nkontinso sampling site gave the least THg concentration (5.68 mg/kg, 3-4 cm). Again, Dunkwa-On-Offin (1) gave the highest range of THg concentration (103-770 mg/kg, *n* = 6) in the soil profile (0-6 cm) with Dunkwa-On-Offin (2) given the least range of THg concentration (7.40-17.7 mg/kg, *n* = 6) in the soil profile (0-6 cm) along the Offin River, Ghana.

Mean THg concetration (mg/kg)
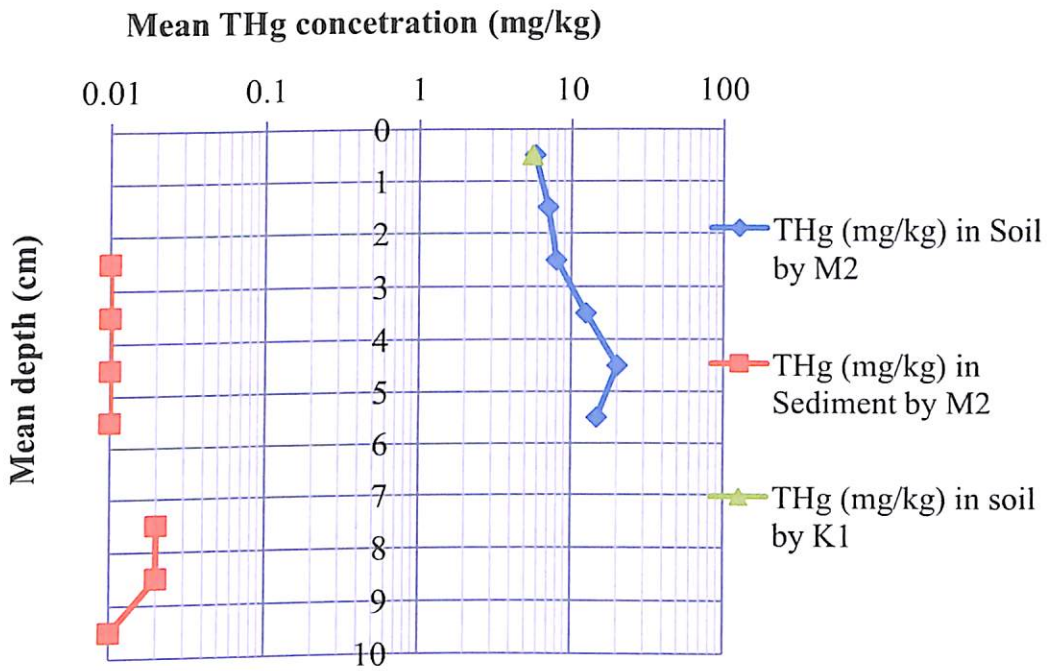
Figure 27: A Graph of Mean THg Concentrations (mg/kg) determined in the Vertical Soil Profile (0-6 cm) and Sediment Core (0-10 cm) from Nnoboamu Sampling site from Anum River in the Pra River Basin Ghana

Mean THg concentration (mg/kg)
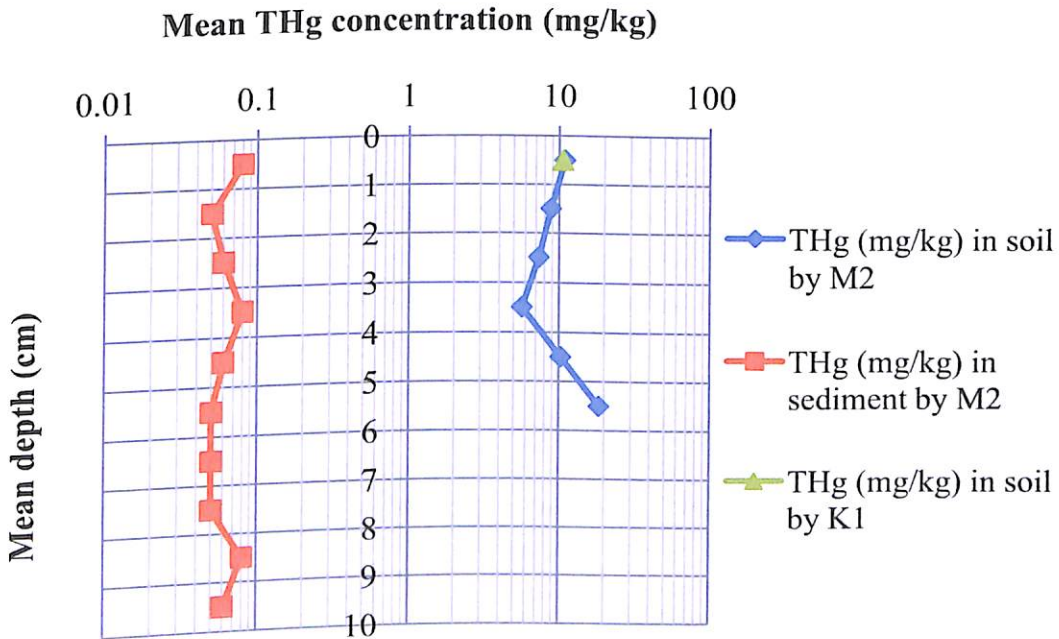
Figure 28: A Graph of Mean THg Concentrations (mg/kg) determined in Vertical Soil Profile (0-6 cm) and Sediment Core (0-10 cm) Nkontinso Sampling site along the Offin River, a Major Tributary in the Pra River Basin, Ghana

Also, Dunkwa-On-Offin (1) sampling site (Figure 29) gave both the highest mean (2.26 mg/kg, $n = 30$, 5-6 cm) THg concentration along the soil

143

profiles investigated and range (0.31-2.26 mg/kg, *n* = 10) of THg concentration in sediment cores in the Offin River. Both the least mean (0.05mg/kg, *n* = 30, 6-7 cm) and range (0.05-0.08 mg/kg, *n* = 10) were registered at Nkontinso sampling site. Offin River is another major tributary of the Pra River Basin, Ghana and the two (2) sampling sites Dunkwa-On-Offin (1) and (2) sampling sites are in the Offin River Basin are marked for Artisanal Gold and small-scale mining (ASGM) activities for years. As indicated in Table 6, ASGM activities coupled with the roasting of gold after gold amalgamation with mercury is scattered in the Dunkwa-On-Offin sampling sites. A perfect positive correlation of 1.0 (*p-value* = 0.00, *n* = 6) between the vertical soil profile (0-6 cm) and THg concentration from soil from Dunkwa-On-Offin (1) sampling site indicates previously impacted ASGM activities than currently in the township. There was a very poor negative correlation of 0.26 (*p-value* = 0.62, *n* = 6) between the vertical depth of soil profile and THg concentration along the soil profile in Dunkwa-On-Offin (2).
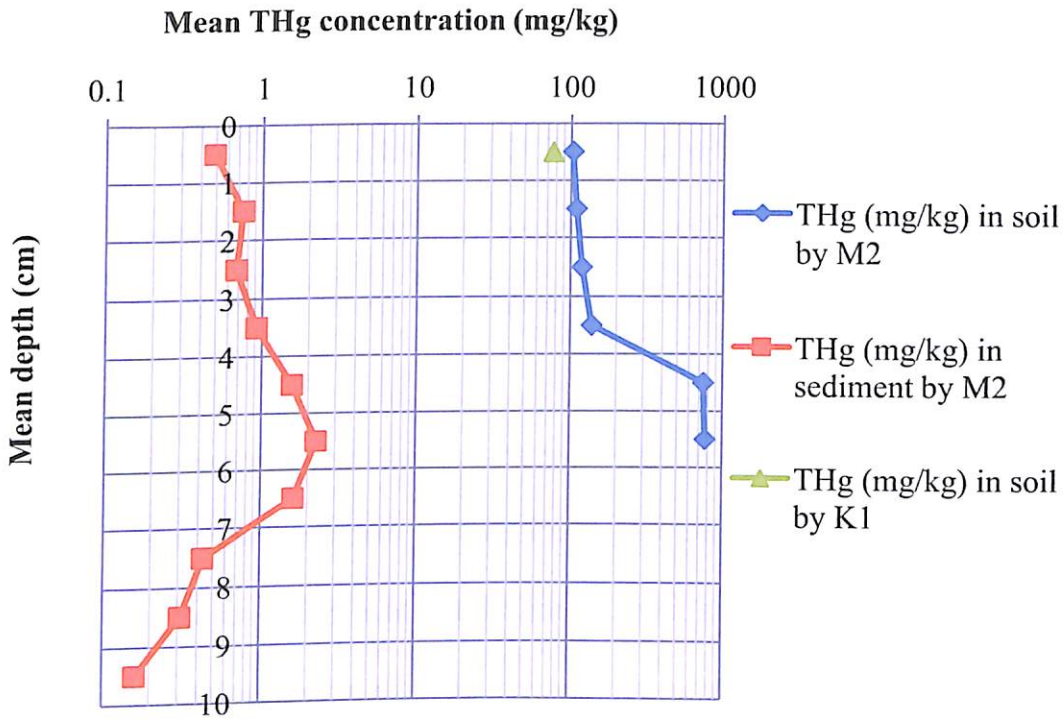
Figure 29: A Graph of Mean THg Concentrations (mg/kg) determined in Vertical Soil Profile (0-6 cm) and Sediment Core (0-10 cm) from Dunkwa-On-Offin (1) sampling site along the Offin River, a Major Tributary in the Pra River Basin, Ghana

In correlating the THg concentration in the sediment core (0-10 cm) and depth of the sediment at Dunkwa-On-Offin (1) sampling site, a negative correlations of 0.35 (p-$value$ = 0.33, n = 10) was established. In order to establish a relationship between THg concentration in soil (0-6 cm) and sediment (0-10 cm) a correlation was drawn and a significant (p-$value$ = 0.01) correlation (0.95) was established. This is an indication of high THg concentration in the soil profile have influenced the elevation of THg concentration in the sediment core through runoffs in the Dunkwa-On-Offin (1) sampling site. In comparing ranges of THg concentrations in the sediment in this research (0.31-2.26 mg/kg, n = 10) to a research conducted in a decade ago (Donkor, Bonzongo, Nartey, & Adotey, 2006) (0.003-0.05 mg/kg, n = 7) it showed that, Hg is elevated in the Offin River Basin. Figure 29 depicts an

increasing order of THg concentration along the soil profile (0-6 cm) from the soil profile (0-6 cm) from Dunkwa-On-Offin (1) sampling site. It must be noted that the soil at Dunkwa-On-Offin (1) cannot be used for agricultural purposes because of the high Hg contamination (Soil-plant-humans or soil-plant-animals-human) which will pose a lot of health hazards to both man and animals.

From upstream to the downstream of the main Pra River, nine (9) sampling sites (Twenedurase, Kwahu Praso, Apreja, Assin Praso, Twifo Praso 1, Daboase, Beposo and, Anlo and Shama) were slated for the determination of THg concentrations (mg/kg) in vertical soil profile (0-6 cm) depth which were sectioned into six (6) sections (0-1 cm, 1-2 cm, 2-3 cm, 3-4 cm, 4-5 cm, and 5-6 cm) each are presented in table 13. At the same time ten (10) sampling sites (Twenedurase, Kwahu Praso, Apreja, Assin Praso, Twifo Praso 1, Twifo Praso 2, Daboase, Beposo and, Anlo and Shama sampling sites at the estuary) were also slated for THg concentration determination in sediment core (0-10 cm) which are presented in Table 14. The Figures 30 to 34 show graphical presentation of THg concentration in both soil (0-6 cm) and sediment core (0-10 cm) from main Pra River starting from upstream to its estuary.
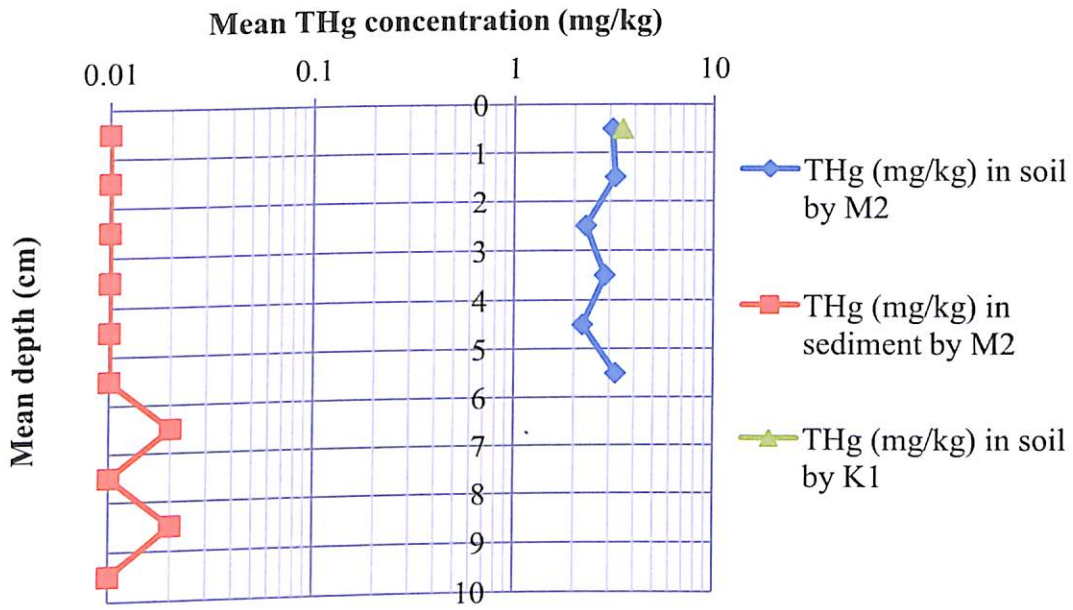
Figure 30: A Graph of Mean THg Concentrations (mg/kg) determined in Vertical Soil Profile (0-6 cm) and Sediment Core (0-10 cm) from Twenedurase Sampling site at the Upstream of the Pra River, Ghana
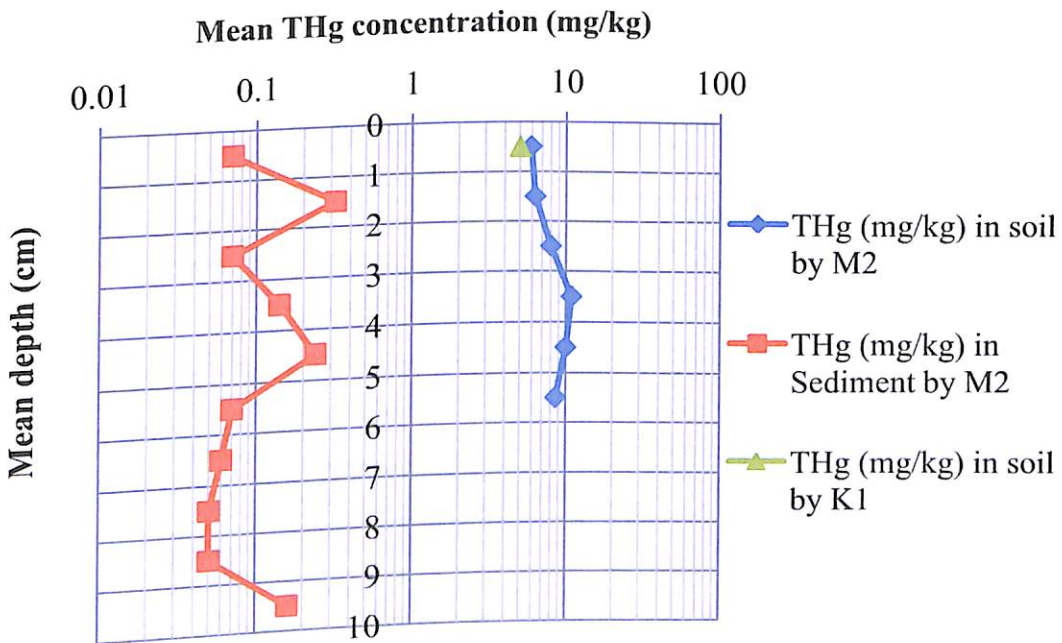
Figure 31: A Graph of Mean THg Concentrations (mg/kg) determined in Vertical Soil Profile (0-6 cm) and Sediment Core (0-10 cm) from Apreja Sampling site along the Main Pra River in Ghana
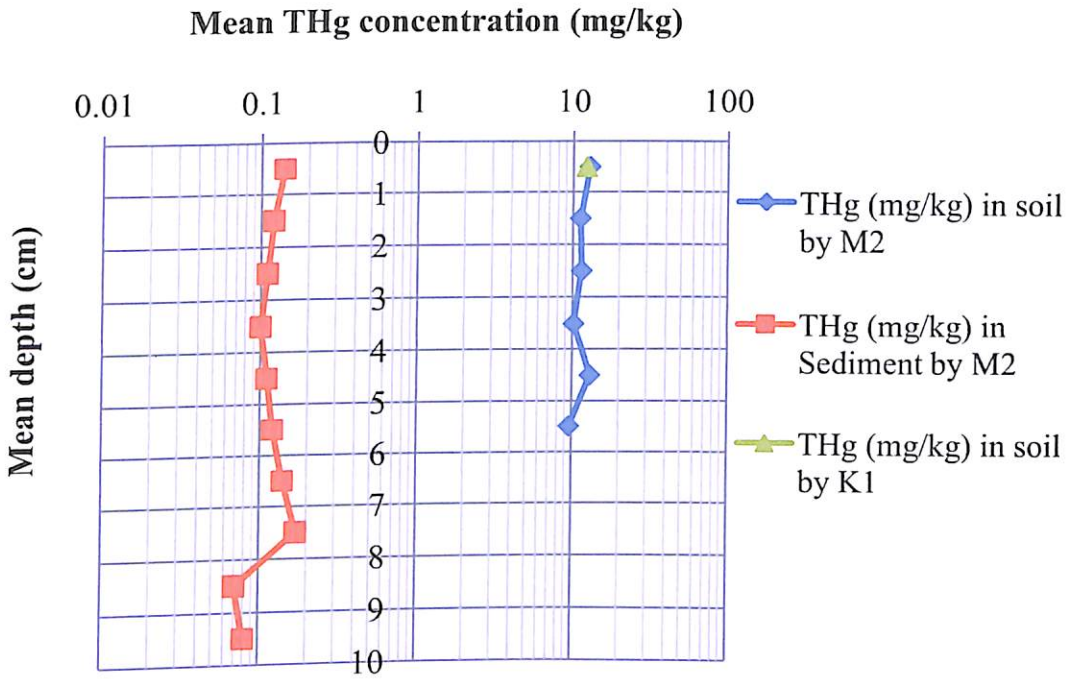
Figure 32: A Graph of Mean THg Concentrations (mg/kg) determined in Vertical Soil Profile (0-6 cm) and Sediment Core (0-10 cm) from Twifo Praso Sampling site along the Main Pra River in Ghana
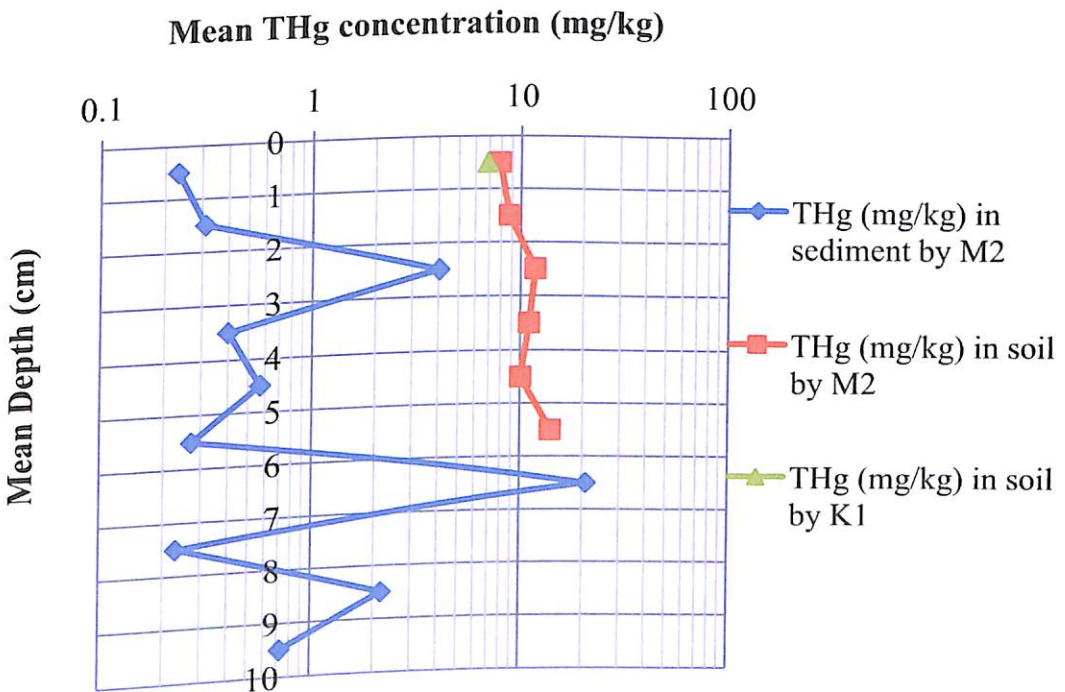
Figure 33: A Graph of Mean THg Concentrations (mg/kg) determined in Vertical Soil Profile (0-6 cm) and Sediment Core (0-10 cm) from Beposo Sampling site at the Downstream of the Pra River Basin in Ghana

Mean THg concentration (mg/kg)
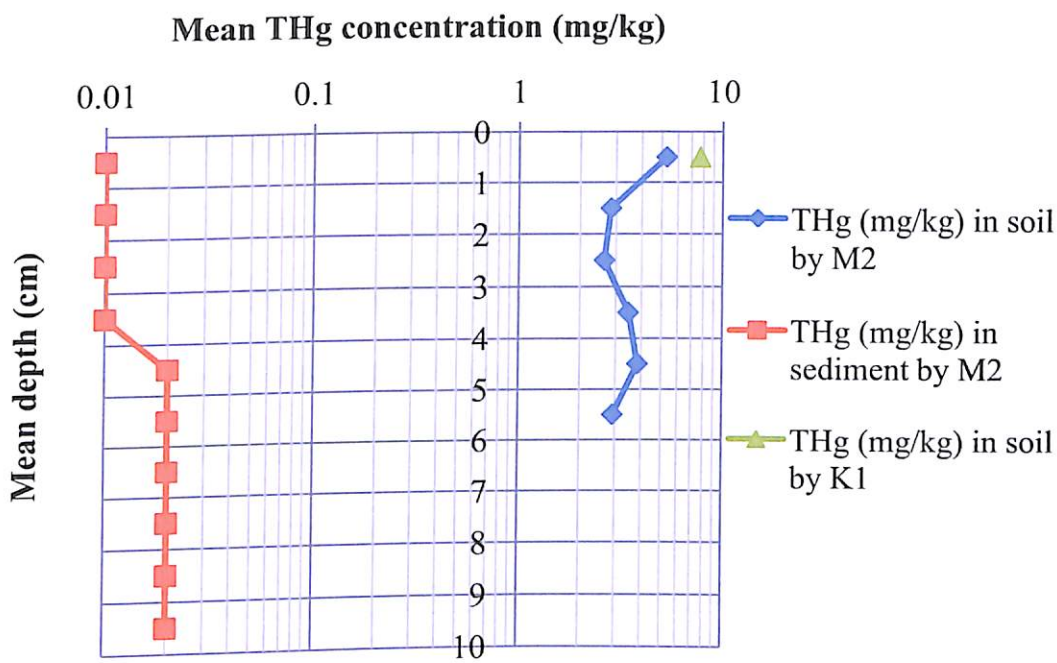
Figure 34: A Graph of Mean THg Concentrations (mg/kg) determined in Vertical Soil Profile (0-6 cm) and Sediment Core (0-10 cm) from Shama Sampling site, at the Estuary of the Pra River Basin, Ghana

Twenedurase sampling site is situated between forest reserves at the time of sampling and there were no human activities. That is, no mining activities whether legal or illegal takes place or any industrial or urban activities like construction works or residential houses located there. Therefore any Hg concentrations above worldwide background (0.07 mg/kg) level in surface soils (Kabata-Pendias, 2011) or critical limit of Hg in soil (Tipping et al., 2010) are as a result of atmospheric deposition from other contaminated sites. The atmosphere is an important reservoir of mercury in which it exists mainly as Hg^0. This is because of the less soluble nature of Hg^0 than other forms of Hg, and more specifically its relatively low deposition velocity and high vapour pressure at ambient conditions. Hg^0 lifetime is between 0.5 and 3 years in the atmosphere (Bank, 2012). Even though local sources are important, a 72-hour travel time trajectory for mercury specifies that some mercury found in rain may originate from sources up to 2,500 km (1,550

149

miles) away (Glass, Easterly, Jones, & Walsh, 1991). Mercury after entering into the environment undergoes many different transformation and transport processes. Although Twenedurase sampling site is a reserved place and no activities on mining takes place, and reported the least range of THg concentration (2.20-3.23 mg/kg, $n = 9$) in the basin, mwas higher than both the background level of Hg of 0.07 mg/kg and the critical limit of 0.3 mg/kg in surface soils (Kabata-Pendias, 2011; Tipping et al., 2010). The higher range of THg concentration registered at Twenedurase sampling site was not due to anthropogenic activities but due to many factors. Wet and dry deposition of Hg from the atmosphere is a factor. Also, the speciation and chemical transformations of Hg in the atmosphere strongly influence its deposition and global cycle (Lin & Pehkonen, 1999). Many researchers have talked about the soil-air exchange which occur bidirectionally. The processes entail the transfer of mercury from the atmosphere to terrestrial surfaces which consist of wet deposition of Hg (II) species; direct dry deposition as gaseous organic matter, gaseous elemental Hg and particulate Hg; and throughfall or litterfall. Mercury deposited in soil by this way can be re-emitted and recycled back to the atmosphere (Liu, Cai, O'Driscoll, Feng, & Jiang, 2012; Ericksen, Gustin, Xin, Weisberg, & Ferbandez, 2006; Schroeder & Munthe, 1998). Also atmospheric deposition (wet and dry) of Hg to forest canopies plays an important role as dry deposition Hg may be washed off plant surfaces, thus elevating concentrations of Hg in throughfall (Iverfeldt, 1991) or held by the leaves and deposited as litterfall to the forest floor (Rea, Keeler, & Schrebatskoy, 1996).

The range of THg concentration of 2.19-6.22 mg/kg ($n = 6$) for soil profile (0-6 cm) and 0.01-0.02mg/kg ($n = 10$) for sediment core (0-10 cm)

were recorded in Apreja sampling site. Apreja sampling sites (Figure 28) at the upstream of the main Pra River is heavily impacted with ASGM activities scattered all over the town and neighbouring villages along the main Pra River. A strong positive correlation of 0.77 (*p-value* = 0.07, *n* = 6) between the soil profile (0-6 cm) depth and THg concentration was established but was insignificant. A range between 0.05 and 0.24 mg/kg (*n* = 10) of THg concentration in the sediment core (0-10 cm) was recorded.

Assin Praso sampling site was previously encroached by ASGM activities. In all the nine (9) sampling sites along the main Pra River, the highest range of THg concentration (5.60-14.8 mg/kg, *n* = 9) in the soil profiles and the highest mean THg concentration (14.8 mg/kg, *n* = 54, 5-6 cm) in the soil profile (0-6 cm) from the main Pra River Basin was recorded at Assin Praso sampling site. The least mean THg concentration (1.4 mg/kg, *n* = 54) in the soil profiles (0-6 cm) from the main Pra River Basin was recorded at the depth of 4-6 cm at Anlo (Estuary) sampling site. There was a perfect positive correlation of 1.0 (*p-value* = 0.00, *n* = 6) which was significant indicating a previously impacted with Hg in Assin Praso sampling site. Assin Praso was previously populated with ASGM activities (Table 6).

In Table 14 Beposo sampling site recorded the highest mean and range of THg concentration of 20.8 mg/kg (*n* = 60, 6-7 cm) and (0.23-20.8 mg/kg, *n* = 10) in sediment corers (0-10 cm) from the main Pra River respectively. Both the least range (0.01-0.02 mg/kg, *n* = 10) and mean (0.01 mg/kg, *n* = 60, 5-6 cm) of THg concentrations in the sediment core (0-10 cm) from the main Pra River were reported at Twenedurase sampling sites. A review on Hg in sediment in Ghana indicate a range of Hg concentration in

151

mining areas (n = 15) as 0.20-186 mg/kg (n = 140) and non-mining areas (n = 13) as ND-0.494 mg/kg (n = 53) which is far higher than THg concentration reported in the main Pra River in this study (Rajaee et al., 2015). A strong negative correlation for both Kwahu Praso (r = 0.73, p-value = 0.02, n = 10) and Daboase (r = 0.76, p-value = 0.01, n = 10) sampling sites were established which indicate a decrease of THg concentrations as the depth of the core increases from the zero (0) to ten (10) centimeters for these two (2) sampling sites. Also, a strong positive significant correlation (r = 0.73, p-value = 0.02, n = 10) was established between the depth (0-10 cm) and THg concentration in the sediment core (0-10 cm) which shows an increase of THg concentration with depth of the sediment core (0-10 cm). Considering the graphical presentation of THg concentration in the sediment core (0-10 cm) in Figure 35, THg is currently elevated in the sediment core (0-10 cm) from Daboase sampling site. Also, there was a significant correlation (r = 0.83, p-value = 0.04, n = 10) between soil profile (0-6 cm) and sediment core (0-6 cm) from Daboase sampling site which indicate that, the presence of THg concentration in the soil profile has had influence through factors like runoffs in the elevation of THg concentration in the sediment core (0-6 cm) at Daboase sampling site.

Identification of Hotspot of THg (mg/kg) in the Pra River Basin in Ghana using Arc Map 10.1

Arc Map 10.1 software was used to plot the ranges of THg concentration (mg/kg) level using each depth (1 cm) from the soil profiles (0-1 cm, 1-2 cm, 2-3 cm, 3-4 cm, 4-5 cm and 5-6 cm) in order to identify hotspots

152

of THg. Each depth from the soil samples along the Pra River Basin, Ghana are shown in Figures 35, 36 and 37. There are ongoing mining activities in the Pra River Basin and mercury is been used in the quest for gold through mercury amalgamation. Table 6 shows the various activities in the Basin.

Dunkwa-On-Offin (1) sampling site exhibited the highest range (Level 4) of THg concentrations in all the soil profiles (0-1 cm-: 12.8-103 mg/kg, 1-2 cm-: 13.0-109 mg/kg, 2-3 cm-: 12.5-119 mg/kg, 3-4 cm-: 13.3-138 mg/kg, 4-5 cm-: 20.1-747 mg/kg, and 5-6 cm-: 15.5-770 mg/kg) which confirms that Dunkwa-On-Offin (1) sampling site is a hotspot for THg contamination in the Pra River Basin. Also, the ranges of THg concentration in all the soil profiles from Dunkwa-On-Offin (1) sampling site are higher than Maximum Allowable Concentration (MAC) and Trigger Action Value (TAV) for agricultural soil which makes the soils from this sampling site unsafe for agricultural purposes due to the fact that, the interaction between plants and nutrient takes place in the rhizosphere. Dunkwa-On-Offin (1) sampling site is a hotspot for mercury contamination. Also, another contamination level (Level 3 with a range between 7.01 and 20.1 mg/kg) was seen in some of the sampling sites (0-1 cm-:Nkontinso, Dunkwa-On-Offin (2), Kade, Dadienem, Kibi, Assin Praso and Anlo sampling sites; 1-2 cm-: Wobiri, Kibi, Nkontinso, Dunkwa-On-Offin (2), Assin Praso, Twifo Praso, and Beposo sampling sites; 2-3 cm-: Wobiri, Kade, Dunkwa-On-Offin (2), Assin Praso, Twifo Praso, and Beposo sampling sites; 3-4 cm-: Nnoboamu, Wobiri, Apreja, AssinPraso, Twifo Praso, and Beposo sampling sites; 4-5 cm-: Nnoboamu, Dunkwa-On-Offin (2), Assin Praso and Twifo Praso sampling sites; and 5-6 cm-: Nnoboamu, Wobiri, Nkontinso, Twifo Praso and Beposo sampling sites).

153

These profile sections in these sampling sites were all in a range (7.01-20.1 mg/kg) that were above the background (0.07 mg/kg compiled by Kabata-Pendias, 2011), Critical Limits (0.13 mg/kg by Tipping et al., 2010), MAC (0.5-5.0 mg/kg by Kabata-Pendias & Sadurski, (2004) and TAV (1.5-10.0 mg/kg by Chen, 1999) which may be classified as Hg hopsopts. Also, in Level 2, the maximum range of THg concentration was recorded at 4-5 cm section with a range between 5.75 and 10.8 mg/kg ($n = 8$) which is again above the TAV making the sampling sites (Kibi, Adonkrono, Kade, Apreja, Wobiri, Nkontinso, Daboase and Beposo sampling sites) hotspots for Hg contaminations.

Depth of 5-6 cm recorded the least range of THg concentration between 1.30 and 3.23 mg/kg ($n = 4$) using the Arc Map 10.1 software to plot the ranges of THg concentration levels in the soil profile (0-6 cm) from various sampling sites from the Pra River Basin. In Figures 32 to 34 and Appendices J, K, and L, Twenedurase, a sampling site at the upstream presented the least range of THg concentration. It is located within three (3) forest reserves (Southern Scarp, Northern Scarp west and North Fomangsu forest) and as indicated in Table 6, free from any activities (whether mining, residential etc). The soil samples from this sampling site may be classified as desolate soils. In desolate soils, GEM dry deposition, as well as Gaseous Organic Mercury (GOM) wet and dry deposition are, chief sources of Hg generating a surface pool available for Hg release over time (Liu, Cai, O'Driscoll, Feng, & Jiang, 2012).
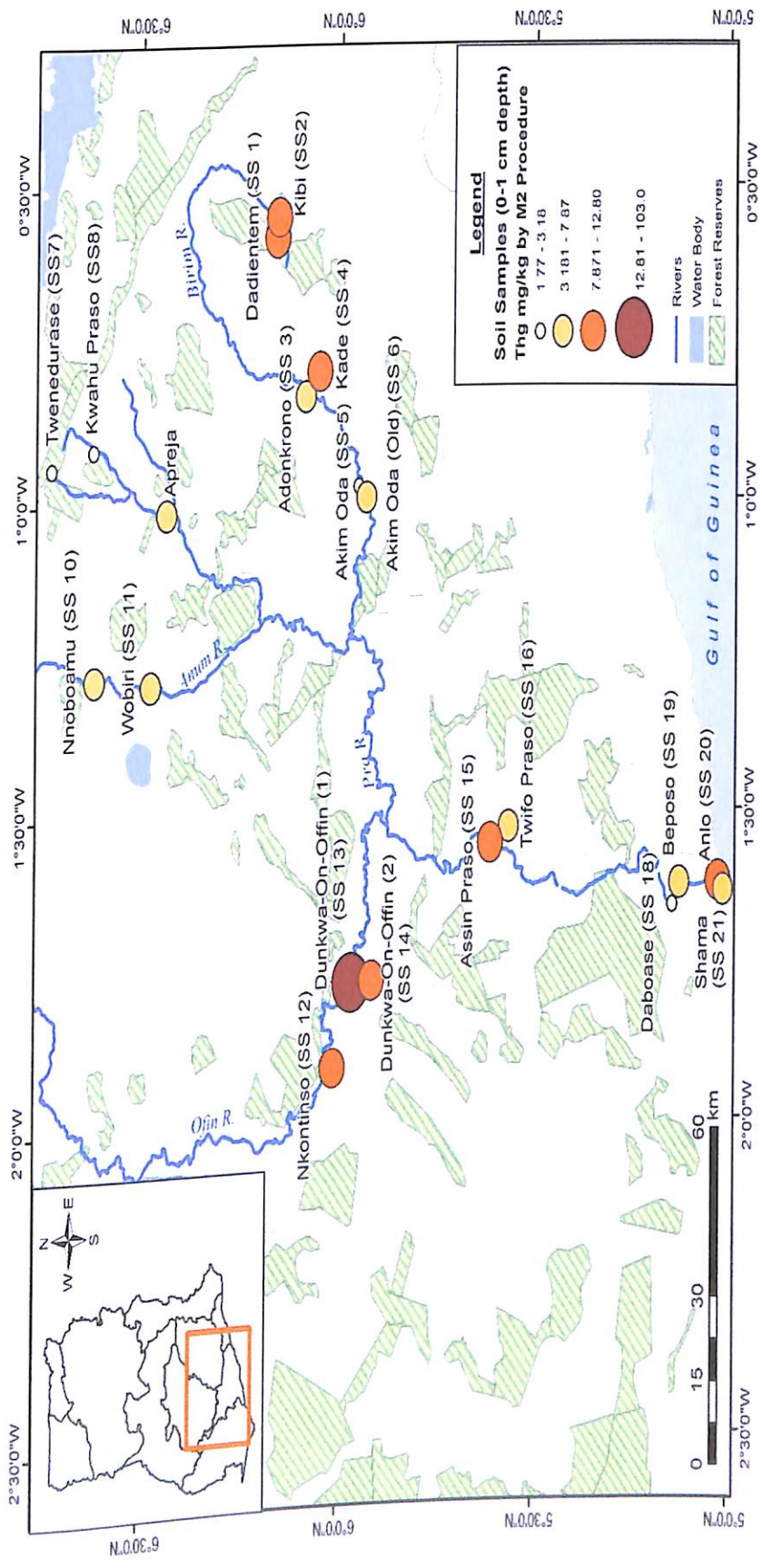
Figure 35: Using Arc Map 10.1 software to plot the distribution of THg Concentration (mg/kg) Level in the 0-1 cm Depth Section of the Soil samples from Twenty (20) Sampling sites from the Pra River Basin, Ghana

Source: Author & Department of Geography and Regional Planning, University of Cape Coast, Cape Coast

155

Figure 36: Using Arc Map 10.1 software to plot the distribution of THg Concentration (mg/kg) Level in the 2-3 cm Depth Section of the Soil samples from Twenty (20) Sampling sites from the Pra River Basin, Ghana

Source: Author Data & Department of Geography and Regional Planning, University of Cape Coast, Cape Coast

156
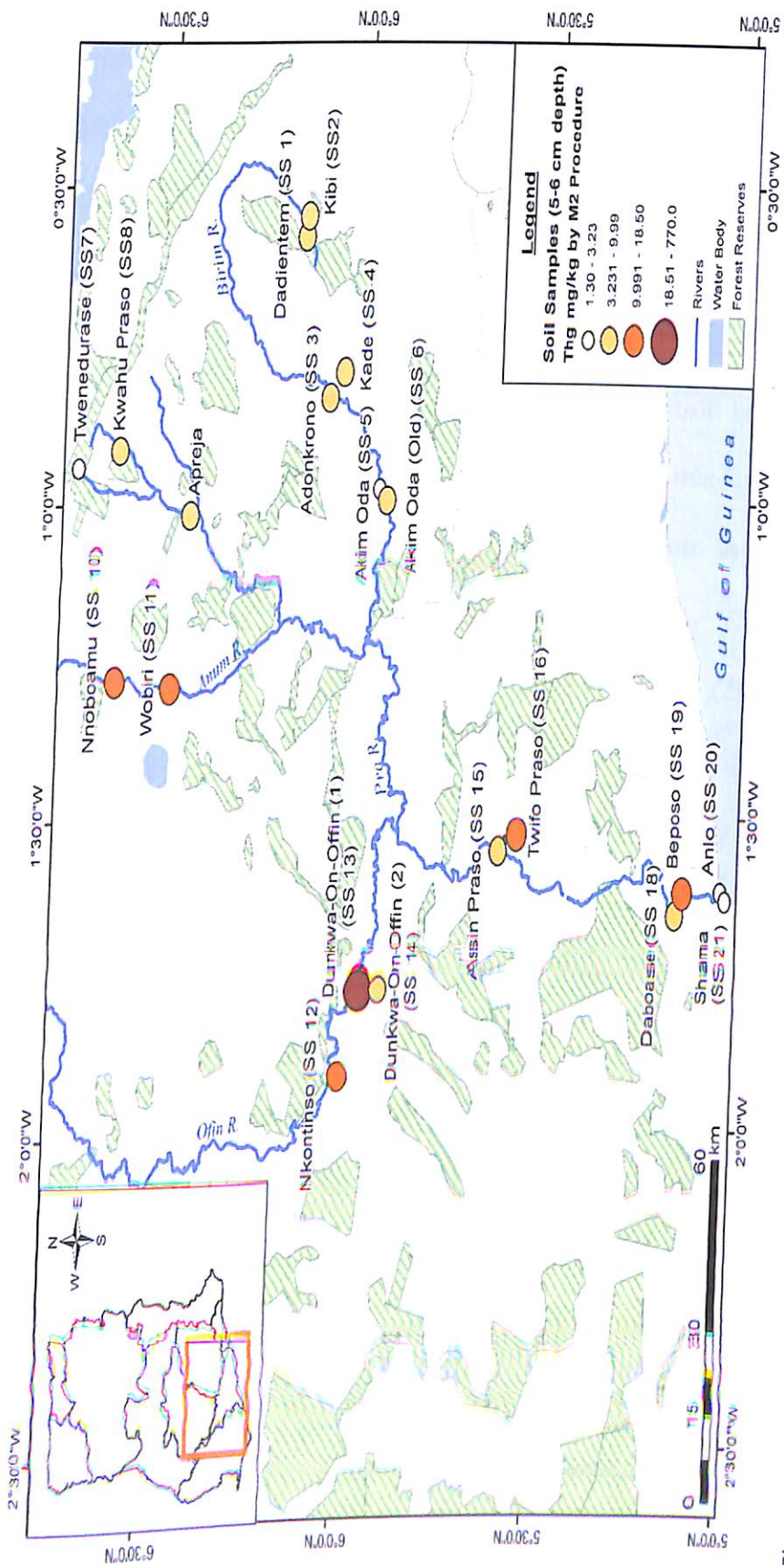
Figure 37: Using Arc Map 10.1 software to plot the distribution of THg Concentration (mg/kg) Level in the 5-6 cm Depth Section of the soil samples from Twenty (20) Sampling sites from the Pra River Basin, Ghana

Source: Author Data & Department of Geography and Regional Planning, University of Cape Coast, Cape Coast

157

Comparing THg concentration from the Pra River Basin to Background, Critical Limit, Maximum Allowable Concentration and Trigger Action Value of Hg

The mean THg concentration in all the soil profiles (0 to 6 cm) from all the twenty (20) sampling sites in the Basin were all above the mean worldwide background of 0.07 mg/kg (Kabata-Pendias, 2011) and critical limit of Hg (0.13 mg/kg) in surface soils (Tipping et al., 2010) as shown in Figures 38, 39 and 40. The soil profiles from the Pra River Basin in Ghana are contaminated with higher Hg concentrations.

Also, linking the range of THg concentration (Appendix O) in the soil profile (0-6 cm) from the twenty (20) sampling sites from the Pra River Basin in this research to the range of Hg for Maximum Allowable Concentration (MAC), that is 0.5-5.0 mg/kg (Kabata-Pendias & Sadurski, 2004) for agricultural soil only three (3) out of the twenty (20), that is, Akim Oda, Twenedurase, and Beposo sampling sites had their ranges of THg concetration (mg/kg) falling within MAC range of 0.5-5.0 mg/kg. The remaining seventeen (17) soil samples had their ranges of THg concentrations above the maximum Allowable concentrations of Hg in the soils. Again, in relating the ranges of THg concentration (mg/kg) determined in the twenty (20) sampling sites along the Pra River Basin to the range of TAV for Hg (Chen, 1999), that is 1.5-10 mg/kg, nine (9) sampling sites (Kibi, Adonkrono, Akim Oda (Old), Akim Oda, Twenedurase, Kwahu Praso, Daboase, Anlo and Shama sampling sites) had the range of THg concentration within (W) the range of Hg for the TAV (1.50-10.0 mg/kg) for agricultural soil. The remaining eleven (11) sampling sites (Dadientem, Kade, Apreja, Nnoboamu, Wobiri, Nkontinso, Dunkwa-On-Offin

(1), Dunkwa-On-Offin (2), Assin Praso, Twifo Praso, Beposo sampling sites) had their range of THg concentration (mg/kg) above (A) the range for TAV (1.5-10 mg/kg) for Agricultural soil. The MAC value of a substance is the highest concentration in which a substance may be present in an environment. In setting limits for trace elements, MAC are based on fundamental criteria such as, the transfer of trace elements especially metals to various organisms and to man. Also, in the assessment of the likely harmful effects, estimation of two threshold values, LOAEC (Lowest Observed Adverse Effect Concentration) and HNOAEC (Highest No Observed Adverse Effect Concentration), and evaluation of metal balance, that is input and output of metals are set. It must be noted that soil contaminated with trace metals like Hg can produce apparently normal crops but unsafe for human or animal consumption (Kabata-Pendias, 2011). None of the soil from the Pra River Basin had range of THg concentration below the background level of Hg, critical limit of Hg or the range for MAC for soils.

Table 15: Mean Concentration of THg (mg/kg) in Soil (Air dried), M2 for CVAAS from Dunkwa-On-Offin Sampling Site, along the Offin River, a Major Tributary of Pra River Basin, Ghana

Name of Sampling Sites	Mean THg concentration (mg/kg) in mining waste								
	M2 procedure								K1
	Depth (cm) (n = 4)						Range (n = 6)	%RSD	(n = 3) 0-1cm
	0-1	1-2	2-3	3-4	4-5	5-6			
SS13S_A	9.32	11.5	13.1	14.4	13.2	9.83	9.32-14.4	2.55	
SS13S_B	19.1	19.1	17.8	16.3	18.6	20.6	16.3-20.6	2.19	
SS13S_C	13.2	13.7	9.39	12.9	11.6	-	9.39-13.2	2.65	
SS13S_D	18.6	21.5	19.5	18.7	17.3	-	17.3-21.5	2.27	19.0±0.70
SS13S_E	10.6	8.29	7.56	6.89	7.75	7.65	6.89-10.6	3.62	
SS13S_F	7.37	8.98	5.6	5.68	5.47	5.74	5.47-8.98	3.04	

NB: M2-5ml (2:1) HNO$_3$/HF + 1ml HCl; K1-k$_0$-INAA.
Source: Author Data, 2014

163

Table 16: Mean Concentration of Total Mercury in mg/kg "Black" Samples ("B") Using Two Different Digestions (M1 and M2) for CVAAS and k_0-INAA (K1) Method from Twelve (12) Pra River Basin, Ghana

"B"	Apreja M2 (n = 4)	Nkontinso M2 (n = 4)	Dunkwa-On-Offin*		Dunkwa-On-Offin** M2 (n = 4)
			M2 (n = 4)	K1 (n = 3)	
1	24.4±0.31	2.12±0.15	1,043±2.10	-	90.0±23.3
2	-	66.2±6.83	1,091±1.42	-	32.1±1.46
3	-	735±7.24	1,673±4.83	-	1.80±0.08
4	-	-	1,190±0.92	1,318±46.0	328±10.8

Source: Author Data, 2014

164

Total Mercury in "Black" and Mining Residues

The abandon of tailings from gold mining after amalgamation can contain highly disintegrated Hg that can later wash into the ecosystem and add more Hg to the environment. Also, residues of Hg in tailings left in the open air evaporate continuously and likewise contribute to pollution of the environment gradually (Kozin & Hansen, 2013). Thus, a total of twelve (12) special mining waste samples called "black" and thirty-four (34) other mining wastes (left in a pit after gold extraction) were analysed for THg concentrations from the Pra River Basin (Apreja, Nkontinso, Dunkwa-On-Offin (1), and Dunkwa-On-Offin (2) sampling sites). Cold Vapour Atomic Absorption Spectroscopy (CVAAS) was used by acid digestion procedure (M2) mentioned earlier in this study. The results from the special mining waste are presented in Table 15 and that for the "Black" samples are presented in Table16.

In using M2 to determine THg in the "black" samples a mean of THg concentration (523±4.95 mg/kg, $n = 12$) was recorded in the Pra River Basin. The least mean THg concentration of 1.80 mg/kg ($n = 12$) by M2 was registered at Apreja sampling site and the highest THg concentration of 1,673 mg/kg ($n = 12$) also recorded by Dunkwa-On-Offin (1) _C "black" sample. In another sampling site at Dunkwa-On-Offin sampling site, special mining residues sampled from six (6) pits were analyzed for THg concentration levels. The highest range of THg concentration in these mining wastes was between 17.3 to 21.5 mg/kg ($n = 6$) and the least range was between 5.47-8.98 mg/kg ($n = 6$). The amount of THg determined in these "blacks' are quite substantial which will be emitted to the environment if measures are not taken. When

these amount of THg get into the ecosystems and the most toxic organometallic compounds of Hg (methyl, ethyl, and phenylmercury) are produced, then an accumulation of methymercury in fish will occur (Drabaek, Iverfeldt, & Stoppler, 1992; Von Burg, 1991). Methylmercury is a neurotoxin and can pose serious health effects on both adults and children.

In performing Hg speciation using some of these "black" and other mining waste samples (as indicated in Table 17), Hg^0, $HgCl_2$, Hg_2Cl_2, HgS, HgO, and Hg_{mc} were present in both the "black" and mining waste samples. If these "black" and mining waste samples are exposed to the environments, then these Hg species will get into the environment. Hg^0, when left on the earth's surface, will constantly evaporate, into the atmosphere and since its lifetime is between 0.5 and 3 years (Bank, 2012) will continuously cycle through the atmosphere. Through oxidation reactions, Hg^0 will be converted into reactive gaseous mercury that represents a mixture of gaseous divalent mercuric compounds and particulate mercury which represents mercury species bound to airborne particles (Liu, Cai, & O'Driscoll, 2012). Hg in any form is toxic and can cause health implications. One can be exposed to mercury from breathing in contaminated air, from swallowing or eating contaminated water or food, or from having skin contact with mercury.

Mercury Speciation in Geological Samples using Temperature Fractionation Technique

Temperature fractionation technique was used to determine the species of mercury that has been released into the environments along the Pra River Basin and may pose health risk to the populate in the Basin. This was also

done to know the temperatures at which each species of mercury can decompose. The temperatures at which each species of mercury is released from the geological samples can be used to recover mercury for remediation purposes. Thus, temperature fractionation technique was purposively used to determine mercury species in thirteen (13) geological samples from the Pra River Basin, Ghana. The geological samples are made up of five (5) soil samples from the zero (0) to one (1) centimeter of selected soils and eight (8) mining wastes from the Pra River Basin, Ghana. The thermograms of mercury species formed after decomposition of mercury in topsoils (0-1 cm), mining waste and "Black" samples from the Pra River Basin in this study are presented in Figures 41 to 52. Table 17 also shows the range and maximum temperatures at which each mercury species decomposed and are compared to other research (Appendix O) done using other samples and standards elsewhere.

The decompositions of single Hg binding forms ($HgCl_2$) were released in all the five (5) topsoil (1-0 cm) samples in this research are presented in Figures 38 to 42. The average temperature range at which $HgCl_2$ decomposed in all the five (5) topsoil samples ranges between 100-388 °C and an average maximum temperature at 205 °C ($n = 5$). This Hg binding formed in this research was compared with two research standards ($HgCl_2$) conducted elsewhere (Hojdová, Navrátil, & Rohovec, 2008; Coufalík, Zvěřina, & Komárek, 2014) and these also confirmed the released of $HgCl_2$ in the topsoils (0-1 cm) from the Pra River Basin. The temperature range for the single sharp peaks of mercury species in this research (100-388 °C) was high than the one conducted using standard (100-300 °C) by other researchers (Hojdova et al.,

2008; Coufalík et al., 2014) with the average maximum temperature (205 °C) falling within 140 °C and 225 °C. Again, two (2) mining waste (SS12-Black-C and SS13-Black-C all grinded) also had single sharp peaks of Hg binding form (Figures 42 to 43) at an average temperature ranging between 63-287 °C ($n = 2$) with maximum peak at a temperature at 202°C ($n = 2$) indicating the possibility of Hg^0. Hg^0 is released at lower temperatures (Biester, Müller, & Schöler, 2002a; Biester, Müller, & Schöler, 2002; Coufalík, Zvěřina, & Komárek, 2014) as indicated in Table 17 (Hojdová, Navrátil, & Rohovec, 2008). Elemental mercury is used to extract gold from ore at the amalgamation process of artisanal and small-scale gold mining and mercury vapor is released into the atmosphere when amalgamation is burned (Spiegel & Veiga, 2006). Kabata-Pendias, (2011) indicate that Hg^0 is easily volatile and can evaporate into the atmosphere at lower temperatures.
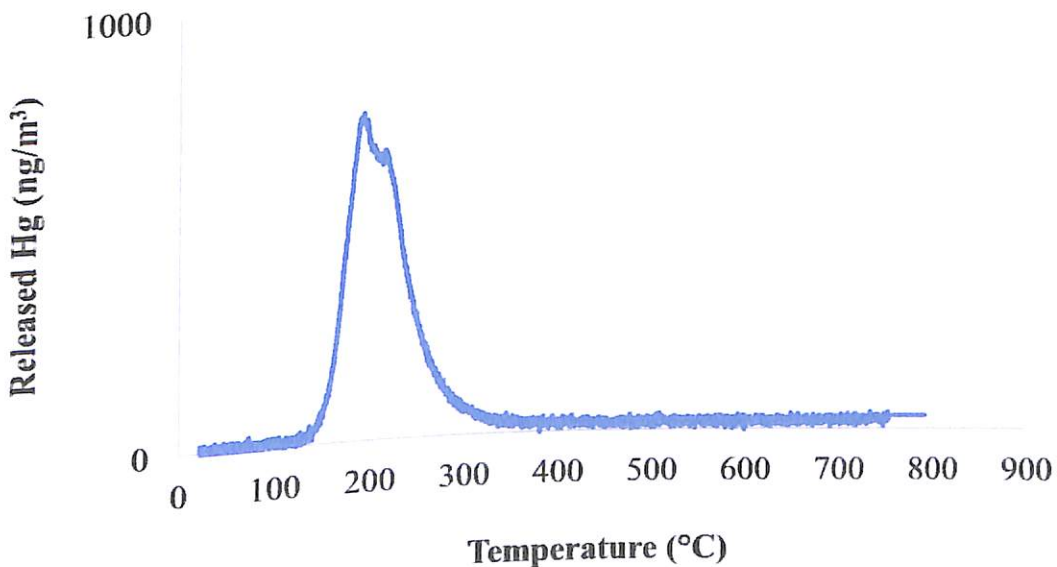
Figure 41: Mercury Species ($HgCl_2$) formed at a Maximum Temperature of 197 °C (709 ng/m^3) from the Topsoil (0-1 cm; grinded) Sampled from Dadientem (SS1), the Upstream of Birim River, Pra River Basin, Ghana
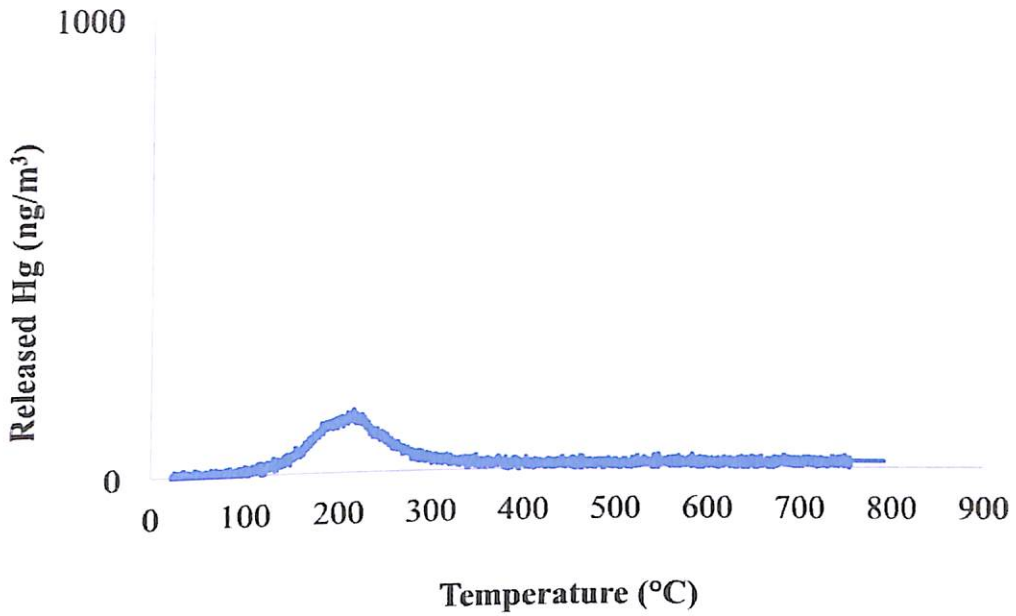
Figure 42: Mercury Species (HgCl$_2$) formed at a Maximum Temperature of 218 °C (108 ng/m^3) from the Topsoil (0-1 cm; grinded) Sampled from Akim Oda 1 (SS5), the Downstream of Birim River, Pra River Basin, Ghana
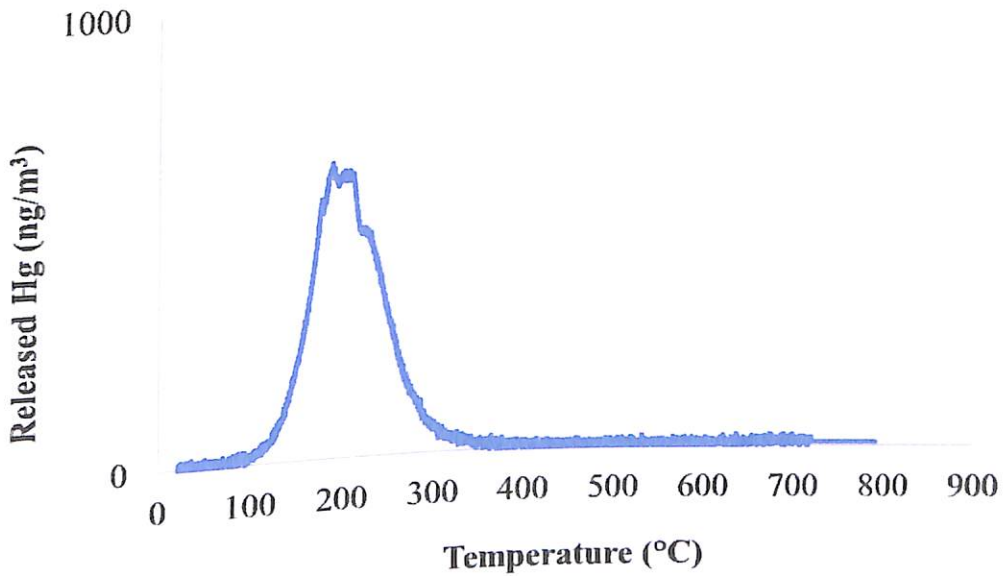
Figure 43: A Single Peak of Mercury Species (HgCl$_2$) formed at a Maximum Temperature of 197 °C (607 ng/m^3) from a Soil (0-1 cm, gringed) sample from Nkontinso (SS12) a Sampling site along the Offin River, Pra River Basin, Ghana

169
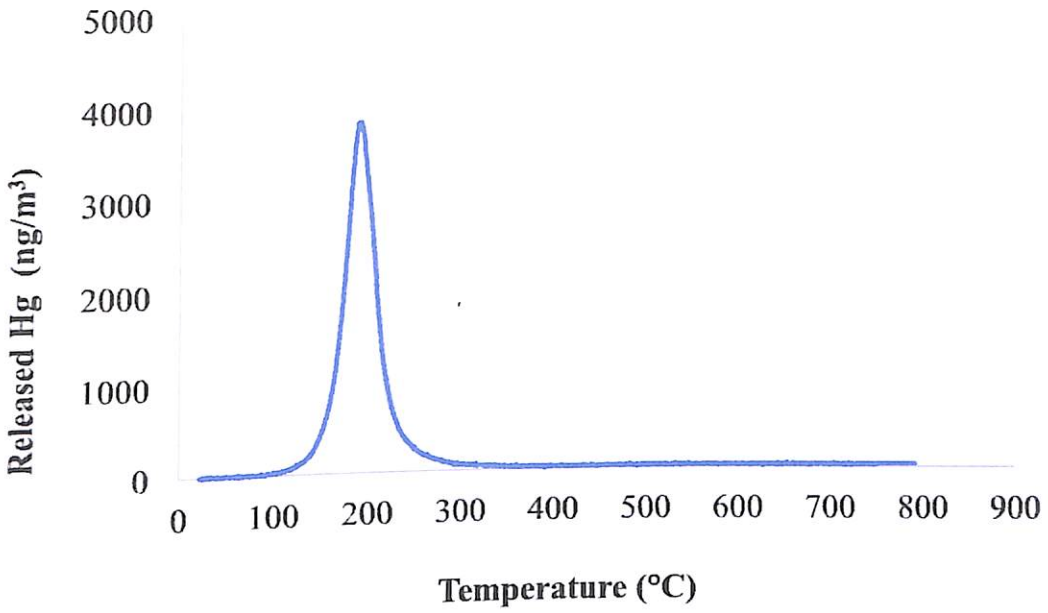
Figure 44: A Single peak of mercury species (HgCl₂) formed at a Maximum Temperature of 192 °C (3,627 g/m³) from a Soil (0-1 cm; grinded) sampled from Dunkwa-On-Offin (1) (SS13) a Sampling site along the Offin River, Pra River Basin, Ghana
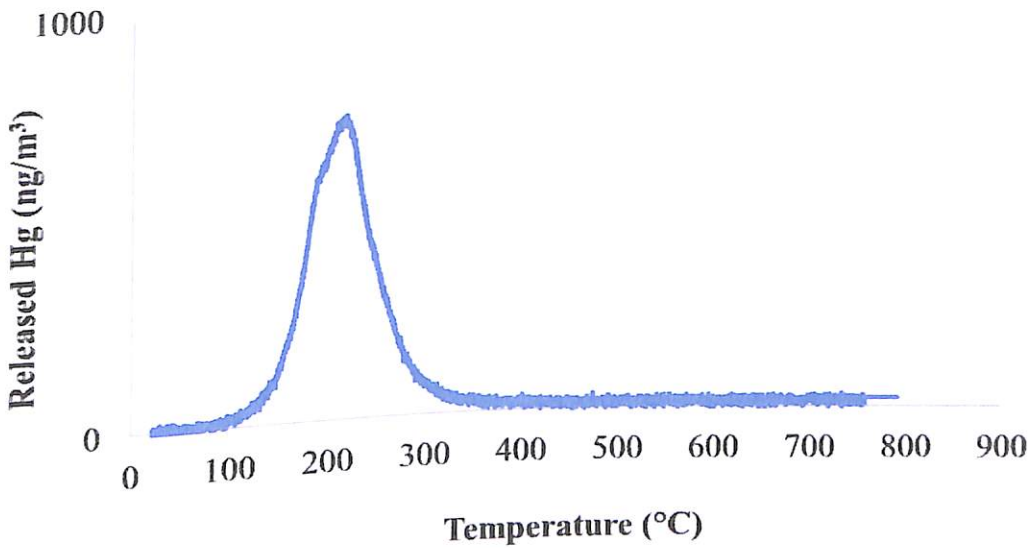
Figure 45: A Single Peak of Mercury Species (HgCl₂) formed at a Maximum Temperature of 221 °C (693 ng/m³) from a soil (0-1 cm, grinded) sampled from Twifo Praso (SS16), a Sampling site along the Main Pra River, Ghana
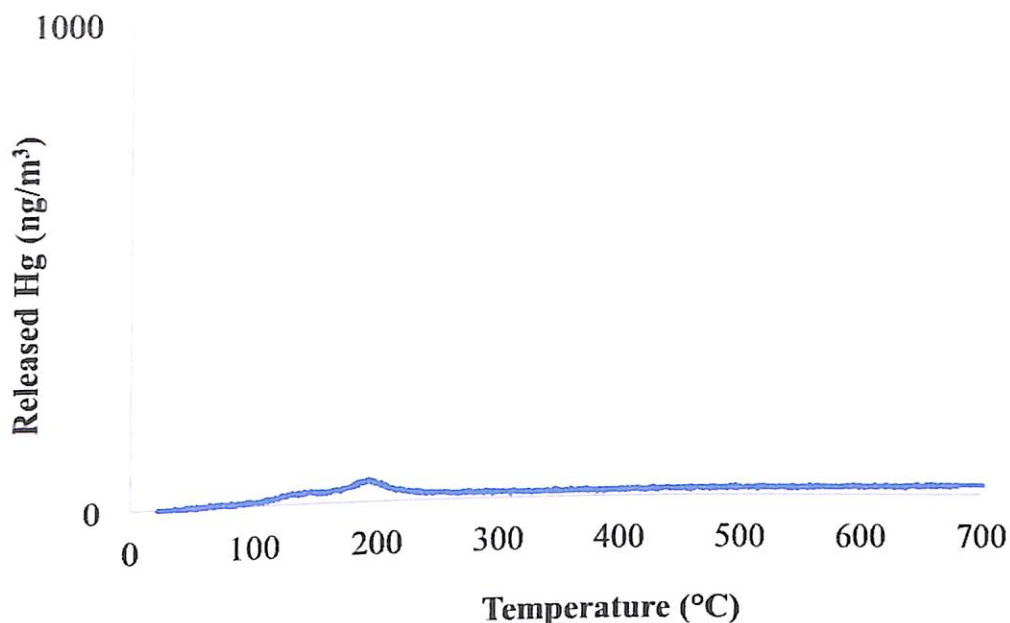
Figure 46: A Single Peak of Mercury Species (Hg^0) formed at a Maximum Temperature of 199 °C (39.4 ng/m^3) in "Black" a Special Mining Waste (SS12-Black-C, grinded) from Nkontinso, a Sampling site along the Offin River, Pra River Basin, Ghana
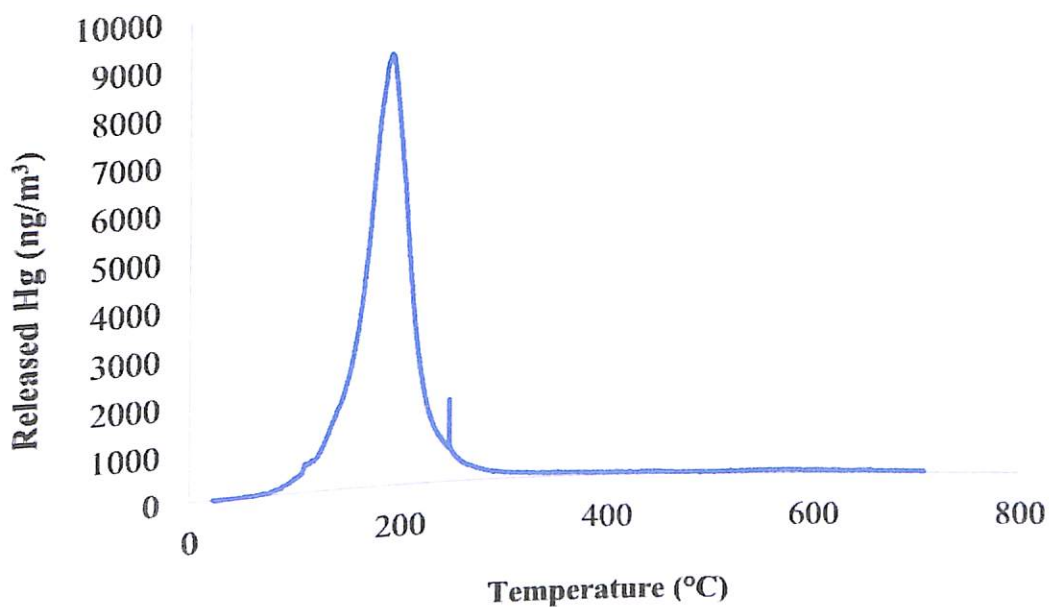
Figure 47: A Single Mercury Species (Hg^0) formed at a Maximum temperature of 193 °C (8,679 ng/m^3) in "Black" (grinded), a Special Mining Waste (SS13-Black-C) from Dunkwa-On-Offin, a Sampling site along the Offin River, Pra River Basin, Ghana

Figures 48 and 49 are the graphical representation of SS13S-D and SS13-Black-B respectively are both mining wastes which released double peaks (higher and smaller peaks of Hg) thermograms showing Hg binding forms of different species released at different temperatures. In Figure 48 the first Hg released was a sharply higher peak which started decomposing at 195 °C and ended at 269 °C which may be the possibility of $HgCl_2$ or Hg_2Cl_2 and HgS formed with the peak reaching its maximum temperature at 195 °C (1,707 ng/m^3). The second peak (a smaller peak of Hg species) occurring between a temperature range of 456-522 °C with a maximum temperature at 492 °C (50.0 ng/m^3) suggests HgO species. The second sample (SS13-Black-B) which also displayed double peaks (Figure 49), had its first Hg released between 70-280 °C (Hg^0) with a maximum temperature at 190 °C (3,895 ng/m^3) and the second (smaller) peak occurring between 530-645 °C (HgO) with a maximum temperature at 570 °C (97.3 ng/m^3).
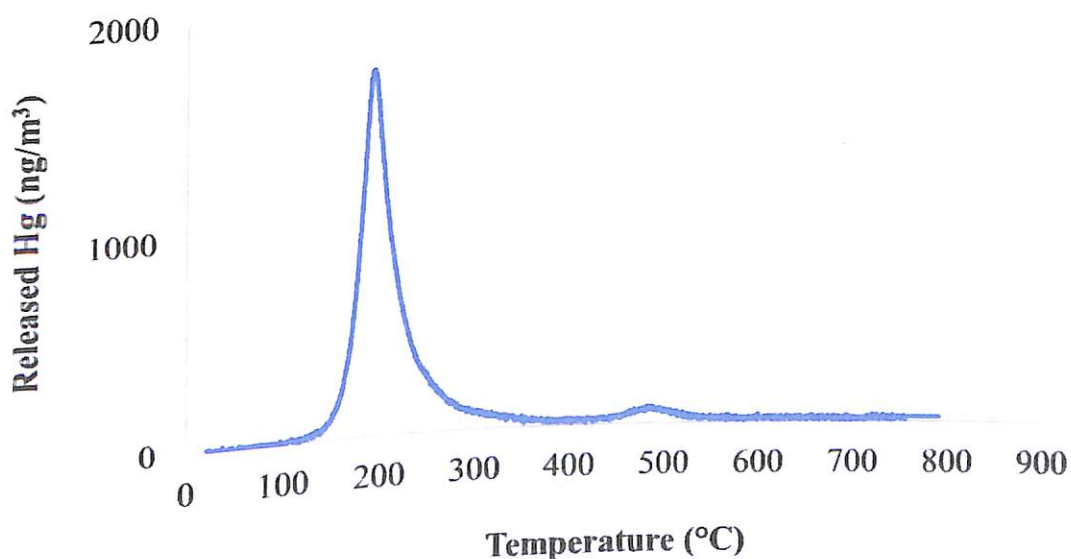
Figure 48: Two (2) Mercury Peaks formed at Maximum Temperatures of 195 °C (1,707 ng/m^3) and 492 °C (50.0 ng/m^3) from SS13S-D a Special Mining Waste (grinded) from Dunkwa-On-Offin, a Sampling site at the Offin River, Pra River Basin, Ghana
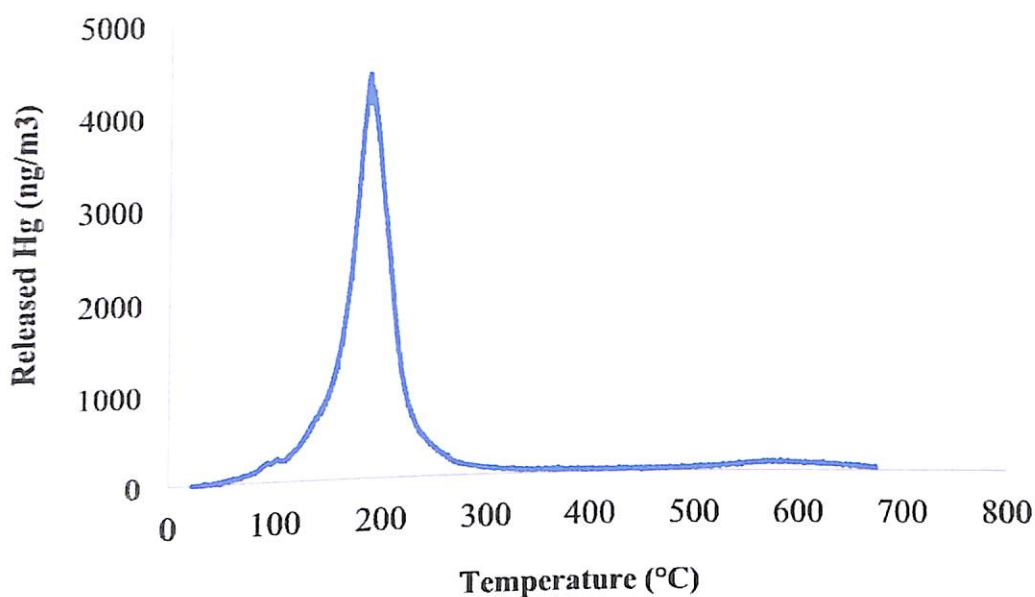
Figure 49: Two (2) Mercury Peaks formed at Maximum Temperatures of 193 °C (3,895 ng/m^3) and 571 °C (97.3 ng/m^3) from by SS13-Black-B Mining Waste (grinded) from Dunkwa-On-Offin, a Sampling site at the Offin River, a Major Tributary of the Pra River Basin, Ghana

SS13-Black-D (ungrinded) and SS13-Black-D (grinded) are the same mining waste sample but one is more homogenized (grinded) and the ungrinded (which was pass through 0.2 mm nylon sieve). After decomposition, each sample gave quite different results. In both samples which are presented in Figures 50 and 51, a peak formed at almost the same temperature range with the maximum temperature at 202 °C for both graphs indicating the same mercury species released. Nevertheless, in Figure 50 (ungrinded sample) another Hg species was released between temperature ranges of 80-285 °C at a maximum temperature at 102 °C. These two peaks observed for ungrinded SS13-Black-D may be probably related to the decomposition of Hg_2Cl_2 in two steps (Lopez-Anton, Yuan, Perry, & Maroto-Valer, 2010).

$$Hg_2Cl_2 \rightarrow Hg^0 + HgCl_2$$

173

$$HgCl_2 \rightarrow Hg^0 + Cl_2$$
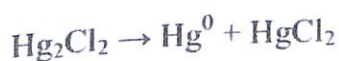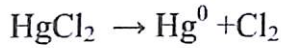
The third Hg peak appeared between the temperature range of 450-510°C and its maximum peak at 478 °C which depicts HgO. Figure 50, is the same sample as in Figure 51 but grinded (more homogenized), the first peak of Hg appeared between 62.7-267 °C with the maximum peak at 202 °C showing the presence of Hg^0. The second and third Hg species HgS and HgO started decomposition form 432-493 °C and 559-609 °C with maximum peaks forming at 437 °C and 566 °C respectively.
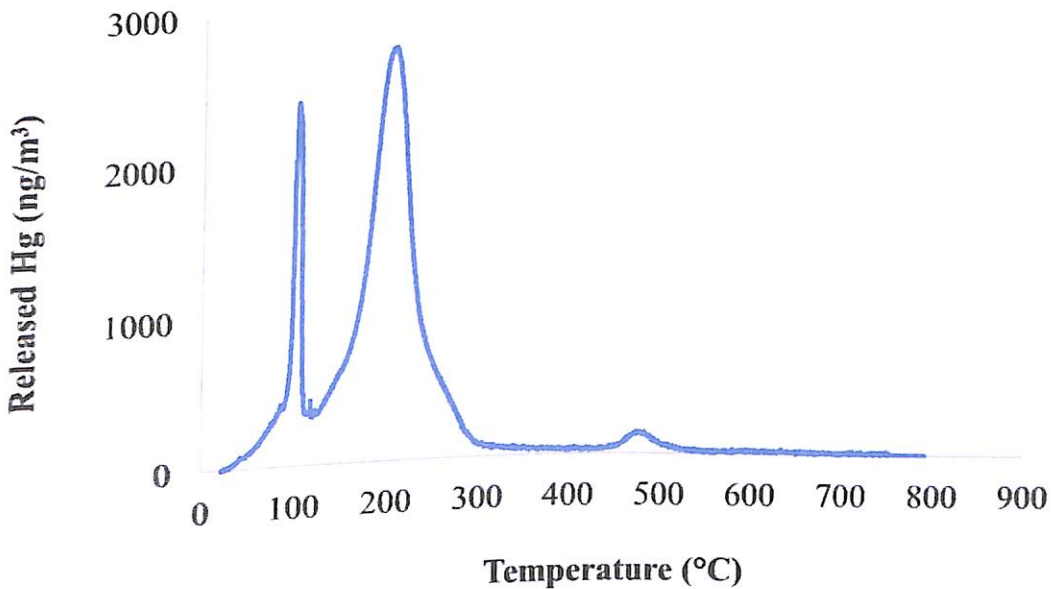
Figure 50: Three (3) Peaks formed at Maximum Temperatures of 102 °C (2,350 ng/m³), 202 °C (270 ng/m³) and 478 °C (116 ng/m³), SS13-Black-D, a Mining Waste (ungrinded) from Dunkwa-On-Offin, a Sampling site at the Offin River, a Major Tributary of the Pra River Basin, Ghana
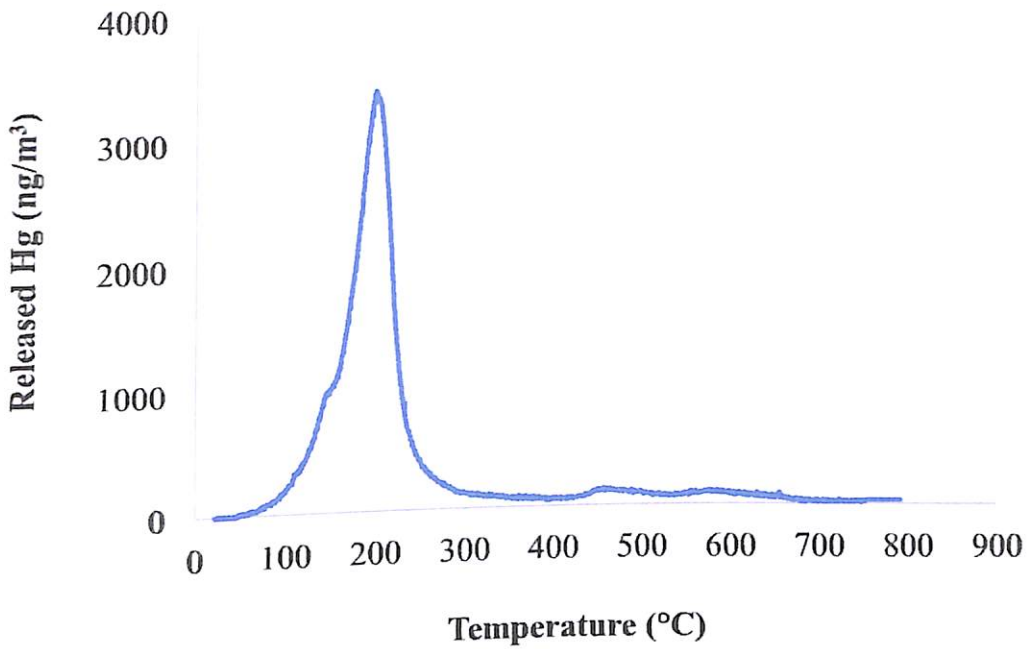
Figure 51: Three (3) peaks formed at Maximum Temperatures of 202 °C (3,239 ng/m³), 437 °C (122 ng/m³) and 566 °C (98.0 ng/m³) after the Mining Waste (SS13-Black-D) was grinded from the Dunkwa-On-Offin, a Sampling site at the Offin River from the Pra Basin River, Ghana

The third sample (SS14-Black-D) in Figure 52 also had three (3) peaks of Hg species with the first peak released within a temperature range from 60 to 245 °C with maximum peaks temperature of 109 °C. The second peak of Hg species formed between the temperature ranges from 141 to 200 °C at a maximum peak at 177 °C with the third peak of Hg species decomposition starting from 203 to 283 °C. The maximum peak at which the third peak formed was 231°C. This also shows the decomposition steps of Hg_2Cl_2 (Lopez-Anton, Yuan, Perry, & Maroto-Valer, 2010).
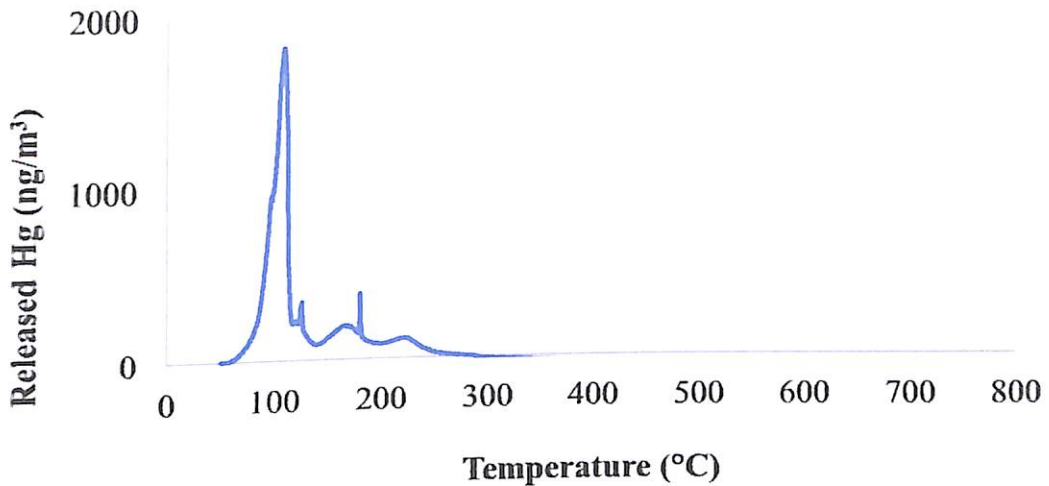
Figure 52: Three (3) Peaks of Hg Species formed at Maximum Temperatures of 109 °C (1,643 ng/m³), 177 °C (178 ng/m³) and 231 °C (107 ng/m³) by SS14-Black-D Mining Waste (grinded) sample from the Dunkwa-On-Offin (2), a Sampling site at the Offin River from the Pra River Basin, Ghana

Another "Black" samples (SS13-Black-A), grinded was presented in Figure 53 gave four (4) peaks which include three (3) small peaks and a one (1) major peak. The first peak of mercury species was a small peak released between the temperatures of 73-130 °C with its maximum temperature peak forming at 126 °C (563 ng/m³) and was identified as Hg^0 (Biester et al., 2002a; Biester et al., 2002b; Coufalík et al., 2014). The second Hg species was the major peak formed between a temperature range of 131-330 °C had its largest peak forming at a maximum temperature of 207 °C (5,509 ng/m³) also identified as Hg_2Cl_2, $HgCl_2$;HgS (Coufalík, Zvěřina, & Komárek., 2014; Hojdová, Navráatil, & Rohovec, 2008; Lopez-Anton, Yuan, Perry, Marotovaler, 2010). The third peak is also a minor peak formed at a temperature ranges of 419-526 °C with its highest peak at a temperature of 473 °C (107 ng/m³) which can also be assumed to be HgO (Biester, Gosar, & Müller, 1999); whilst the last peak formed within the temperature range of

556-616 °C at a higher peak of 589 °C which is an indication of HgO released

from the mining waste.
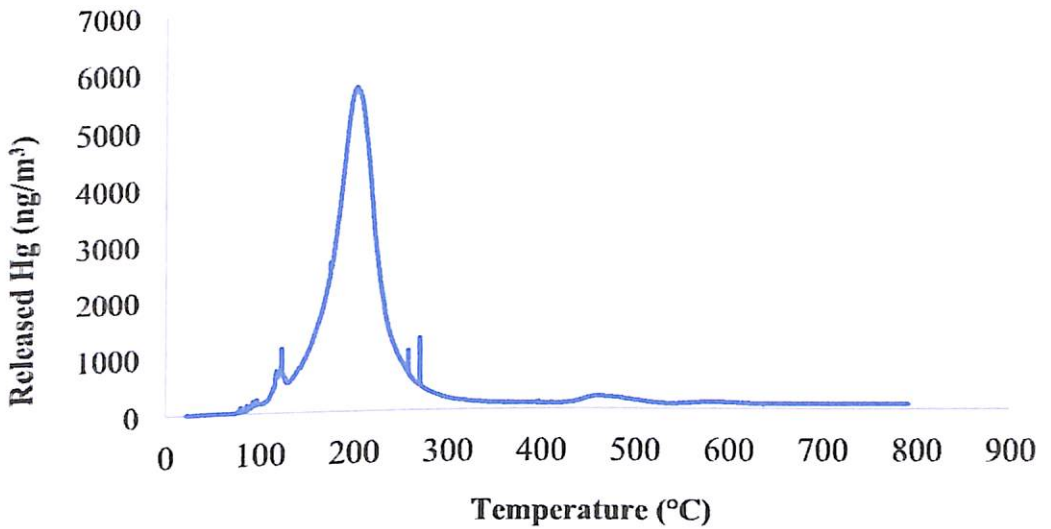
Figure 53: Four (4) Peaks formed at Maximum Temperatures of 126 °C (563 ng/m³), 207 °C (5,509 ng/m³), 473 °C (198 ng/m³) and 480 °C (107 ng/m³) by SS13–Black–A Mining Waste (grinded) sample from Dunkwa-On-Offin, a Sampling site at the Offin River, a Major Tributary Pra River Basin, Ghana

In Figures 41, 43, 46, 49, 51 and 52, the peaks were not sharp as a

result of difficult matrices of the samples (soil, mining waste, and "Black")

from the Pra River Basin. In analyzing THg in these samples from the Pra

River Basin, $HNO_3/HClO_3/H_2SO_4$ Wet Acid Digestion (M1) was not able to

total digest THg into solution but rather more robust digestion procedure

involving HF acid combination had to be used to totally digest THg into

solution for measurements. This was due to other elements (As, Hf, Se, Zr, U,

Sb, W, and Au) in the samples (presented in Appendices Q and R) which

bonded THg (Appendix S) to the lattice of the silicate and therefore prevented

THg liberation from the sample's matrices for measurements. Unlike cinnabar

crystal (HgS), species of Hg are bond chemically or physically to samples

(Coufalík, Zvěřina, & Komárek, 2014) thus, the binding interactions of

analytes in the matrix and their stability thus making it difficulty for Hg species to be released easily (sharp peak) but rather broaden peaks.

Different Hg species have a different health effect. The brain is the critical organ for Hg^0 toxicity. Meanwhile, the salts of H^{++} ($HgCl_2$ and HgS) in the kidney are the most sensitive organ expose to H^{++} salts and affect it greatly. It also damages the renal glomerulus through an autoimmune reaction resulting in albuminuria. In the body, the highest concentrations of H^{++} are found in the liver and kidney. Also, long term inhalation exposure of Hg^0 can lead to Hg^{++}. HgO is a toxic substance which can be absorbed into the body by inhalation of its aerosol, through the skin and by ingestion. The substance is irritating to the eyes, the skin and the respiratory tract and may have effects on the kidneys too, resulting in kidney impairment. In the food chain important to humans, bioaccumulation takes place, specifically in aquatic organisms. In general, Hg can cross the placenta and accumulate in the fetal tissue, thus developing foetuses are most at risk. In babies, mercury can be transferred from mother to child through breast milk. However, the health effects of highly exposed populations and wildlife are also a great concern (Gundacker & Hengstschläger, 2012; Driscoll, Mason, Chan, Jacob, & Pirrone, 2013). Mercury may have toxic effects on the nervous, digestive and immune systems, and on lungs, kidneys, skin, and eyes (WHO, 2017). Aside health issues, impacts of Hg have been also assessed for three potential future anthropogenic Greenhouse Gas (GHG) emissions on climate change (Driscoll, Mason, Chan, Jacob, & Pirrone, 2013). Thus the exposure of these Hg species, that is Hg^0, $HgCl_2$, Hg_2Cl_2, HgS, HgO, and Hg_{mc} into the environment will pose a lot of health risk which needs to be looked at.

Table 17: Hg Binding forms in Soil, "Black" and Mining Waste Samples which were determined by Temperature Fractionation Method in this Study

Study	Sample name	Name of Sampling site	Material	THg mg/kg	Possible Hg Compounds released	Θ °C range	θ °C max.
This study	SS1 (0-1 cm)*	Dadientem	Soil	11.1	Single peak ($HgCl_2$)	132-330	197
	SS5 (0-1 cm)*	Akim Oda (1)	Soil	1.77	Single peak ($HgCl_2$)	103-341	218
	SS12 (0-1cm)*	Nkontinso	Soil	10.9	Single peak ($HgCl_2$)	102-348	197
	SS13 (0-1 cm)	Dunkwa-On-Offin	Soil	103	Single peak ($HgCl_2$)	100-314	192
	SS16 (0-1 cm)*	Twifo Praso	Soil	13.2	Single peak ($HgCl_2$)	104-360	221
	SS12–Black–C	Nkontinso	Black	735	Single peak (Hg^0)	66.0-264	199
	SS13–Black–C	Dunkwa-On-Offin	Black	1,673	Single peak (Hg^0)	60.0-310	204
	SS13S–D	Dunkwa-On-Offin	Mining [w]	18.7	1st peak ($HgCl_2$,Hg_2Cl_2,HgS) / 2nd Peak (HgO)	145-269 / 456-522	195 / 492
	SS13–Black–B	Dunkwa-On-Offin	Black	1,091	1st peak (Hg^0) / 2nd peak (HgO)	70-280 / 530-645	190 / 570

179

Table 17 Cont'd

Sample	Location	Colour		Peak		
SS13–Black–A	Dunkwa-On-Offin	Black	1,043	1st peak (Hg^0)	73-130	126
				2nd peak	131-330	207
				($HgCl_2,Hg_2Cl_2;HgS$)		
				3rd peak (HgS)	419-26	473
				4th peak (HgO)	556-616	589
SS13–Black–D (grinded)	Dunkwa-On-Offin	Black	1,318	1st peak (Hg^0)	62.7-267	202
				2nd peak (HgS	432-493	437
				3rd peak (HgO)	559-609	566
SS13–Black–D (ungrinded)	Dunkwa-On-Offin	Black	1,773	1st peak (Hg^0)	80.0-113	102
				2nd peak	130-285	202
				($HgCl_2,Hg_2Cl_2;HgS$)		
				3rd peak (HgO)	450-510	478
SS14–Black–D	Dunkwa-On-Offin [2]	Black	328	1st peak (Hg^0)	60-137	110
				2nd peak	141-200	177
				($HgCl_2,Hg_2Cl_2;HgS$)		
				3rd peak (Hg_{mc})	203-283	231

Note: *The temperature were estimated from the reported Hg release curves; Hg_{mc} = Hg bound to the matrix components.
Source: Author Data, 2014

Table 18: Fish Samples from Seven (7) Sampling Sites from the Pra River
Basin, Ghana

Sampling sites	Herbivorous	Carnivorous	Omnivorous
SS12	*Oreochromis niloticus, Sarotherodon melanotheron,*	*Chrysichthys nigrodigitatus, Synodontis eupterus, Schilbe schilbe,*	*Parachana obscura*
SS13	*Sarotherodon melanotheron, Oreochromis niloticus, Barbus/Brycinus*	*Chrysichthys nigrodigitatus, Synodontis eupterus, electric fish.*	*Parachana obscura, Clarias sp., Heterobranchus*
SS16	*Tilapia zillii*	*Synodontis eupterus, Chrysichthys nigrodigitatus,*	*Parachana obscura*
SS17	*Brycinus nurse, Tilapia zilli*	*tilapia*	
SS18	*Tilapia zillii*	*Chrysichthys nigrodigitatus, Hemichromis fascitus, Parachana obscura*	*Heterobranchus*
SS20	*Sarotheron melanotheron,*	*Elops lacerta, Bathygobius sp., Brachydeuterius aurita,*	*Liza falcipinnis.*
SS21	*Tilapia zillii*	*Chrysichthys nigrodigitatus,*	*Liza falcipinnis.*

Source: Author Data, 2013

Table 19: Number of Fish Species Sampled from each Sampling Sites from the Pra River Basin

Species of Fish	SS12	SS13	SS16	SS17	SS18	SS20	SS21	Sub Total
Oreachromis niloticus	15							15
Sarotheron melanotheron	11					40		51
Brycinus				10				10
Tilapia zillii			36	21	24		25	106
Elaps laurta						5		5
Bathygobius sp.						7		7
Brachydeuterus aurita				10		6		16
Heterobranchus catfish		4			12			16
Chrysichthys nigrodigitatus	24	32	2				70	128
Synodontis eupterus	25	14	19					58
Electric fish		1						1
Parachana obscura	5	3						8
Schilbe schilbe	7							7
Clarias sp		5						5
Liza sp						49		49
Sole						1		1
Cynoglossus spp								
Kribia sp						2		2
Snake head			8		3			11
Hemichromis				17	6			23
Total								516

Source: Author Data, 2013

Total Mercury and Methylmercury in Carnivorous Fish Muscle and Skin from Pra River Basin

Methylmercury (MeHg) is a neurotoxin, the most toxic form of Hg species which presents many concerns in the ecology. This is because it tends to accumulate in the tissues of the animal which through the food chain gets to humans, thus influences the health and evolution of the organism. Fish and

182

fish products are the dominant source of methylmercury in food. Seven (7) species of carnivorous fish (*Chrysichthys nigrodigitatus, Synodontis eupterus, Scilbe schilbe, Hemichromis fascitatus, Elops lacerta, Bathygobius sp., Brachydeuterius aurita*) samples of varying standard length (cm) were categorized using length intervals of 4.9 cm in each sets of carnivorous fish samples. These carnivorous fish samples are presented in Table 19. The standard length (cm) of the carnivorous fish samples used for analysis ranges between 0.1 cm and 55.1 cm. Each set of the carnivorous fish sample was analyzed for both THg (muscle and skin) and methylmercury (muscle) in wet weight. In all, a total number of three hundred and twenty-seven (327) carnivorous fish samples (Table 8) were used for the determination of THg and MeHg in this research.

Out of the eight (8) sets of carnivorous fish muscle analyzed, 24 % of the carnivorous fish (most consumed fish) had THg higher than that of the Mercury Reference Concentrations of 0.3 µg/g (EPA, 2001). The results of THg and methylmercury in µg/g and percentages of MeHg in the carnivorous fish muscle in this study are presented in Table 19.

Fish sample (0.10-5.00 cm) from Anlo sampling site gave a mean THg concentration of 0.021 µg/g ($n = 4$, $std = 0.011$) which was lower than the Mercury Reference Concentration (0.30 µg/g) with 76.2 % MeHg (0.016 µg/g). The carnivorous fish muscle with the standard length 5.10-10.0 cm from the Pra River Basin had a mean THg concentration of 0.162 µg/g ($n = 5$; mean MeHg = 0.131, mean % MeHg = 80.9 %). Meanwhile the range of THg concentration in the carnivorous fish muscle (5.1-10 cm) was between 0.045 and 0.397 µg/g ($n = 5$; range of MeHg = 0.036-0.132 µg/g; range of % MeHg

183

between 65.0 and 100 %) with the maximum THg concentration of 0.397 µg/g

(% MeHg = 76.3 %) recorded from Nkontinso, a sampling site from the Offin

River. Fish appear to bind methylmercury strongly. Thus, approximately 100

percent of mercury that bioaccumulates in predator fish is MeHg which was

also exhibited in the carnivorous fish muscle samples (standard length = 5.10-

10.0 cm) from Twifo Praso sampling site with a percentage (100 %) of MeHg

in the fish muscles been the highest recorded in this category of fish sample.

MeHg is toxic and it ingestion by humans will create lots of health problems,

therefore fish in this category of standard length (5.10-10.0 cm) will pose lots

of health problems to people in the catchments areas when used as food.

The next category of carnivorous fish with standard length 10.1-15.0

cm that was analysed for THg and MeHg were from five (5) sampling sites

had the highest concentration of 0.380 µg/g (n = 4, % MeHg = 96.3 %) was

again registered at Nkontinso sampling site from the Offin River which was

also higher than the Mercury Reference Concentration of 0.30 µg/g (EPA,

2001). Figure 12 is a portion of Offin River at Nkontinso, a sampling site that

is impacted with a lot of ASGM activities as indicated in Table 8. The THg

concentration in this set of standard length (10.1-15.0) ranges from 0.032 to

0.380 µg/g (n = 7; mean of THg = 0.166 µg/g; mean of MeHg = 0.155 µg/g;

range % MeHg = 84.8 to 108 %). The Highest methylmercury in standard

length (10.1-15.0 cm) carnivorous fish was 108 % (THg = 0.103 µg/g, n = 4;

MeHg = 0.111 µg/g, n = 4) which was from Shama sampling site, the estuary

at the main Pra River. The highest percentage of methylmercury (108 %) in

the 10.1-15.0 cm (standard length) in this studies was higher than a proposed

percentage of greater than 94 % of methylmercury in a small freshwater fish

of approximately 10-15 cm (Drysdale, Burgess, Entremont, Carter, & Brun, 2005; Scheuhammer, Atchison, Wong, & Evers, 1998). Meanwhile a larger predatory fish, muscle tissue contains 40 > 90 % MeHg (Lasorsa & Allen-Gil, 1995). It must be noted that the highest percentage of methylmercury (108 %) in the standard length (10.1-15.0 cm) was higher than the highest percentage of methylmercury (100 %) in standard length (5.10-10.0 cm). The mean percentage methylmercury of 82.9 % (n = 5) for standard length (5.10-10.0 cm) was lower than the mean percentage of methylmercury of 95.7 % (n = 5) for standard length (10.1-15.0 cm) from the Pra River Basin in this study.

The third group of standard length was 15.1-20.0 cm carnivorous fish muscle analysed (n = 5) and the utmost THg concentration registered was 0.376 µg/g (n = 4, % MeHg = 92.3 %) was yet again from Nkontinso sampling site from the Offin River. THg concentrations ranges from 0.079 to 0.376 µg/g (n = 5, mean THg = 0.219 µg/g, range of % MeHg between 88.8 and 110 %). This time the highest methylated fish was 110 % MeHg (THg = 0.079 µg/g, MeHg = 0.087 µg/g) and this set of fish came from Daboase sampling site from the main Pra River. Only one sampling site (Twifo Praso 1) from the main Pra river had carnivorous fish samples for standard length 20.1-25.0 cm and it had THg concentration of 0.175 µg/g (n = 4, MeHg = 0.211 µg/g, % MeHg = 121 %).

In the carnivorous fish muscle of the standard length of 25.1-30.0 cm group, three (3) out of the four (4) fish muscle analysed had their THg concentration 0.983 µg/g (n = 4, % MeHg = 81.9 %), 0.313 µg/g (n = 4, % MeHg = 118 %), and 0.371 µg/g (n = 4, % MeHg = 72.2 %) from Nkontinso (Offin River), Dunkwa-On-Offin (Offin River) and Twifo Praso (Main Pra

River) respectively above the Mercury Reference Concentration of 0.30 µg/g (EPA, 2001). The range of THg concentration was between 0.055 to 0.983 µg/g (n = 4, range of MeHg = 0.060-0.805 µg/g, % MeHg range between 72.2-118 %) with the highest percentage methylated carnivorous fish muscle having 118 % MeHg (THg = 0.313 µg/g and MeHg = 0.356 µg/g) from Dunkwa-On-Offin (Offin River) sampling site. This indicates that carnivorous fish with the standard length between 25.1 and 30.0 cm groups along the food chain may accumulate Hg in their tissues. MeHg is water soluble and its bioavailable due to its stronger binding compared to Hg (II) it bioaccumulates in living organisms and also increases in the food chain with increasing trophic levels (Rimondi, Gray, Costagliola, Vaselli, & Lattanzi, 2012). Daboase was the only sampling site that had these two sets of standard length 35.1-40.0 cm and 55.1-60.0 cm from the Pra River Basin and their THg concentration were 0.146 µg/g (n = 4, MeHg = 0.156, % MeHg = 107 %) and 0.060 µg/g (n = 4, MeHg = 0.040 µg/g, % MeHg = 71.8 %) respectively. *Chrysichthys nigrodigitatus* a carnivorous fish from the Offin River (Kaniago, Buabuasin, and Baadoa) one of the tributaries of the Pra River Basin which was studied (Dankwa et al., 2005) gave a mean Hg concentration to be 0.23 µg/g. Hg input to ecosystems largely occurs as Hg^{2+}, which enters aquatic ecosystem by means of atmospheric deposition or from point sources such as wastewater and storm drainage discharges from hotspots or contaminated sites. Inputs of Hg can be retained in sediments which have reduced to gaseous elemental mercury (GEM) and transported through drainage water to sites of net methylation (Grigal, 2003).

The same carnivorous fish samples were analyzed to determined THg concentration (µg/g) in the carnivorous fish skin were also presented in Table 20. All the THg concentration in the skin of all the standard length (0.10-60.0 cm) of carnivorous fish skin samples in this study were below the Mercury Reference Concentration of 0.30 µg/g. The THg concentration in the carnivorous fish skin ranges from 0.016 to 0.060 µg/g (n = 4, mean = 0.038 µg/g) in 5.10-10.0 cm standard length with the highest from Nkontinso (Offin River) sampling site; 0.010 to 0.072 µg/g (n = 6, mean = 0.040 µg/g) with standard length 0.10-5.00 cm, Twifo Praso (1) sampling site with standard length 20.1-25.0 cm, Daboase with standard lengths 35.1-40.0 cm and 55.1-60.0 cm were single carnivorous fish samples found in the mentioned sampling sites and their THg concentrations in the skin are 0.027 µg/g, 0.025 µg/g, 0.011 and 0.005 respectively. Most Hg found in fish is in methylated form consequently it is easily transferred to man as the intestinal absorption of MeHg is extremely high (Veiga, Baker, Fried, & Withers, 2004).

Table 20: Results of THg (*n* = 4) and MeHg *(n* = 4) in mg/kg; Mean (*n* = 4), Minimum, Maximum, Standard Deviation of various Standard Lengths (cm) of Carnivorous Fish (muscles and skin) from Pra River Basin, Ghana

Sampling site	Fish sample n	Standard length (cm)	Carnivorous Fish			
				Muscle		Skin
			THg	MeHg	%(ab)	THg
Anlo (Estuary)	5	0.10-5.00	0.021	0.016	76.2	0.026
Nkontinso	10	5.10-10.0	0.397*	0.303	76.3	0.060
Dunkwa-On-Offin	20		0.141	0.132	93.6	-
Twifo Praso (1)	7		0.109	0.109	100	0.023
Anlo (Estuary)	5		0.045	0.036	80.0	0.016
Shama (Estuary)	28		0.119	0.077	64.7	0.054
Mean (*n = 5*)			**0.162**	**0.131**	**82.9**	**0.038**
Minimum			**0.045**	**0.036**	**64.7**	**0.016**
Maximum			**0.397**	**0.303**	**100**	**0.060**
STD			**0.136**	**0.102**	**14.0**	**0.022**
Twifo Praso (1)	6	10.1-15.0	0.085	0.087	102	0.019
Twifo Praso (2)	7		0.158	0.142	89.9	0.010
Daboase	6		0.197	0.167	84.8	0.071
Anlo (Estaury)	5		0.032	0.030	93.8	0.032
Shama (Estuary)	29		0.103	0.111	108	0.038
Mean (*n* = 5)			**0.166**	**0.155**	**95.7**	**0.040**
Minimum			**0.032**	**0.030**	**84.8**	**0.010**
Maximum			**0.380**	**0.366**	**108**	**0.072**
STD			**0.166**	**0.106**	**9.26**	**0.026**
Nkontinso	10	15.1-20.0	0.376*	0.347	92.3	0.125
Dunkwa-On-Offin	7		0.217	0.206	94.9	-
Twifo Praso (1)	9		0.143	0.127	88.8	0.028
Daboase	4		0.079	0.087	110	0.017
Shama (Estuary)	13		0.280	0.293	105	0.051
Mean (n = 5)			**0.219**	**0.212**	**98.2**	**0.055**
Minimum			**0.079**	0.087	**110**	**0.017**
Maximum			**0.376**	**0.347**	**110**	**0.125**
STD			**0.116**	**0.109**	**8.89**	**0.049**
Nkontinso	15	25.1-30.0	0.983*	0.805	81.9	0.154
Dunkwa-On-Offin	12		0.313*	0.356	114	-
Twifo Praso (2)	10		0.371*	0.268	72.2	0.070
Daboase	4		0.055	0.06	109	0.012

Table 20 Conti'd

Mean (n = 4)	0.431*	0.372	99.6	0.079
Minimum	0.055	0.06	72.2	0.012
Maximum	0.983	0.805	118	0.154
STD	0.393	0.314	21.6	0.071

NOTE: *a*- denotes fish samples from estuary of the Pra River Basin; (*) denote carnivorous fish muscles whose THg concentration is higher than that of the Mercury Reference Concentrations of 0.3 µg/g (EPA, 2001); *b*- denote single fish standard length found in the Pra River Basin.

Source: Author Data, 2014
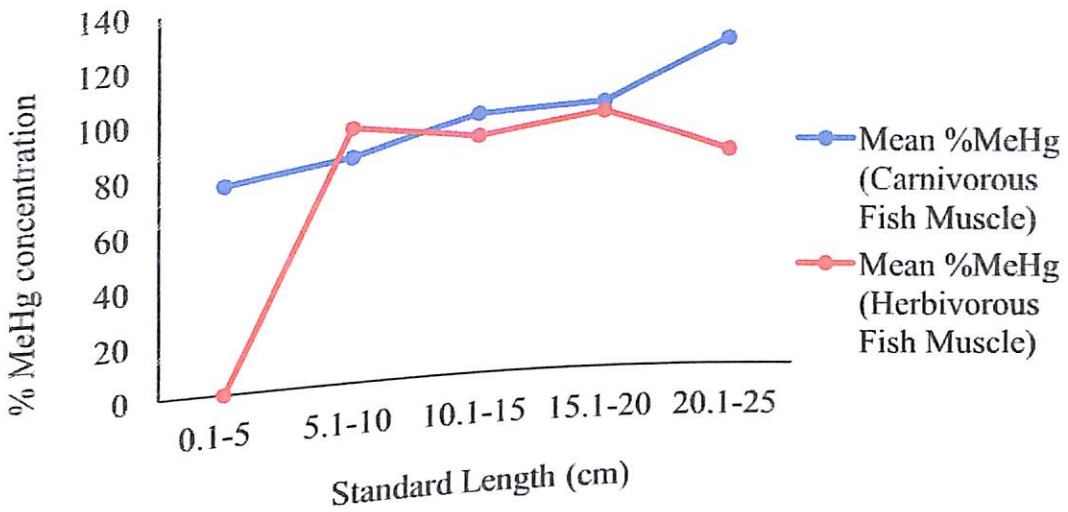
Figure 54: The mean percentage (MeHg/Hg *100) in both carnivorous and herbivorous fish muscle of different standard length (cm) from the Pra River Basin, Ghana

A graphical representation in Figure 54 shows the mean percentages (%) of MeHg increases as standard length increases (5.10-10.0 cm, 10.1-15.0 cm, 15.1-20.0 cm and 25.1-30.0 cm) in the carnivorous fish muscle but that of herbivorous fish muscle decreased with the standard length from the Pra River Basin.

Total Mercury and Methylmercury in Herbivorous Fish Muscle and Skin from Pra River Basin, Ghana.

A total number of one hundred and eighty nine (189) herbivorous fish (*Oreochromis niloticus, Sarotherodon melanotheron, Barbus, Tilapia zillii,* and *Brycinus nurse*) samples which were grouped into four different standard length (5.10-10.0 cm = 72 fishes; 10.1-15.0 cm = 64 fishes; 15.1-20.0 cm = 36 fishes; and 20.1-25.0 cm = 17 fishes) from four (4) different sampling sites from the Pra River Basin (Nkontinso, Twifo Praso-1, Twifo Praso-2 and Daboase sampling sites) were analyzed for both THg and MeHg. The THg was determined in the fish muscle and skin using CVAAS method whilst the MeHg was determined via CVAFS method. The results of both THg and MeHg in the herbivorous fish samples from the four (4) sampling sites from the Pra River Basin are presented in Table 21.

The THg concentration in herbivorous fish for standard length 5.10-10.0 cm ranged from 0.031 to 0.205 µg/g ($n = 5$, mean = 0.099 µg/g) and that of MeHg also had 0.029 to 0.178 µg/g ($n = 5$, mean = 0.094 µg/g). The highest percentage of methylmercury in this category of fish muscle was 104 % (MeHg = 0.199 µg/g, THg = 0.191 µg/g) from Daboase a sampling site in the main Pra River. Meanwhile, the highest THg concentration in this category of fish was from Nkontinso sampling site from the Offin river catchment area. Herbivorous fish skin in this category of fish also had a range of THg concentration between 0.016 and 0.110 µg/g ($n = 5$, mean THg = 0.035). Herbivorous fish ($n = 60$) muscle from five (5) sampling sites with standard length 10.1 to 15.0 cm had a range of THg concentration from 0.043 to 0.262 µg/g ($n = 5$, mean = 0.118 µg/g). Also, the MeHg concentration from the same

190

fish muscle samples gave concentration ranging between 0.029 and 0.178 µg/g

(n = 5, mean = 0.098 µg/g) with 104 % (THg = 0.048 µg/g and MeHg = 0.050

µg/g) been the highest MeHg which was from Twifo Praso (1) a sampling site

from the main Pra River. The skin of the same fish samples gave a range

between 0.012 and 0.115 µg/g (n = 5, mean = 0.041 µg/g). A total of twenty-

eight (28) herbivorous fish with standard lengths from 15.1 to 20.0 cm from

three (3) sampling sites from the Pra River Basin were analyzed to determine

THg (muscle and skin) and MeHg (muscle). The ranges of THg concentration

was between 0.045 and 0.092 µg/g (n = 3, mean = 0.070 µg/g) while MeHg

concentration ranging from 0.037 to 0.108 µg/g (n = 3, mean = 0.065) with

117 % methylation taken place at Daboase sampling site, a town at the main

Pra River catchment area. The fish skin recorded a THg concentration ranging

from 0.010 to 0.029 µg/g (n = 3, mean = 0.019). The highest standard length

(20.1-25.0 cm) of herbivorous fish (n = 19) sampled from the Pra River Basin

(Nkontinso, Twifo Praso 1, and Twifo Praso 2 sampling sites) were analyzed

for THg using both muscle and skin, and MeHg in the fish muscle only. The

THg concentration ranges from 0.014 to 0.097 µg/g (n = 3, mean = 0.049

µg/g) and that of MeHg also ranged between 0.012 and 0.056 (n = 3, mean =

0.034 µg/g) with the utmost percentage methylation 94.9 % taken place at

Twifo Praso (2) sampling site from the main Pra River. The THg

concentration in the fish skin ranges from 0.007 to 0.026 µg/g (n = 3, mean =

0.017 µg/g). Three (3) of the herbivorous fish muscles had more than hundred

percent (104 % of MeHg from Daboase; 104 % of MeHg from Twifo Praso

(1); and 117 % of MeHg from Daboase) methylation and the least methylated

herbivorous fish from the Pra River Basin was 58.2 % of MeHg (20.1-25.0

cm) from Twifo Praso. The percentage of methylation of the herbivorous fish muscle ranges from 86.8 to 104 % MeHg for 5.1-10.0 cm ($n = 5$); 75.0- 104 % MeHg ($n = 5$); 84.0-117 % MeHg ($n = 3$); and 58.2-94.9 % MeHg ($n = 3$). The results show that all the concentrations of THg were lower than the Mercury Reference Concentration of 0.30 μg/g but there were a degree of methylation in all the fish muscles which may pose a health risk to consumers. In other studies (Dankwa et al., 2005) on two (2) herbivorous fishes (*Brycinu nurse* and *Tilapia zillii*) from both Offin River (Kaniago, Buabuasin and Baadoa) and main Pra River (Twifo Praso), the Hg concentration in the *Tilapia zillii* from Twifo Praso sampling site gave 0.06 mg/g whilst that of *Brycinu nurse* from Kaniago-0.33 mg/g, Buabuasin-0.13 mg/g, Baadoa-0.13 mg/g and Twifo Praso-0.70 mg/g.

Even though the THg concentration in all the herbivorous fish muscle and skin were below the Mercury Reference Concentration (0.3 μg/g) there were higher methylations of THg. The percentage methylation ranges between 58.2 to 117 % in the herbivorous fish muscle from the Pra River Basin in this study with a range of THg concentration in the fish muscle given as 0.014 to 0.262 μg/g. The highest percentage (117 %) of methylation in the herbivorious fish in the Pra River Basin occurred at Daboase (15.1-20.0 cm fish muscle) sampling site along the main Pra River. Meanwhile, Shama sampling site (Estuary) at the Pra River Basin of Ghana, gave the highest THg concentration (0.262 μg/g, $n = 5$) in its fish muscles (10.1-15.0 cm). Even though the correlation of 0.84 between THg concentration and the standard length (cm) was very good it was not significant (*p-value* = 0.164, $n = 4$)

indicating the THg accumulation does not depend on the herbivorous fish muscle.

Table 21: Results of THg (a) ($n = 4$) and MeHg (b) ($n = 4$) Concentrations ($\mu g/g$); Mean ($n = 4$), Minimum, Maximum, Standard Deviation of various Standard Lengths (cm) of Herbivorous fish (muscle and skin) from Pra River Basin including its Estuary (e), Ghana

Sampling site	Standard Length (cm)	Herbivorous Fish			
		Muscle			Skin
		THg (a)	MeHg (b)	%	THg
Nkontinso	5.10-10.0	0.205	0.178	86.8	0.110
Twifo Praso (1)		0.031	0.030	96.8	0.018
Twifo Praso (2)		0.037	0.034	91.9	0.015
Daboase		0.191	0.199	104	0.017
Anlo[e]		0.033	0.029	87.8	0.016
Mean (n = 5)		0.099	0.094	93.5	0.035
Minimum		0.031	0.029	86.8	0.016
Maximum		0.205	0.178	104	0.11
STD		0.090	0.087	7.49	0.042
Nkontinso	10.1-15.0	0.150	0.113	75.3	0.042
Twifo Praso (1)		0.048	0.05	104	0.012
Twifo Praso (2)		0.043	0.042	97.7	0.012
Daboase		0.100	0.082	82.0	0.026
Shama[e]		0.262	0.205	78.2	0.115
Mean (n = 5)		0.118	0.098	87.4	0.041
Minimum		0.043	0.050	75.0	0.012
Maximum		0.262	0.205	104	0.12
STD		0.091	0.066	12.7	0.043
Nkontinso	15.1-20.0	0.059	0.050	84.7	0.029
Twifo Praso (1)		0.045	0.037	82.2	0.010
Daboase		0.092	0.108	117	0.017
Mean (n = 3)		0.070	0.065	94.6	0.019
Minimum		0.045	0.037	84.0	0.010
Maximum		0.092	0.108	117	0.029
STD		0.024	0.038	20.4	0.010
Nkontinso	20.1-25.0	0.014	0.012	85.7	0.026
Twifo Praso (1)		0.097	0.056	57.7	0.007
Twifo Praso (2)		0.037	0.035	94.6	0.018
Mean (n = 3)		0.049	0.034	79.3	0.017
Minimum		0.014	0.012	58.2	0.007
Maximum		0.097	0.056	94.9	0.026
STD		0.043	0.022	19.2	0.010

Source: Author Data, 2014

Total Mercury and other Elements in the Pra River Basin, Ghana

k_0-INAA was used to determined other elements (As, Au, Ag, Cs, Na, K, Ca, Cd, Cr, Sc, Cr, Eu, Fe, Co, Zn, Ga, Se, Br, Rb, Sr, Sb, Zr, Mo, Ba, La, Ce, Nd, Sm, Yb, Hf, Ta, W, Tb, Th, U, W, and Hg) in twenty (20) topsoil (0-1 cm) samples from twenty (20) sampling sites (Dadientem, Kibi, Adonkrono, Kade, Akim Oda, Akim Oda Old, Twenedurase, Kwahu Praso, Apreja, Nnoboamu, Wobiri, Nkontinso, Dunkwa-On-Offin (1), Dunkwa-On-Offin (2), Assin Praso, Twifo Praso, Daboase, Beposo, Anlo and Shama sampling sites) in the Pra River Basin, Ghana. The mean concentrations of the results are presented in Appendices P (Sc, Ce, Eu, La, Nd, Sn, Tb and Yb), Q (As, Br, Cs, Hf, Se, Zr, Ba, Th, U, Sr, Sb, Rb, and Mo), and R (Ag, Au, Co, Sn, Cd, Cr, Ga, and Ta). The normal and partial correlation (Appendix S) using Pearson correlation with SPSS (Version 16) was used to determine if there were a linear relationship between THg concentration and the other elements (mentioned above) in the Pra River Basin, Ghana. The pH and percentage (%) moisture content were used as controlled variables. The exact behavior of the pH-dependent adsorption of metals, including Hg, depends on the adsorption that is adsorbate ratio thus pH is the most important controlling factor (Amirbahman, Reid, Haines, Kahl, & Arnold, 2002; Dzombak & Morel, 1990; Tiffreau, Lützenkirchen, & Behra, 1995).

In determining the normal and partial correlation between THg and the thirty four (34) elements (Appendix S), only eight (8) of the elements (As/THg, Hf/THg, Se/THg, Zr/THg, U/THg, Sb/THg, W/THg and Au/THg) had significant (p-value < 0.05) correlations (normal correlation range = 0.55-0.98, p-value = 0.00-0.01, n = 8; partial correlation ranges = 0.51-0.99, p-

intentionally introduced through the use of Hg in mining gold from Au-rich arsenopyrite which has also introduced As into the catchment areas. Mercury is a pollutant and toxic to human health as well as arsenic in the inorganic forms which is also highly toxic to human health.

Also, both normal correlations ($r = 0.98$, *p-value* $= 0.00$, $n = 20$) and partial correlation ($r = 0.99$, *p-value* $= 0.00$, $n = 20$) between Sb and THg were significant indicating Hg was used in the Pra River Basin. In a multiple correlation ($r = 1.00$, *p-value* $= 0.00$, $n = 20$) between Sb/As and Sb/Au which were all positive and very significant, shows the presence of Aurostibite (gold mineral bearing) in the Ashante gold deposite which was a source of gold for extraction using mercury in the Pra River Basin. There was also a significant positive correlation ($r = 0.99$, *p-value* $= 0.00$, $n = 5$) between Hf and Zr which indicate their association as an element but a negative moderate correlation ($r = 0.51$- 0.55, *p-value* $= 0.01 - 0.03$) between Sb/Hf and Sb/Zr.

Another element that was considered in this research was Selenium (Se), an element that has similar properties as S and has an exceptional high binding affinity with Hg. In using k_0-INAA in determining Se in the topsoil (0-1 cm) from the Pra River Basin only five (5) out of the twenty (20) sampling sites were above the detection limit (DL). The correlations between THg and Se in the topsoil (0-1 cm) from twenty (20) sampling sites from the Pra River Basin gave normal correlation ($r = 0.86$, *p-value* $= 0.00$, $n = 5$) and partial correlation ($r = 0.85$, *p-value* $= 0.00$, $n = 5$) which were positive and significant. Se and Hg react to form insoluble compound HgSe in a molar ratio 1:1 in the rhizosphere which is as a results of the Se in rhizosphere soils significantly inhibiting the accumulation of inorganic Hg in the portions of

plants above the roots (Mounicou, Vonderheide, & Shann, 2006b; Mounicou, Shah, Meija, Caruso, & Vonderheide, 2006a; Yathavakilla, 2007; Zhao , 2013a, b). Zircon is one of the heavy minerals associates with sedimentary gold found in many places in Ghana (Wright, 1985) and is considered to behave as "identical twins" during magmatic processes with Hf (Taylor & McLennan, 1985). In correlating Zr and Hf for twenty (20) soil (0-1 cm) from twenty (20) sampling sites from the Pra River Basin, Ghana, a perfect correlation of 0.99 (p-value = 0.00, n = 20) was established which is significant. Also, in correlating THg with Zr and, THg with Hf, both correlation gave negatively significantly correlations (r = -0.55, p-value = 0.01, n = 20; partial correlation = -0.62, p-value = 0.01, n = 20) for THg and Zr, and (r = -0.60, p-value = 0.01, n = 20; partial correlation = -0.67, p-value = 0.00, n = 20) respectively, indicating Hf is also associated with the sedimentary gold mineral associated with Zircone. Mercury amalgamation is been used in mining gold from the sedimentary gold mineral from the Pra River Basin, Ghana.

Another element that was determined in the topsoil (0-1 cm) samples from the twenty (20) sampling sites which had a positive perfect correlation (r = 0.85, p-value = 0.00, n = 15; partial correlation = 0.84, p-value = 0.00, n = 15) with THg is Tungsten (W). Also, in determining the multi correlation presented in Table 22, W with the other elements (As, Hf, Se, Zr, U, Sb and Au) which also had significant correlation with THg in the Pra River Basin, Ghana, five (5) out of the seven (7) elements (As, Hf, Zr, Sb, and Au) had correlations which were perfect and significant. The mean concentration of W was 2.17 mg/kg (n = 15, RSD = 0.14) with maximum concentration of W

(10.4±0.80 mg/kg, n = 3) recorded at Dunkwa-On-Offin (1) sampling site and the minimum concentration of W (1.58±0.17 mg/kg, n = 3) recorded at Twenedurase sampling site. It must be noted that the background level of W reported by Kabata-Pendias (2011) was 1.70 mg/kg and this was lesser than both the maximum and the mean concentration reported in the Pra River Basin, Ghana. Table 22 presents the multiple correlation (*correl.*) and *p-value* between Sc, As, Hf, Se, Zr, U, Sb, W and Au from the Pra River Basin, Ghana.

Table 22: Multiple Correlation (*correl.*) and *p-value* between Sc, As, Hf, Se, Zr, U, Sb, W and Au from the Pra River Basin, Ghana

		As	Hf	Se	Zr	U	Sb	W	Au
As	*correl.*	1.00	-0.55	0.92	-0.51	0.30	1.00	0.92	1.00
	p-value	1.00	0.01	0.03	0.02	0.22	0.00	0.00	0.00
Hf	*correl.*		1.00	-0.82	0.99	-013	-0.55	-0.75	-0.57
	p-value		1.00	0.09	0.00	0.61	0.01	0.00	0.02
Se	*correl.*			1.00	-0.92	0.11	0.92	0.91	0.92
	p-value			1.00	0.03	0.99	0.03	0.10	0.08
Zr	*correl.*				1.00	-0.20	-0.51	-0.68	-0.53
	p-value				1.00	0.42	0.02	0.01	0.03
U	*correl.*					1.00	0.09	0.45	-0.19
	p-value					1.00	0.73	0.10	0.49
Sb	*correl.*						1.00	0.91	1.00
	p-value						1.00	0.00	0.00
W	*correl.*							1.00	0.91
	p-value							1.00	0.00
Au	*correl.*								1.00
	p-value								1.00

Source: Author Data, 2014

Rare Earth Elements and THg concentration in the Pra River Basin, Ghana.

Multielemental analysis was performed using k_0INAA method (K1) to determined thirty-five elements in twenty (20) topsoil (0-1cm depth) samples, one (1) "Black" and one (1) mining waste in all the sampling sites (Dadientem, Kibi, Adonkrono, Kade, Akim Oda, Akim Oda (Old), Twenedurase, Kwahu Praso, Apreja, Nnoboamu, Wobiri, Nkontinso, Dunkwa-On-Offin (1), Dunkwa-On-Offin (2), Assin Praso, Twifo Praso, Daboase, Beposo, Anlo and Shama). The results of eight (8) Rare Earth Elements (Eu, Ce, La, Sc, Sm, Nb, Tb, Yb) presented in Appendix U. The two (2) mining waste analyzed using k_0-INAA for rare earth elements from Dunkwa-On-Offin sampling site.

In correlating THg with the eight (8) REEs (Sc, Eu, Ce, La, Nd, Sm, Tb, and Yb), determined in this studies (Appendix S), all the correlations were insignificant with their *p-value* > 0.05 which shows REEs in the Pra River Basin does not have influence on THg binding to the soils samples.

Cerium (Ce) is the most abundant of all the REEs and forms several minerals including monazite $(Ce,La,Nd,Th)PO_4$ and xenotime $(Y,Ce)PO_4$, the rarer bastnaesite $(Ce,La)CO_3(F,OH)$ and cerite $(Ce,La)_9(Mg,Fe)Si_7(O,OH,F)_{28}$. In this research, a pie chart in Figure 55 shows the percentage of eight REE and Ce (43 %) designate the most abundant of all the eight (8) REE's. The percentages are as follow: Ce (43 %), La (19 %), Nd (18 %), Sc (12 %), Sm (3 %), Yb (3 %), Tb (1 %), and Eu (1 %). Meanwhile, the percentage shares of estimated global production of REEs in 2015 are Ce (40 %), La (27 %), Nd (18 %), Sm (2 %), Tb (0.2 %), and Eu (0.4 %) (Kingsnorth, 2010) which is almost similar to that obtained in this research. In nature four (4) types of monazite exist and they are: monazite-Ce $(Ce, La, Nd, Th)PO_4$, monazite-La $(La, Ce, Nd)PO_4$, monazite-Nd $(Nd, La, Ce)PO_4$, and monazite-Sm (Sm, Gd, Ce, Th)PO_4 with the attached element indicating the highest concentration. There were strong correlations (r = 0.59-0.87, *p-value* = 0.00-0.01, *n* = 8) between Th, and Ce, Se, Eu, Nd, La, Sm, Tb and Yb. Also, the percentage (Figure 59) obtained between the REEs in this study shows the highest REE to be Ce with 43 % and this coupled with significant correlations (*p-values* < 0.00, *n* = 20) in Table 23 clearly indicates the presence of monazite-Ce in the Pra River Basin, Ghana. Mean while monazite was discovered in stream gravels in many parts of Ghana (Overstreet, 1967) which is an indication of REEs in the Pra River Basin not being an anthropogenic source but a

geological deposit. Also, in a report by the members of the Gold Coast Geological Survey, some interesting mineral associated with ninety-one (91) concentrates (out of 639 concentrates) were monazite bearing with five (5) concentrates given the most abundant heavy minerals (Junner, 1959).

Kibi sampling site (upstream of Birim River) had the highest concentration (Sc-: 21.4±0.80 mg/kg; Ce-: 67.7±2.40 mg/kg; Eu-: 1.50±0.06 mg/kg; La-: 29.4±1.00 mg/kg; Nd-: 28.6±1.50 mg/kg; Sm-: 4.83±0.17 mg/kg; Tb-: 0.91±0.03 mg/kg; and Yb-: 3.85±0.14 mg/kg) of all the REEs determined in this study. The least concentrations of Sc (2.39±0.08 mg/kg) , Ce (6.41±0.24 mg/kg), La (3.00±0.11 mg/kg), Nd (3.27±0.20 mg/kg), and Sm (0.62±0.02 mg/kg), were obtained from Akim Oda sampling site; Eu (0.26±0.02 mg/kg) and Tb (0.14±0.01 mg/kg) were obtained from Akim Oda (Old); and Yb (0.70±0.04 mg/kg) was obtained from Dunkwa-On-Offin (1) sampling site. The percentage abundance of eight (8) rare earth elements are shown in Figure 55 whilst Table 23 represents the Pearson Correlation between Eight (8) REE and Th determined in topsoils from twenty (20) sampling sites in the Pra River Basin, Ghana. The associate of Th and U with REEs in the soils along the Pra River Basin must be also look at since Th and U are of radiological impact and may washed into the rivers which is also an environmental concern.
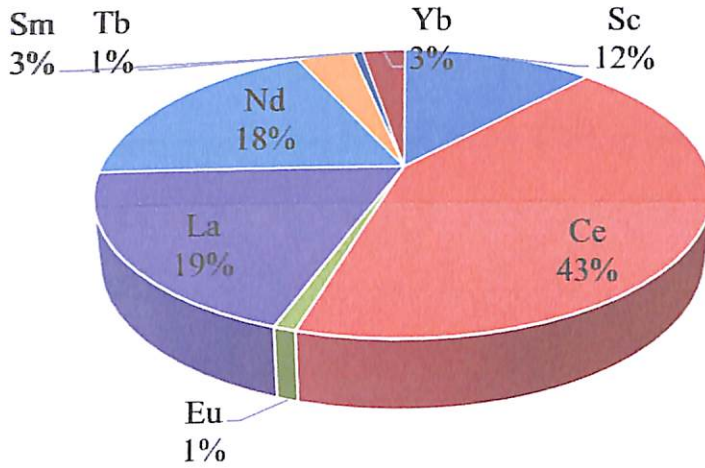
Figure 55: The percentage abundance of eight (8) rare earth elements (Ce>La>Nd>Sc>Sm>Yb>Tb>Eu) average concentrations ($n = 20$) in 0-1 cm soil samples from Pra Basin, Ghana using k_0-INAA

Table 23: Pearson Correlation between Eight (8) REE and Th Determine in Topsoil (0-1 cm) from the Twenty (20) Sampling Sites from the Pra River Basin, Ghana

		Sc	Ce	Eu	La	Nd	Sm	Tb	Yb	Th
Sc	correl.	1.00	0.52	0.55	0.71	0.69	0.47	0.47	0.61	0.68
	p-value	0.00	0.01	0.00	0.00	0.00	0.03	0.03	0.00	0.00
Ce	correl.		1.00	0.88	0.74	0.74	0.98	0.80	0.38	0.84
	p-value		0.00	0.00	0.00	0.00	0.00	0.00	0.08	0.00
Eu	correl.			1.00	0.62	0.63	0.88	0.96	0.57	0.82
	p-value			0.00	0.00	0.00	0.00	0.01	0.01	0.00
La	correl.				1.00	0.91	0.75	0.57	0.56	0.87
	p-value				0.00	0.00	0.00	0.01	0.01	0.00
Nd	correl.					1.00	0.73	0.59	0.57	0.81
	p-value					0.00	0.00	0.01	0.01	0.00
Sm	correl.						1.00	0.80	0.34	0.80
	p-value						0.00	0.00	0.13	0.00
Tb	correl.							1.00	0.65	0.73
	p-value							0.00	0.00	0.00
Yb	correl.								1.00	0.59
	p-value								0.00	0.01
Th	correl.									1.00
	p-value									0.00

Source: Author Data, 2014

Evaluation of Soil (0-1 cm) contamination using Enrichment Factor

The qualities of twenty (20) topsoils (0-1 cm) from twenty sampling sites were determined using enrichment factor (EF) in normalizing; Ce, Eu, La, Nd, Sm, Tb, Yb (Appendix U); As, Br, Cs, Hf, Se, Zr, Ba, Th, U, Sr, Sb, Rb, and Mo (Appendix V); and Ag, Au, Co, Cr, Ga, Ta, and W (Appendix W) using Sc as nornamilizing agent.

Scandium (Sc) can hardly be found in nature, as it occurs in very small amounts. Few studies used Sc as a normalizing agent (Ackermann, 1980; Grousset, Quetel, Thomas, Donard, & Lambert, 1995) and in this research, Sc was used to normalize the twenty five (25) elements determined in the soil (0-1 cm) from the Pra River Basin, Ghana. The highest EF of four (4) out of the twenty-five (25) elements, that is Ag (74.3), As (2,663), Sb (179) and Au (22,028) were extremely high enrichments in the soil samples from Dunkwa-On-Offin (1) sampling site. Also, the EF (22.0) for Se was a very high enrichment in the soil (0-1 cm) from Dunkwa-On-Offin (1) and the highest in all the sampling sites. Again, a significant enrichment of W with EF to be 18.5 was registered at Dunkwa-On-Off (1). Moreover, the highest EF for Co (2.96) and Cr (2.55) among the twenty (20) sampling sites were both recorded at Dunkwa-On-Offin (1) and they were both moderate enrichment in the soil (0-1 cm) sample. Dunkwa-On-Offin (1) is an encroached sampling site with many ASGM activities exploring gold in mineral like arsenopyrite which is present in the Offin basin (Oberthür et. al., 1997), thus exposure of the environment to extremely high content of As, Au, Ag and Sb in soil samples from Dunkwa-On-Offin (1) sampling site. Anlo sampling site recorded the least EF of As (0.31), Sb (0.15), Se (1.41), and Co (0.29), whilst Dadientem, Kibi, and Kade

had THg above the background level. Dunkwa-On-Offin and Nkontinso both along the Offin River were noted to be contaminated in their soil and fish respectively. Various species of mercury has become available in the Pra River Basin. Beposo noted to have high contamination of THg sunk in the sediment. Monazite-Ce was discovery in an appreciable quantity in the topsoil at Kade.

CHAPTER FIVE

SUMMARY, CONCLUSIONS AND RECOMMENDATIONS

Overview

Quality control of all the entire instruments used for CVAAS, CVAFS, Temperature Fractionation, and k_0-INAA were very important in ensuring accuracy and precision of the instruments to achieve good results. The results were in good agreements. This chapter presents summary and conclusions of the findings from this study and recommendations.

Summary

The continuous use of mercury (Hg) in gold mining is on the verge of becoming an ecological and human health disaster. Pra River Basin is a basin in Ghana that is rich in natural resources especially gold, therefore gold mining activities is a major economic activity along the Basin. Mercury is being used in the Pra River Basin, therefore the concentration of mercury and its species, and other elements (Ag, As, Au, Ba, Br, Ca, Cd, Ce, Co, Cr, Cs, Eu, Fe, Ga, Hg, K, La, Mo, Na, Nd, Rb, Sb, Sc, Se, Sm, Sn, Sr, Ta, Tb, Th, U, W, Yb, Zn, and Zr) were determined in different compartment along three major tributaries including Anum, Offin, Birim and main Pra River from the Pra River Basin. The concentrations of total mercury (THg) were determined in soil profiles (0-6 cm), sediments core (0-10 cm), mining wastes, carnivorous fish (muscle and skin), and herbivorous fish (muscle and skin) using Cold Vapour Atomic Absorption Spectroscopy (CVAAS). Whilst merthylmercury was determined in the fish (carnivorous and herbivorous) muscles using Cold Vapour Absorption Fluorescence Spectroscopy (CVAFS).

In testing for the appropriate procedure that will totally digest total mercury from geological samples into solution for CVAAS measurements, M2 (5ml (2:1) HNO_3/HF + 1ml HCl) digestion acid gave a reliability test that yielded a high interclass correlation coefficient of 98.4 % (between M2 and K1) with a narrower confidence interval between 95.9 to 99.4. This indicates that statistically, M2 acid digestion procedure is one of the best procedures for total mercury digestion in geological samples from the Pra River Basin in Ghana.

In sampling zero (0) to six (6) centimeters of soil from twenty (20) sampling sites (Dadientem, Kibi, Adonkrono, Kade, Akim Oda, Akim Oda (Old), Twenedurase, Kwahu Praso, Apreja, Nnoboamu, Wobiri, Nkontinso, Dunkwa-On-Offin (1), Dunkwa-On-Offin (2), Assin Praso, Twifo Praso, Daboase, Beposo, Anlo and Shama) from the Pra River Basin (Birim, Anum, Offin and main Pra Rivers), the results indicated that, the highest mean concentration (770 mg/kg, $n = 120$) of THg was registered at the 4-5 cm depth at Dunkwa-On-Offin (1) sampling sites whilst the least mean concentration (1.30 mg/kg, $n = 120$) of THg was registered at the depth of 5-6 cm at Anlo sampling site. The highest range of THg (103-770 mg/kg, $n = 6$) was registered at Dunkwa-On-Offin (1) sampling site at the Offin River with the least range of THg concentration (2.20-3.23 mg/kg, $n = 6$) registered at Twenedurase, a sampling site at the upstream of the Pra River Basin. All the THg concentrations in all the soil profile in the twenty (20) sampling sites along the Pra River Basin are above the background level (0.07 mg/kg) tabulate by Kabata-Pendias, (2011); Critical Limit (0.13 mg/kg) of Hg in soils (Tipping et al., 2010); MAC range (0.5-5.0 mg/kg) of Hg in soil (Kabata-

Pendias & Sadurski, 2004); and TAV range of Hg (1.5-10 mg/kg) in soil by Chen, (1999).

The highest mean THg concentration (20.8 mg/kg, $n = 210$) in sediment corers (0-10 cm) was recorded at the 6-7 cm depth at Beposo sampling site whilst the least mean concentration (0.00 mg/kg) was recorded at the depth of 6-7 cm at Nnoboamu sampling site. Meanwhile, the highest range of THg concentration (0.23-20.8 mg/kg, $n = 10$) was recorded at Beposo sampling site again with the least range of THg concentration (0.01-0.02 mg/kg, $n = 10$) which was recorded at Kwahu Praso sampling site at the upstream of the Pra River Basin. Out of the twenty-one (21) sampling sites, three (3) sampling sites (Adonkrono, Kwahu Praso, and Daboase) gave a trend of current deposition of THg along their sediment core (0-10 cm) as there were negatively significant correlations between the depth of sediment cores and THg concentrations. Also, five (5) among the twenty-one (21) sampling sites (Dadientem, Kade, Nnoboamu, Wobiri, and Shama) gave a previously deposition of THg concentrations as there were positively significant correlations (p-value<0.05) between the sediment cores and THg concentrations.

The THg concentration in the soil profiles from only three (3) sampling sites (Nnoboamu, Dunkwa-On-Offin (1) and Daboase) had an influence in the upload of the THg concentration in their various sediment cores since there were significant correlations between the THg concentrations in their soil profiles and sediment corers. All the THg concentrations in the soil cores from the eighteen (18) sampling sites (Dadientem, Kibi, Adonkrono, Kade, Akim Oda, Akim Oda (Old), Twenedurase, Kwahu Praso, Apreja,

Nnoboamu, Wobiri, Nkontinso, Dunkwa-On-Offin (1), Dunkwa-On-Offin (2), Assin Praso, Twifo Praso (1), Twifo Praso (2), Daboase, Beposo, Anlo, and Shama) had no influence in the upload of THg concentrations in their various sediment cores. A positively significant correlation between THg concentration and soil profile, THg concentration and sediment core; and soil profile and sediment core indicate that the THg concentration from the soil profile had an influence in the upload of THg concentration in the sediment core at Nnoboamu sampling site.

Out of the thirteen (13), geological samples analyzed for Hg species decomposition, five (5) soils (0-1 cm) and two (2) "black" samples released single sharp peaks. All the soil samples gave out $HgCl_2$ sharp peaks and all "black" samples gave out Hg^0 either as a singles sharp peak or as their first peak Hg species. In multiple peaks of Hg species released in three (3) "blacks" and a mining waste, $HgCl_2$, Hg_2Cl_2, HgS were released. Also, in the multiple peaks released, four (4) "blacks" and the mining waste gave out HgO species. Again, HgS was released in four (4) "blacks" as part of the multiple peaks of Hg species released. Only one "black" gave out Hg_{mc} as one of the Hg species in that sample.

In determining THg and MeHg in carnivorous fish muscles from the Pra River Basin, Nkontinso sampling site had the THg concentrations (a range between 0.376 to 0.983 µg/g, $n = 4$) in all the groups (5.1-10 cm, 10.1-15 cm, 15.1-20 cm, 20.1-25 cm, 25.1-30 cm) of carnivorous fish muscle which were above the Mercury Reference Concentration of 0.3 µg/g (EPA, 2001).The percentage of methylmercury as compared with THg in the carnivorous fish muscle from the Pra River Basin ranges between 65.0 to 121 % ($n = 24$). The

carnivorous fish muscle with the highest MeHg percentage (121 % MeHg, 20.1-25 cm fish) was from Twifo Praso (1) sampling site from the main Pra River. A good positive correlation of 0.94 ($n = 6$, *p-value* = 0.01) between the THg concentration and the standard length of the carnivorous fish muscle was established. Thus, there is bioaccumulation of THg in carnivorous fish as it ages.

Also, in herbivorous fish from the Pra River Basin, THg concentration range (0.014 and 0.262 µg/g) in the fish muscle and skin (0.007-0.12 µg/g) were below the Mercury Reference Concentration of 0.3 µg/g (EPA, 2001). Meanwhile, the percentage of MeHg as compared to total mercury ranges between 58.2 to 117 % in the herbivorous fish muscle from the Pra River Basin with the highest occurres at Daboase (15.1-20 cm fish muscle) sampling site with 117 %. Shama sampling site as estuary in the Pra River Basin gave the highest THg concentration (0.205 µg/g, $n = 5$) in herbivorous fish muscles (10.1-15 cm) whilst the least THg concentration (0.014 µg/g, $n = 3$) was recorded in the fish muscle from Nkontinso sampling site from the Offin River. There was no relationship between the THg concentration and the standard length of the herbivrious fish muscle form the Pra River Basin as the correlation of -0.84 was not significant (*p-value* = 0.16, $n = 4$).

Out of the thirty five (35) elements determined in the topsoil (0-1 cm) from the Pra River Basin, only eight (8) of the elements (As/THg, Hf/THg, Se/THg, Zr/THg, U/THg, Sb/THg, W/THg and Au/THg) had significant (*p-value* < 0.05) correlations (normal correlation range = 0.55-0.98, *p-value* = 0.00-0.01, $n = 8$; partial correlation ranges = 0.51-0.99, *p-value* = 0.00 - 0.03, $n = 8$) with THg. In a multiple correlation between these eight (8) elements

(As, Hf, Se, Zr, U, Sb, W, and Au), U had no correlations with any of the seven (7) elements. The significant correlations between As, Hf, Zr, Sb, W, and Au indicate the presence of Arsenopyrite, Aurostibite (gold mineral bearing) and Hf associated sedimentary gold mineral with zircon deposits in the Pra River Basin, Ghana (AZOmining, 2013; Hirdes & Nunoo, 1994; Oberthür et al., 1995) which were used as sources of gold deposits for exploration. Therefore, Hg amalgamation with gold uses rudiment methods which have exposed the Pra River Basin to high THg concentrations and other elements. Meanwhile, Se also had significant correlations with only Zr and Sb.

There were no correlations between THg and Rare Earth Elements (REEs) from the Pra River Basin which clearly shows REEs in the basin had no influence on the THg binding effect to the matrix of geological samples in the Pra River Basin. The significant correlation (p-value < 0.05) between the REEs (Ce, Eu, La, Nd, Sc, Tb, and Yb) and also, REEs with Th coupled with high percentage of Ce (43 %) as compared with the other REEs (La-: 19 %, Nd-: 18 %, Sc-: 12 %, Sm-: 3 %, Yb-: 3 %, Tb-: 1 %, and Eu-: 1 %) indicates that, monazite-Ce is present in the Pra River Basin, Ghana and an appreciable quantities are deposited in Kibi sampling site. Kibi sampling site recorded the highest REEs in the Pra River Basin. Meanwhile, the least REE, were recorded at Akim Oda sampling site.

In using the enrichment factor (EF) to evaluate twenty-five (25) elements in the soil (0-1 cm) samples from the Pra River Basin, four (4) elements Ag (EF= 74.3), As (EF = 2663), Sb (EF = 179) and Au (EF = 22028) were found to be extremely enriched in the soil (0-1 cm) from Dunkwa-On-Offin (1) sampling site. Also, very high EF for Se (EF = 22), significant of W

(EF = 18.5) and, moderate of Co (EF = 2.96) and Cr (EF = 2.55) have been exposed to the environment of Dunkwa-On-Offin (1) sampling site due to the exploration of gold from the mineral deposites. Also, Hf (EF = 7.32), Zr (EF = 7.74) and Zn (EF = 8.00) were all extensively enriched in the soil (0-1 cm) samples from Akim Oda (Hf and Zr) and Shama (Zn).

The soil pH along the Pra River Basin, Ghana was basically acidic as out of the twenty (20) soil profile (0-6 cm) tested for pH ranges, fourteen (14) sampling sites (Dadientem, Kibi, Adonkrono, Kade, Akim Oda (Old), Twenedurase, Kwahu Praso, Anlo, Apreja, Twifo Praso, Beposo, Nnoboamu, Wobiri, and Nkontinso) had strong correlations ($p < 0.05$) between depth and soil pH as the acidity increased vertically downwards the soil profiles. The six (6) sampling sites that had insignificant ($p > 0.05$) correlation are Assin Praso, Daboase, Akim Oda, Shama, Dunkwa-On-Offin (1) and Dunkwa-On-Offin (2). The acidity of the soil profiles was from extremely acidic to strongly alkaline using the Soil Survey Manual (2011).

The moisture content of the soils based on the weight loss upon heating at 105 °C in the Pra River Basin ranges from 0.06 % (topsoil of 0-1 cm at Akim Oda from the Birim River Basin) to 3.53 % (at the 1-2 cm depth at Twenedurase the upstream of the main Pra River). It must be noted that the soils were air dried at room temperature before heat dried at 105 °C.

Conclusion

In conclusion, after validating both procedures M1 and M2 with k_0-INAA method, HF acid combination (M2) was found to be the appropriate acid digestion procedure in the decomposition of THg in geological samples

from the Pra River Basin, Ghana. All the soils from the Pra River Basin were contaminated with THg concentration. Dunkwa-On-Offin (1) sampling site has become Hg hotspot in the Pra River Basin and will distribute Hg in the Basin and beyond. Nnoboamu, Dunkwa-On-Offin (1), and Assin Praso sampling sites showed previous deposition of THg concentration in the soil, which indicate a buried of THg within the rhizosphere of the soil. Anlo sampling site gave a current deposition of THg in the immediate topsoil and will pollute the environment and affect the health of the populace in the catchment area. The species of Hg ($HgCl_2$, Hg_2Cl_2, Hg0, HgS, and Hg_{mc}) present in the River Basin poses risk to humans and the environment as each species has it own health effect. Mercury in the Pra River Basin was bonded to eight (8) elements, Au, As, Hf, Se, Zr, U, Sb, and W which will help mercury live in the environment for longer time. The Rare Earth Elements (REE), Ce, Eu, La, Nd, Sc, Tb, and Yb found in the basin were significant but associated with U and Th. REE associated with U and Th may be radioactive which may also be washed into our rivers and pollute our river bodies therefore get through the food chain. Monazite-Ce is present in the topsoil (0-1 cm) from Kibi sampling site in the Pra River Basin.

Also, carnivorous fish muscles from the Nkontinso sampling site in the Pra River Basin are contaminated with both Hg and MeHg which make fishes from Nkontinso not safe to be consumed. Also, there is bioaccumulation of THg in carnivorous fishes as it grows with age in the Pra River Basin, Ghana. Again, eventhough THg in Herbivorous fishes from the Pra River Basin were below USEPA (2001) recommended value methylation (58.2-117 %) was

high. Most soil (0-6 cm) samples from the Pra River Basin were found to be more acidic.

Recommendations

The following recommendations were made after this study:

- Further studies should be carried out to determined atmospheric deposition of Hg in the Pra River Basin.

- Remediation research must be carried out in all contaminated sites in this research.

- Humans must be used as indicators to determine the health status of people living in the catchment areas in this research.

- Further research must be carried out to know if the mercury in the soil and sediments has become methylated.

- Plants (example dandelion) in contaminated sites with high uptake of metals must be research into to know the uptake of plants on contaminates especially Hg in the Pra River Basin.

- REEs must be studied in the Pra River Basin extensively that is, beyond 0-1 cm section of the soil to see if monazite and other concentrates of REEs can be mined in Ghana.

- Monazite-Ce should be studied in Kibi and Dadientem extensively.

- Fish from the Pra River basin may not be safe for food therefore further research must be conducted periodically.

- Further research must be conducted on the quality of the water from the Pra River Basin.

REFERENCES

Ackermann, F. (1980). A procedure for correcting the grain size effect in heavy metal analyses of estuarine and coastal sediments. *Environmental Technology, 1*(11), 518-527.

Adriano, D. (1986). Trace elements in the terrestrial environment Springer-Verlag. *New York*, 219-262.

Agbesinyale, P. K. (2003). *Ghana's Gold Rush and Regional Development: The Case of Wassa West District*. SPRING Centre, University of Dortmund.

Akabzaa, T. M. (2001). *Boom and dislocation: The environmental and social impacts of mining in the Wassa West District of Ghana*. Third World Network.

Akagi, H., & Nishimura, H. (1991). Advances in mercury toxicology. *ed. T. Suzuki, N. Imura and TW Clarkson*. pp 53-76.

AMAP/UNEP. (2013). Technical Background Report for the Global Mercury Assessment. *Arctic Monitoring and Assessment Programme*. pp 74-78.

Amirbahman, A., Reid, A. L., Haines, T. A., Kahl, J. S., & Arnold, C. (2002). Association of methylmercury with dissolved humic acids. *Environmental Science & Technology, 36*(4), 690-695.

Amonoo-Neizer, E., Nyamah, D., & Bakiamoh, S. (1996). Mercury and arsenic pollution in soil and biological samples around the mining town of Obuasi, Ghana. *Water, Air, & Soil Pollution, 91*(3), 363-373.

Amponsah-Tawiah, K., & Dartey-Baah, K. (2011). The mining industry in Ghana: a blessing or a curse. *International Journal of Business and Social Science, 2*(12), 62-69.

Ariya, P. A., Khalizov, A., & Gidas, A. (2002). Reactions of gaseous mercury with atomic and molecular halogens: kinetics, product studies, and atmospheric implications. *The Journal of Physical Chemistry A, 106*(32), 7310-7320.

Asiamah, R. (1987). Soil resources and their agricultural utilization in Ghana. In *National Conference on resources conservation for Ghana's sustainable development.* pp. 28-30.

Audi, G., Wapstra, A., & Thibault, C. (2003). The AME2003 atomic mass evaluation:(II). Tables, graphs and references. *Nuclear Physics A, 729*(1), 337-676.

Ault, T., Krahn, S., & Croff, A. (2015). Radiological impacts and regulation of rare earth elements in non-nuclear energy production. *Energies, 8*(3), 2066-2081.

AZOmining. (2013). Aurostibite-occurence, Properties and Distribution. 1-3.

Babut, M., Sekyi, R., Rambaud, A., Potin-Gautier, M., Tellier, S., Bannerman, W., & Beinhoff, C. (2003). Improving the environmental management of small-scale gold mining in Ghana: a case study of Dumasi. *Journal of Cleaner Production, 11*(2), 215-221.

Bank, M. S. (2012). *Mercury in the environment: pattern and process.* Univ of California Press. pp 3-19.

Beaty, R., & Kerber, J. (1993). Control of analytical interferences. *Concepts, Instrumentation and Techniques in Atomic Absorption Spectrophotometry*, 3-5.

Becker, D. S, & Bigham, G. N. (1995). Distribution of mercury in the aquatic food web of Onondaga Lake, New York. In *Mercury as a Global Pollutant* (pp. 563-571). Springer.

Bermudez-Lugo, O. (2008). Gold Fields Mineral Survey. *Ghana Chamber of Mines Factoid.*

Biester, H, Müller, G., & Schöler, H. (2002). Estimating distribution and retention of mercury in three different soils contaminated by emissions from chlor-alkali plants: part I. *Science of the Total Environment, 284*(1), 177-189.

Biester, Harald, Gosar, M., & Müller, G. (1999). Mercury speciation in tailings of the Idrija mercury mine. *Journal of Geochemical Exploration, 65*(3), 195-204.

Biester, Harald, Müller, G., & Schöler, H. (2002). Binding and mobility of mercury in soils contaminated by emissions from chlor-alkali plants. *Science of the Total Environment, 284*(1), 191-203.

Birke, M., Rauch, U., & Stummeyer, J. (2011). Urban geochemistry of Berlin, Germany. *Mapping the Chemical Environment of Urban Areas*, 245-268.

Bityukova, L., & Birke, M. (2011). Urban Geochemistry of Tallinn (Estonia): Major and Trace-Elements Distribution in Topsoil. *Mapping the Chemical Environment of Urban Areas*, 348-363.

Bonzongo, J., Heim, K., Warwick, J., & Lyons, W. (1996). Mercury levels in surface waters of the Carson River-Lahontan Reservoir system, Nevada: influence of historic mining activities. *Environmental Pollution, 92*(2), 193-201.

Bohr, A., & Mottelson, B. R. (1998). *Nuclear structure* (Vol. 1). World Scientific. pp. 438-447.

Bose-O'Reilly, S., McCarty, K. M., Steckling, N., & Lettmeier, B. (2010). Mercury exposure and children's health. *Current Problems in Pediatric and Adolescent Health Care, 40*(8), 186-215.

Bouffard, A., & Amyot, M. (2009). Importance of elemental mercury in lake sediments. *Chemosphere, 74*(8), 1098-1103.

Bravo, A. G., Cosio, C., Amouroux, D., Zopfi, J., Chevalley, P. A., Spangenberg, J. E., Ungureanu, V.G & Dominik, J. (2014). Extremely elevated methyl mercury levels in water, sediment and organisms in a Romanian reservoir affected by release of mercury from a chlor-alkali plant. *Water research, 49*, 391-405.

Brown, A. S., Brown, R. J., Corns, W. T., & Stockwell, P. B. (2008). Establishing SI traceability for measurements of mercury vapour. *Analyst, 133*(7), 946-953.

Cai, Y. (2000). Speciation and analysis of mercury, arsenic, and selenium by atomic fluorescence spectrometry. *TrAC Trends in Analytical Chemistry, 19*(1), 62-66.

Calvert, J. G., & Lindberg, S. E. (2005a). Mechanisms of mercury removal by O_3 and OH in the atmosphere. *Atmospheric Environment, 39*(18), 3355-3367.

Calvert, J. G., & Lindberg, S. E. (2005b). Mechanisms of mercury removal by O_3 and OH in the atmosphere. *Atmospheric Environment, 39*(18), 3355-3367.

CAMEP. (2013). Mercury concentrations in fish and human in Puerto Maldonado. *Research Brief*, (1), 1-2.

Chemicals, U. N. E. P. (2002). Global mercury assessment. United Nations Environmental Programme. Chemicals. *Inter-Organization Programme for the Sound Managements of Chemicals. Geneva, Switzerland, 258pp.*Chen, Z.-S. (1999). *Selecting indicators to evaluate soil quality.* Food & Fertilizer Technology Center.

Chojnicki, J. (2000). Rare earth elements in the alluvial soils of central Vistula valley and Zulawy. *Roczniki Gleboznawcze (Poland).*

Clark, R. (1986). *The Handbook of Environmental Monitoring. A GEMS/UNEP Publication.* Clarendon Press, Oxford.

Clarkson, T. W., & Magos, L. (2006). The toxicology of mercury and its chemical compounds. *Critical Reviews in Toxicology, 36*(8), 609-662.

Coakley, G. J. (2003). *The mineral industry of Ghana. Washington, DC: US Geological Survey, Minerals Information.* v. III, pp. 17.1-17.8.

Connelly, N. G. (2005). *Nomenclature of inorganic chemistry: IUPAC recommendations 2005.* Royal Society of Chemistry.

Cornelis, R., Caruso, J. A., Crews, H., & Heumann, K. G. (2005). *Handbook of elemental speciation II: species in the environment, food, medicine and occupational health.* John Wiley & Sons.

Costa, M.F., Landing, W.M., Kehrig, H.A., Barletta, M., Holmes, C.D., Barrocas, P.R., Evers, D.C., Buck, D.G., Vasconcellos, A.C., Hacon,

S.S. & Moreira, J. C. (2012). Mercury in tropical and subtropical coastal environments. *Environmental research, 119*, 88-100.

Cottenie, A., & Verloo, M. (1984). Analytical diagnosis of soil pollution with heavy metals. In *Environmental Research and Protection* (pp. 389-393). Springer.

Coufalík, P., Zvěřina, O., & Komárek, J. (2014). Determination of mercury species using thermal desorption analysis in AAS. *Chemical Papers, 68(4)*, 427-434.

Csuros, M., & Csuros, C. (2016). *Environmental sampling and analysis for metals*. CRC Press.

Currie, L. A. (1968). Limits for qualitative detection and quantitative determination. Application to radiochemistry. *Analytical chemistry, 40(3)*, 586-593.

Dankwa, H., Biney, C., & others. (2005). Impact of mining operations on the ecology of river Offin in Ghana. *West African Journal of Applied Ecology, 7(1)*.

Das, A., Sherameti, I., & Varma, A. (2012). Contaminated soil: physical, chemical and biological components. In *Bio-Geo Interactions in Metal-Contaminated Soils* (pp. 1-15). Springer.

de BC Menezes, M., de VS Sabino, C., Amaral, A., & Maia, E. (2000). k0-NAA applied to certified reference materials and hair samples: evaluation of exposure level in a galvanising industry. *Journal of Radioanalytical and Nuclear Chemistry, 245(1)*, 173-178.

De Corte, F, Simonits, A., Bellemans, F., Freitas, M., Jovanović, Smodiš, B., Erdtmann, G., Petri, H., & De Wispelaere, A. (1993). Recent advances

in the k0-standardization of neutron activation analysis: extensions, applications, prospects. *Journal of Radioanalytical and Nuclear Chemistry, 169*(1), 125-158.

De Corte, Frans. (1987). The k0-standardization method, a move to the optimization of neutron activation analysis. Aggregé Thesis, Gent University, Belgium.

De Corte, Frans, & Simonits, A. (1989). k0-Measurements and related nuclear data compilation for (n, γ) reactor neutron activation analysis: IIIb: Tabulation. *Journal of Radioanalytical and Nuclear Chemistry, 133*(1), 43-130.

Diaz, R., Herrera, P., Alvarez, P., & Manso, G. (2002). Implementation and evaluation of k0-INAA for environmental studies. Conference : Vienan Memories at Rio de Janeriro, Brazil. pp 1-6.

Donkor, A., Bonzongo, J., Nartey, V., & Adotey, D. (2006). Mercury in different environmental compartments of the Pra River Basin, Ghana. *Science of the Total Environment, 368*(1), 164-176.

Drabaek, I., Iverfeldt, A., & Stoppler, M. (1992). *Hazardous Metals in the Environment.* Elsevier Science Publisher, Amsterdam, The Netherlands.

Drasch, G., Böse-O'Reilly, S., Maydl, S., & Roider, G. (2004). Response to the letter of the Human Biomonitoring Commission. Int. J. Hyg. Environ. Health 207, 179-181 (2004). *International Journal of Hygiene and Environmental Health, 207*(2), 183-184.

Drysdale, C., Burgess, N., d'Entremont, A., Carter, J., & Brun, G. (2005). Mercury in brook trout, white perch, and yellow perch in Kejimkujik

National Park. *Mercury Cycling in a Wetland-Dominated Ecosystem: A Multidisciplinary Study. SETAC Press, Pensacola, FL.*

DSNR, (1990). Soil standard test method; Soil moisture content. Authorised by B. Craze. pp 1-5.

Dzombak, D. A., & Morel, F. M. (1990). *Surface complexation modeling: hydrous ferric oxide.* John Wiley & Sons.

Ehmann, W., & Vance, D. (1991). *Advantages and Disadvantages of Nuclear Activation Methods, in Radiochemistry and Nuclear Methods of Analysis.* Wiley Interscience Publication, NY.

EPA, L. (2001). *Water quality criteriun fur the pruerinn af hunnan health: methylmercury.* EPA-ER-U1-11. Wislingtı. DC: Clie u Water, LL5. Envirinentil Pritetin Agely.

Erdtmann, G., & Petri, H. (1986). Nuclear activation analysis: fundamentals and techniques. *Treatise on analytical chemistry, 14*(1), 643.

Evers, D. C., Mason, R. P., Kamman, N. C., Chen, C. Y., Bogomolni, A. L., Taylor, D. L., Hammerschmidt, C.R., Jones, S.H., Burgess, N.M., Munney, K. & Parsons, K. C. (2008). Integrated mercury monitoring program for temperate estuarine and marine ecosystems on the North American Atlantic coast. *EcoHealth, 5*(4), 426-441.

Fitzgerald, W., & Lamborg, C. (2005). in the Environment. *Environmental Geochemistry, 9,* 107.

Flight, A. J., D. M. A. &.Scheib. (2011). Soil geochemical baselines in UK urban centres: The G-BASE project. In *The G-BASE project, In Johnson, J. C. C. Demetriades, A. Locutura, J. & Ottesen, R.T. (eds.).* ohn Wiley &Sons, West Sussex, UK.

Garcia, J. L., & de Castro, M. L. (2002). *Acceleration and automation of solid sample treatment* (Vol. 24). Elsevier.

Gaudino, S., Galas, C., Belli, M., Barbizzi, S., de Zorzi, P., Jaćimović, R., Jeran, Z., Pati, A. & Sansone, U. (2007). The role of different soil sample digestion methods on trace elements analysis: a comparison of ICP-MS and INAA measurement results. *Accreditation and Quality Assurance, 12*(2), 84-93.

Gelinas, Y., Venkatesh Iyungar, G., & Barnes, R. M., (1998). *Fressenius, J. Anal. Chem., 362, 483.*

Glass, L. R., Easterly, C. E., Jones, T. D., & Walsh, P. J. (1991). Ranking of carcinogenic potency using a relative potency approach. *Archives of Environmental Contamination and Toxicology, 21*(2), 169-176.

Glascock, M. D. (2011). Comparison and contrast between XRF and NAA: Used for characterization of Obsidian Sources in Central Mexico. In *X-ray fluorescence spectrometry (XRF) in geoarchaeology* (pp. 161-192). Springer, New York, NY.

Grandjean, P., Cordier, S., Kjellström, T., Weihe, P., & Jørgensen, E. (2005). Health Effects and Risk Assessment. *Dynamics of Mercury Pollution on Regional and Global Scales:*, 511-538.

Grandjean, P., Weihe, P., White, R. F., Debes, F., Araki, S., Yokoyama, K., Sørensen, N., Dahl, R. & Jørgensen, P. J. (1997). Cognitive deficit in 7-year-old children with prenatal exposure to methylmercury. *Neurotoxicology and Teratology, 19*(6), 417-428.

Griesbauer, L. (2007). Methylmercury contamination in fish and shellfish. *ProQuest Discovery Guides.*

Griffis, R., Barning, K., Agezo, F., & Akosah, F. (2002). Gold deposits of Ghana. *Mineral Commission, Accra, Ghana.*

Grigal, D. (2003). Mercury sequestration in forests and peatlands. *Journal of Environmental Quality, 32*(2), 393-405.

Grousset, F., Quetel, C., Thomas, B., Donard, O., Lambert, C., Guillard, F., & Monaco, A. (1995). Anthropogenic vs. lithogenic origins of trace elements (As, Cd, Pb, Rb, Sb, Sc, Sn, Zn) in water column particles: northwestern Mediterranean Sea. *Marine Chemistry, 48*(3-4), 291-310.

Ghana Statistical Service (GSS), (2012). 2010 Population and Housing Census: Summary Report of final Results.

Gustin, M. S., & Stamenkovic, J. (2005). Effect of watering and soil moisture on mercury emissions from soils. *Biogeochemistry, 76*(2), 215-232.

Haitzer, M., Aiken, G. R., & Ryan, J. N. (2003). Binding of mercury (II) to aquatic humic substances: Influence of pH and source of humic substances. *Environmental Science & Technology, 37*(11), 2436-2441.

Hall, B., Bodaly, R., Fudge, R., Rudd, J., & Rosenberg, D. (1997). Food as the dominant pathway of methylmercury uptake by fish. *Water, Air, & Soil Pollution, 100*(1), 13-24.

Hammerschmidt, C. R., Lamborg, C. H., & Fitzgerald, W. F. (2007). Aqueous phase methylation as a potential source of methylmercury in wet deposition. *Atmospheric Environment, 41*(8), 1663-1668.

Harada, M., Nakanishi, J., Yasoda, E., Maria da Conceicão, N. P., Oikawa, T., de Assis Guimarâes, G., da silva Cardoso, B., Kizaki, T. & Ohno, H. (2001). Mercury pollution in the Tapajos River basin, Amazon:

mercury level of head hair and health effects. *Environment International, 27*(4), 285-290.

Harkinson, J. (2003). Confessions of a Dangerous Mine: Illegal Gold Mining in Ghana shafts Locals. *Health and the Environment, Grist Magazine, 24.*

Health, U. D. of, Services, H., & others. (1991). USDHHS (1999). *Profile Of State And Territorial Public Health System.*

Hilson, G., & Pardie, S. (2006). Mercury: An agent of poverty in Ghana's small-scale gold-mining sector? *Resources Policy, 31*(2), 106-116.

Hirdes, W., & Nunoo, B. (1994). The Proterozoic paleoplacers at Tarkwa gold mine, SW Ghana: sedimentology, mineralogy, and precise age dating of the Main Reef and West Reef, and bearing of the investigations on source area aspects. *Geologisches Jahrbuch D, 100,* 247-311.

Hissler, C., & Probst, J. L. (2006). Impact of mercury atmospheric deposition on soils and streams in a mountainous catchment (Vosges, France) polluted by chlor-alkali industrial activity: the important trapping role of the organic matter. *Science of the Total Environment, 361*(1-3), 163-178.

Høgdahl, O. (1962). *Neutron absorption in pile neutron activation analysis.* Michigan. Univ., Ann Arbor. Michigan Memorial-Phoenix Project.

Hojdová, M., Navrátil, T., & Rohovec, J. (2008). Distribution and speciation of mercury in mine waste dumps. *Bulletin of Environmental Contamination and Toxicology, 80*(3), 237-241.

Honda, S., Hylander, L., & Sakamoto, M. (2006). Recent advances in evaluation of health effects on mercury with special reference to

methylmercury: A mini review. *Environmental Health and Preventive Medicine, 11*(4), 171-176.

Hooper, M., M. .. &.Anderson. (2009). Soil toxicity and bioassessment test methods for ecologicology risk assessment; Toxicity test methods for soil microorganisms, terrestrial plants, terrestrial invertebrates and vertebrates. *Critical Reviews in Analytical Chemistry, 25*(2), 1-3.

Horvat, M. (2005). Determination of mercury and its compounds in water, sediment, soil and biological samples. In *Dynamics of Mercury Pollution on Regional and Global Scales:* (pp. 153-190). Springer, Boston, MA.

Horvat, M., Kotnik, J., Logar, M., Fajon, V., Zvonarić, T., & Pirrone, N. (2003). Speciation of mercury in surface and deep-sea waters in the Mediterranean Sea. *Atmospheric Environment, 37,* 93-108.

Howe, L. M., Jervis, R. E., & Eastwood, T. A. (1962). The development of a dilute aluminum-gold alloy for thermal and resonance neutron flux measurements. *Nuclear Science and Engineering, 12*(2), 185-189.

https://en.wikipedia.org/wiki/Pra_River_(Ghana) Retrived on 6/04/2012

Hurst, C. (2010). *China's rare earth elements industry: What can the west learn?* DTIC Document.

Hynes, A. J., Donohoue, D. L., Goodsite, M. E., & Hedgecock, I. M. (2009). Our current understanding of major chemical and physical processes affecting mercury dynamics in the atmosphere and at the air-water/terrestrial interfaces. In *Mercury fate and transport in the global atmosphere* (pp. 427-457). Springer, Boston, MA.

Iverfeldt, A. (1991). Occurrence and turnover of atmospheric mercury over the Nordic countries. *Water, Air, & Soil Pollution, 56*(1), 251-265.

Jaćimović, R. (2003). Evaluation of the use of the TRIGA Mark II reactor for the k0-method of activation analysis. *University of Ljubljana.*

Janesseus, K. Vincze, L., Vekemans, B., Williams, C. T., Radtke, M., Haller, M., & Knöchel, A. (1999). *Fressenius, J. Anal. Chem., 363, 413.*

Johansson, K., Bergbäck, B., & Tyler, G. (2001). Impact of atmospheric long range transport of lead, mercury and cadmium on the Swedish forest environment. *Water, Air and Soil Pollution: Focus, 1*(3-4), 279-297.

Junner, N. R. (1959). The occurrence of uranium in ancient conglomerates; reply. *Economic Geology, 54*(7), 1320-1323.

Kabata-Pendias, A. (2010). *Trace elements in soils and plants.* CRC Press

Kabata-Pendias, A, & Pendias, H. (2001). *Trace element in soil and plants. Boca Raton. FL: CRC Press.*

Kabata-Pendias, A. (2011a). Trace Elements in Soils and Plants. CRC Press, Taylor and Francis Group.

Kabata-Pendias, Alina, & Sadurski, W. (2004). Trace elements and compounds in soil. *Elements and Their Compounds in the Environment: Occurrence, Analysis and Biological Relevance, Second Edition,* 79-99.

Kaiser, G. T. N., G. &.Olg. (1980). Handbook of Environmental Chemistry, Part A. *Springer-Verlag, 3*(131), 322-323.

Kesse, G. O. (1985). The mineral and rock resources of Ghana.

Kingsnorth, D. J. (2010, February). Rare earths: facing new challenges in the new decade. In *Presented by Clinton Cox, SME Annual Meeting.*

Kinniburgh, D., & Jackson, M. (1978). Adsorption of mercury (II) by iron hydrous oxide gel. *Soil Science Society of America Journal, 42*(1), 45-47.

Kitazume, M. & Terash, M. (2013). The deep mixing method. CRC Press/ Balkema, Leiden, the Netherlands.

Kocman, D., & Horvat, M. (2010). A laboratory based experimental study of mercury emission from contaminated soils in the River Idrijca catchment. *Atmospheric Chemistry and Physics, 10*(3), 1417-1426.

Kozin, L. F., & Hansen, S. C. (2013). *Mercury handbook: chemistry, applications and environmental impact.* Royal Society of Chemistry.

Kučera, J., & Zeisler, R. (2004). Do we need radiochemical separation in activation analysis? *Journal of Radioanalytical and Nuclear Chemistry, 262*(1), 255-260.

Kulkarni, P., Chellam, S., & Fraser, M. P. (2006). Lanthanum and lanthanides in atmospheric fine particles and their apportionment to refinery and petrochemical operations in Houston, TX. *Atmospheric Environment, 40*(3), 508-520.

Lacerda, L. D., de Souza, M., & Ribeiro, M. G. (2004). The effects of land use change on mercury distribution in soils of Alta Floresta, Southern Amazon. *Environmental Pollution, 129*(2), 247-255.

Lajunen, L. H., & Perämäki, P. (2004). *Spectrochemical analysis by atomic absorption and emission.* Royal Society of Chemistry. pp 276-285.

Lasorsa, B., & Allen-Gil, S. (1995a). The methylmercury to total mercury ratio in selected marine, freshwater, and terrestrial organisms. In *Mercury as a Global Pollutant* (pp. 905-913). Springer.

.& Allen-Gil, S. (1995b). The methylmercury to total mercury ratio in selected marine, freshwater, and terrestrial organisms. In *Mercury as a Global Pollutant* (pp. 905-913). Springer.

Lenntech. (2010). Heavy Metals. pp. 1-3. www.lenntech.com Retrieved on 2nd July, 2012.

Leo. (2005). *Chromatographic analysis of the environment* (3rd ed., Vol. 93). Taylor & Francis, CRC.

Levich, R. A. (2010). Alluvial gold minning-Offin River area.

Lin, C.-J., & Pehkonen, S. O. (1999). The chemistry of atmospheric mercury: a review. *Atmospheric Environment, 33*(13), 2067-2079.

Lin, X., & Henkelmann, R. (2003). Contents of arsenic, mercury and other trace elements in Napoleon's hair determined by INAA using the k0-method. *Journal of Radioanalytical and Nuclear Chemistry, 257*(3), 615-620.

Liu, G., Cai, Y., & O'Driscoll, N. (2011). *Environmental chemistry and toxicology of mercury.* John Wiley & Sons.

Liu, G., Cai, Y., O'Driscoll, N., Feng, X., & Jiang, G. (2012a). Overview of mercury in the environment. *Environmental Chemistry and Toxicology of Mercury,* 1-12.

Liu, G., Cai, Y., O'Driscoll, N., Feng, X., & Jiang, G. (2012b). Overview of mercury in the environment. *Environmental Chemistry and Toxicology of Mercury,* 1-12.

Locutura, J., & Bel-Lan, A. (2011). Systematic urban geochemistry of Madrid, Spain, based on soils and dust. *Mapping the Chemical Environment of Urban Areas,* 307-347.

Lopez-Anton, M. A., Yuan, Y., Perry, R., & Maroto-Valer, M. M. (2010). Analysis of mercury species present during coal combustion by thermal desorption. *Fuel, 89*(3), 629-634.

Marcoux, E., Bonnemaison, M., Braux, C., & Johan, Z. (1989). Distribution de Au, Sb, As et Fe dans l'arsénopyrite aurifère du Châtelet et de Villeranges (Creuse, Massif central français). *Comptes Rendus de l'Académie Des Sciences. Série 2, Mécanique, Physique, Chimie, Sciences de L'univers, Sciences de La Terre, 308*(3), 293-300.

Mason, R. P., Fitzgerald, W. F., & Morel, F. M. (1994). The biogeochemical cycling of elemental mercury: anthropogenic influences. *Geochimica et Cosmochimica Acta, 58*(15), 3191-3198.

Mason, R. P., & Sullivan, K. A. (1998). Mercury and methylmercury transport through an urban watershed. *Water Research, 32*(2), 321-330.

McLean, J., & Bledsoe, B. (1992). Behaviour of metals in soils (EPA Ground Water Issue, EPA 540-S-92-018: 25 pp). *Washington, USA: Environmental Protection Agency.*

Meili, M. (1997). Mercury in lakes and rivers. *Metal Ions in Biological Systems, 34*, 21-51.

Mercury, W. I. (1991). Environmental Health Criteria 118. *Geneva: World Health Organization, 107.*

Millán, R., Gamarra, R., Schmid, T., Sierra, M. J., Quejido, A. J., Sánchez, D. M. Cardona, A.I., Fernández, M. & Vera, R. (2006). Mercury content in vegetation and soils of the Almadén mining area (Spain). *Science of the Total Environment, 368*(1), 79-87.

Mounicou, S, C. J., Vonderheide AP, Shann JR. (2006b). Comparing a selenium accumulator plant (Brassica juncea) to a nonaccumulator plant (Helianthus annuus) to investigate selenium-containing proteins. *Anal Bioanal Chem.*, *5*(386), 1367-1378.

Mounicou, S, S. J., Shah M, Meija J, Caruso JA, Vonderheide AP. (2006a). Localization and speciation of selenium and mercury in Brassica juncea: implications for Se-Hg antagonism. *J Anal At Spectrom*, *21*(4), 404-412.

Mulligan, C. N., Yong, R. N., & Gibbs, B. F. (2001). Remediation technologies for metal-contaminated soils and groundwater: an evaluation. *Engineering geology*, *60*(1-4), 193-207.

Mumin, A., Fleet, M., & Chryssoulis, S. (1994). Gold mineralization in As-rich mesothermal gold ores of the Bogosu-Prestea mining district of the Ashanti gold belt, Ghana: Remobilization of invisible gold. *Mineralium Deposita*, *29*(6), 445-460.

Murata, K., Budtz-Jørgensen, E., & Grandjean, P. (2002). Benchmark Dose Calculations for Methylmercury-Associated Delays on Evoked Potential Latencies in Two Cohorts of Children. *Risk Analysis*, *22*(3), 465-474.

Muresan, B., Cossa, D., Coquery, M., & Richard, S. (2008). Mercury sources and transformations in a man-perturbed tidal estuary: The Sinnamary Estuary, French Guiana. *Geochimica et Cosmochimica Acta*, *72*(22), 5416-5430.

Nriagu, J., & Becker, C. (2003). Volcanic emissions of mercury to the atmosphere: global and regional inventories. *Science of the Total Environment, 304*(1), 3-12.

Obeng, H. (2000). Soil classification in Ghana. *Selected Economic Issues*, (3), 1-35.

Oberthür, T., Hirdes, W., Höhndorf, A., Schmidt Mumm, A., Vetter, U., Weiser, T. Davis, D.W., Blenkinsop, T.G., Amanor, J.A. & Loh, G. (1995). A review of gold mineralisation in the Ashanti Belt of Ghana and its relation to the crustal evolution of the terrane. *Communications of the Geological Survey of Namibia, 10,* 121-127.

Oberthür, T., Weiser, T., Amanor, J., & Chryssoulis, S. (1997). Mineralogical siting and distribution of gold in quartz veins and sulfide ores of the Ashanti mine and other deposits in the Ashanti belt of Ghana: genetic implications. *Mineralium Deposita, 32*(1), 2-15.

Obodai, E., Yankson, K., & Blay Jr, J. (1991). Seasonal changes in hydrographic factors and breeding in two popula nons of crassostrea tulipa (lamarck). *Ghana Journal of Science.*

Obodai, E. A., Boamponsem, L. K., Adokoh, C. K., Essumang, D. K., Villawoe, B. O., Aheto, D. W., & Debrah, J. S. (2011). Concentrations of heavy metals in two Ghanaian Lagoons. *Arch. Appl. Sci. Res, 3*(3), 177-187.

Ogrinc, N., Monperrus, M., Kotnik, J., Fajon, V., Vidimova, K., Amouroux, D., Kocman, D., Tessier, E., Žižek, S. & Horvat, M. (2007). Distribution of mercury and methylmercury in deep-sea surficial sediments of the Mediterranean Sea. *Marine Chemistry, 107*(1), 31-48.

Oppong, S., Voegborlo, R., Agorku, S., & Adimado, A. (2010). Total mercury in fish, sediments and soil from the River Pra Basin, southwestern Ghana. *Bulletin of Environmental Contamination and Toxicology*, *85*(3), 324-329.

Ottesen, R. T., Birke, M., Finne, T. E., Gosar, M., Locutura, J., Reimann, C., & Tarvainen, T. (2013). Mercury in European agricultural and grazing land soils. *Applied geochemistry*, *33*, 1-12.

Overstreet, W. C. (1967). *The geologic occurrence of monazite*. US Geological Survey.

Pacyna, J. M., Munthen, J., Wilson, S., Maxon, P., Sundseth, K., Pacyna, E. G., Harper, E., Kindbom, K., Wangberg, I., Panasiuk, D. & Glodek, A. (2008). Technical background report to the global atmospheric mercury assessment. *Arctic Monitoring and Assessment Programme/UNEP Chemical Branch*.

Paraquetti, H. H., Lacerda, L. D., Almeida, M. D., Marins, R. V., & Mounier, S. (2007). Mercury speciation changes in waters of the Sepetiba Bay, SE Brazil during tidal events and different seasons. *Journal of The Brazilian Chemical Society*, *18*(6), 1259-1269.

Parsons, M. B., & Percival, J. B. (2005). A brief history of mercury and its environmental impact. *Mercury: Sources, Measurements, Cycles, and Effects*, *34*, 1-20.

Pesch, G. G., & Wells, P. G. (2004). Tides of Change Across the Gulf. *An Environmental Report on the Gulf of Maine and the Bay of Fundy. Gulf of Maine Council on the Marine Environment*.

Petersen, J., Sack, D., & Gabler, R. E. (2010). *Fundamentals of physical geography.* Cengage Learning. pp 460-461.

Pfeil, D. (2011). ATOMIC PERSPECTIVES-Measurement Techniques for Mercury: Which Approach Is Right for You? The advantages and disadvantages of measuring mercury with cold vapor atomic absorption spectroscopy, cold vapor atomic fluorescence spectroscopy, and direct analysis by thermal decomposition are explained. *Spectroscopy-Eugene, 26(9),* 40.

Rahn, K., & Sturdivan, L. (2004). Neutron activation and the JFK assassination, Part I. Data and interpretation. *Journal of Radioanalytical and Nuclear Chemistry, 262(1),* 205-213.

Rajaee, M., Obiri, S., Green, A., Long, R., Cobbina, S., Nartey, V., Buck, D., Antwi, E. & Basu, N. (2015). Integrated assessment of artisanal and small-scale gold mining in Ghana-Part 2: Natural sciences review. *International journal of environmental research and public health, 12(8),* 8971-9011.

Rayment, G., & Higginson, F. R. (1992). *Australian laboratory handbook of soil and water chemical methods.* Inkata Press Pty Ltd.

Rea, A. W., Keeler, G. J., & Scherbatskoy, T. (1996). The deposition of mercury in throughfall and litterfall in the Lake Champlain watershed: a short-term study. *Atmospheric Environment, 30(19),* 3257-3263.

RH Richards, C. L. (1940). *Textbook of Ore Dressing.* McGraw-Hill, New York.

Rice, G., Ambrose, R., Bullock, O., & Swartout, J. (1997). *Mercury study report to Congress. Volume 3. Fate and transport of mercury in the*

environment. Environmental Protection Agency, Research Triangle Park, NC (United States). Office of Air Quality Planning and Standards.

Rimondi, V., Gray, J. E., Costagliola, P., Vaselli, O., & Lattanzi, P. (2012). Concentration, distribution, and translocation of mercury and methylmercury in mine-waste, sediment, soil, water, and fish collected near the Abbadia San Salvatore mercury mine, Monte Amiata district, Italy. *Science of the Total Environment, 414,* 318-327.

Robertson, C. (2006). Atmospheric Pollutions in and around Manchester United Kingdom, 1-39.

Rodgers, D. (1994). *You are what you eat and a little bit more: bioenergetics-based models of methylmercury accumulation in fish revisited* (Vol. 427). Lewis Publishers, Boca Raton.

Roulet, M., Lucotte, M., Saint-Aubin, A., Tran, S., Rheault, I., Farella, N., Dezencourt, J., Passos, C. J. S., Soares, G.S., Guimaraes, J. R. & Mergler, D. (1998). The geochemistry of mercury in central Amazonian soils developed on the Alter-do-Chao formation of the lower Tapajos River Valley, Para state, Brazil. *Science of the Total Environment, 223*(1), 1-24.

Rytuba, J. (2005). Geogenic and mining sources of mercury to the environment. *Mercury: Sources, Measurements, Cycles, and Effects, 34,* 21-41.

Rytuba, J. (2003). Mercury from mineral deposits and potential environmental impact. *Environmental Geology, 43*(3), 326-338.

Sajn, R. (2003). Distribution of chemical elements in attic dust and soil as reflection of lithology and anthropogenic influence in Slovenia. In *Journal de Physique IV (Proceedings)* (Vol. 107, pp. 1173-1176). EDP sciences.

Salminen, R., Batista, M. J., Bidovec, M., Demetriades, A., De Vivo, B., De Vos, W., Duris, M., Gilucis, A., Gregorauskiene, V., Halamić, J. & Heitzmann, P. (2005). *Geochemical atlas of Europe, part 1, background information, methodology and maps.* Geological survey of Finland.

Sánchez, D. M., Quejido, A. J., Fernández, M., Hernández, C., Schmid, T., Millán, R. González, M., Aldea, M., Martín, R. & Morante, R. (2005). Mercury and trace element fractionation in Almaden soils by application of different sequential extraction procedures. *Analytical and Bioanalytical Chemistry, 381*(8), 1507-1513.

Sánchez-Rodas, D., Corns, W., Chen, B., & Stockwell, P. (2010). Atomic fluorescence spectrometry: a suitable detection technique in speciation studies for arsenic, selenium, antimony and mercury. *Journal of Analytical Atomic Spectrometry, 25*(7), 933-946.

Scheuhammer, A. M., Atchison, C. M., Wong, A. H., & Evers, D. C. (1998a). Mercury exposure in breeding common loons (Gavia immer) in central Ontario, Canada. *Environmental Toxicology and Chemistry, 17*(2), 191-196.

Scheuhammer, A. M., Atchison, C. M., Wong, A. H., & Evers, D. C. (1998b). Mercury exposure in breeding common loons (Gavia immer) in central

Ontario, Canada. *Environmental Toxicology and Chemistry, 17(2),* 191-196.

Schroeder, W. H., & Munthe, J. (1998). Atmospheric mercury: an overview. *Atmospheric Environment, 32(5),* 809-822.

Sedlar, M., Pavlin, M., Jacimovic, R., Stergarsek, A., Frkal, P., & Horvat, M. (2015). Temperature Fractionation (TF) of Hg Compounds in Gypsum from Wet Flue Gas Desulfurization System of the Coal Fired Thermal Power Plant (TPP). *American Journal of Analytical Chemistry, 6(12),* 939.

Selin, N. E., Jacob, D. J., Yantosca, R. M., Strode, S., Jaeglé, L., & Sunderland, E. M. (2008). Global 3-D land-ocean-atmosphere model for mercury: Present-day versus preindustrial cycles and anthropogenic enrichment factors for deposition. *Global Biogeochemical Cycles, 22(2).*

Semu, E., Singh, B., & Selmer-Olsen, A. (1987). Adsorption of mercury compounds by tropical soils II. Effect of soil: solution ratio, ionic strength, pH, and organic matter. *Water, Air, and Soil Pollution, 32(1–2),* 1-10.

Sherene, T. (2010). Mobility and transport of heavy metals in polluted soil environment. In *Biological Forum: An International Journal* (Vol. 2, pp. 112-121).

Sholupov, S., Pogarev, S., Ryzhov, V., Mashyanov, N., & Stroganov, A. (2004). Zeeman atomic absorption spectrometer RA-915+ for direct determination of mercury in air and complex matrix samples. *Fuel Processing Technology, 85(6),* 473-485.

Simon, M. & Wuhl-Couturier, M. (2002). Mercury. In F. Bohnet ed. Ulmann's encyclopedia of industrial chemistry, 6th completely revised edition. Weinheim, Germany: Wully-VCH.

Simonits, A., Moens, L., De Corte, F., De Wispelaere, A., Elek, A., & Hoste, J. (1980). ko-measurements and related nuclear data compilation for (n, γ) reactor neutron activation analysis. *Journal of Radioanalytical Chemistry, 60(2),* 461-516.

Singh, R., Gautam, N., Mishra, A., & Gupta, R. (2011). Heavy metals and living systems: An overview. *Indian journal of pharmacology, 43(3),* 246.

Skoog, D. A., West, D. M., Holler, F. J., & Crouch, S. (2013). *Fundamentals of analytical chemistry.* Nelson Education.

Snoj, L., Trkov, A., Jaćimović, R., Rogan, P., Žerovnik, G., & Ravnik, M. (2011). Analysis of neutron flux distribution for the validation of computational methods for the optimization of research reactor utilization. *Applied Radiation and Isotopes, 69(1),* 136-141.

Soerensen, A. L., Jacob, D. J., Streets, D. G., Witt, M. L., Ebinghaus, R., Mason, R. P., Andersson, M. & Sunderland, E. M. (2012). Multi-decadal decline of mercury in the North Atlantic atmosphere explained by changing subsurface seawater concentrations. *Geophysical Research Letters, 39(21).*

Spiegel, S., & Veiga, M. (2006). Interventions to Reduce Mercury Pollution in Artisanal Gold Mining Sites-lessons from the UNDP. In *GEF/UNIDO Global Mercury Project, NIMD Forum* (pp. 1-18).

Steane, A., (2002). Atomic Physics: A high-precision quantum Mechancic systems and the interaction of light and matter. pp. 67-71.

Sunderland, E. M., Krabbenhoft, D. P., Moreau, J. W., Strode, S. A., & Landing, W. M. (2009). Mercury sources, distribution, and bioavailability in the North Pacific Ocean: Insights from data and models. *Global Biogeochemical Cycles, 23(2).*

Swartzendruber, P., & Jaffe, D. (2012). Sources and Transport. *Mercury in the Environment: Pattern and Process, 3.*

Taylor, K. (2007). Urban environments. *Environmental Sedimentology,* 190-222.

Taylor, S. R., & McLennan, S. M. (1985). The continental crust: its composition and evolution.

Telmer, K., & Veiga, M. (2008). World emissions of mercury from small scale artisanal gold mining and the knowledge gaps about them. *Mercury Fate and Transport in the Global Atmosphere: Measurements Models and Policy implications.(N. Pirrone Y R. Mason, Eds.) United Nations Environment Programme,* 96-129.

Thode, H. C. (2002). *Testing for normality.* CRC press.

Tiffreau, C., Lützenkirchen, J., & Behra, P. (1995). Modeling the adsorption of mercury (II) on (hydr) oxides: I. Amorphous iron oxide and α-quartz. *Journal of Colloid and Interface Science, 172(1),* 82-93.

Tipping, E., Lofts, S., Hooper, H., Frey, B., Spurgeon, D., & Svendsen, C. (2010). Critical limits for Hg (II) in soils, derived from chronic toxicity data. *Environmental Pollution, 158(7),* 2465-2471.

Tsuguyoshi, S. (2004). Mercury analysis manual. *Ministry of the Environment, Japan.*

UNEP/FAO/IOC/IAEA (1997). Reference Methods for Marine Pollution Studies No "AE". Determination of selected organophosphorus contaminants in marine sediments.

USEPA. (1997a). *Fate and Transport of mercury in the environment* (Vol. 3). Washington D. C., USA: US. Environmental Protection Agency.

USEPA. (1997). *Fate and Transport of mercury in the environment* (Vol. 3). Washington D. C., USA: US. Environmental Protection Agency.

Vahedpour, M., Tozihi, M., & Nazari, F. (2011). Mechanistic Study on the Ozone-Mercury Reaction and the Effect of Water and Water Dimer Molecules. *Journal of the Chinese Chemical Society*, *58*(3), 398-407.

Veiga, Marcello M, Maxson, P. A., & Hylander, L. D. (2006). Origin and consumption of mercury in small-scale gold mining. *Journal of Cleaner Production*, *14*(3), 436-447.

Veiga, Marcello Mariz, Baker, R. F., Fried, M. B., & Withers, D. (2004). *Protocols for environmental and health assessment of mercury released by artisanal and small-scale gold miners*. United Nations Publications.

Von Burg, R. M., B. .. &.Greenwood. (1991). Mercury. In Metals and Their Compounds in the Environment, 1045-1089.

Walker, F. W., Feiner, F., & Parrington, J. R. (1989). *Nuclides and isotopes*. GE Nuclear Energy.

Wan, D., G. Q. ..Kim, D. ..Diony, Siou, D. D. ..Soria, L. G. A. .. &.Timber Lake. (2004). Sources and remediation for mercury contamination in aquatic systems-a literature review. *Critical Reviews in Analytical Chemistry*, *3*(131), 322-323.

Wang, S., & Mulligan, C. N. (2006). Occurrence of arsenic contamination in Canada: sources, behavior and distribution. *Science of the Total Environment, 366*(2), 701-721.

Watras, C., Back, R., Halvorsen, S., Hudson, R., Morrison, K., & Wente, S. (1998). Bioaccumulation of mercury in pelagic freshwater food webs. *Science of the Total Environment, 219*(2), 183-208.

Watras, C. J., & Bloom, N. S. (1992). Mercury and methylmercury, in individual zooplankton: Implications for bioaccumulation. *Limnology and Oceanography, 37*(6), 1313-1318.

Wei, B., & Yang, L. (2010). A review of heavy metal contaminations in urban soils, urban road dusts and agricultural soils from China. *Microchemical Journal, 94*(2), 99-107.

Welz, B., & Sperling, M. (1999). The techniques of atomic absorption spectrometry. *Atomic Absorption Spectrometry, Third Edition*, 335–475.

WHO. (2017). Mercury and Health. *Media Centre Fact Sheet*.

Wiener, J. G., Krabbenhoft, D. P., Heinz, G. H., & Scheuhammer, A. M. (2003). Ecotoxicology of mercury. *Handbook of Ecotoxicology, 2*, 409-463.

Williams, M. L., Jercinovic, M. J., & Hetherington, C. J. (2007). Microprobe monazite geochronology: understanding geologic processes by integrating composition and chronology. *Annu. Rev. Earth Planet. Sci., 35*, 137-175.

Wiltsche, H., & Knapp, G. (2014). Flow digestion systems with microwave and conductive heating. In *Microwave-Assisted Sample Preparation for Trace Element Analysis*. Elsevier. pp. 253-280).

Wolfe, M. F., Schwarzbach, S., & Sulaiman, R. A. (1998). Effects of mercury on wildlife: a comprehensive review. *Environmental Toxicology and Chemistry, 17*(2), 146-160.

World Bank Group (July, 1998). Pollution prevention and abatement handbook; Project Guidelines pollutants. 219-222.

WRC. (2010b). Baseline studies and water balance assessment for Pra and Tano basins towards the development of National.

WRC. (2010a). National baseline studies and institutional analysis towards the development of the national.

WRC. (2010c). Pra Basin Baseline study.

WRC. (2012). Pra River Basin- Integrated Water Resources Management Plan.

Wright, J. B., Hastings, D. A., Jones, W. B., & Williams, H. R. (1985). Geology and mineral resources of West Africa. 46-47Wu, X., & Delbove, F. (1989). Hydrothermal synthesis of gold-bearing arsenopyrite. *Economic Geology, 84*(7), 2029-2032.

Xin, M., Gustin, M., & Johnson, D. (2007). Laboratory investigation of the potential for re-emission of atmospherically derived Hg from soils. *Environmental Science & Technology, 41*(14), 4946-4951.

Yahaya, A., Adegbe, A., & Emurotu, J. (2012). Assessment of heavy metal content in the surface water of Oke-Afacanal Isolo. Lagos, Nigeria. *Archives of Applied Science Research, 4*(6), 2322-2326.

Yathavakilla, SKV, C. J. (2007). A study of Se-Hg antagonism in Glycine max (soybean) roots by size exclusion and reversed phase HPLC-ICPMS. *Anal Bioanal Chem, 3*(398), 715-723.

Yoneda, S., & Suzuki, K. T. (1997). Equimolar Hg-Se complex binds to selenoprotein P. *Biochemical and Biophysical Research Communications, 231*(1), 7-11.

Zaichick, V. (2006). INAA of Ca, Cl, K, Mg, Mn, Na, P, and Sr contents in the human cortical and trabecular bone. *Journal of Radioanalytical and Nuclear Chemistry, 269*(3), 653-659.

Zhang, C. (2007). *Fundamentals of environmental sampling and analysis.* John Wiley & Sons.

Zhao, J, C. Z., Gao Y, Li Y.F, Hu Y, Peng X, Dong Y, Li B, Chen C. (2013a). Selenium inhibits the phytotoxicity of mercury in garlic (Allium sativum). *Environ Res, 125,* 75-81.

Zhao, J, C. Z., Hu Y, Gao Y, Li Y, Li B, Dong Y. (2013b). Mercury modulates selenium activity via altering its accumulation and speciation in garlic (Allium sativum). *Metallomics, 5*(7), 896-903.

Žižek, S., Horvat, M., Gibičar, D., Fajon, V., & Toman, M. J. (2007). Bioaccumulation of mercury in benthic communities of a river ecosystem affected by mercury mining. *Science of the Total Environment, 377*(2), 407-415.

APPENDICES

APPENDIX A

MEAN pH ($n = 3$) OF VERTICAL SOIL PROFILE (0-6 cm DEPTH) INTO 1 cm SECTIONS FROM TWENTY (20) SAMPLING SITES ALONG THE PRA RIVER BASIN, GHANA

Name of Sampling Sites	Mean pH ($n = 3$) for each soil Depth (cm)						Range ($n = 6$)	%RSD
	0-1	1-2	2-3	3-4	4-5	5-6		
Dadientem	5.28	4.65	4.58	4.68	4.55	4.62	4.55-5.28[c-d]	2.07
Kibi	4.16	4.14	4.10	4.12	4.03	4.09	4.03- 4.16[b]	0.89
Adonkrono	7.12	6.93	6.97	6.89	6.77	6.54	6.54-7.12[g]	0.70
Kade	5.00	4.75	4.69	4.71	4.53	4.36	4.36-5.00[c]	0.85
Akim Oda	8.25	8.13	8.18	8.38	8.36	8.34	8.18-8.34[j]	0.27
Akim Oda Old	7.15	6.60	6.23	6.29	6.01	5.69	5.69-7.15[e-g]	1.26
Twenedurase	6.03	5.70	5.41	5.67	5.43	5.39	5.39- 6.03[d-e]	2.50
Kwahu Praso	7.40	7.12	6.01	5.69	5.57	5.63	5.57-7.40[e-h]	1.59
Apreja	6.40	6.03	6.01	6.01	5.52	5.42	5.42-6.40[d-f]	1.77
Nnoboamu	6.23	5.94	5.89	5.90	5.33	5.03	5.03-6.23[d-f]	1.77
Wobiri	5.73	5.41	5.37	5.22	5.26	5.19	5.19-5.73[d-e]	1.52
Nkontinso	4.49	4.17	4.00	3.93	3.96	3.89	3.89-4.49[b-c]	2.89
Dunkwa-On-Offin (1)	7.85	7.73	7.63	7.76	7.43	7.71	7.43-7.85[h-i]	2.38
Dunkwa-On-Offin (2)	4.69	4.81	4.83	4.68	4.71	4.54	4.54-4.83[c]	3.02
Assin Praso	5.36	5.40	5.21	5.30	5.33	5.27	5.21-5.40[d]	3.38

245

APPENDIX A Cont'd

Name of Sampling Sites	Mean pH ($n = 3$) for each soil Depth (cm)						Range ($n = 6$)	%RSD	Source: (Author Data, 2014)
	0-1	1-2	2-3	3-4	4-5	5-6			
Twifo Praso	5.25	5.25	4.85	4.79	4.20	4.08	4.08-5.25[b-d]	2.40	
Daboase	5.23	5.01	5.02	5.04	5.05	4.96	4.96-5.23[c-d]	2.70	
Beposo	5.90	5.75	5.58	5.73	5.59	5.33	5.33-5.90[d-e]	2.66	
Anlo	6.26	5.67	5.28	4.90	4.66	4.40	4.40-6.26[b-f]	3.37	
Shama	9.03	8.89	8.75	8.74	8.81	8.89	8.74-9.03[j]	1.43	

Source: Author Data, 2014

APPENDIX B

MEAN pH ($n = 3$) OF SPECIAL MINING WASTE FROM THE DUNKWA-ON-OFFIN SAMPLING SITE, A SAMPLING SITE FROM THE OFFIN RIVER, A MAJOR TRIBUTARY OF PRA RIVER BASIN, GHANA

Name of Samples	Mean pH ($n = 3$) for Mining waste						Range	n
	0-1 (cm)	1-2 (cm)	2-3 (cm)	3-4 (cm)	4-5 (cm)	5-6 (cm)		
SS13S-A	7.07	7.32	7.48	7.46	7.50	7.83	7.07-7.83[g-h]	6
SS13S-B	8.69	8.60	8.72	8.73	8.80	8.90	8.60-8.90[j]	6
SS13S-C	7.82	7.70	7.73	8.23	7.86	-	7.70-8.23[h-i]	5
SS13S-D	7.48	7.66	7.55	7.57	7.52	-	7.48-7.66[h]	5
SS13S-E	7.48	7.46	7.51	7.48	7.54	7.51	7.46-7.54[h]	6
SS13S-F	8.11	8.22	8.37	8.25	8.35	8.37	8.11-8.37[i]	6

NB: Classification of pH range: Ultra acid (<3.5)[a]; Extremely acidic (3.5-4.4)[b]; Very strongly acid (4.5-5.0)[c]; Strong acid (5.1-5.5)[d]; Moderately acid (5.6-6.0)[e]; Slightly acid (6.1-6.5)[f]; Neutral (6.6-7.3)[g]; Slightly alkaline (7.4-7.8)[h]; Moderately alkaline (7.9-8.4)[i]; Strongly alkaline (8.5-9.0)[j]; Very Strongly alkaline (>9.0)[k] (Soil Survey Manual, 2011).

Source: Author Data, 2014

APPENDIX C

MEAN pH ($n = 3$) OF TWELVE (12) "BLACK" SAMPLES FROM FOUR (4) SAMPLING SITES IN THE PRA RIVER BASIN, GHANA

"Black" Sample	Apreja	Nkontinso	Dunkwa-On-Offin (1)	Dunkwa-On-Offin (2)
Sampling site A	6.36±0.03[f]	5.48±0.09[d]	7.13±0.35[g]	5.33±0.21[d]
Sampling site B	-	5.36±0.11[d]	7.51±0.19[g]	6.46±0.14[f]
Sampling site C	-	8.26±0.42[i]	6.47±0.15[g]	5.62±0.05[e]
Sampling site D	-	-	7.56±0.28[h]	8.44±0.17[i]

Source: Author Data, 2014

APPENDIX D

PHYSIOCHEMICAL PROPERTIES OF THE RIVER IN TWENTY-ONE (21) SAMPLING SITES ALONG THE PRA RIVER BASIN, GHANA

Sampling Site	pH	Dissolved Oxygen (mg/L)	Conductivity (µs/cm)	Total Dissolved Solid (ppm)	Salinity (ppm)	Temperature (°C)	Water Depth (m)
Dadientem	6.71	4.06	150	77.6	77.7	23.1	3.80
Kibi	6.70	-	-	-	-	-	-
Adonkrono	6.69	4.32	100	52.4	54.6	27.4	7.00
Kade	6.73	4.91	105	55.4	57.6	27.6	6.20
Akim Oda (old)	6.79	4.99	107	56.9	58.0	26.2	5.10
Akim Oda	6.84	5.01	110	57.6	58.9	26.1	5.00
Twenedurase	5.37	6.47	52.4	27.9	32.3	22.5	3.40
Kwahu Praso	6.66	3.91	153	72.0	72.0	23.7	5.60
Apreja	6.95	4.14	134	70.2	70.4	24.2	5.40
Nnoboamu	7.16	4.51	150	78.3	78.3	27.3	6.80
Wobiri	6.58	4.09	142	76.4	73.9	27.2	2.50
Nkontinso	7.09	6.48	176	92.1	91.6	31.0	8.20
Dunkwa-On-Offin (1)	7.22	6.05	195	101	100	29.7	5.80
Dunkwa-On-Offin (2)	6.81	5.98	198	100	99.8	29.7	7.60
Assin Praso	6.96	3.81	122	57.0	59.0	26.1	5.00

APPENDIX D Cont'd

Sampling Site	pH	Dissolved Oxygen (mg/L)	Conductivity (μs/cm)	Total Dissolved Solid (ppm)	Salinity (ppm)	Temperature (oC)	Water Depth (m)
Twifo Praso (1)	6.86	3.73	125	65.5	54.6	28.9	7.00
Twifo Praso (2)	6.80	5.90	128	67.6	68.2	28.6	4.20
Daboase	6.72	2.59	158	82.4	83.2	26.6	2.80
Beposo	6.77	3.22	169	87.5	88.1	27.4	5.00
Anlo	7.20	-	-	-	-	29.1	4.00
Shama	7.60	-	-	-	-	26.0	2.10
Mean	6.82	4.64	138	71.1	71.1	26.8	5.32
std	0.41	1.11	35.2	17.9	17.2	2.34	1.67
n	21.0	19.0	19.0	19.0	19.0	19.0	19.0

Source: Author Data, 2014

250

APPENDIX D Cont'd

Sampling Site	pH	Dissolved Oxygen (mg/L)	Conductivity (µs/cm)	Total Dissolved Solid (ppm)	Salinity (ppm)	Temperature (oC)	Water Depth (m)
Twifo Praso (1)	6.86	3.73	125	65.5	54.6	28.9	7.00
Twifo Praso (2)	6.80	5.90	128	67.6	68.2	28.6	4.20
Daboase	6.72	2.59	158	82.4	83.2	26.6	2.80
Beposo	6.77	3.22	169	87.5	88.1	27.4	5.00
Anlo	7.20	-	-	-	-	29.1	5.00
Shama	7.60	-	-	-	-	26.0	4.00
Mean	6.82	4.64	138	71.1	71.1	26.8	2.10
std	0.41	1.11	35.2	17.9	17.2	2.34	5.32
n	21.0	19.0	19.0	19.0	19.0	19.0	1.67
							19.0

Source: Author Data, 2014

250

PERCENTAGE MOISTURE CONTENT (%MC) OF VERTICAL SOIL PROFILE OF 0-6 cm (SECTIONED INTO 1 cm) FROM THE UPSTREAM (*) AND PRA ESTUARY (**) OF THE MAIN PRA RIVER BASIN, GHANA.

Sampling Site	Soil Profile (0-6 cm) ($n = 3$)						Range ($n = 6$)	%RSD ($n = 6$)
	0-1	1-2	2-3	3-4	4-5	5-6		
Dadientem*	2.80	2.61	2.77	3.12	3.35	2.36	2.36-3.12	2.01
Kibi*	1.43	1.96	1.68	1.56	1.96	1.66	1.43-1.96	3.84
Adonkrono	0.39	0.65	0.52	0.63	0.41	0.59	0.39-0.65	1.18
Kade	1.49	1.02	1.24	1.14	0.82	0.70	0.70-1.49	2.55
Akim Oda	0.55	0.10	0.10	0.10	0.12	0.11	0.10-0.55	0.55
Akim Oda (Old)	0.06	0.52	0.56	0.28	0.16	0.19	0.06-0.56	0.89
Twenedurase*	3.40	3.53	3.13	3.00	2.42	1.94	1.94-3.53	1.98
Kwahu Praso	2.08	1.82	1.50	1.34	1.16	0.84	0.84-2.08	3.62
Apreja	0.55	0.55	0.56	0.73	0.71	0.64	0.55-0.73	0.29
Nnoboamu	0.65	0.70	0.97	0.88	0.78	0.91	0.65-0.97	1.09
Wobiri	0.39	0.39	0.47	0.63	0.53	0.54	0.39-0.63	3.22
Nkontinso	0.94	0.94	1.33	0.89	0.86	0.99	0.86-0.99	3.87
Dunkwa-On-Offin (1)	0.23	0.23	0.31	0.12	0.11	0.10	0.11-0.31	1.09
Dunkwa-On-Offin (2)	0.79	0.79	1.06	0.84	0.83	1.08	0.83-1.09	2.22
Assin Praso	0.61	0.61	1.49	0.49	0.77	0.75	0.49-1.49	0.99
Twifo Praso	0.61	0.61	0.44	0.51	3.03	0.93	0.44-3.03	1.42
Daboase	0.60	0.60	0.58	0.48	0.75	0.51	0.48-0.75	2.17
Beposo	0.95	0.95	1.03	1.40	0.96	1.23	0.95-1.40	5.60

APPENDIX E Cont'd

| Sampling Site | Soil Profile (0-6 cm) (n = 3) | | | | | | Range | %RSD |
	0-1	1-2	2-3	3-4	4-5	5-6	(n = 6)	(n = 6)
Anlo**	0.82	1.20	0.82	0.91	0.97	0.85	0.82-1.20	2.87
Shama**	0.64	0.51	0.98	1.18	1.35	1.10	0.51-1.35	3.46

NB: * indicate the sampling site is at the upstream of the River; and ** indicate the sampling site is at the Pra River Estuary.

Source: Author Data, 2014

APPENDIX F

MEAN THg CONCENTRATION (mg/kg) IN 1cm SECTIONS OF VERTICAL SOIL (SECTIONED INTO 1 cm) PROFILE, USING M1 (n = 4) FROM TWENTY (20) SAMPLING SITES ALONG THE PRA RIVER BASIN, GHANA

Name of Sampling site	Mean concentration of THg (mg/kg) in Soil Profile depth (cm) (n = 4)						Range (n = 6)	%RSD (n = 6)
	0-1	1-2	2-3	3-4	4-5	5-6		
Dadientem	10.6	4.38	3.95	5.15	4.55	4.81	3.95-10.6	0.55
Kibi	3.63	3.12	2.79	2.23	2.3	5.73	2.23-5.73	2.10
Adonkrono	0.94	0.57	2.54	1.92	1.63	1.37	0.57-2.54	1.85
Kade	2.79	2.54	2.28	1.1	1.37	0.52	0.52-2.79	2.27
Akim Oda	0.51	0.88	0.81	0.67	1.11	1.43	0.51-1.43	1.40
Akim Oda (Old)	2.09	2.27	2.45	2.57	1.66	1.43	1.43-2.57	2.68
Twenedurase	2.39	2.86	3.25	2.31	1.86	3.13	1.86-3.25	1.54
Kwahu Praso	3.48	3.17	2.29	2.23	2.04	6.89	2.04-6.89	0.79
Apreja	2.35	2.24	2.14	2.40	2.44	2.30	2.14-2.44	1.95
Nnboamu	1.79	2.54	2.60	3.52	4.03	5.00	1.79-5.00	1.95
Wobiri	3.59	3.69	2.40	2.28	1.91	1.82	1.82-3.69	2.14
Nkontinso	0.77	0.91	0.99	0.62	1.00	0.77	0.62-1.00	3.80
Dunkwa-On-Offin 1	82.9	82.5	101	129	143	122	82.5-143	2.46
Dunkwa-On-Offin 2	6.88	9.58	2.20	0.60	1.65	0.71	0.60-9.58	3.11
Assin Praso	1.50	1.97	3.81	2.56	5.00	6.95	1.50-6.95	3.11
Twifo Praso	3.62	2.03	1.64	1.54	1.84	2.34	1.54-3.62	3.94
Daboase	1.14	2.18	2.06	2.21	2.41	2.68	1.14-2.68	3.92

APPENDIX F Cont'd

Name of Sampling site	Mean concentration of THg (mg/kg) in Soil Profile depth (cm) ($n = 4$)						Range ($n = 6$)	%RSD ($n = 6$)
	0-1	1-2	2-3	3-4	4-5	5-6		
Beposo	2.72	3.39	2.50	1.40	1.90	3.59	1.40-3.59	1.06
Anlo	4.95	2.15	0.60	0.71	0.90	0.65	0.60-5.95	2.01
Shama	6.69	4.98	3.42	3.89	4.48	3.50	3.42-6.69	1.52

Source: Author Data, 2013

254

APPENDIX G

MEAN THg CONCENTRATION (n = 4) (mg/kg) IN SEDIMENT CORE (0-10 cm) SECTIONED INTO 10 SECTIONS, USING M1 BY CVAAS FROM TWENTY ONE (21) SAMPLING SITES FORM THE PRA RIVER BASIN, GHANA

Name of Sampling site	M1 for CVAAS Mean THg (g/g) sediment core (n = 4) depth (cm)										Range (n = 10)	%RSD (n = 10)
	0-1	1-2	2-3	3-4	4-5	5-6	6-7	7-8	8-9	9-10		
Dadientem	0.02	0.01	0.01	0.02	0.03	0.02	0.04	0.04	0.04	0.03	0.01 - 0.04	1.22
Kibi	0.03	0.03	0.03	0.03	0.04	0.04	0.04	0.05	0.04	0.04	0.03 - 0.05	5.09
Adonkrono	0.07	0.07	0.06	0.05	0.04	0.05	0.04	0.04	0.05	0.04	0.04 - 0.07	3.36
Kade	0.05	0.05	0.07	0.06	0.06	0.09	0.09	0.12	0.15	0.15	0.05 - 0.15	3.21
Akim Oda	0.05	0.03	0.04	0.04	0.04	0.04	0.04	0.04	0.04	0.04	0.03 - 0.05	4.04
Akim Oda (Old)	0.07	0.08	0.08	0.08	0.08	0.09	0.11	0.10	0.09	0.05	0.05 - 0.11	0.97
Twenedurase	0.01	0.01	0.01	0.01	0.01	0.01	0.01	0.09	0.01	0.08	0.01 - 0.09	7.40
Kwahu Praso	0.02	0.01	0.01	0.01	0.02	0.01	0.01	0.01	0.01	0.01	0.01 - 0.02	11.4
Apreja	0.20	0.15	0.15	0.19	0.16	0.15	0.10	0.08	0.08	0.03	0.03 - 0.20	1.00
Nnoboamu	0.01	0.01	0.01	0.01	0.01	0.01	0.01	0.02	0.02	0.01	0.01 - 0.02	7.83
Wobiri	0.01	0.01	0.01	0.01	0.01	0.01	0.01	0.01	0.01	0.02	4.78 - 15.6	11.8
Nkontinso	0.06	0.06	0.05	0.05	0.07	0.05	0.05	0.04	0.05	0.05	0.04 - 0.07	0.98
Dunkwa-On-Offin 1	0.43	0.38	0.19	0.28	1.14	1.55	1.38	0.35	0.20	0.09	0.19 - 1.55	1.28

255

APPENDIX G Cont'd

Name of Sampling site	M1 for CVAAS Mean THg (g/g) sediment core ($n = 4$) depth (cm)										Range ($n = 10$)	%RSD ($n = 10$)
	0-1	1-2	2-3	3-4	4-5	5-6	6-7	7-8	8-9	9-10		
Dunkwa-On-Offin 2	0.09	0.08	0.07	0.05	0.06	0.06	0.06	0.06	0.08	0.06	0.05 - 0.09	2.15
Assin Praso	0.05	0.04	0.04	0.04	0.03	0.07	0.03	0.04	0.04	0.11	0.03 - 0.04	1.20
Twifo Praso 1	0.14	0.12	0.11	0.10	0.11	0.12	0.14	0.17	0.07	0.08	0.06 - 0.11	0.79
Twifo Praso 2	0.10	0.23	0.20	0.09	0.23	0.41	0.25	0.14	0.15	0.12	0.10 - 0.33	0.79
Daboase	0.14	0.16	0.14	0.14	0.26	0.23	0.18	0.20	0.10	0.12	0.10 - 0.26	0.82
Beposo	0.23	5.39	0.51	1.36	0.31	0.20	0.16	0.13	7.94	0.16	0.16 - 7.94	1.90
Anlo	0.01	0.01	0.01	0.02	0.03	0.04	0.03	0.01	0.01	0.01	0.01 - 0.04	9.72
Shama	0.01	0.01	0.01	0.01	0.01	0.01	0.01	0.01	0.02	0.01	0.01 - 0.02	10.2

Source: Author Data, 2013

APPENDIX H

MEAN THg CONCENTRATIONS (mg/kg) IN 0-1 cm SECTION OF SOIL (AIR DRIED MASS) FROM PRA RIVER BASIN, GHANA, BY TWO ACID DIGESTION PROCEDURES (M1 AND M2) OF CVAAS AND k_0-INAA

Name of Sampling Site	THg mg/kg M1 procedure (n = 4)	THg mg/kg M2 procedure (n = 4)	THg mg/kg K1 method (n = 3)
Dadientem	10.6±0.33	11.1±0.36	11.9±0.50
Kibi	3.63±0.05	9.25±0.06	8.00±0.30
Adonkrono	0.94±0.048	6.27±0.12	5.54±0.20
Kade	2.79±0.11	11.9±0.26	10.2±0.40
Akim Oda (old)	0.51±0.03	1.77±0.10	1.73±0.07
Akim Oda	2.09±0.07	5.20±0.14	4.78±0.17
Twenedurase	2.39±0.10	3.09±0.079	3.48±0.13
Kwahu Praso	3.48±0.03	3.06±0.046	3.10±0.12
Apreja	2.35±0.09	5.91±0.17	5.01±0.18
Nnoboamu	3.59±0.09	5.66±0.13	5.52±0.21
Wobiri	1.79±0.03	7.38±0.03	6.44±0.23
Nkontinso	0.77±0.00	10.9±0.09	10.6±0.40
Dunkwa-On-Offin (1)	82.9±2.12	103±1.90	79.6±2.80
Dunkwa-On-Offin (2)	6.88±0.02	11.7±0.06	11.2±0.40
Assin Praso	1.50±0.02	5.60±0.06	4.88±0.18
Twifo Praso (1)	3.62±0.07	13.2±0.22	12.2±0.50
Daboase	2.72±0.19	6.38±0.03	3.95±0.15
Beposo	1.14±0.02	7.44±0.06	6.87±0.24
Anlo	4.95±0.16	9.34±0.12	9.29±0.35
Shama	6.69±0.09	5.28±0.03	7.73±0.29
SS13S_D	11.1±0.14	18.6±0.10	18.7±0.70
SS13 "BLACK" D	1,773±19.0	1,188±0.97	1,318±46.0

NB: *a* denote M1 which comprises acid digestion with H_2SO_4; *b* denote M2 which comprises acid digestion with HF; *c* denotes K1 which is a method that used k_0-INAA method

Source: Author Data, 2014

CORRELATION, AND *p-value* BETWEEN THg CONCENTRATION (USING M2) AND DEPTH OF VERTICAL SOIL PROFILE (0-6 cm) FROM TWENTY (20) SAMPLING SITES ALONG THE PRA RIVER BASIN, GHANA

Name of Sampling sites	THg in soil (mg/kg) /depth (cm)		THg in sediment (mg/kg) /depth (cm)		Soil/Sediment	
	Correlation (n = 6)	P-values (n = 6)	Correlation (n = 10)	P-values (n = 10)	Correlation (n = 6)	P-values (n = 6)
Dadientem	-0.03	0.96	0.81	0.01	-0.12	0.83
Kibi	-0.75	0.08	0.40	0.26	0.15	0.78
Adonkrono	0.31	0.54	-0.62	0.05	0.38	0.46
Kade	-0.37	0.47	0.81	0.00	0.73	0.10
Akim Oda	0.14	0.79	0.49	0.15	0.12	0.83
Akim Oda (Old)	-0.03	0.96	-0.02	0.96	0.70	0.15
Twenedurase	-0.03	0.96	0.20	0.58	0.53	0.28
Kwahu Praso	-0.09	0.87	-0.73	0.02	0.09	0.86
Apreja	0.77	0.07	0.32	0.38	0.37	0.47
Nnoboamu	0.94	0.01	0.66	0.04	0.81	0.05
Wobiri	0.37	0.47	0.73	0.02	0.26	0.62
Nkontinso	0.20	0.70	-0.20	0.58	0.49	0.33
Dunkwa-On-Offin (1)	1.00	-0.00	-0.12	0.74	0.95	0.01
Dunkwa-On-Offin (2)	-0.26	0.62	-0.08	0.84	0.49	0.33
Assin Praso	1.00	-0.00	0.47	0.17	0.09	0.87
Twifo Praso (1)	-0.37	0.47	0.29	0.42	0.20	0.70
Twifo Praso (2)	-	-	-0.01	0.96	-	-

APPENDIX I Cont'd

Name of Sampling sites	THg in soil (mg/kg) /depth (cm)		THg in sediment (mg/kg) /depth (cm)		Soil/Sediment	
	Correlation (r) (n = 6)	P-values (n = 6)	Correlation (r) (n = 6)	P-values (n = 6)	Correlation (r) (n = 6)	P-values (n = 6)
Daboase	0.71	0.11	-0.76	0.01	0.83	0.04
Beposo	0.77	0.07	0.17	0.64	0.37	0.47
Anlo	-0.83	0.04	0.08	0.83	0.66	0.16
Shama	-0.09	0.87	0.69	0.03	0.26	0.62

Source: Author Data, 2014

APPENDIX M

SUMMARY OF THE RANGES OF THg CONCENTRATION (mg/kg) IN EACH DEPTH (1 cm) OF THE SOIL PROFILES (0-6 cm) SAMPLED FROM THE PRA RIVER BASIN, GHANA THAT WERE DETERMINED BY USING ARC MAP 10.1 SOFTWARE

Contamination levels of THg	Range of THg concentrations in each depth from the soil profile (0 - 6 cm)						NB: n represents the number of sampling sites
	0-1 cm	1-2 cm	2 - 3 cm	3 - 4 cm	4 - 5 cm	5 - 6 cm	
Level 1 = ⚬	1.77-3.16 ($n=4$)	2.32- 4.63 ($n=7$)	1.57-4.42 ($n=6$)	1.54-3.66 ($n=6$)	1.62-0.75 ($n=7$)	1.30-3.23 ($n=4$)	
Level 2 = ◉	3.16-7.87 ($n=7$)	4.63-7.01 ($n=5$)	4.42-8.91 ($n=7$)	3.66-8.85 ($n=6$)	5.75-10.8 ($n=8$)	3.23-9.98 ($n=10$)	
Level 3 = ⬤	7.87-12.8 ($n=7$)	7.01-13.0 ($n=7$)	8.91-12.5 ($n=6$)	8.85-13.3 ($n=6$)	10.8-20.1 ($n=4$)	9.99-15.5 ($n=5$)	
Level 4 = ⬤	12.8-103 ($n=1$)	13.0-109 ($n=1$)	12.5-119 ($n=1$)	13.3-138 ($n=1$)	20.1-747 ($n=1$)	15.5-770 ($n=1$)	

Source: Author Data, 2014

263

MERCURY BINDING SPECIES IN SOIL FROM OTHER STUDIES

Study	Sample name	Name of Sampling site	Material	THg mg/kg	Possible Hg Compounds released	T°C range	T°C max.
Biester et al., 1999	-	-	Tailings	43-1,640	1st peak (Metallic Hg)	<100	-
					2nd peak (Hg_{mc})	-	150-250
					3rd peak (Cinnabar)	-	250-350
					4th peak (HgO)	420-550	-
					5th peak (unknown)	630 - 670*	650
Biester et al., (2002a, b)	-		Standard	-	Hg^0 from Schists (Idrija)	50-180*	120*
				-	Metacinnabar (synthetic cinnabar)	190-330	270*
				-	Incubated Hg^0 on Fe oxyhydroxide	50-300*	110*,190*
				-	Hg in humic acids	190-330*	250*
	Site 1 (0-5)	Exact location confidential (Europe)	Topsoil	0.024-4.19	One peak (Hg_{mc})	180-300	200-250
	Site 2 (0-5)			0.122-3.01	One peak (Hg_{mc})	180-300	200-250
	Site 3 (0-5)			0.094-2	One peak (Hg_{mc})	150-280	200

APPENDIX N Cont'd

Study	Sample name	Name of Sampling site	Material	THg mg/kg	Possible Hg Compounds released	T°C range	T°C Max.
Hojdová et al., (2008)	-	-	Standard	-	HgS	280-480	415
					HgO	280-700	380, 590
					HgCl$_2$	100-300	
					Hg^0 in sand	150-460	225
					Hg (II) adsorbed onto goethite	200-700*	230,325
					Hg (II) adsorbed onto lepidocrocite	100-650*	330,450
					Hg (II) adsorbed onto humic acid	200-450*	300,520
					Hg (II) adsorbed onto Kaoline	150-500*	380
					Hg (II) adsorbed onto montmorillonite	200-500*	350
Hojdová et al., (2008	0-10, 100	Jedová & Svatá (Czech Republic)	Mining waste	90.7-120	1st peak (Hg$_{mc}$)	-	320-340,
					2nd peak (Cinnabar)	-	438-456

APPENDIX N Cont'd

Study	Sample name	Name of Sampling site	Material	THg mg/kg	Possible Hg Compounds released	T°C range	T°C Max.
Coufalik et al., (2014)			Standard		Hg^0	60-120	95
					$HgCl_2$	100-190	140
					HgO	110-400	240
					$HgSO_4$	165-450	255
					Hg in humic acid	270-340	305
					Cinnabar	250-435	365
					Incubated Hg^0 on Sand	50-200	125
					Incubated Hg^0 on kaolinite	100-300	158
					Incubated Hg^0 on ash	50-450	150,300
					Incubated Hg^0 on peat	150-400	300
					Incubated Hg^0 on ground granite	200-450	300-350

Note:*The temperature were estimated from the reported Hg release curves; Hg_{mc}= Hg bound to the matrix components

266

COMPARING THE RANGE OF THg CONCENTRATIONS OF SOIL PROFILE (0-6 cm) SAMPLES IN THIS STUDIES (PRA RIVER BASIN) TO THE RANGE OF THE MAXIMUM ALLOWABLE CONCENTRATION AND TRIGGER ACTION VALUE FOR AGRICULTURAL SOIL TO SHOW IF THG CONCENTRATIONS IN THIS STUDIES ARE BELOW (B), WITHIN (W) OR ABOVE (A)

Sampling Site	Range in this Studies mg/kg M2 (n = 6)	MAC (0.5-5.0) mg/kg M2	TAV (1.5-10) mg/kg M2
Dadientem	3.32-11.1	A	A
Kibi	6.54-9.25	A	W
Adonkrono	6.05-8.91	A	W
Kade	6.53-11.9	A	A
Akim Oda	1.77-3.55	W	W
Akim Oda (Old)	5.20-6.70	A	W
Twenedurase	2.20-3.23	W	W
Kwahu Praso	2.19-6.22	A	W
Apreja	5.91-10.9	A	A
Nnoboamu	5.71-20.1	A	A
Wobiri	7.38-13.3	A	A
Nkontinso	5.68-18.5	A	A
Dunkwa-On-Offin (1)	10.3-770	A	A
Dunkwa-On-Offin (2)	7.14-17.7	A	A
Assin Praso	5.60-14.8	A	A
Twifo Praso	9.57-13.0	A	W
Daboase	2.58-9.99	A	A
Beposo	7.87-14.0	W	W
Anlo	1.30-9.34	A	W
Shama	2.63-5.29	A	

Source: Kabata-Pendias & Sadurki, 2004; Chen, 1999

APPENDIX P

BASIC STATISTICAL PARAMETERS (MEAN, MINIMUM, MAXIMUM, STANDARD DEVIATION) OF REE MEAN CONCENTRATION (mg/kg) IN TWENTY (20) SOILS (0–1 cm) AND TWO (2) MINING WASTE DETERMINED BY k_0-INAA (K1, $n = 3$) FROM THE PRA BASIN, GHANA

Sampling Sites	Sc	Ce	Eu	La	Nd	Sm	Tb	Yb
Dunkwa-On-Offin*	2.22*	54.8*	1.34*	LD*	LD*	4.50*	0.74*	LD*
Akim Oda	2.39	6.41	0.30	3.00	3.27	0.62	0.20	1.31
Akim Oda (old)	2.91	8.95	0.26	3.97	3.33	0.65	0.14	0.94
Shama	3.47	26.7	0.43	11.8	13.2	2.46	0.28	0.96
Dunkwa-On-Offin*	3.54*	15.9*	0.40*	8.89*	8.45*	1.60*	0.20*	0.58*
Twenedurase	3.75	37.1	0.64	17.7	17.0	3.13	0.50	1.88
Apreja	3.84	20.2	0.47	8.42	8.55	1.63	0.29	1.40
Dunkwa-On-Offin 1	4.01	15.9	0.39	8.00	6.40	1.56	0.22	0.70
Adonkrono	4.46	12.5	0.63	6.38	6.09	1.30	0.62	3.29
Wobiri	4.58	16.1	0.35	5.81	5.48	1.13	0.25	1.44
Nnboamu	4.77	30.7	0.53	14.7	13.5	2.26	0.34	1.37
Kwahu Praso	4.80	17.5	0.40	8.13	7.31	1.52	0.26	1.24
Twifo Praso (1)	4.81	26.8	0.58	11.6	11.8	1.93	0.31	1.34
Daboase	6.17	22.2	0.56	10.1	9.66	1.91	0.32	1.23
Assin Praso	6.31	20.5	0.50	9.17	8.38	1.64	0.29	1.41

APPENDIX P Cont'd

Sampling Sites	Sc	Ce	Eu	La	Nd	Sm	Tb	Yb
Beposo	7.21	22.6	0.56	11.0	9.30	1.81	0.31	1.44
Nkontinso	9.81	39.5	0.93	17.5	17.9	3.24	0.49	1.94
Kade	10.4	30.7	0.80	13.9	13.4	2.69	0.49	2.13
Anlo	10.8	24.0	0.50	11.8	9.25	1.82	0.23	0.82
Dunkwa-On-Offin (2)	14.0	41.3	1.00	17.6	17.7	3.32	0.53	1.91
Dadientem	20.4	51.2	1.29	20.8	22.6	4.40	0.77	3.04
Kibi	21.4	67.7	1.50	29.4	28.6	4.83	0.91	3.85
Mean	7.57	27.4	0.64	12.3	11.9	2.24	0.39	1.65
std	5.44	14.3	0.32	6.00	6.28	1.07	0.20	0.87
Minimum	2.39	6.41	0.26	3.00	3.27	0.62	0.14	0.70
Maximum	21.4	67.7	1.50	29.4	28.6	4.83	0.91	3.85

NB: (*) are not inclusive in the statistic. They are mining waste or "Black" samples not soil (0-1 cm) samples.
Source: Author Data, 2014

269

APPENDIX Q

TRACE ELEMENTS (As, Ba, Br, Cs, Hf, Mo, Rb, Se, Sb, Sr, Th, U AND Zr) IN mg/kg DETERMINED IN SURFACE SOIL (0-1 cm) FROM TWENTY (20) SAMPLING SITES FROM THE PRA RIVER BASIN, GHANA BY k_0-INAA METHOD

Sampling sites	As	Br	Cs	Hf	Se	Zr	Ba	Th	U	Sr	Sb	Rb
Akim Oda	1.74	0.43	0.34	9.62	LD	422	28.8	1.96	0.90	19.0	0.19	3.84
Akim Oda (old)	1.56	2.17	0.76	7.69	LD	321	58.6	2.39	1.07	17.0	0.16	9.97
Shama	19.9	11.1	0.59	12.8	LD	519	189	3.35	2.19	508	0.52	23.2
Twenedurase	8.33	6.38	1.49	9.81	LD	410	119	5.20	1.92	30.7	0.34	40.9
Apreja	2.25	2.41	0.73	11.5	LD	501	94.4	3.03	1.31	30.0	0.73	10.3
Dunkwa-On-Offin (1)	6193	1.24	1.27	1.72	3.53	87.7	83.4	1.37	LD	61.2	43.0	16.1
Adonkrono	2.02	2.68	0.79	7.91	LD	339	77.9	3.61	1.84	22.5	0.27	16.9
Wobiri	6.46	2.71	0.98	10.3	LD	438	66.5	2.46	1.14	28.5	0.31	8.31
Nnboamu	159	2.44	1.96	6.68	1.03	264	185	4.18	2.08	LD	0.50	34.7
Kwahu Praso	4.29	3.69	0.71	13.0	LD	573	154	2.58	1.06	87.0	0.30	15.8
Twifo Praso	5.54	4.09	0.98	9.25	LD	400	133	3.57	1.05	50.7	0.36	16.1
Daboase	9.07	2.18	1.57	5.62	LD	229	224	2.84	1.22	63.9	0.29	23.9
Assin Praso	4.35	3.74	1.45	8.42	0.44	343	208	3.13	1.32	57.3	0.45	22.7
Beposo	5.15	6.81	2.39	7.45	LD	285	372	4.09	2.07	70.0	0.41	39.6
Nkontinso	10.9	1.67	2.82	7.16	LD	288	278	4.44	1.90	79.0	0.32	42.4
Kade	6.96	5.00	1.58	7.70	1.75	313	169	4.40	1.76	31.1	0.52	23.3
Anlo	1.95	13.9	0.56	5.70	0.61	228	40.2	6.97	2.45	19.2	0.10	10.5

270

APPENDIX Q Cont'd

Sampling sites	As	Br	Cs	Hf	Se	Zr	Ba	Th	U	Sr	Sb	Rb
unkwa-On-Offin (2)	21.3	2.08	2.18	4.15	LD	178	268	3.85	1.30	85.6	1.61	35.3
Dadientem	13.2	11.3	1.63	7.40	LD	320	275	5.93	1.64	66.6	0.74	34.0
Kibi	21.6	2.07	2.20	10.7	LD	459	233	7.21	2.23	43.6	1.18	40.9
Mean	325	4.40	1.35	8.23	1.47	346	163	3.83	1.60	72.2	2.62	23.4
std	1382	3.71	0.70	2.79	1.26	121	93.7	1.56	0.48	108	9.51	12.5
Minimum	1.56	0.43	0.34	1.72	0.44	87.7	28.8	1.37	0.90	17.0	0.10	3.84
Maximum	6193	13.9	2.82	13.0	3.53	573	372	7.21	2.45	508	43.0	42.4

Source: Author Data, 2014

TRACE METALS (Ag, Au, Co, Cd, Ta, Cr, Ga, Sn &W) IN mg/kg DETERMINED IN SURFACE SOIL (0-1 cm) FROM TWENTY (20) SAMPLING SITES FROM THE PRA RIVER BASIN, GHANA BY k₀-INAA METHOD

Sampling sites	Ag	Au	Co	Sn*	Cd*	Cr	Ga*	Ta	W*
Akim Oda	LD	LD	2.65	LD	LD	23.0	1.70	0.822	1.40
Akim Oda (old)	LD	0.0011	4.42	LD	LD	26.8	3.18	0.702	0.63
Shama	LD	0.0021	7.21	LD	LD	36.0	7.50	0.573	LD
Twenedurase	LD	0.0016	5.27	LD	LD	18.5	6.35	0.500	0.58
Apreja	LD	0.2250	3.13	LD	LD	38.0	4.58	0.524	0.87
Dunkwa-On-Offin (1)	2.98	26.500	11.5	LD	LD	52.1	LD	0.287	10.4
Adonkrono	LD	0.0017	2.78	LD	LD	54.0	4.86	0.891	4.14
Wobiri	LD	0.0014	6.75	LD	LD	28.2	4.00	0.659	0.87
Nnboamu	LD	0.0045	3.42	LD	LD	56.2	9.42	0.707	3.58
Kwahu Praso	LD	0.0022	5.50	LD	LD	30.1	5.87	0.410	LD
Twifo Praso	LD	0.0189	4.94	LD	LD	43.4	5.75	0.542	LD
Daboase	LD	0.0118	8.30	LD	LD	46.5	8.25	0.601	0.96
Assin Praso	LD	0.0018	9.66	LD	LD	48.4	6.81	0.730	1.18
Beposo	LD	0.0060	7.69	LD	LD	51.8	11.0	0.846	1.10
Nkontinso	LD	0.0091	9.71	LD	LD	71.4	12.5	0.830	1.48
Kade	LD	0.0031	7.67	LD	LD	23.0	9.76	0.891	1.72
Anlo	LD	DL	3.05	LD	LD	36.0	7.50	0.881	LD

APPENDIX R Cont'd

Sampling sites	Ag	Au	Co	Sn*	Cd*	Cr	Ga*	Ta	W*
Dunkwa-On-Offin (2)	LD	0.0172	15.1	LD	LD	105	12.8	0.666	LD
Dadientem	LD	0.0043	21.8	LD	LD	164	19.5	0.946	1.81
Kibi	LD	DL	28.9	LD	LD	83.9	21.3	1.240	1.79
n	1	17	20	-	-	20	19	20	15
Mean	2.98	1.5800	8.47	-	-	51.8	8.56	0.710	2.17
std	0.11	6.4200	6.71	-	-	1.94	0.43	0.027	0.14
Minimum	2.98	0.0011	2.65	-	-	18.5	1.70	0.287	0.58
Maximum	2.98	26.500	28.9	-	-	105	21.3	1.240	10.4

Source: Author Data, 2014

273

ZERO-ORDER (PEARSON) CORRELATIONS BETWEEN MEAN THg CONCENTRATION (mg/kg) AND OTHER ELEMENTS DETERMINED BY k_0-INAA METHOD USING SOIL (0-1 cm) FROM THE TWENTY (20) SAMPLING SITES ALONG THE PRA RIVER BASIN, GHANA

Element	Correlations			Control Variables (pH & %MC)		
	None Controlled Variables					
	Hg			Hg		
	Correlation	p-value	n	Correlation	p-value	n
As	0.98	0.00	18	0.99	0.00	16
Au	0.98	0.00	18	0.97	0.00	16
Br	-0.12	0.60	18	-0.10	0.70	16
Cs	0.05	0.84	18	0.31	0.22	16
Hf	-0.60	0.01	18	-0.67	0.00	16
Se	0.86	0.00	18	0.85	0.00	16
Zr	-0.55	0.01	18	-0.62	0.01	16
Ba	-0.12	0.61	18	0.01	0.97	16
Th	-0.27	0.25	18	-0.15	0.57	16
U	-0.55	0.01	18	-0.51	0.03	16
Sr	0.01	0.96	18	-0.08	0.75	16
Sb	0.98	0.00	18	0.99	0.00	16
Rb	-0.07	0.77	18	0.14	0.58	16
Sc	-0.03	0.90	18	0.20	0.42	16
Ce	-0.07	0.79	18	0.21	0.41	16
Eu	-0.06	0.80	18	0.20	0.43	16
La	-0.05	0.85	18	0.23	0.36	16
Nd	-0.08	0.74	18	0.17	0.50	16
Sm	-0.02	0.94	18	0.28	0.27	16
Tb	-0.12	0.63	18	0.08	0.75	16
Yb	-0.22	0.35	18	-0.10	0.70	16
Fe	0.24	0.31	18	0.38	0.12	16
Na	-0.02	0.95	18	0.00	1.00	16
K	-0.05	0.85	18	0.11	0.67	16
Ca	-0.03	0.90	18	-0.16	0.53	16
Zn	0.32	0.16	18	0.29	0.24	16
Fe	0.24	0.31	18	0.38	0.12	16
Mo	-0.08	0.75	18	-0.13	0.61	16
Ag	-0.10	0.67	18	0.00	0.10	16
Co	0.19	0.43	18	0.40	0.10	16
Cr	0.11	0.63	18	0.27	0.28	16
Ga	-0.25	0.30	18	-0.10	0.70	16
Ta	-0.40	0.08	18	-0.36	0.15	16
W	0.85	0.00	18	0.84	0.00	16

NB: Using SPSS version 16

APPENDIX T

MEAN ELEMENTAL CONCENTRATION OF Ca, K, Zn, Fe, Na AND Mo (mg/kg) AND pH DETERMINED IN TWENTY (20) TOPSOIL (0-1 cm) FROM THE PRA RIVER BASIN, GHANA BY k_0-INAA METHOD

Sampling sites	Na	K	Ca	Zn	Fe	Mo
Akim Oda	144	451	779	17.0	7795	LD
Akim Oda (old)	211	1179	884	28.9	9384	LD
Shama	6409	5975	51696	166	30970	0.85
Twenedurase	199	6454	2774	29.7	12560	LD
Apreja	735	1960	1233	81.3	12450	0.52
Dunkwa-On-Offin (1)	1318	2906	2254	92.9	33540	LD
Adonkrono	185	1947	1705	58.8	13970	LD
Wobiri	468	1007	DL	21.7	11720	LD
Nnboamu	334	6063	DL	24.2	15470	1.31
Kwahu Praso	3022	2809	7153	36.3	14610	LD
Twifo Praso	2959	3055	DL	51.1	11950	0.70
Daboase	3953	4812	2329	37.1	14680	LD
Assin Praso	3248	4062	DL	36.3	14020	LD
Beposo	2492	7386	2022	42.7	15570	LD
Nkontinso	2966	7839	2026	43.6	17870	LD
Kade	1603	3651	1527	46.2	24540	LD
Anlo	192	1742	DL	29.2	49660	1.20
Dunkwa-On-Offin (2)	2155	6622	DL	36.7	31790	1.06
Dadientem	4044	5738	2214	82.3	68080	LD
Kibi	1241	5381	DL	80.7	62670	LD
Mean	1894	4052	6046	52.1	23665	0.94
n	20	20	13	20	20	6
std	1721	2287	13808	34.7	17604	0.30
Minimum	144	451	779	17.0	7795	0.52
Maximum	6409	7839	51696	166	68080	1.31

Source: Author Data, 2014

APPENDIX U

ENRICHMENT FACTORS OF Ce, Eu, La, Nd, Sm, Tb, AND Yb DETERMINED USING Sc AS NORMALIZING AGENT IN 0 TO 1 cm SOIL FROM THE PRA RIVER BASIN

Sampling Sites	Ce	Eu	La	Nd	Sm	Tb	Yb
Akim Oda	0.55	1.05	1.30	0.62	0.67	1.67	2.49
Akim Oda (old)	0.63	0.74	1.72	0.52	0.57	0.96	1.47
Shama	1.59	1.03	5.11	1.71	1.82	1.61	1.26
Twenedurase	2.04	1.42	7.66	2.04	2.14	2.67	2.28
Apreja	1.08	1.02	3.65	1.00	1.09	1.51	1.66
Dunkwa-On-Offin 1	0.82	0.81	3.46	0.72	1.00	1.10	0.79
Adonkrono	0.58	1.18	2.76	0.62	0.75	2.78	3.35
Wobiri	0.72	0.64	2.52	0.54	0.63	1.09	1.43
Nnboamu	1.33	0.93	6.36	1.27	1.21	1.43	1.31
Kwahu Praso	0.75	0.69	3.52	0.69	0.81	1.08	1.17
Twifo Praso (1)	1.15	1.00	5.02	1.11	1.03	1.29	1.27
Daboase	0.74	0.76	4.37	0.71	0.79	1.04	0.91
Assin Praso	0.67	0.66	3.97	0.60	0.67	0.92	1.02
Beposo	0.65	0.65	4.76	0.58	0.64	0.86	0.91
Nkontinso	0.83	0.79	7.58	0.58	0.85	1.00	0.90
Kade	0.61	0.64	6.02	0.82	0.66	0.94	0.93
Anlo	0.46	0.39	5.11	0.58	0.43	0.43	0.35
Dunkwa-On-Offin (2)	0.61	0.60	7.62	0.39	0.61	0.76	0.62
Dadientem	0.52	0.53	9.00	0.57	0.55	0.75	0.68
Kibi	0.65	0.58	12.7	0.50	0.58	0.85	0.82

APPENDIX V

ENRICHMENT FACTORS OF As, Br, Cs, Hf, Se, Zr, Ba, Th, U, Sr, Sb, Rb AND Mo USING Sc AS A NORMALIZING AGENT IN 0 TO 1 cm SOIL FROM THE PRA RIVER BASIN

Sampling Sites	As	Br	Cs	Hf	Se	Zr	Ba	Th	U	Sr	Sb	Rb	Mo
Akim Oda	1.26	0.21	0.33	7.32	LD	7.74	0.22	1.04	1.45	0.53	1.32	0.28	LD
Akim Oda (old)	0.92	0.88	0.61	4.80	LD	4.84	0.37	1.04	1.41	0.39	0.92	0.59	LD
Shama	9.89	3.76	0.40	6.71	LD	6.56	1.00	1.22	2.43	9.76	2.50	1.15	2.72
Twenedurase	3.83	2.00	0.92	4.76	LD	4.80	0.58	1.76	1.97	0.55	1.51	1.88	LD
Apreja	1.01	0.74	0.44	5.45	LD	5.72	0.45	1.00	1.31	0.52	3.17	0.46	1.50
Dunkwa-On-Offin (1)	2663	0.36	0.74	0.78	22.0	0.96	0.38	0.43	LD	1.02	179	0.69	LD
Adonkrono	0.78	0.71	0.41	3.22	LD	3.33	0.32	1.02	1.59	0.34	1.01	0.65	LD
Wobiri	2.43	0.70	0.50	4.09	LD	4.19	0.27	0.68	0.96	0.41	1.13	0.31	LD
Nnoboamu	57.4	0.60	0.96	2.55	5.40	2.43	0.71	1.11	1.68	LD	1.75	1.25	3.05
Kwahu Praso	1.54	0.90	0.34	4.92	LD	5.24	0.59	0.68	0.85	1.21	1.04	0.57	LD
Twifo Praso	1.99	1.00	0.47	3.50	LD	3.65	0.51	0.94	0.84	0.70	1.25	0.58	1.62
Daboase	2.53	0.42	0.59	1.66	LD	1.63	0.66	0.58	0.76	0.69	0.78	0.67	LD
Assin Praso	1.19	0.70	0.53	2.43	1.74	2.38	0.60	0.63	0.80	0.61	1.19	0.62	LD
Beposo	1.23	1.11	0.77	1.88	LD	1.73	0.94	0.72	1.10	0.65	0.95	0.95	LD
Nkontinso	1.92	0.20	0.67	1.33	LD	1.29	0.52	0.57	0.74	0.54	0.54	0.74	LD

277

APPENDIX V Cont'd

Sampling Sites	As	Br	Cs	Hf	Se	Zr	Ba	Th	U	Sr	Sb	Rb	Mo
Kade	1.15	0.57	0.35	1.35	4.21	1.32	0.30	0.54	0.65	0.20	0.83	0.39	LD
Anlo	0.31	1.50	0.12	0.96	1.41	0.93	0.07	0.82	0.87	0.12	0.15	0.17	1.23
Dunkwa-On-Offin(2)	2.62	0.17	0.36	0.54	LD	0.56	0.35	0.35	0.36	0.41	1.92	0.43	0.84
Dadientem	1.12	0.65	0.19	0.66	LD	0.69	0.25	0.37	0.31	0.22	0.60	0.29	LD
Kibi	1.74	0.11	0.24	0.91	LD	0.94	0.20	0.43	0.40	0.14	0.92	0.33	LD

APPENDIX W

ENRICHMENT FACTORS OF Ag, Au, Co, Sn, Cd, Cr, Ga, Ta, AND W USING Sc AS A NORMALIZING AGENT IN 0 TO 1 cm SOIL FROM THE PRA RIVER BASIN

Sampling Sites	Ag	Au	Co	Sn*	Cd*	Cr	Ga*	Ta	W*
Akim Oda	LD	LD	1.14	LD	LD	1.89	0.55	2.87	4.18
Akim Oda (old)	LD	1.26	1.57	LD	LD	1.81	0.84	2.01	1.55
Shama	LD	2.02	2.14	LD	LD	2.04	1.66	1.38	LD
Twenedurase	LD	1.42	1.45	LD	LD	0.97	1.30	1.11	1.10
Apreja	LD	195	0.84	LD	LD	1.94	0.92	1.14	1.62
Dunkwa-On-Offin (1)	74.3	22028	2.96	LD	LD	2.55	LD	0.60	18.5
Adonkrono	LD	1.27	0.64	LD	LD	2.38	0.84	1.66	6.63
Wobiri	LD	1.02	1.52	LD	LD	1.21	0.67	1.20	1.36
Nnboamu	LD	3.14	0.74	LD	LD	2.31	1.52	1.24	5.36
Kwahu Praso	LD	1.53	1.18	LD	LD	1.23	0.94	0.71	LD
Twifo Praso	LD	13.1	1.06	LD	LD	1.77	0.92	0.94	LD
Daboase	LD	6.37	1.39	LD	LD	1.48	1.03	0.81	1.11
Assin Praso	LD	0.95	1.58	LD	LD	1.51	0.83	0.96	1.34
Beposo	LD	2.77	1.10	LD	LD	1.41	1.17	0.98	1.09
Nkontinso	LD	3.09	1.02	LD	LD	1.43	0.98	0.71	1.08
Kade	LD	0.99	0.76	LD	LD	0.43	0.72	0.71	1.18
Anlo	LD	LD	0.29	LD	LD	0.65	0.53	0.68	LD

APPENDIX W Cont'd

Sampling Sites	Ag	Au	Co	Sn*	Cd*	Cr	Ga*	Ta	W*
Dunkwa-On-Offin (2)	LD	4.10	1.11	LD	LD	1.47	0.70	0.40	LD
Dadientem	LD	0.70	1.10	LD	LD	1.58	0.74	0.39	0.63
Kibi	LD	LD	1.39	LD	LD	0.77	0.77	0.48	0.60

CARNIVOROUS FISH (*Schilbe schilbe*) SAMPLES FROM THE PRA
RIVER BASIN, GHANA

CARNIVOROUS FISH (*Synodontis eupterus* (SPOTTED) AND *Chrysichthys*
sp) FROM THE PRA RIVER BASIN, GHANA

Source: Author Data, 2014

APPENDIX Y

THE SAME STANDARD LENGTH OF TWO (2) CARNIVOROUS FISH SAMPLES (*Synodontis auratus* AND *Chrysichthys nigrodigitatus)* FROM NKONTINSO SAMPLING SITE

Source: Author Data, 2014

APPENDIX Z

VEGETATION AROUND THE OFFIN RIVER AT NKONTINSO SAMPLING SITE, ONE OF THE MAJOR TRIBUTARIES OF THE PRA RIVER BASIN

Source: Author Data, 2014